



Virginia Commonwealth University
VCU Scholars Compass

Theses and Dissertations

Graduate School

2017

Design, Synthesis, and Biological Screening of Selective Mu Opioid Receptor Ligands as Potential Treatments for Opioid Addiction

Samuel Obeng
Virginia Commonwealth University

Follow this and additional works at: <https://scholarscompass.vcu.edu/etd>

 Part of the [Medicinal and Pharmaceutical Chemistry Commons](#), and the [Nervous System Diseases Commons](#)

© Samuel Obeng

Downloaded from

<https://scholarscompass.vcu.edu/etd/4771>

This Dissertation is brought to you for free and open access by the Graduate School at VCU Scholars Compass. It has been accepted for inclusion in Theses and Dissertations by an authorized administrator of VCU Scholars Compass. For more information, please contact libcompass@vcu.edu.

© Samuel Obeng 2017

All Rights Reserved

Design, synthesis, and biological screening of selective mu opioid receptor ligands as
potential treatments for opioid addiction

A dissertation submitted in partial fulfillment of the requirements for the degree of Doctor
of Philosophy in Medicinal Chemistry at Virginia Commonwealth University.

by

Samuel Obeng,

B. Pharmacy, Kwame Nkrumah University of Science and Technology, 2010

M.Phil. Pharmaceutical Chemistry, Kwame Nkrumah University of Science and
Technology, 2014

Director: Dr. Yan Zhang,

Professor, Medicinal Chemistry

Virginia Commonwealth University

Richmond, Virginia

05/2017

Acknowledgment

I would first want to thank God for his guidance and providence all these years in graduate school. I would also like to thank my advisor Dr. Yan Zhang for his guidance and encouragement he provided me through my years in the graduate school at VCU. I would also like to thank my research advisory committee: Dr. Dana Selley, Dr. Glen Kellogg, Dr. Phillip Gerk and Dr. Shijun Zhang for providing me feedback about my research progress and helping me with my dissertation. I would also like to thank Dr. Yunyun Yuan for teaching me the synthetic techniques used in organic chemistry. I would like to thank Dr. Dana Selley for allowing me to train in his laboratory to conduct radioligand binding assays. I would like to thank Abdulmajeed Jali for teaching me the radioligand binding assays. I would also like to thank my wife, Rebecca, and my daughter, Audrey for their love, support, and patience through these years in graduate school. I would also like to thank my parents, my brother, and my friends for their unending love and support. Finally, I would like to thank all members of Dr. Yan Zhang and Dr. Dana Selley's laboratory for the friendly environment in the laboratory.

Table of Contents

Acknowledgment.....	ii
Table of Contents.....	iii
List of Tables.....	vii
List of Figures.....	ix
List of Schemes.....	xi
List of Abbreviations and Symbols	xii
Abstract.....	ii
1.0 INTRODUCTION.....	1
1.1 History of opioids.....	2
1.2 Opioid abuse statistics	3
1.3 Opioids and opioid receptors	4
1.4 G-protein signaling.....	5
1.5 Types of opioid receptors.....	5
1.6 Opioid receptor ligands	6
1.6.1 Peptides.....	6
1.6.2 Non-peptides	7

1.7 Functions of opioid receptors	8
1.7.1 Ionic homeostasis	9
1.7.2 Cell proliferation	9
1.7.3 Neuroprotection	10
1.7.4 Hibernation	10
1.7.5 Pain modulation	11
1.7.6 Emotional response	12
1.7.7 Immune Function	12
1.7.8 Obesity.....	13
1.7.9 Drug Abuse/Addiction	13
1.7.10 Other functions of opioid receptors	14
1.8 Current treatment of opioid addiction	15
1.9 Goal	18
1.10 Specific aims.....	18
1.10.1 Aim 1.....	18
1.10.2 Aim 2.....	18
1.10.3 Aim 3.....	18
2.0 DESIGN, SYNTHESIS, AND PHARMACOLOGICAL CHARACTERIZATION OF INDOLE ANALOGS OF 6 α / β -NALTREXAMINE.....	19
2.1 Molecular design.....	19

2.2 Specific Aims	23
2.2.1 Aim 1: Synthesis of compounds.....	23
2.2.2 Aim 2: In vitro and in vivo screening of compounds obtained from Aim 1	24
2.2.3 Aim 3: Molecular modeling studies of compounds identified after biological screening	24
2.3 Results and Discussion.....	24
2.3.1 Synthesis (Chemistry).....	24
2.3.2 Pharmacological characterization of the indole analogs of 6 α -naltrexamine .	27
3.0 SYNTHESIS OF NAQ FOR STUDIES IN MONKEYS AND DESIGN AND SYNTHESIS OF THIRD GENERATION NAQ ANALOGS	46
3.1 Specific Aim	46
3.2 Design of the third generation NAQ analogs.....	46
3.2.1 Specific Aim	48
3.3 Results and Discussion.....	48
4.0 QUANTITATIVE STRUCTURE PHARMACOKINETIC (PK) RELATIONSHIP STUDIES FOR NOVEL OPIOID COMPOUNDS.....	51
4.1 Introduction	51
4.2 Aim of QSPKR project.....	52
4.3 Results and Discussion.....	52
4.4 Summary of QSPKR study.....	58

5.0 CONCLUSIONS	60
6.0 EXPERIMENTAL SECTION.....	68
6.1 Chemical synthesis	68
6.2 Characterization of compounds	75
6.3 Instruments used for characterization	93
6.4 Pharmacological assays	94
6.4.1 Cell culture.....	94
6.4.2 Cell membrane harvesting.....	95
6.4.3 Competition binding assay.....	96
6.4.4 [³⁵ S]GTP γ S functional assay.....	98
6.4.5 warm-water immersion assay	101
6.4.6 Opioid withdrawal assay	102
6.5 Molecular modeling study	102
6.5.1 Molecular docking study	103
6.5.2 Molecular dynamics simulation	103
6.6 QSPKR study.....	104
List of References	106
Appendix	140
Vita	181

List of Tables

Table 1. Site-directed mutagenesis study in MOR.....	22
Table 2. Designed indole derivatives of 6 α / β -naltrexamine.....	23
Table 3. Percentage yield obtained for indole analogs of 6 α / β -naltrexamine HCl.....	26
Table 4. Binding affinity and selectivity of indole derivatives of 6 α -naltrexamine.....	27
Table 5. Binding affinity and selectivity of indole derivatives of 6 β -naltrexamine.....	30
Table 6. MOR [³⁵ S]GTP γ S binding functional assay results of indole derivatives of 6 α -naltrexamine.....	34
Table 7. MOR [³⁵ S]GTP γ S binding functional assay results of indole derivatives of 6 β -naltrexamine.....	37
Table 8. Binding scores of compound 6 in the two poses obtained after docking.....	43
Table 9. RMSD score after MD simulation.....	44
Table 10. Designed third generation NAQ analogs.....	47
Table 11. Opioid QSPKR obtained from Dr. Jurgen Venitz laboratory	54

Table 12. Comparison of predicted f_u and CL_{tot} to actual of NTX, NAP and NAQ.....56

List of Figures

Figure 1. Opioid receptor ligands.....	7
Figure 2. Compounds used in the treatment of opioid addiction.....	16
Figure 3. MOR selective compounds.....	17
Figure 4. Compounds designed using the “message address” concept.....	19
Figure 5. MOR selective ligands designed and synthesized in Dr. Yan Zhang’s laboratory.....	20
Figure 6. Docked poses of NAQ in MOR, KOR, and DOR.....	21
Figure 7. Warm-water tail immersion assay in mice.....	39
Figure 8. Dose dependent studies on compound 6.....	40
Figure 9. Compound 6 (s.c.) in opioid-withdrawal assays in chronic morphine-exposed mice	41
Figure 10. Docked poses of compound 6 in the mu opioid receptor.....	42

Figure 11. RMSD plot for MD simulation of compound 6 for the two binding poses obtained observed	43
Figure 12. MD simulation results for compound 6 in the mu opioid receptor	45
Figure 13. Second generation NAQ analogs.....	47

List of Schemes

Scheme 1. Synthesis of 6 α / β naltrexamine HCl.....	25
Scheme 2. Coupling of naltrexamine to indole carboxylic acids.....	25
Scheme 3. Synthesis of the third generation NAQ analogs.....	49
Scheme 4. Metabolic pathway of NTX in rodents.....	53

List of Abbreviations and Symbols

Å	angstroms
^3H	tritiated
β -FNA	beta-funaltrexamine
δ	delta
$^{\circ}\text{C}$	degrees celcius
γ	gamma
κ	kappa
μ	mu
μg	micrograms
μL	microliter
B_{max}	receptor density

CHO	Chinese hamster ovarian
CL _{tot}	total body clearance
CNS	central nervous system
d	doublet
DD	dihydrodiol cytosolic dehydrogenases
DPN	diprenorphine
DMEM	Dulbecco's modified Eagle's medium
DMF	dimethylformamide
DMSO	dimethyl sulfoxide
DOR	delta opioid receptor
DPM	disintegrations per minute
EC ₅₀	half maximal effective concentration
EDTA	ethylenediaminetetraacetic acid
EGTA	ethylene glycol tetraacetic acid
E _{max}	maximum response
FBS	fetal bovine serum
FDA	Food and Drug Administration
F _{oral}	oral bioavailability

f_u [%]	percentage unbound
g (centrifuge)	g-force
G418	geneticin
GDP	guanosine diphosphate
GNTI	5-guanidinonaltrindole
GPCR	g-protein coupled receptor
GTP	guanosine triphosphate
GTP γ S	guanosine 5'-O-[gamma-thio] triphosphate
h	hours
HPLC	High performance liquid chromatography
IC ₅₀	half maximal inhibitory concentration
IR	infrared spectroscopy
K ₂ CO ₃	potassium carbonate
K _i	binding affinity
K _d	dissociation constant
KOR	kappa opioid receptor
m	multiplet
M	molar

MD	molecular dynamics
MHz	megahertz
mM	millimolar
MOR	mu opioid receptor
HRMS	high resolution mass spectroscopy
N ₂	Nitrogen gas
Na ⁺	sodium ion
NaCl	sodium chloride
NaOH	sodium hydroxide
NH ₄ OH	ammonium hydroxide
NLX	naltrexone
nM	nanomolar
NMR	nuclear magnetic resonance
NTI	naltrindole
NTX	naltrexone
norBNI	norbinaltorphimine
RMSD	root-mean-square deviation
s	singlet

SAR	structure activity relationship
TEA	triethylamine
THF	tetrahydrofuran
Tris	trihydroxymethylaminomethane
Ugt2b1	UDP-glucuronosyltransferase

Abstract

DESIGN, SYNTHESIS, AND BIOLOGICAL SCREENING OF SELECTIVE MU OPIOID RECEPTOR LIGANDS AS POTENTIAL TREATMENTS FOR OPIOID ADDICTION

Samuel Obeng, Doctor of Philosophy in Medicinal Chemistry

A dissertation submitted in partial fulfillment of the requirements for the degree of Doctor of Philosophy in Medicinal Chemistry at Virginia Commonwealth University.

Virginia Commonwealth University, 2017

Dr. Yan Zhang, Professor, Department of Medicinal Chemistry

Today, more Americans die each year because of drug overdoses than are killed in motor vehicle accidents. In fact, in 2015, more than 33,000 individuals died due to an overdose of heroin or prescription opioids. Sadly, 40-60 % of patients on current opioid addiction treatment medications relapse. Studies have shown that the addiction/abuse liability of opioids are abolished in mu opioid receptor (MOR) knock-out mice; this indicates that the addiction and abuse liability of opioids are mainly mediated through MOR. Utilizing the “message-address concept”, the our laboratory reported a novel non-peptide, reversible MOR selective ligand 17-cyclopropylmethyl-3,14 β -dihydroxy-4,5 α -epoxy-6 α (isoquinoline-3-carboxamido)morphinan (NAQ). Molecular modeling and mutagenesis studies revealed that the selectivity of NAQ for MOR is because of the π - π stacking of the isoquinoline ring of NAQ with W318.

Therefore, other heterocyclic ring systems were explored to obtain a diverse library of compounds with similar or different molecular interactions and pharmacologic characteristics as NAQ. The newly designed compounds were indole analogs of 6 α / β -naltrexamine. The compounds were synthesized and the affinity and selectivity for MOR determined using the radioligand binding assay while the functional activity at MOR was determined using the [³⁵S]GTP γ S binding assay. The indole analog of 6 α -naltrexamine substituted at position 7 (compound **6**) was found to be very potent and had the lowest efficacy in the [³⁵S]GTP γ S functional assay while the indole analog of 6 β -naltrexamine substituted at position 2 (compound **10**) was identified as a MOR agonist and had the greatest efficacy. In vivo studies were conducted using the warm-water immersion assay to find whether the synthesized compounds had antinociceptive effects and/or blocked the antinociceptive effects of morphine. Not surprisingly, compound **10** was

identified as an opioid agonist while compound **6** almost completely blocked morphine's antinociceptive effects. The opioid antagonist effect of compound **6** was found to be dose dependent with an AD_{50} of 2.39 mg/kg (0.46-12.47). An opioid withdrawal assay was conducted on compound **6** using morphine-pelleted mice. Compound **6** produced significantly less withdrawal symptoms at 50 mg/kg than naltrexone at 1 mg/kg. Therefore, compound **6** has the potential to be used in opioid addiction and withdrawal treatment.

CHAPTER 1

1.0 INTRODUCTION

It is estimated that between 26.4 million and 36 million people abuse opioids such as heroin, morphine, and other prescription pain relievers worldwide, which is a serious global problem affecting health, social, and economic welfare of every demographic group.¹ In the United States, an estimated 4.4 million people aged 12 or older suffer from substance use disorders related to prescription opioids and an estimated 435,000 addicted to heroin.² Opioid addiction has devastating effects on societies and an alarming observation is that opioid misuse is on the rise. For example, the number of unintentional overdose deaths from opioid prescription analgesics has soared in the United States, more than quadrupling since 1999.³ Therefore, opioid addiction has become a global epidemic and has affected the economies of many countries.

In addition to the detrimental effects of drug abuse on health and well-being, drug abuse has a huge economic burden on the United States of America costing over \$600 billion annually due to crime, violence, abuse, and the associated health care costs. Effective drug addiction treatment has been shown to reduce associated health and social cost

by far more than the cost of treatment itself. For example the cost of 1 full year of methadone maintenance therapy is approximately \$4,700 per patient whereas 1 full year of imprisonment costs approximately \$24,000 per person.⁴ Therefore, treating opioid addicts rather than imprisoning them might help drive down the huge cost associated with substance abuse. However, 40-60% of patients being treated for opioid addiction suffer relapse.⁴ Opioid antagonists such as naltrexone and naloxone have been shown to curb drug craving and prevent relapse. On the other hand, severe side effects have been reported on the use of these drugs as long-term treatments for opioid addiction. Therefore, there is the need to develop new opioid addiction medications with fewer side effects. This chapter seeks to review the history and pharmacology of opioids and provides a review on the statistics and current treatments for opioid addiction. Finally, the goal and specific aims of this project are also outlined in this chapter.

1.1 History of opioids

The Sumerians in Mesopotamia were among the first people identified to have cultivated the poppy plant around 3400 BC. The poppy plant was named Hul Gil, the “joy plant”. The cultivation of the poppy plant then spread through major civilizations in Europe and Asia and was used to treat pain and many other diseases.⁵⁻⁸ In 1806, the German chemist Friedrich Serturmer isolated the opium alkaloids, one of them being morphine named after Morpheus, the god of dreams. However, it was not until 167 years later that the pharmacology of morphine was defined at the receptor level. In 1877, Dr. Eduard Livenstein for the first time demonstrated that morphine is addictive and had withdrawal effects. He also argued that the craving produced by morphine was a physiological response.⁹⁻¹¹ Due to the developments in the 19th century that

transformed the practice of medicine, there was a struggle to either use opioids for their medicinal benefits or to abandon the use of opioids because of their abuse liability and the devastating effects for individuals and the society at large.^{5,12} On the other hand, in the twentieth century there were many research advances that led to changes in the way opioids were used for the treatment of pain and addiction.^{13,14} For example, the opioid maintenance therapy for the treatment of opioid addiction was introduced and it was recognized that pain itself is a debilitating disease and thus, opioids are essential for the treatment of pain.^{15,16}

1.2 Opioid abuse statistics

In the 1990's, the use of opioids for chronic pain started to increase, showing a substantial year-to-year rise that continues up to today. The increased use of opioids for legitimate treatment of acute and chronic pain has been accompanied by a substantial increase in the prevalence of nonmedical use of prescription opioids.^{17,18} Nonmedical use of prescription pain relievers, particularly opioid analgesics, is a major public health concern in the United States as evidenced by the increased numbers of emergency department visits, treatment admissions, and fatal overdoses.^{19,20} Opioids accounted for 61% of all drug-related overdose deaths in 2014 —a rate that has nearly quadrupled since 2000. In addition, opioid-related hospitalizations increased 150% between 1993 and 2012.²¹⁻²⁴ If this is not disturbing enough, the national survey on drug use and health estimated that over 10 million people in the United States used prescription opioids for nonmedical use in 2014.² This finding is a substantial concern because people who misuse prescription opioid painkillers are 40 times more likely to become addicted to heroin than those who do not misuse prescription opioids, and 80% of new

heroin users have previously misused prescription opioids.^{25,26} Currently, more Americans die each year as a result of drug overdoses (both prescription and illegal drug use) than are killed in motor vehicle accidents.²⁷ In fact, in 2015, more than 33,000 individuals died due to an overdose of heroin or prescription opiate drugs, with deaths due to heroin-related causes surpassing those due to gun homicides.^{28–30} The reason why patients on prescription opioids are able to shift easily to heroin use is because heroin is affordable and easily accessible.³ It is therefore necessary to know the pharmacology of opioids to be able to treat opioid addiction.

1.3 Opioids and opioid receptors

An opioid is any compound that binds to the opioid receptor, while the term opiate is used to describe opioid alkaloids obtained from the opium poppy such as morphine and codeine. Opioids can either be semi-synthetic or synthetic. Examples of semi-synthetic opioids include heroin and oxycodone, which are synthesized from morphine and thebaine, respectively. Examples of synthetic opioids include fentanyl, methadone, and propoxyphene.¹⁷ Opioids produce their pharmacological effects by binding to specific proteins, called opioid receptors. These receptors are widely distributed and can be found both in the central and peripheral nervous system.^{31,32} Opioid receptors have high sequence homology and belong to the large superfamily of seven transmembrane-spanning G protein-coupled receptors (GPCRs). GPCRs play an important role in the body by mediating the actions of most known neurotransmitters and hormones. Activation of opioid receptors leads to adenylyl cyclase inhibition, which leads to decreased production of cAMP, closing of voltage-gated Ca²⁺ channels, and activation of inwardly rectifying K⁺ channels.³³ Also, activation of opioids results in activation of

phospholipase C (PLC) and subsequent mobilization of the inositol 1,4,5- trisphosphate (IP3)-sensitive which results in the release of intracellular Ca^{2+} from the endoplasmic reticulum.³⁴ The effects of opioids are mainly inhibitory and results in strong inhibition of nerve firing and reduction in neurotransmitter release. There are four main types of opioid receptors.^{35,36}

1.4 G-protein signaling

GPCRs associate with heterotrimeric G-proteins which are composed of three different subunits: alpha, beta, and gamma. Opioid receptors are mainly coupled to $G_{\alpha i/o}$. In an inactive state, GDP is bound to the G_{α} subunit of the G-protein. G_{α} is bound to the $\beta\gamma$ -complex. When an opioid agonist binds to an opioid receptor, it results in a conformational change in the receptor thereby resulting in the exchange of GTP for GDP on the G_{α} subunit. This results in the activation of the G-protein. The GTP bound G_{α} subunit dissociates from the $\beta\gamma$ -complex. Both the G_{α} and $\beta\gamma$ -complex diffuse along the membrane to modulate target proteins. Since the G_{α} subunit has intrinsic GTPase activity, GTP is hydrolyzed to GDP thereby resulting in the re-association of the $\beta\gamma$ -complex with the G_{α} subunit to form the inactive G-protein.^{37,38}

1.5 Types of opioid receptors

Since opioid-binding sites were first proposed in the early 1950s and 1960s and discovered in mammalian brain tissue in 1973, extensive pharmacological studies have uncovered different types of opioid receptors.^{10,39–42} To date, four opioid receptors have been cloned, the mu opioid receptor (MOR, mu for morphine), the kappa opioid receptor (KOR, kappa for ketocyclazocine), the delta opioid receptor (DOR, delta for deferens because it was first identified in mouse vas deferens), and the opioid receptor-like

orphan receptor (ORL), or nociceptin/orphanin FQ receptor (NOP) .⁴³⁻⁴⁶ Each of these receptors have their own repertoire of ligands.

1.6 Opioid receptor ligands

Opioid receptor ligands can be categorized into two main groups based; peptides and non-peptides.

1.6.1 Peptides

Some endogenous peptides have been found to bind to opioid receptors that are involved in pain modulation and other functions. Endogenous opioid peptides include enkephalins, dynorphins and β -endorphin that are derived from three precursor molecules pro-enkephalin, pro-dynorphin and proopiomelanocortin, respectively (**Figure 1**). These peptides are present in the CNS. Their presence have also been confirmed in peripheral tissues.⁴⁷ The tetrapeptide sequence Tyr-Gly-Gly-Phe at the N-terminus is present in all endogenous peptides derived from these precursors. Enkephalin, dynorphin and β -endorphin have varying affinities for MOR, DOR, and KOR and have negligible affinity for the ORL receptor. However, none of these peptides bind exclusively to one opioid receptor type. On the other hand, recently discovered endogenous peptides endomorphin-1 and endomorphin-2 have high selectivity for MOR. Nociceptin/orphanin FQ, derived from pro-nociceptin, is the endogenous ligand for the ORL/NOP receptor.⁴⁶ The major difference between Nociceptin and the endogenous peptides mentioned above is that nociceptin's N-terminal amino acid is Phe instead of Tyr. In addition to endogenous opioid peptides, synthetic opioid agonists

such as DAMGO ([D-Ala², N-MePhe⁴, Gly-ol]-enkephalin) and DADLE ([D-Ala², D-Leu⁵]-Enkephalin) have also been identified.^{48,49}

PEPTIDES

Tyr-Gly-Gly-Phe-Met-Thr-Ser-Glu-Lys-Ser-Gln-Thr-Pro-Leu-Val-Thr-Leu-Phe-Lys-Asn-Ala-Ile-Ile-Lys-Asn-Ala-Tyr-Lys-Lys-Gly-Glu
β-endorphin

Phe-Gly-Gly-Phe-Tyr-Gly-Ala-Arg-Lys-Ser-Ala-Arg-Lys-Leu-Ala-Asn-Gln
Nociceptin

Tyr-Gly-Gly-Phe-Leu-Arg-Arg-Ile-Arg-Pro-Lys-Leu-Lys

Dynorphin A

Tyr-Gly-Gly-Phe-Leu-Arg-Arg-Gln-Phe-Lys-Val-Val-Thr

Dynorphin B

Tyr-Gly-Gly-Phe-Met
Met-enkephalin

Tyr-Gly-Gly-Phe-Leu
Leu-enkephalin

H-Tyr-D-Ala-Gly-N-MePhe-Gly-OH
DAMGO

Tyr-D-Ala-Gly-Phe-D-Leu
DADLE

NON-PEPTIDES

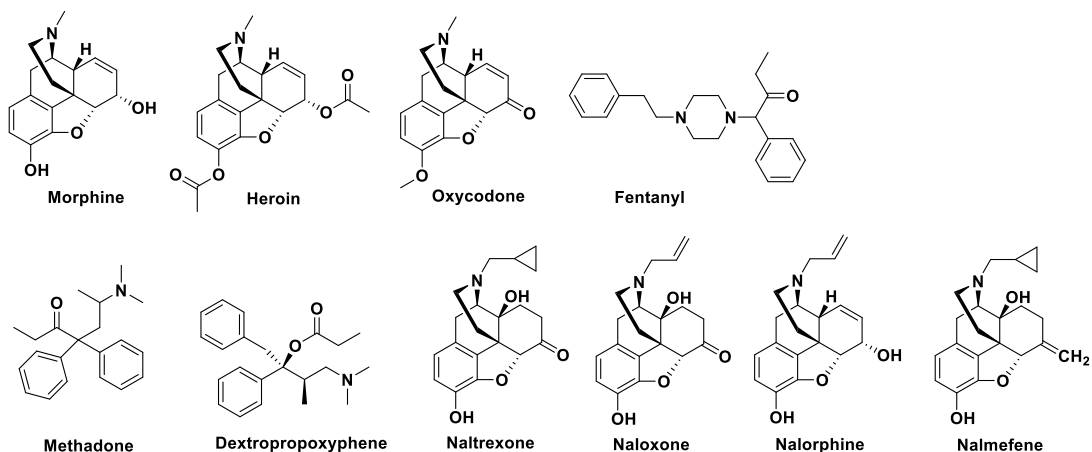


Figure 1. Opioid receptor ligands

1.6.2 Non-peptides

Agonists: The first known opioid alkaloid was morphine and its chemical structure was elucidated in 1923.⁵⁰ Morphine and other opioids are widely used in clinical practice for

blockage of severe pain syndromes or for anesthetic purposes. Morphine is primarily an agonist ligand at MOR. Its affinities for DOR and KOR are low and it is therefore used as a selective MOR ligand in pharmacological studies.⁵¹ Opioid agonists include semi-synthetic (heroin and oxycodone) and synthetic (fentanyl, methadone, and propoxyphene) compounds (**Figure 1**). These compounds are full opioid agonists since they produce over 90% stimulation of the opioid receptor. Opioid partial agonists such as buprenorphine produce 25 to 70% stimulation relative to the full agonists.⁵²

Antagonists: Naloxone and naltrexone are the most frequently used opioid antagonists.⁵³ Nalorphine was the first compound to be recognized as an opioid antagonist while naloxone was the first pharmacologically neutral antagonist identified and it is non-selective.^{54,55} For a compound to be characterized as an opioid agonist, its effects have to be “naloxone-reversible”.⁵⁶ Naloxone and naltrexone bind to all three opioid receptors, but have greater affinity for MOR over KOR and DOR.⁵⁷ Nalmefene is another opioid antagonist that is used for the treatment of alcoholism.⁵⁸ Activation or blockage of each receptor type by agonists or antagonists results in different physiological effects. By definition, antagonists produce no efficacy. However, antagonists have been shown to produce low efficacy (5-25% stimulation relative to the full agonist) in the GTPγS assay.⁵⁹

1.7 Functions of opioid receptors

Opioid receptors in the CNS are part of the most extensive and diverse peptidergic transmission systems and are involved in numerous functions in the body. Some of the physiological functions of these receptors include pain, mood, and stress modulation. Opioid receptors are also involved in regulatory functions such as thermoregulation and

regulation of the respiratory, gastrointestinal, and cardiovascular systems. Abuse of opioid compounds leads to addiction, which affects homeostasis and brain function.⁶⁰

1.7.1 Ionic homeostasis

Opioid receptors have been shown to be involved in the regulation of ionic homeostasis. Under normal conditions, the extracellular Na⁺ concentration is about 13 to 38 times the intracellular concentration while the intracellular K⁺ concentration is about 50 times the extracellular concentration. This difference in concentration creates a steep electrochemical gradient across the plasma membrane which is essential for normal functioning of the neurons. Studies have shown that opioids are involved with the regulation of ionic homeostasis under both normal oxygen blood levels and hypoxic conditions. DOR activation attenuates hypoxia induced increase in extracellular K⁺ and decrease in extracellular Na⁺.⁶¹⁻⁶⁴ This demonstrates that opioids play an important role in the regulation of ionic homeostasis under environmental stress. Under normal conditions, all opioid agonists either lead to an increase of intracellular Ca²⁺ or an inhibition of Ca²⁺. However, the predominant effect of opioid agonists on Ca²⁺ homeostasis is inhibitory, which is consistent with classical recognition of the opioids as inhibitory regulators in the brain.⁶⁵⁻⁷¹

1.7.2 Cell proliferation

In a study conducted by Malendowicz et al., it was observed that activation of MOR and DOR results in the inhibition of growth of immature adrenals, stimulates adrenal regeneration, and does not affect proliferation of cultured adrenocortical cells.⁷² On the other hand, Narita et al. found that SNC80, a DOR selective agonist, promoted neural differentiation from multipotent neural stem cells obtained from embryonic C3H mouse

forebrains.⁷³ However, neither MOR nor KOR activation produced these effects. This demonstrates that DOR plays a crucial role in neurogenesis.

1.7.3 Neuroprotection

One of the most exciting findings of the past decade in opioid receptor function is the discovery that DOR mediates neuroprotection against hypoxic/ischemic injury. Several studies conducted in the past had opposing results for the role of opioids in neuronal responses to hypoxic/ischemic insults. While some researchers showed that opioid receptor activation protects the brain from ischemia and extended the animal survival time during severe hypoxia,^{74–78} others demonstrated that opioid receptor inhibition protects the brain from ischemia-induced injury.^{79–84} A series of studies conducted recently have showed that DOR is neuroprotective against hypoxic stress in the brain. The mechanism for DOR neuroprotection involves the stabilization of ionic homeostasis, increase in intracellular transduction of pro-survival signals and attenuation of oxidative injury as well as regulation of DOR expression.^{85–92} This clarified the historical controversies on the important functions that opioids and their receptors play in ischemic/hypoxic neuronal injury.^{85,87,93–103} Other studies showed that DOR is neuroprotective because its activation protects neocortical neurons from glutamate excitotoxicity.¹⁰⁴

1.7.4 Hibernation

Mammalian hibernation is associated with depletion of energy stores, intracellular acidosis, and hypoxia, which are similar to the effects observed during hypoxia. DOR activation triggers physiological features such as analgesia and respiratory depression that are associated with hibernation.¹⁰⁵ It has also been observed that circulating levels

of opioid peptides in hibernating animals are increased dramatically, which is considered a “hibernation induction trigger”.^{106–109} Mammalian hibernation can be reversed by opioid antagonists.^{108,110} Thus, DOR plays a significant role in hibernation.

1.7.5 Pain modulation

Most of the studies with opioids are associated with analgesia.^{111–113} When injury occurs, there is a release of endogenous opioids and a rise in level of opioids in blood which helps alleviate the pain resulting from the injury. For instance, there is a significant increase in the circulating levels of β -endorphin following muscle injury, fixed-pressure hemorrhagic shock and lipopolysaccharide (LPS) administration in animal models.¹¹⁴ The analgesic effects experienced after an acute insult can be partially reversed by naloxone, an opioid antagonist. This demonstrates the involvement of endogenous opioids in stress-induced analgesia.¹¹⁵

Using MOR knockout mice, it was demonstrated that MOR plays a central role in analgesia.¹¹² MOR knockout mice have increased sensitivity to heat, however, DOR- and KOR-deficient mice do not show any alteration in heat perception.^{112,116} This suggests that MOR modulates thermal nociception through crosstalk with the transient receptor potential vanilloid type 1 (TRPV1) ion channel. It has also been observed that, after knocking out MOR, the analgesic effects of DOR agonists are unchanged or diminished while the analgesic effects of MOR agonists are abolished.^{117–119} DOR agonists can enhance the analgesic effects of MOR agonists and DOR antagonists can prevent or reduce the addictive properties of MOR agonists.¹²⁰ Compared to MOR and DOR, KOR mainly mediates analgesia to visceral pain.^{117,121}

1.7.6 Emotional response

The role of the opioid system in regulating emotional response is not well documented as its role in controlling pain and addiction.¹²² Studies have demonstrated that DOR acts as a natural inhibitor of anxiety and stress.¹²³ Thus, DOR agonists have antidepressant and anxiolytic effects. Also, studies have shown that DOR agonists increase the expression of brain-derived neurotrophic factor (BDNF) mRNA, an effect produced by some antidepressants. Thus, DOR agonists have antidepressant and anxiolytic effects. In depression paradigms, studies showed that KOR mediates a variety of stressors, and produces despair-like responses. KOR agonists have been shown to produce dysphoric and psychomimetic effects.¹²⁴

1.7.7 Immune Function

Opioids like cytokines, interact with their receptors in the CNS and peripheral neurohumoral system to modulate immune response.^{125–128} Studies have shown that, acute and chronic opioid administration leads to inhibition of the humoral and cellular response.^{126,127,129–131} Activation of opioid receptors suppresses multiple components of the immune defense response including, phagocytosis, neutrophil complement and immunoglobulin receptor expression, natural killer cell activity, and chemokine-induced chemotaxis.^{132–135} MOR, KOR, and DOR have been found to be present in cells of the immune system. Morphine modulates immune functions such as macrophage phagocytosis and secretion of TNF- α . This effect of morphine is not observed in MOR knock-out mice, which suggests that MOR modulates the immune functions of opioids.¹³⁶

1.7.8 Obesity

Studies have shown that stimulation of MOR leads to an increase in the intake of a high fat diet. Osborne-Mendel rats which have increased levels of MOR in the hypothalamus have preference for a high fat diet and increased susceptibility to obesity.^{137,138} In a study conducted by Czyzyk et al., they found that KOR-knockout mice had 28% lower body weight and 45% lower fat mass than wild-type mice fed a high-energy diet.¹³⁹ They further observed that there was attenuation of triglyceride synthesis in KOR-knockout mice. Therefore, KOR plays an important physiological role in the control of hepatic lipid metabolism, and activation of KOR is a signal for fat storage.

1.7.9 Drug Abuse/Addiction

Using opioids continuously can lead to the development of opioid addiction, which is now considered a neurological pathology. Symptoms of opioid addiction include high probability of relapse even after prolonged drug-free periods, compulsive drug-seeking and persistent abuse of substances despite the often irreparable social consequences and deterioration of physical health.¹⁴⁰ Drug abuse and addiction treatment is the most expensive of all the neuropsychiatric disorders associated with personality disorders and a diminished quality of life.^{141,142} The rewarding, dependence-producing and analgesic effects of opioids result from activation of MORs in several brain regions.^{143–}

145

Opioid abuse leads to the development of tolerance due to receptor desensitization and internalization.¹⁴⁶ Studies have shown that there is upregulation of cAMP/PKA and cAMP response element-binding signaling and also MAPK cascades in opioid sensitive neurons. This upregulation leads to the development of tolerance and withdrawal and

synaptic plasticity during the cycles of intoxication and withdrawal.¹⁴⁷ Messengers such as G proteins, cyclic AMP, MAP kinases, and some transcription factors involved in the transmission of signals upon receptor activation have been found to be involved in the development of opioid tolerance and dependence. The involvement of transcription factors can lead to the modification of the expression of target genes which leads to long-lasting neural plasticity induced by opioids.^{147,148} In β arrestin-3 knockout mice, it was observed that the acute antinociceptive response to morphine or heroin was enhanced while both acute and chronic tolerance to the antinociceptive effects of morphine was significantly attenuated.^{149–151} Studies have shown that deletion of the genes for DOR inhibits the development of morphine tolerance in antinociceptive tests without affecting the developmental adaptations observed during morphine withdrawal.^{152–154} Activation of KOR has been found to mediate the aversive effects of stress and reinstate drug seeking behavior.¹⁵⁵ Opioids can directly or indirectly affect various neurotransmitter systems, especially glutamatergic and dopaminergic systems.^{156,157} Positive reinforcement produced by opioids has been linked to the activation of dopaminergic neurons resulting in an increase in dopamine in the mesolimbic area of the brain. In summary, drug abuse induces adaptive changes in opioid receptors that occur following chronic (e.g., desensitization and/or internalization) and chronic (e.g., adaptive tolerance and down-regulation) opioid use.^{158–160}

1.7.10 Other functions of opioid receptors

The opioid system has been found to play a role in epileptogenesis and epileptic seizure. It is been proposed that opioid receptors have both anticonvulsant and proconvulsant effects.^{161–167} Also, opioid agonists and antagonists have corresponding

stimulatory and inhibitory effects on feeding, thereby playing a role in the regulation of feeding.^{168,169} Opioids also play a role in the regulation of other systems such as the respiratory and cardiovascular system. Activation of opioids leads to respiratory depression due to the direct action of opioids MOR in the brain.^{170,171} Both DOR and KOR have been shown to mediate cardioprotection by preconditioning with myocardial ischemia and metabolic inhibition.¹⁷²⁻¹⁸⁰ Finally, opioids have been found to play a role in neurodegenerative diseases. Several lines of evidence show that opioid antagonists inhibit the onset and progression of multiple sclerosis and that DOR agonists have a therapeutic effect on Parkinson's disease.¹⁸¹⁻¹⁸³

1.8 Current treatment of opioid addiction

Breaking free of opioid addiction takes much more than willpower; medication and counseling is required for addicts to overcome their addiction. The drugs that are currently approved by the Food and Drug Administration (FDA) to treat opioid addiction include methadone (an opioid agonist) and buprenorphine (a partial opioid agonist).¹⁸⁴ Both methadone (Dolophine) and buprenorphine (Subutex) are used during both the detoxification and maintenance stages of opioid addiction treatment. Methadone and buprenorphine are used in agonist replacement therapy and hence suppress withdrawal and reduce drug cravings.¹⁸⁵ However, 40-60 % of patients after cessation of methadone and buprenorphine relapse. Interestingly, opioid receptor antagonists such as naltrexone and naloxone have also been shown to block relapse and curb drug craving in abstinent addicts.¹⁸⁶⁻¹⁸⁸ As a result, a combination of naloxone with buprenorphine (Bunavail, Suboxone and Zubsolv) has been added as a detoxification

and maintenance treatment for opioid addiction. Also, naltrexone has been added to the current treatment regimen for opioid addiction to prevent relapse (**Figure 2**).

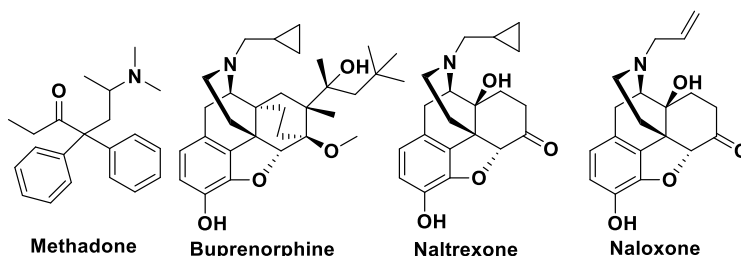


Figure 2. Compounds used in the treatment of opioid addiction

Opioid addicts must be completely detoxified from opioids before taking naltrexone as the interaction will cause immediate opioid withdrawal.¹⁸⁵ However, some severe side effects have been reported on the use of naltrexone and naloxone as a long-term treatment for opioid addiction. For example, patients receiving naltrexone for opioid dependence reported depression and dysphoria and showed high rates of overdose and suicide.^{189,190} Naloxone has also been found to cause pulmonary edema and cardiac arrhythmias.¹⁹¹ Studies have shown that the severe side effects observed are due to the lack of selectivity for MOR over other opioid receptors. For instance, DOR activation has antidepressant and anxiolytic effects and also plays an important role in neuroprotection and cell proliferation.^{73,104,123} Also, naltrexone's side effects could be due to its partial agonist effects at KOR due to the fact that KOR agonists and partial agonists produce psychotomimetic and dysphoric effects.^{192,193} Moreover, studies using MOR knock-out mice have shown that the addiction/abuse liability, respiratory depression, and constipation associated with opioids are abolished; this indicates that the addiction and abuse liability of opioids are mainly mediated through MOR.^{117,194,195}

Therefore, an ideal agent to treat opioid addiction without the severe side effects of naltrexone and naloxone would be a highly selective MOR antagonist.

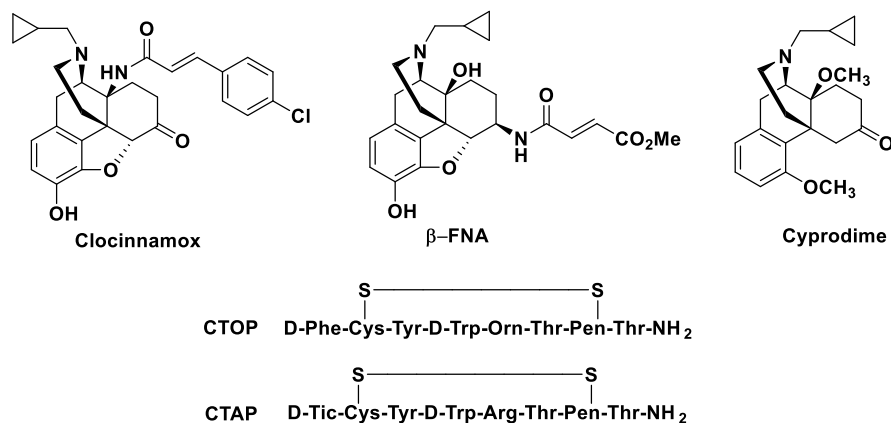


Figure 3. MOR selective compounds

Some selective MOR antagonist such as β -FNA and clocinnamox have been developed, but these agents bind irreversibly to MOR via a Michael addition reaction (**Figure 3**).^{196,197} Compounds that bind irreversibly to receptors form covalent interactions with the receptor, which limits their use as drugs. Usually, reversible antagonists are preferred since their effects can be reversed by other drugs that bind to the same receptor competitively. Cyprodime is a reversible MOR antagonist that has been intensively studied. However, it has a lower affinity for MOR than naltrexone and naloxone and it has only moderate selectivity for MOR (KOR/MOR \approx 10, DOR/MOR \approx 39).^{198,199} The highly selective MOR antagonists that have been identified are conformationally constrained peptides such as D-Phe-Cys-Tyr-D-Trp-Orn-Thr-Pen-Thr-NH₂ (CTOP) and D-Phe-Cys-Tyr-D-Trp-Arg-Thr-Pen-Thr-NH₂ (CTAP). CTOP and CTAP have limited bioavailability and have poor blood-brain barrier penetration capacity. This makes them unsuitable as drug development candidates.^{200,201} Therefore, the

development of a nonpeptide, potent, selective, and reversible antagonist for MOR remains highly desirable.

1.9 Goal

The goal of this project is to design and synthesize small molecule reversible MOR selective antagonists as potential treatments for opioid addiction.

1.10 Specific aims

1.10.1 Aim 1: Design, synthesize, and pharmacologically characterize indole derivatives of $6\alpha/\beta$ -naltrexamine.

1.10.2 Aim 2: Synthesize at large scale NAQ, a MOR selective ligand identified in our laboratory, for studies in rhesus monkeys. Design and synthesize third generation NAQ analogs.

1.10.3 Aim 3: Develop a quantitative structure pharmacokinetic relationship (QSPKR) model for opioids that can be used to predict the pharmacokinetic properties of newly designed opioids.

CHAPTER 2

2.0 DESIGN, SYNTHESIS, AND PHARMACOLOGICAL CHARACTERIZATION OF INDOLE ANALOGS OF 6 α / β -NALTREXAMINE

2.1 Molecular design

Norbinaltorphimine (norBNI) and naltrindole (NTI) are selective for KOR and DOR, respectively (**Figure 4**). The selectivity of these compounds has been rationalized in terms of the “message address concept”. The “message” moiety binds to the same binding site in all three receptors and is responsible for the pharmacologic activity of the compound while the “address” moiety is responsible for the selectivity of these compounds.

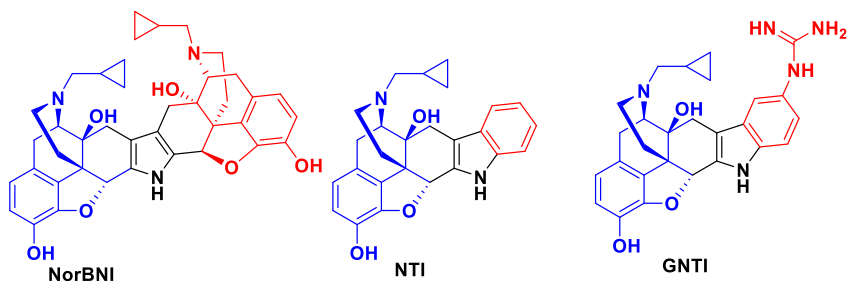


Figure 4. Compounds designed using the “message address” concept. Message part of the compound is in blue whilst address is in red

The address domain aids in selectivity by either increasing the affinity for a particular type of receptor or by decreasing the affinity at other types of receptors.^{199,202,203}

The “message address concept” has been utilized to design and synthesize 5'-Guanidinonaltrindole (GNTI), an opioid antagonist that is 5x more potent and 500 times more selective than norBNI (Figure 3).²⁰⁴ These compounds are widely used as selective ligands in pharmacological studies. Utilizing the “message-address concept”, the Yan Zhang laboratory group reported novel, non-peptide, reversible ligands 17-cyclopropylmethyl-3,14 β -dihydroxy-4,5 α -epoxy-6 α (isoquinoline-3-carboxamido)morphinan (NAQ) and 17-Cyclopropylmethyl-3,14 β -dihydroxy-4,5 α -epoxy-6 β -(4'-pyridylcarboxamido)morphinan (NAP) that were experimentally characterized through in vitro and in vivo studies as MOR selective antagonists (Figure 5).^{205–207} Further pharmacokinetic and functional characterization revealed that NAP is a P-glycoprotein substrate and therefore acts mainly peripherally whilst NAQ can also act in the central nervous system.^{208,209}

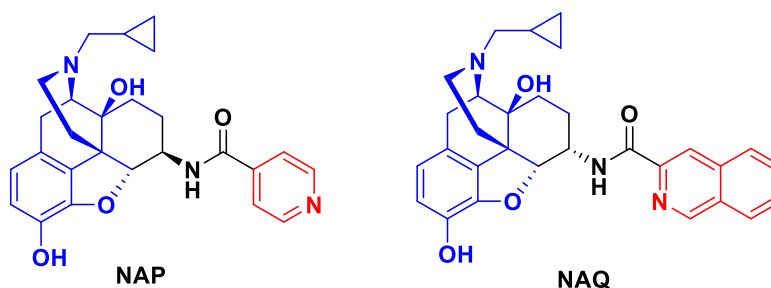


Figure 5. MOR selective ligands designed and synthesized in our laboratory. Message part of the compound is in blue whilst address is in red

Thus, NAQ holds tremendous promise as a candidate or lead compound to treat opioid addiction. NAQ has an affinity of 0.55 nM to MOR with over 100-fold selectivity for MOR over the DOR and 10-fold selectivity over KOR. NAQ acted as a low-efficacy MOR partial agonist in the [³⁵S]GTPγS binding assay, but antagonized the effects of DAMGO (an MOR full agonist) and morphine in the [³⁵S]GTPγS binding assay and warm-water tail immersion assay, respectively.

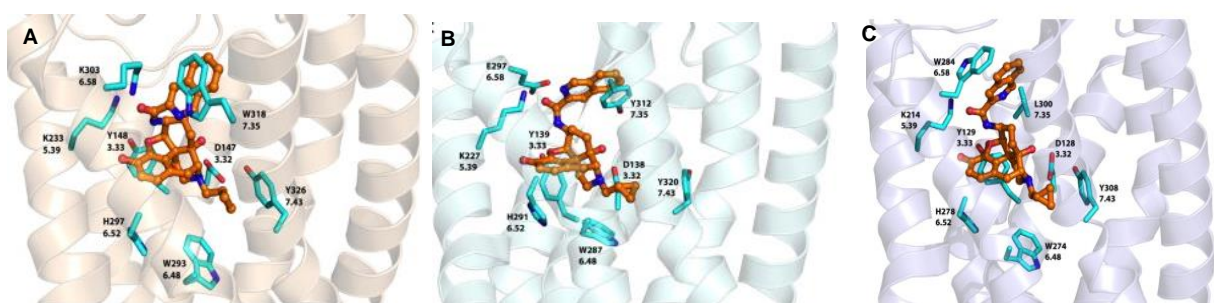


Figure 6. Docked poses of NAQ in (A) MOR, (B) KOR, and (C) DOR. NAQ atoms: carbon (orange); amino acid residue atoms carbon: (cyan), oxygen (red), nitrogen (blue), sulfur (yellow).

Further pharmacological characterization showed that NAQ acts in the CNS and significantly reversed morphine withdrawal-associated depression of intracranial self-stimulation (ICSS) in rats. The ICSS results thus agreed with the in vitro characterization data of NAQ and indicate that NAQ may serve as a relatively safe option for treatment of opioid withdrawal or dependence.^{209,210} However, NAQ's selectivity for MOR over DOR (146 fold) is lower than that of naltrexone (435 fold).²¹¹ Even though NAQ has low efficacy at KOR, it has high efficacy and moderate potency at DOR. Studies have demonstrated that DOR activation is involved in the development of morphine dependence and also, deletion of the genes for DOR inhibits the development of morphine tolerance.^{153,154,212} Thus, new compounds having less efficacy

at DOR in addition to retaining NAQ's low efficacy at KOR with high selectivity for MOR might have more therapeutic value in treating opioid addiction.

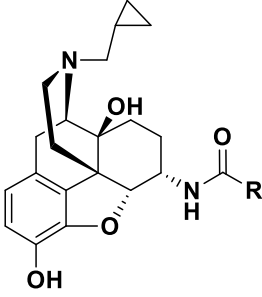
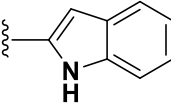
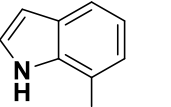
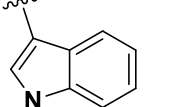
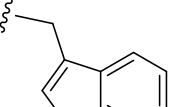
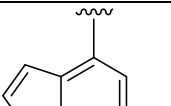
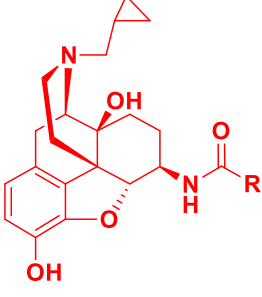
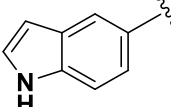
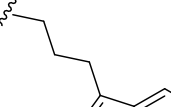
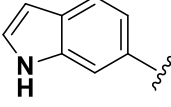
Table 1. Site-directed mutagenesis study in MOR²¹³

Compd	Wild type MOR (nM) ± SEM		Y210A MOR (nM) ± SEM		W318A MOR (nM) ± SEM	
	IC50	Ki	IC50	Ki	IC50	Ki
NTX	3.90 ± 2.96	1.85 ± 1.41	0.95 ± 0.49	0.45 ± 0.23	10.35 ± 1.64	4.91 ± 0.78
NAP	2.29 ± 0.15	1.09 ± 0.07	1.61 ± 0.17	0.77 ± 0.08	>1000	NDa
NAQ	5.42 ± 0.70	2.57 ± 0.33	3.31 ± 1.71	1.57 ± 0.81	>1000	NDa

Through molecular modeling and mutagenesis studies, it was demonstrated that the selectivity of NAQ for MOR is likely to be due to its π - π stacking with W318 (**Table 1**) (**Figure 6**).²¹³ To explore whether other heterocyclic ring systems that might form π - π interactions with W318, new compounds were designed in which the isoquinoline ring of NAQ was replaced with an indole ring. Introducing other heterocyclic ring systems will increase the diversity of compounds that bind to MOR and also obtain other “address” moieties that can help explain opioid receptor selectivity using the “message address concept”. Again, exploring other heterocyclic ring systems might yield compounds with improved pharmacologic (increased selectivity and reduced partial agonist effect) and drug-like properties (improved absorption, distribution, metabolism, and excretion properties), which might lead to the identification of new lead compounds. Furthermore, compounds with different alkyl chain lengths between the indole ring and naltrexamine were designed to determine if the distance between the indole ring and naltrexamine

influences binding, selectivity, and activity. The newly designed compounds were indole analogs of 6 α / β -naltrexamine (**Table 2**).

Table 2. Designed indole derivatives of 6 α / β -naltrexamine

	Compound	R	Compound	R
 6 α -naltrexamine analogs	1 10		6 15	
	2 11		7 16	
	3 12		8 17	
 6 β -naltrexamine analogs	4 13		9 18	
	5 14			

9 indole carboxylic acids were coupled to both 6 α -naltrexamine HCl and 6 β -naltrexamine HCl. A total of 18 compounds were synthesized. The compound IDs for the 6 α -naltrexamine derivatives are in black while the compound IDs for the 6 β -naltrexamine derivatives are in red.

2.2 Specific Aims

2.2.1 Aim 1: Synthesis of compounds

The first aim of this project was to synthesize indole analogs of naltrexamine. High yield, cost-effective synthetic schemes were used to achieve this aim.

2.2.2 Aim 2: In vitro and in vivo screening of compounds obtained from Aim 1

Radioligand binding assays were used to assess the affinity and selectivity of the compounds obtained under aim 1 for MOR over DOR and KOR. The [³⁵S]GTPγS binding assay, an in vitro functional assay, was used to determine the relative efficacy of the compounds synthesized at MOR. The warm-water tail immersion assay was used to assess whether the compounds synthesized had antinociceptive effect and/or blocked morphine's antinociceptive effects. The opioid withdrawal assay using morphine pelleted mice was used to determine whether the compounds precipitated morphine withdrawal in opioid dependent mice.

2.2.3 Aim 3: Molecular modeling studies of compounds identified after biological screening

Molecular modeling studies were conducted with compound **6** (this compound blocked morphine's antinociceptive effect) to understand its molecular interactions with MOR.

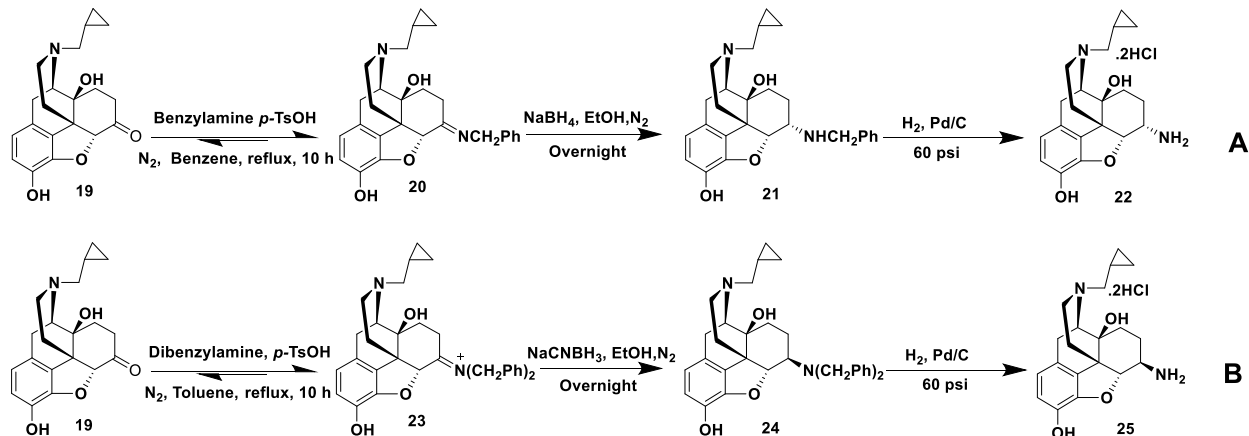
2.3 Results and Discussion

2.3.1 Synthesis (Chemistry)

2.3.1.1 Synthesis of 6α/β naltrexamine

Naltrexone was used as the starting material in the synthesis of both 6α-naltrexamine (**22**) and 6β-naltrexamine (**25**). In the synthesis of 6α-naltrexamine HCl (**Scheme 1, route A**), a reductive amination was conducted between naltrexone and benzyl amine. The Schiff base formed (**22**) was reduced and the benzyl group cleaved off using hydrogenation. However, dibenzyl amine was refluxed with naltrexone to synthesize 6β-

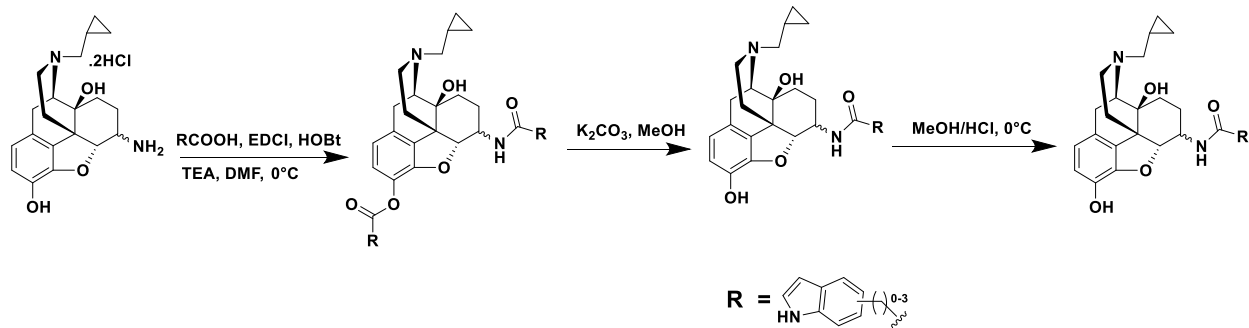
naltrexamine HCl.²¹⁴ The reduction of Schiff base of benzyl naltrexamine yielded the 6 α -



Scheme 1. Synthesis of 6 α / β naltrexamine HCl

isomer because the ring adopts a chair-like conformation. Therefore, hydride transfer occurs on the β -face leading to the formation of the 6 α -isomer. On the other hand, the Schiff base of dibenzyl naltrexamine adopts a boat conformation. Therefore, hydride transfer from NaCNBH₃, occurs exclusively on the more accessible α face, thereby leading to the 6 β isomer.

2.3.1.2 Synthesis of indole analogs substituted at 6 position of naltrexamine

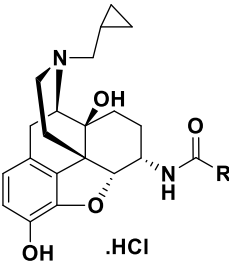
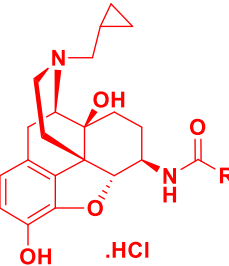
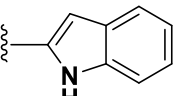
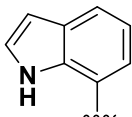
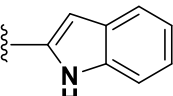
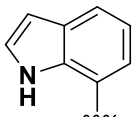
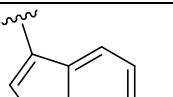
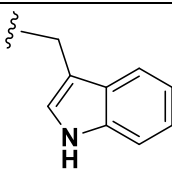
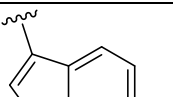
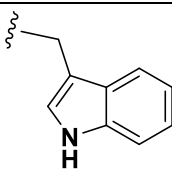
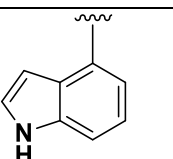
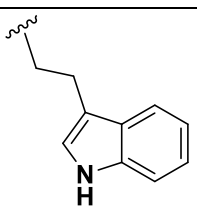
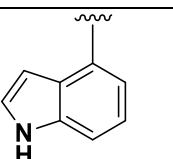
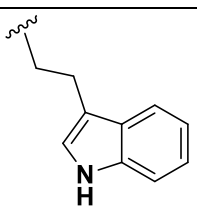
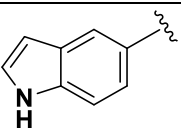
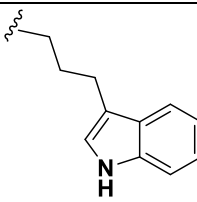
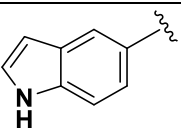
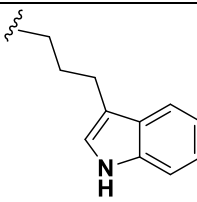
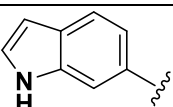
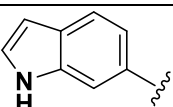


Scheme 2. Coupling of naltrexamine to indole carboxylic acids

The 6 α / β naltrexamine HCl compounds were coupled to their respective indole carboxylic acids using 1-Ethyl-3-(3-dimethylaminopropyl)carbodiimide (EDCI) coupling

(Scheme 2). This coupling reaction also results in the formation of an ester at position 3. The ester group was then hydrolyzed since esters are more susceptible to hydrolysis

Table 3. Percentage yield obtained for indole analogs of 6 α / β -naltrexamine HCl

	Compd.	R	Yield	Compd.	R	Yield
		1		81%	6	
10			32%	15		56%
2			29%	7		80%
11			23%	16		49%
3			80%	8		55%
12			31%	17		51%
4			50%	9		34%
13			61%	18		39%
5			75%			
14		29%				

9 indole carboxylic acids were coupled to both 6 α -naltrexamine HCl and 6 β -naltrexamine HCl. A total of 18 compounds were synthesized. The compound IDs and the respective % yields for the 6 α -naltrexamine derivatives are in black while the compound IDs and the %yields for the 6 β -naltrexamine derivatives are in red.

than amides. The final compounds synthesized were converted to the HCl salts and the percentage yield obtained for each compound is shown in **Table 3**. The percentage

yield obtained for the 6 α -naltrexamine derivatives ranged from 22-81% while that for the 6 β -naltrexamine derivatives ranged from 23-61%.

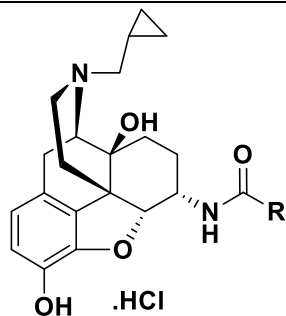
The final compounds were characterized by ¹HNMR, ¹³CNMR, HRMS and IR and the purity determined by HPLC.

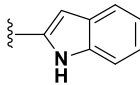
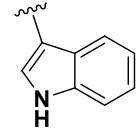
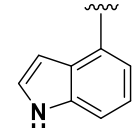
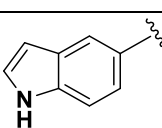
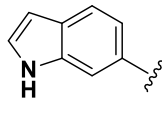
2.3.2 Pharmacological characterization of the indole analogs of 6 α -naltrexamine

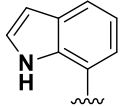
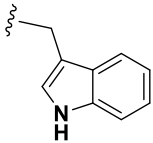
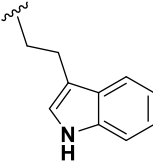
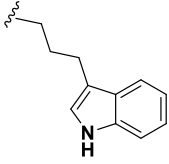
2.3.2.1 Radioligand binding assay

The radioligand binding assays were performed to study the selectivity and affinity of the newly synthesized ligands using mono-cloned opioid receptors expressed in CHO cells. [³H] naloxone was used to label MOR whilst [³H] diprenorphine was used to label both DOR and KOR. The radioligands employed for the biological assays are highly selective for their corresponding receptors. The K_d values for the tritirated compounds and the B_{max} value for the CHO cell lines expressing the different opioid receptors have been previously determined in the laboratory. In this assay, varying concentrations of the naltrexamine derivatives compete with a constant concentration of the radioligand, usually set between 1 to 2 times their K_d values. Non-specific binding was determined at MOR, KOR and DOR using 5 μ M of cold naltrexone, U50,488 and SNC 80 respectively. The potency of the new compounds in displacing the specific binding of the radioligand was determined using linear regression analysis of Hill plots. The IC₅₀ values are then calculated and corrected to K_i values using the Cheng-Prusoff equation, $K_i = IC_{50}/(1+[L]/K_d)$.²¹⁵ The K_i values obtained for the indole analogs of 6 α -naltrexamine at MOR, KOR and DOR and the selectivities for MOR over KOR and DOR are shown in **Table 4** whilst those for the indole analogs of 6 β -naltrexamine are shown in **Table 5**.

Table 4. Binding affinity and selectivity of indole derivatives of 6 α -naltrexamine



Compd	R	K _i (nM) ± SEM			Selectivity Ratio	
		μ	κ	δ	κ/μ	δ/μ
NTX^a		0.33 ± 0.02	1.44 ± 0.11	144 ± 14	4.4	435
NAQ^b		1.11 ± 0.07	13.3 ± 1.1	162 ± 15	12	146
1		0.36 ± 0.03	0.93 ± 0.13	14.2 ± 2.8	2.6	39.2
2		0.29 ± 0.04	0.98 ± 0.13	10.5 ± 29	3.4	37.0
3		0.26 ± 0.04	1.49 ± 0.35	9.3 ± 2.8	5.6	35.1
4		0.76 ± 0.11	3.45 ± 0.99	26.7 ± 7.7	4.5	35.0
5		0.43 ± 0.05	1.63 ± 0.28	12.8 ± 3.4	3.8	29.4

6		0.23 ± 0.02	1.69 ± 0.35	10.9 ± 2.9	7.4	47.7
7		0.84 ± 0.12	3.14 ± 0.45	9.2 ± 2.7	3.7	11.0
8		0.44 ± 0.04	1.36 ± 0.18	31.2 ± 8.1	3.1	71.5
9		0.29 ± 0.04	0.15 ± 0.03	6.73 ± 0.40	0.5	23.0

^a The K_i values of NTX and ^b NAQ were obtained from experiments previously conducted in Dr. Selley's laboratory.²¹¹

2.3.2.1.1 MOR binding

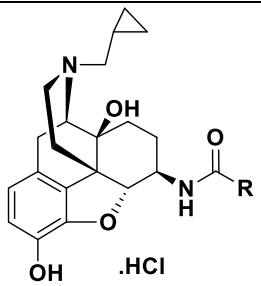
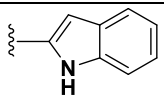
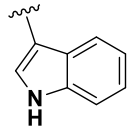
2.3.2.1.1.1 MOR binding for indole analogs of 6 α -naltrexamine

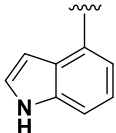
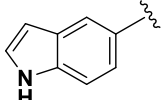
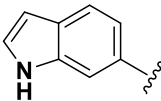
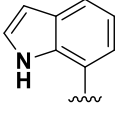
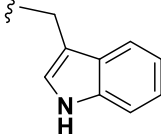
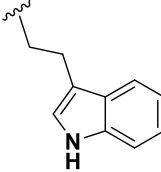
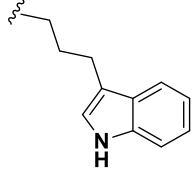
From the results obtained, it was observed that the position of the substitution on the indole ring did not affect the binding affinities significantly. Among the indole analogs of 6 α -naltrexamine, compound **4** had the least binding affinity, which was 3.3 fold worse than compound **6**, which had the best binding affinity at MOR. Also, increasing alkyl chain length at position 3 did cause a significant change in binding affinity at MOR. Compound **7** with the one carbon linker had the least binding affinity, which was approximately 3 fold worse than compound **3** that has its carbonyl group directly attached to position 3 and compound **9** with the three carbon linker. The binding affinities of the compounds at MOR were similar to the binding affinities of NTX at MOR.

2.3.2.1.1.2 MOR binding for indole analogs of 6β-naltrexamine

The binding affinities at MOR for the indole analogs of 6β-naltrexamine were higher than their respective 6α-naltrexamine analogs. The K_i of all the indole analogs of 6β-naltrexamine at MOR was approximately 0.2 nM. Thus, neither the substitution position nor the length of the alkyl group at position 3 produced a significant change in binding affinity at MOR.

Table 5. Binding affinity and selectivity of indole derivatives of 6β-naltrexamine

						
Compd	R	K_i (nM) \pm SEM			Selectivity Ratio	
		μ	κ	δ	κ/μ	δ/μ
NTX^a		0.33 \pm 0.02	1.44 \pm 0.11	144 \pm 14	4.4	435
NAQ^b		1.11 \pm 0.07	13.3 \pm 1.1	162 \pm 15	12	146
10		0.29 \pm 0.04	0.18 \pm 0.002	1.54 \pm 0.47	0.6	5.4
11		0.19 \pm 0.02	0.16 \pm 0.01	7.17 \pm 1.2	0.83	37.3

12		0.24 ± 0.03	1.94 ± 0.30	45.9 ± 16.3	8.2	195.2
13		0.26 ± 0.04	0.51 ± 0.04	17.7 ± 4.8	2.0	68.2
14		0.25 ± 0.04	0.17 ± 0.01	6.2 ± 0.8	0.7	25
15		0.19 ± 0.01	0.52 ± 0.09	30.4 ± 9.5	2.8	162
16		0.24 ± 0.03	0.95 ± 0.11	37.0 ± 1.2	3.9	153.6
17		0.17 ± 0.01	0.39 ± 0.05	49.0 ± 4.7	2.3	293.5
18		0.20 ± 0.03	0.18 ± 0.04	25.3 ± 4.3	0.86	124.6

^a The K_i values of NTX and ^b NAQ were obtained from experiments previously conducted in Dr. Selleys laboratory.²¹¹

2.3.2.1.2 KOR binding

2.3.2.1.2.1 KOR binding for indole analogs of 6 α -naltrexamine

The binding affinities for the indole analogs of 6 α -naltrexamine was lower at KOR compared to MOR. Compound 4 with a substitution at position 5 had the least binding to

KOR. The binding affinities at KOR for the indole analogs of 6 α -naltrexamine were similar to that of naltrexone at KOR. The position of substitution on the indole ring did not have a significant effect on the binding of the compounds at KOR. Also, increasing the alkyl chain length at position 3 on the indole ring did not have any significant effect on KOR binding; however, compound **9** which had a three carbon linker had a greater binding affinity at KOR than MOR. Compound **9** was the only indole derivatives of 6 α -naltrexamine that had a greater affinity at KOR than MOR.

2.3.2.1.2.1 KOR binding for indole analogs of 6 β -naltrexamine

Again, the binding affinities at KOR for the indole analogs of 6 β -naltrexamine were higher than their respective 6 α -naltrexamine analogs. Among the indole analogs of 6 β -naltrexamine, compound **12** (with substitution at position 4) had the least affinity for KOR. Also, increasing the alkyl chain at position 3 did not significantly alter the binding affinity. Most of the indole analogs of 6 β -naltrexamine might either be dual MOR and KOR agonist or antagonists.

2.3.2.1.3 DOR binding

2.3.2.1.3.1 DOR binding for indole analogs of 6 α -naltrexamine

The indole analogs of 6 α -naltrexamine had the least binding affinities at DOR compared to MOR and KOR. Compound **8** with substitution at position 3 and a two carbon linker had the least binding to DOR. The position of substitution on the indole ring did not have a significant effect on the binding of the compounds at DOR. However, it was observed the analog that was substituted at position 4 (had best binding affinity when substitution was moved around indole ring) had a binding affinity that was 3 fold better than substitution at position 5 (had worst binding affinity when substitution was moved

around indole ring). Interestingly, it was observed that when the alkyl chain at position 3 was increased to 1 carbon chain, there was little change in the binding affinity.

However, upon increasing the chain length to 2 carbon atoms, the binding affinity decreased by three fold. On the other hand, when the chain length was increased to 3 carbon atoms the binding affinity improved.

2.3.2.1.3.2 DOR binding for indole analogs of 6 β -naltrexamine

Among the indole analogs of 6 β -naltrexamine, compound **10** (with substitution at position 1) had the best binding affinity for DOR whilst compound **17** (with 2 carbon chain linker substituted at position 3) had the least binding affinity for DOR. It was also observed that, increasing the alkyl chain length at position 3 resulted in a reduction in DOR binding.

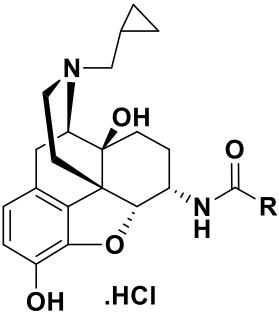
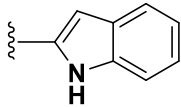
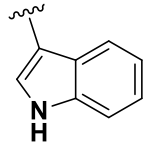
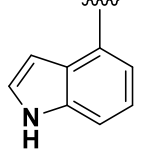
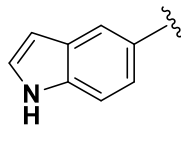
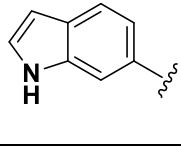
2.3.2.1.4 Selectivity for MOR over KOR and DOR of synthesized compounds

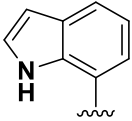
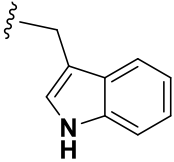
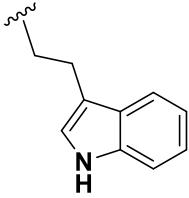
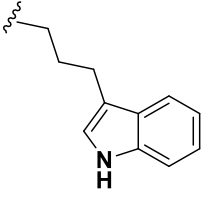
Compound **6** and compound **12** had the best selectivity for MOR over KOR whilst compound **17** had the greatest selectivity for MOR over DOR. However, it is worth noting that among the 6 α -naltrexamine analogs, compound **6** and compound **8** had good selectivity for MOR over DOR. Thus, compound **6** and **12** had good selectivities when considering selectivity for MOR over both KOR and DOR.

2.3.2.2 MOR [³⁵S]GTP γ S functional assay

The [³⁵S]GTP γ S functional assay was conducted to determine the efficacy of the compounds at MOR. In this assay, 10 μ g of MOR-CHO membrane protein was incubated with 10 μ M GDP, 0.1 nM [³⁵S]GTP γ S and varying concentrations of the compounds under investigation for 90 minutes in a 30°C water bath. GTP γ S was used

Table 6. MOR [³⁵S]GTP_γS binding functional assay results of indole derivatives of 6α-naltrexamine

			
Compound	R	EC ₅₀ (nM) ± SEM	E _{max} (% DAMGO) ± SEM
NTX^a		0.16 ± 0.04	5.4 ± 0.8
NAQ^a		3.3 ± 0.4	20.8 ± 1.2
1		3.3 ± 1.3	52.0 ± 13.5
2		1.1 ± 0.1	35.4 ± 4.8
3		5.0 ± 2.2	28.9 ± 1.0
4		1.6 ± 0.1	32.2 ± 1.3
5		5.4 ± 1.5	27.0 ± 0.3

6		1.0 ± 0.1	21.0 ± 4.4
7		4.9 ± 0.4	33.9 ± 1.4
8		1.9 ± 0.4	41.1 ± 6.5
9		0.6 ± 0.1	48.4 ± 5.2

^a The EC_{50} and E_{max} (%DAMGO) values of NTX and ^b NAQ were obtained from experiments previously conducted in Dr. Selley's laboratory.²¹¹

instead of GTP because $GTP\gamma S$ cannot be hydrolyzed by GTPase. Therefore, when $GTP\gamma S$ binds to the $G\alpha$ subunit it remains bound and the $G\alpha$ subunit remains in the active form. Since $GTP\gamma S$ is radiolabeled, the amount of $GTP\gamma S$ that is bound to the $G\alpha$ subunit can be quantified to determine the relative efficacy of the compounds. The Bradford protein assay was utilized to determine and adjust the concentration of protein required for the assay. Non-specific binding was determined with 20 μM unlabeled $GTP\gamma S$. TME buffer (50 mM Tris-HCl, 3 mM $MgCl_2$, 0.2 mM EGTA, pH 7.4) with 100mM NaCl was used to increase agonist stimulated binding and the final volume in each assay tube was 500 μl . Furthermore, 3 μM of DAMGO was included in the assay as

maximally effective concentration of a full agonist for MOR. The net stimulation produced by each compound was normalized to the stimulation produced by 3 μM of DAMGO, which was considered to be 100%. After the incubation, the bound radioactive ligand was separated from the free radioligand by filtration through a GF/B glass fiber filter paper and rinsed three times with ice-cold wash buffer (50 mM Tris-HCl, pH 7.2) using the Brandel harvester. The results were determined by utilizing a scintillation counter. All assays were determined in triplicate and repeated at least three times. Percent DAMGO-stimulated [^{35}S]GTP γ S binding was defined as (net-stimulated binding by ligand/net-stimulated binding by 3 μM DAMGO) x 100%.and the results obtained are shown in **Table 6** (indole analogs of 6 α -naltrexamine) and **Table 7** (indole analogs of 6 β -naltrexamine).

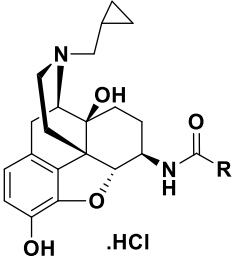
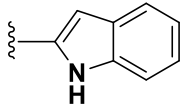
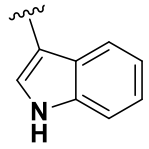
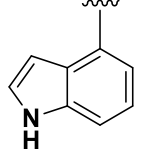
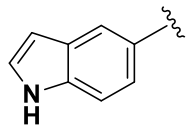
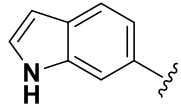
2.3.2.2.1 [^{35}S]GTP γ S functional assay for indole analogs of 6 α -naltrexamine

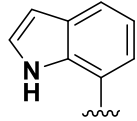
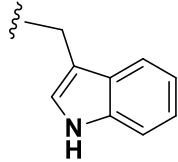
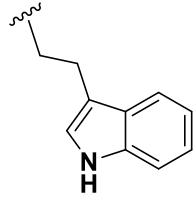
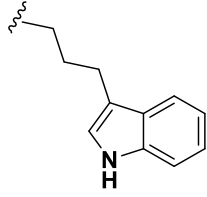
From the results obtained, it was observed that position of substitution on the indole ring did not significantly affect potency and efficacy. All the compounds had a partial agonist effect at MOR. Compound **6** (substitution at position 7) had the highest potency, but the lowest efficacy at MOR. Compound **6** was more potent than NAQ but had similar efficacy as NAQ. Compound **1** had the highest efficacy at MOR. Increasing the length of the alkyl chain at position 3 did not produce a significant change in potency and efficacy. Compound **9** with the three carbon linker was the most potent and efficacious.

2.3.2.2.2 [^{35}S]GTP γ S functional assay for indole analogs of 6 β -naltrexamine

Compound **10**, **11** and **14** were the most potent compounds and these compounds were the most efficacious having E_{max} values greater than 70%. In fact, compound **10** with

Table 7. MOR [³⁵S]GTP_γS binding functional assay results of indole derivatives of 6β-naltrexamine

			
Compound	R	EC ₅₀ (nM) ± SEM	E _{max} (% DAMGO) ± SEM
NTX^a		0.16 ± 0.04	5.4 ± 0.8
NAQ^a		3.3 ± 0.4	20.8 ± 1.2
10		0.21 ± 0.01	92.4 ± 2.8
11		0.30 ± 0.03	70.5 ± 0.9
12		1.97 ± 0.12	15.2 ± 3.13
13		2.28 ± 0.19	20.2 ± 4.4
14		0.19 ± 0.02	71.8 ± 4.4

15		0.75 ± 0.20	32.0 ± 4.6
16		0.56 ± 0.18	50.2 ± 7.8
17		0.39 ± 0.11	40.4 ± 5.3
18		1.04 ± 0.17	36.3 ± 4.1

^a The EC₅₀ and E_{max} (%DAMGO) values of NTX and ^b NAQ were obtained from experiments previously conducted in Dr. Selley's laboratory.²¹

substitution at position 2 had the greatest efficacy among both the indole analogs of 6 α and β naltrexamine, with an E_{max} value of 92%. From the results obtained, it was observed that substitution at position 2, 3 and 6 had a significant effect on potency and efficacy. Compound **12** was identified as the compound with the least efficacy at MOR. It was also observed that increasing the alkyl chain length at position 3 did not significantly affect potency. However, as the alkyl chain increased, the efficacy decreased correspondingly.

According to previous studies conducted in Dr. Selley's laboratory, it has been observed that in the [³⁵S]GTP γ S functional assay, compounds with efficacies less than 25% tend

to be opioid antagonists.²⁰⁷ Therefore, compound **6**, **12** and **13** may be MOR antagonists.

2.3.2.3 Warm-water immersion assay

The warm-water immersion assay was conducted to determine whether the compounds

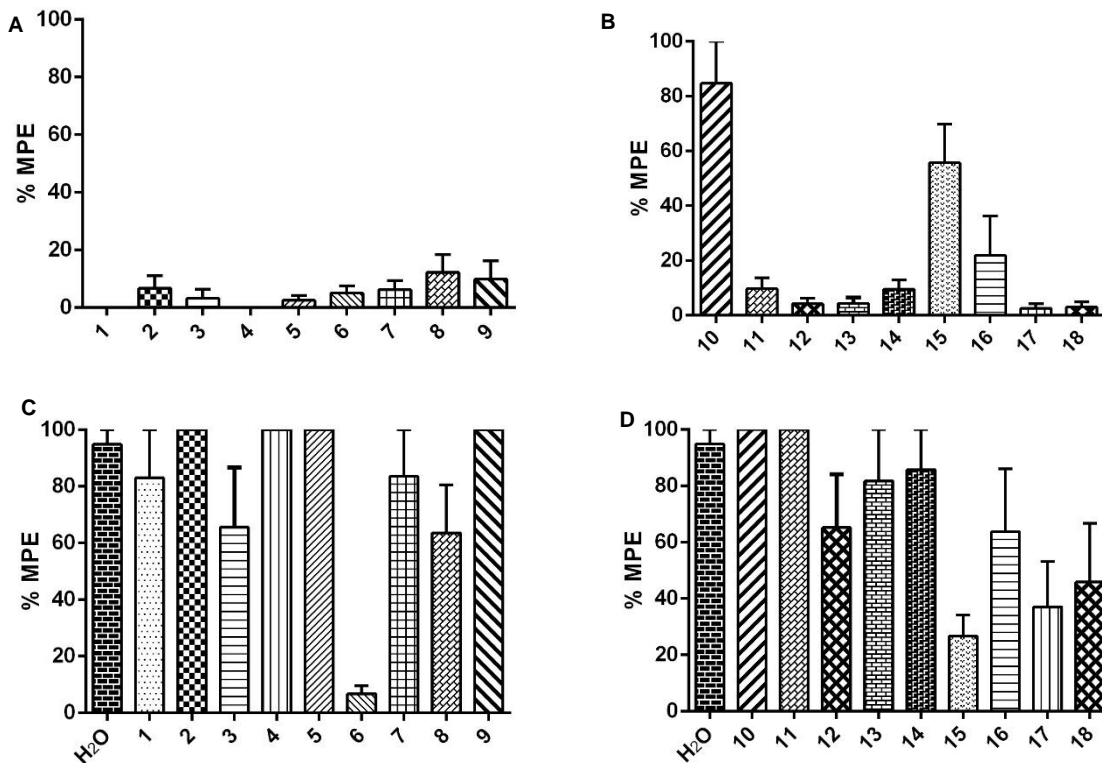


Figure 7. Warm-water tail immersion assay in mice ($n=5$) at 56 ± 0.1 °C. All tested compounds were administered subcutaneously (s.c.). Antinociceptive effects of (A) indole analogs of 6α -naltrexamine (B) indole analogs of 6β -naltrexamine. Compounds (10 mg/kg) were injected at Time 0. Twenty minutes after injection, tail flick was assessed with hot water. Blockage of the antinociceptive effect of morphine by (C) indole analogs of 6α -naltrexamine (D) indole analogs of 6β -naltrexamine. Tested compounds (10 mg/kg) were injected at Time 0. Five minutes later, morphine (10 mg/kg) was administered. Twenty minutes after morphine injection, tail flick was tested using hot water.

synthesized were opioid agonists or antagonists. Each indole analog of naltrexamine was tested for its ability to produce antinociception and/or to antagonize the antinociceptive effects of morphine in mice. The tail-flick test was conducted 20 minutes after injection of the compounds because morphine's effect starts to peak at 20 minutes

after s.c. administration. The results are interpreted as the percentage of maximum possible effect (% MPE) which is a measure of antinociception. A higher % MPE indicates a stronger antinociception effect by the ligand. **Figure 7A** shows the

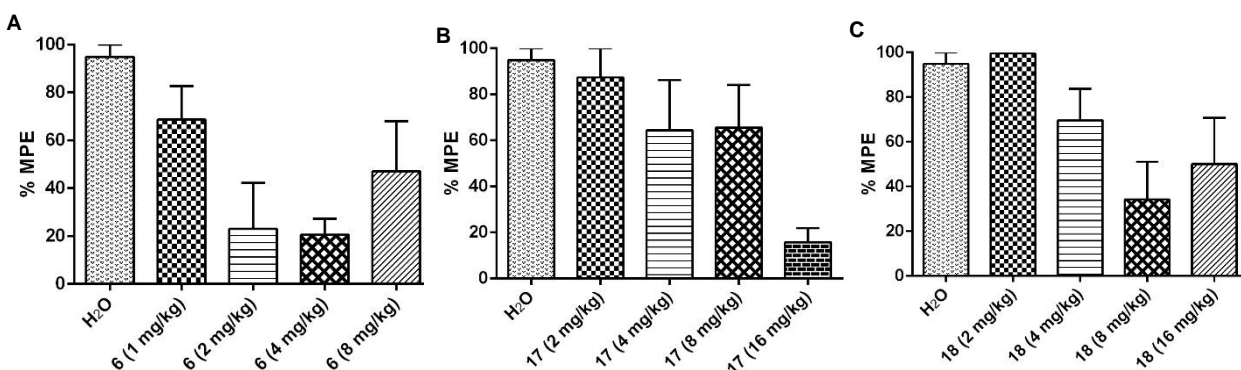


Figure 8. Dose dependent studies on compound **6** (A), **17** (B), and **18** (C) for opioid antagonist effect. Compounds **6**, **17**, and **18** had AD₅₀ values of 2.39 (0.46-12.47), 7.30 (3.38-15.74), and 9.64 (3.17-29.29) mg/kg (95% CL) respectively.

antinociceptive effects of the indole analogs of 6 α -naltrexamine, while **Figure 7B** shows the antinociceptive effects of the indole analogs of 6 β -naltrexamine. Not surprisingly, compound **10** which was identified as a potent and efficacious MOR agonists was also identified as an opioid agonist in the warm-water immersion assay. Compound **15** and **16** were identified as partial opioid agonists. Figure 7C and D shows the antinociceptive effect of morphine at 10 mg/kg in the presence of each indole analog of 6 α -naltrexamine (**Figure 7C**) and 6 β -naltrexamine (**Figure 7D**) at 10 mg/kg. Not surprisingly, compound **6** that had a high potency and a low efficacy in the [³⁵S]GTP γ S functional assay was identified as the most potent opioid antagonist in the warm-water immersion assay. However, compound compounds **12** and **13** which also had low efficacies in the [³⁵S]GTP γ S functional assay did not significantly inhibit morphine's antinociceptive effect. This could be due to the lower potencies of these compounds compared to compound **6**. Compounds **17**, and **18** also showed opioid antagonist effects. The opioid

antagonist effects of compound **6**, **17**, and **18** were dose dependent and their AD₅₀ values were 2.39 (0.46-12.47), 7.30 (3.38-15.74), and 9.64 (3.17-29.29) mg/kg (95% CL) respectively (**Figure 8**). The slight increase in the %MPE for compound **6** at 8 mg/kg in the dose response study could be due to the partial agonist effects of compound **6** or could be due to variability in the mice.

2.3.2.4 Opioid withdrawal studies

Compound **6** had the most promising pharmacological characteristics in the invitro studies conducted compared to the other compounds synthesized. Compound **6** was also identified as the most potent opioid antagonist in the warm-water immersion assay. Therefore further in vivo studies were conducted on compound **6** using morphine-

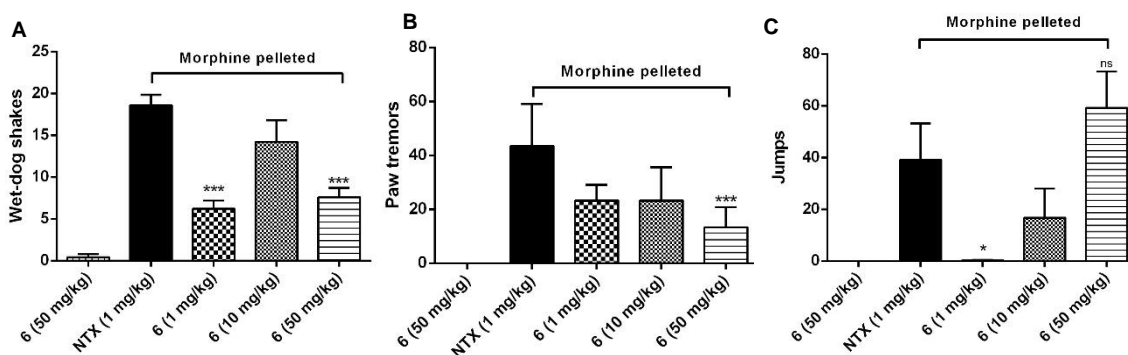


Figure 9. Compound **6** (s.c.) in opioid-withdrawal assays in chronic morphine-exposed mice (n=5): (A) Wet-dog shakes, (B) Escape jumps, and (C) Paw tremors. The first column in each figure represents placebo-pelleted mice while the second to the fourth represent morphine-pelleted mice. *** Indicates P < 0.05, compared to 1 mg/kg naltrexone (NTX, s.c.), whilst * indicates P < 0.1, compared to 1 mg/kg naltrexone (NTX, s.c.) .

pelleted mice to determine if compound **6** had opioid withdrawal effects (**Figure 9**). In this study, somatic symptoms of opioid withdrawal in mice (wet-dog shakes, paw tremors, and jumps) are observed for a period of 20 min after injecting the mice with the test compound. From the opioid withdrawal studies conducted, it was observed that compound **6** itself did not induce any significant withdrawal symptoms in placebo-

pelleted mice at 50 mg/kg (**Figure. 9A, B and C**, first columns). Again, compound **6** at 1 mg/kg produced significantly less wet-dog shakes, paw tremors and jumps than naltrexone at 1 mg/kg (**Figure. 9A, B and C**, third columns) in morphine pelleted mice. Moreover, compound **6** at 50 mg/kg produced significantly less wet-dog shakes and paw tremors than naltrexone at 1 mg/kg (**Figure. 9A and B**, fifth columns).. However, compound **6** at a dose of 50 mg/kg produced escape jumps that were not significantly different from naltrexone at 1 mg/kg(**Figure. 9C**, fifth column). Thus, compound **6** produced significantly less withdrawal symptoms than naltrexone.

2.3.3 Molecular modeling studies

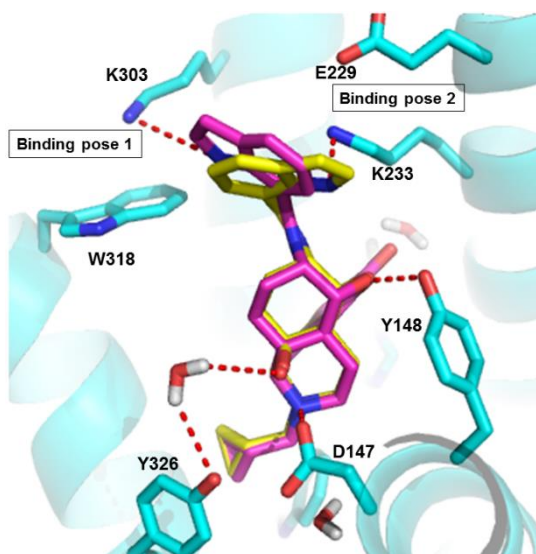


Figure 10. Docked poses of compound **6** in the mu opioid receptor in binding pose 1 and binding pose 2. Compound **6** atoms in binding site 1: carbon (magenta); Compound **6** atoms in binding site 2: carbon (yellow); amino acid residue atoms carbon: (cyan), oxygen (red), nitrogen (blue).

Molecular modeling studies were conducted to try to understand the pharmacological characteristics observed for compound **6**, which will provide guidance in the future molecular design of analogs of compound **6**.

2.3.3.1 Docking of compound **6** in MOR

Compound **6** was first sketched with sybylx2.1 and then docked into the

crystal structure of MOR (4dki). From the docking results obtained, it was observed that compound **6** clustered into two poses (**Figure 10**). The morphinan part of the compound was docked in the same position in both sites, however, the indole ring was docked

differently. The morphinan group formed ionic interactions with D148 and hydrogen bonding interactions with Y148. In binding site 1, the nitrogen of the indole ring was hydrogen bonded to K303 and the indole ring formed pi-pi interactions with W318. In binding site 2, the nitrogen of the indole ring formed hydrogen bonds with K233. The orientation of the indole ring was away from W318 and π - π stacking was not observed. The CHEM-PLP scores for the two binding sites were quite similar, however binding pose 1 had a better GOLD score than binding pose 2 (**Table 8**).

Table 8. Binding scores of compound **6** in the two poses obtained after docking

Pose	CHEM-PLP score	GOLD score
Binding pose 1	80.0451	0.7027
Binding pose 2	81.1141	-4.4924

2.3.3.2 MD simulation of compound 6 in binding pose 1 and 2

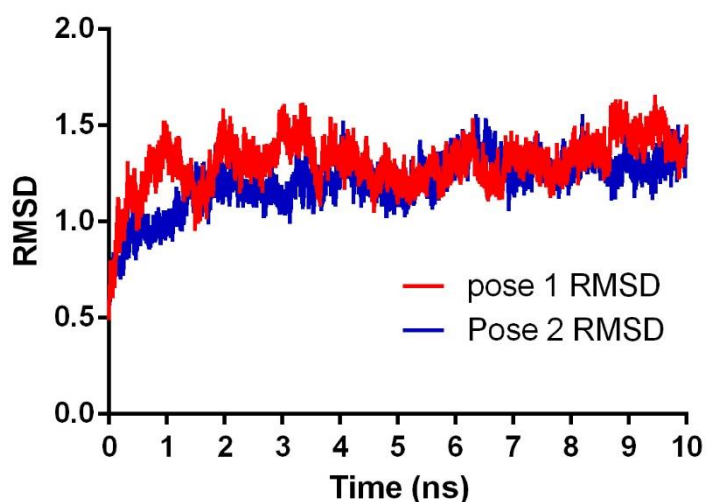


Figure 11. RMSD plot for MD simulation of compound 6 for the two binding poses observed.

Since the CHEM-PLP scores for the two solutions were very similar, an MD simulation was conducted using NAMD 2.8 on the best CHEM-PLP scored solution obtained for the two binding poses to determine the most likely interactions. The simulation

system consisted of the receptor–ligand complex embedded in a lipid (POPC) bilayer

surrounded with saline solution created in VMD 1.9.1. The temperature of the simulation was maintained at 310 K and the simulation was conducted for 10 ns. The RMSD obtained for the ligand receptor complex during the simulation revealed that the simulation was stable after 4 ns (**Figure 11**). The average distances from 4 ns to 10 ns between the residues W318, K303, K233, E229 and the indole ring of compound **6** were determined. The result for binding pose 1 after 10 ns of simulation revealed that the average distances between the indole ring of compound **6** and W318 and K303 was longer than the average distances between the indole ring of compound **6** and K233 and E229; thus, the indole ring of compound **6** moved into the binding pocket occupied by binding pose 2 (**Figure 12A and B**). In the case of binding pose 2, it was observed that the average distances between the indole ring of compound **6** and W318 and K303

Table 9. RMSD score after MD simulation

Pose	RMSD 1 ns	RMSD 10 ns
Binding pose 1	1.5038	1.4260
Binding pose 2	1.0586	1.3984

was longer than the average distances between the indole ring of compound **6** and K233 and E229; thus, there was no change in the position of the indole ring before and after 10 ns of simulation. Moreover, the RMSD for the simulation of pose 2 was slightly lower than that for pose 1 (**Table 9**). Thus, the indole ring (the address domain) of compound **6** most likely interacts with K233 and E229 (binding pose 2).

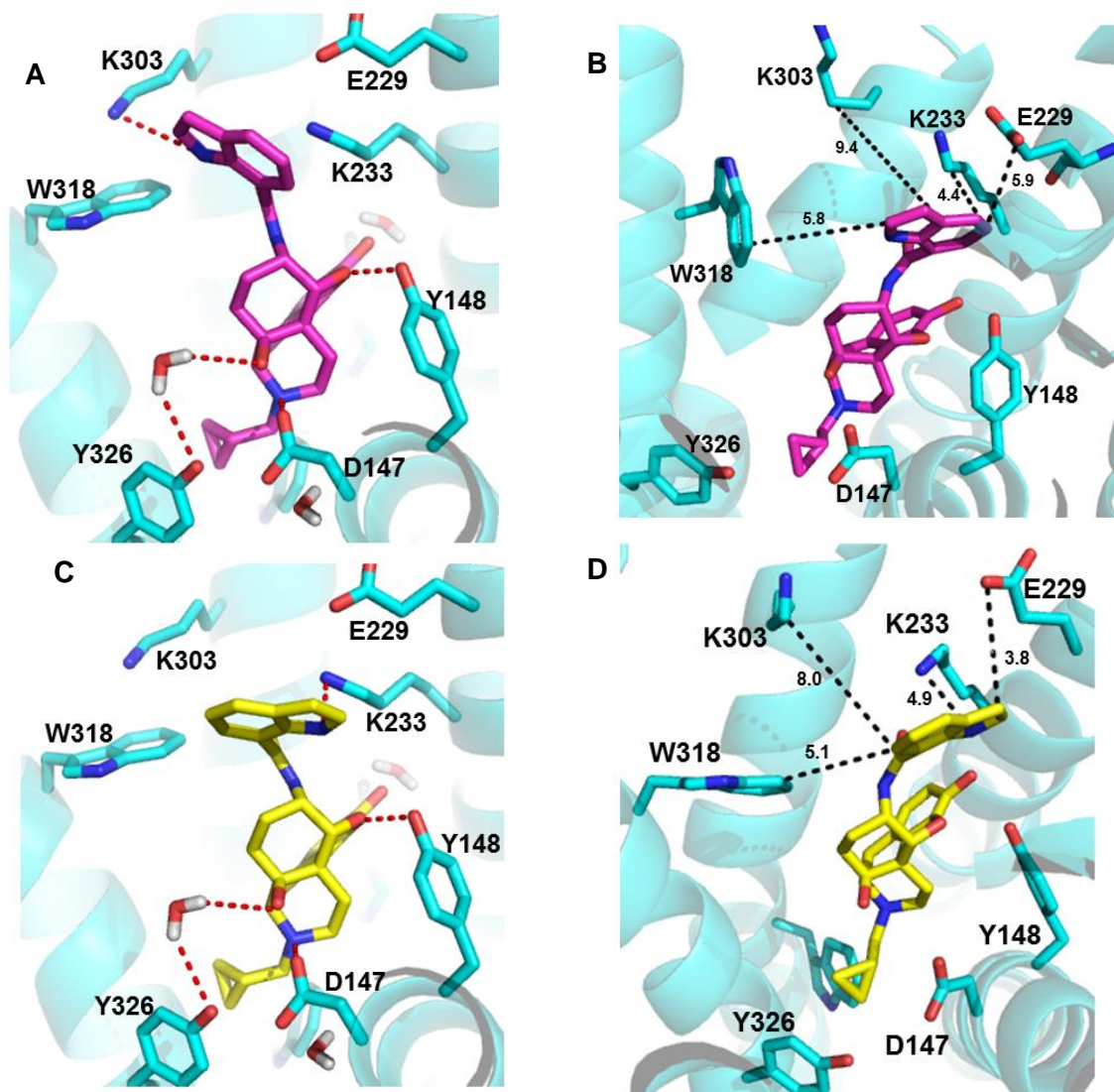


Figure 12. MD simulation results for compound **6** in the mu opioid receptor. (A) Compound **6** in MOR binding pose 1 before simulation. (B) Compound **6** in MOR binding pose 1 after 10 ns simulation. (C) Compound **6** in MOR binding pose 2 before simulation. (D) Compound **6** in MOR binding pose 2 after 10 ns simulation. Compound **6** atoms in binding site 1: carbon (magenta); Compound **6** atoms in binding site 2: carbon (yellow); amino acid residue atoms carbon: (cyan), oxygen (red), nitrogen (blue). The red dotted lines show hydrogen bond interactions between compound **6** and MOR while the black dotted lines show average distances between compound **6** and residues

CHAPTER 3

3.0 SYNTHESIS OF NAQ FOR STUDIES IN MONKEYS AND DESIGN AND SYNTHESIS OF THIRD GENERATION NAQ ANALOGS

NAQ is a non-peptide selective MOR ligand that has been previously designed and synthesized in Dr. Yan Zhang's laboratory.²⁰⁷ To further study the pharmacological effects of NAQ in primates, a project was proposed to study the effects of NAQ in Rhesus monkeys. Therefore, large scale synthesis of NAQ was conducted. Again, to further obtain compounds with improved pharmacological profile, design and synthesis of the third generation NAQ analogs was conducted.

3.1 Specific Aim

The aim was to conduct large scale synthesis of NAQ for studies in Rhesus monkeys.

3.2 Design of the third generation NAQ analogs

NAQ showed relatively high efficacy and moderate potency in the DOR [³⁵S]GTPγS binding assay.²⁰⁵ It has been proposed that DOR activation is also involved in the development of morphine dependence.²¹² Again, NAQ has KOR partial agonists effects.

Evidence has shown that activation of KOR produces psychotomimetic and dysphoric effects. Therefore the second generation NAQ analogs were designed.²¹¹

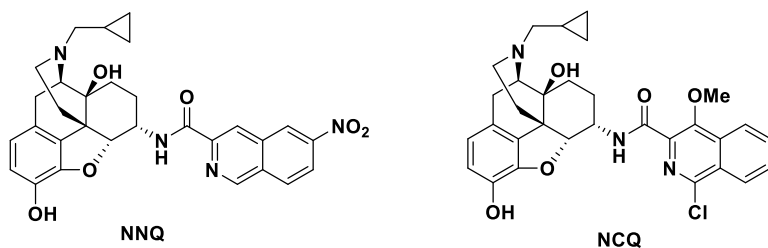
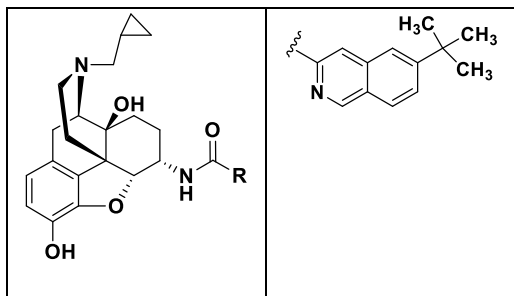


Figure 13. Second generation NAQ analogs

Two second generation analogs of NAQ, 17-Cyclopropylmethyl-3,14 β -dihydroxy-4,5 α -epoxy-6 α -(1-chloro-4-methoxyisoquinoline-3-carboxamido)morphinan (NCQ) and 17-Cyclopropylmethyl-3,14 β -dihydroxy-4,5 α -epoxy-6 α -(6-nitroisoquinoline-3-carboxamido)morphinan (NNQ) were identified as MOR ligands (**Figure 12**). Using the Warm-water tail immersion assay, NCQ was identified as an agonist while NNQ was identified as an antagonist. Both NCQ and NNQ and all the NAQ derivatives synthesized thus far have electron withdrawing groups on the isoquinoline ring.²¹¹ To understand the structure activity relationship (SAR) of substituents on NAQ, the synthesis of the third generation of NAQ analogs with electron donating groups (alkyl groups) on the isoquinoline ring of NAQ was proposed (**Table 10**).

Table 10. Designed third generation NAQ analogs

	R

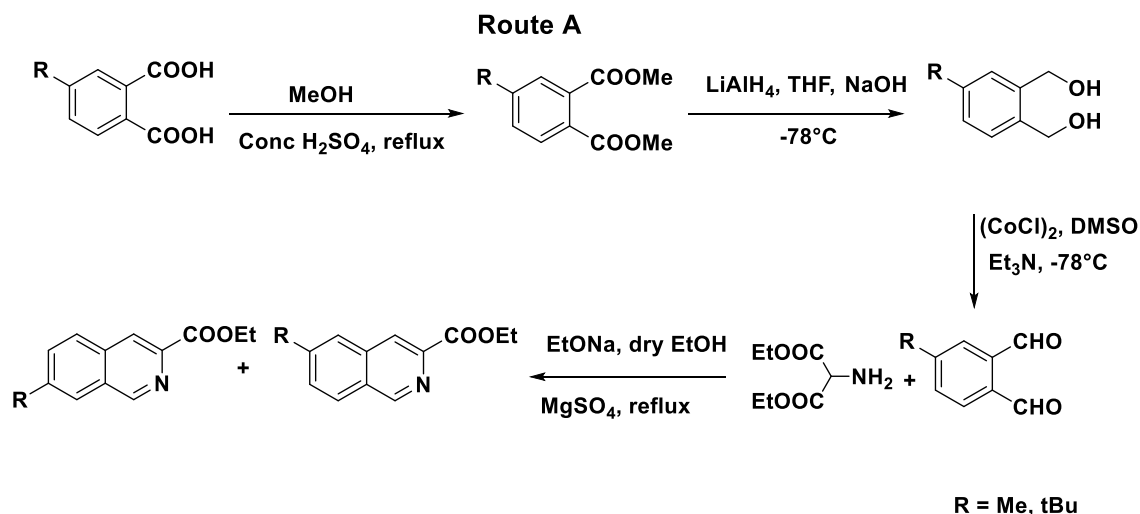


3.2.1 Specific Aim

The aim was to conduct synthesis of third generation NAQ analogs which have alkyl groups substituted at position 6 on the isoquinoline ring of NAQ.

3.3 Results and Discussion

To study the effects of alkyl substitution at position 6 of the isoquinoline group of NAQ, synthesis of the third generation NAQ analogs was proposed. The first reaction that was conducted was the synthesis of 6 α -naltrexamine HCl as shown in the previous chapter (**scheme 1 A**). 4-methyl phthalic acid was used as the starting material in the synthesis of the synthesis of 6-methyl isoquinoline-3-carboxylate whilst 4-tertbutyl-o-xylene was the starting material to synthesize 6-tertbutyl isoquinoline-3-carboxylate. Thus, 4-tertbutyl-o-xylene had to be oxidized to get the corresponding phthalic acid. The phthalic acid derivatives were first esterified and then converted to a diol using lithium aluminum hydride. A Swern oxidation was then used to convert the diol into the dialdehyde. This reaction failed initially until the reagents and the reaction vessels were thoroughly dried and then carried out under nitrogen protection. The dialdehyde formed was reacted with freshly prepared diethyl amino malonate to obtain the substituted isoquinoline-3-carboxylate (**scheme 3A**).²¹⁶ The product spot was separated by column chromatography and characterized by ¹HNMR, ¹³CNMR, and HRMS. However, the



Scheme 3. Synthesis of the third generation NAQ analogs

¹HNMR data obtained revealed that the product was a mixture of the 6 and 7 methyl isoquinoline carboxylate isomers. The two isomers had the same R.F. value and could not be separated by column chromatography nor by recrystallization. The reason why this reaction led to the formation of the mixture of the two isomers could be due to the reductive amination occurring at both aldehyde 1 or 2 of the dialdehyde. Therefore, another synthetic route was used to try and synthesize the 6-methyl isoquinoline-3-carboxylate (**scheme 3B**). In this route, 2-bromo-4-methylbenzaldehyde was refluxed with methyl 2-acetamidoacrylate in the presence of tris-*o*-tolyl phosphine and palladium acetate. However, the reaction was not successful and the product could not be obtained. The reaction was then conducted under microwave conditions but it still failed. Because of the difficulty in obtaining 6-methyl isoquinoline carboxylate, the 6 ethyl and tert-butyl isoquinoline carboxylate analogs were not synthesized.

Pharmacological characterization of NAQ in vitro and in vivo revealed that NAQ is a selective MOR ligand that has opioid antagonist effect. Further studies conducted revealed that NAQ does not precipitate opioid withdrawal in morphine pelleted mice and significantly reversed morphine withdrawal-associated depression of intracranial self-stimulation (ICSS) in rats. Thus, to study the effects of NAQ in primates, an in vivo study with rhesus monkeys was proposed. Large amounts of NAQ was needed for this study, thus 8 g of NAQ was synthesized in 48% yield and was characterized by ¹HNMR, ¹³CNMR and HRMS.

CHAPTER 4

4.0 QUANTITATIVE STRUCTURE PHARMACOKINETIC (PK) RELATIONSHIP STUDIES FOR NOVEL OPIOID COMPOUNDS

4.1 Introduction

Since the 1990s, studies have demonstrated a link between lipophilicity, molecular weight, hydrogen bonding and other molecular properties with oral bioavailability and systemic disposition characteristics of drugs. Numerous studies have shown that physicochemical properties of a molecule can help predict the “drug likeness” of that compound.²¹⁷ Absorption, distribution, metabolism and excretion (ADME) properties are important for determining the bioavailability and duration of action of drugs. In particular, total body clearance (CL_{tot}) and oral bioavailability (F_{oral}) are the main determinants for drug concentrations in plasma (“systemic exposures”), and subsequently, therapeutic and toxic effects, resulting from oral drug administration.²¹⁸ ADME properties can be determined by in vitro and in vivo methods. However, these methods are expensive and time consuming, especially in early drug discovery. As a result, in silico methods have been developed to quickly predict the pharmacokinetic (PK) properties of compounds

early in the drug discovery process. Quantitative structure pharmacokinetic relationship (QSPKR) studies use theoretical descriptors that are calculated from the physicochemical properties of the molecule. Once a QSPKR model is generated, it can be used to predict the PK properties of similar drug molecules.

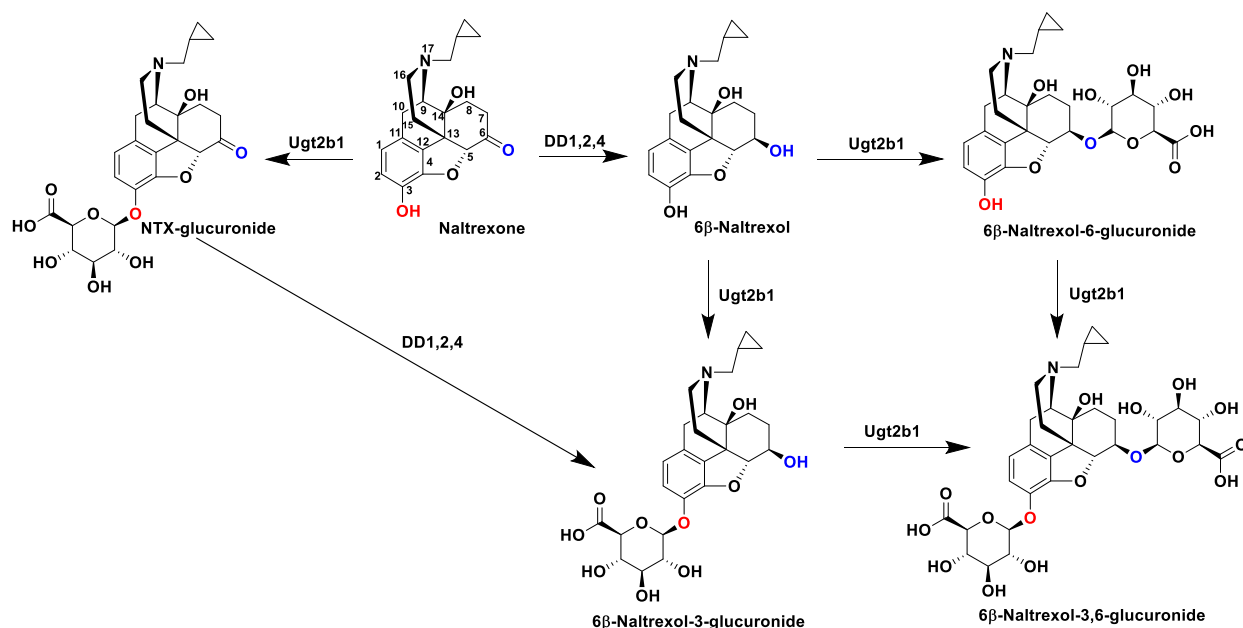
4.2 Aim of QSPKR project

The aim of the project was to generate a QSPKR model for opioid compounds designed and synthesized in our laboratory group. The QSPKR model might then be used to predict the pharmacokinetic properties of newly designed and synthesized compounds.

4.3 Results and Discussion

All the compounds used to build the QSPKR model were derivatives of Naltrexone (NTX). Although well absorbed orally (i.e., possessing sufficient GI solubility and permeability at oral doses in the low mg range), NTX is subject to significant first-pass GI and hepatic metabolism with F_{oral} estimates ranging from 5 to 40%. NTX is mainly metabolized to 6 β -naltrexol by dihydrodiol cytosolic dehydrogenases (DD1, DD2 and DD4), present in most body tissues.^{219,220} 6 β -naltrexol formation has not been detected in the microsomal fraction, suggesting a lack of involvement of cytochrome P450 enzymes. In vitro studies with human plasma show NTX to be 21% bound to plasma proteins over the therapeutic plasma concentration range. After I.V. administration, NTX was found to have a very large volume of distribution at steady-state ($V_{d_{ss}}$) of 18 L/kg - indicating extensive extravascular tissue distribution – as well as a high value for total body clearance (CL_{tot}) of 46.7 mL/min/kg – exceeding hepatic blood flow (20 mL/min/kg) and demonstrating extrahepatic metabolism, resulting in a relatively short half-life for NTX of 267 minutes.

Studies have demonstrated that 6 β -naltrexol is present in much higher concentrations in plasma than the parent drug after an oral dose of NTX, indicating its formation as result of high NTX first-pass metabolism. Also, 6 β -naltrexol remains much longer in the systemic circulation as shown by its longer half-life of about 12 hours compared with ~4 hours for parent NTX.²²¹ 6 β -naltrexol is the major urinary excretion product of NTX in man after intravenous and oral (IV/PO) administration. In a study conducted by Wall et al, it was found out that approximately 60% of the total (radioactively-labeled) NTX dose is excreted in the urine within 48-72 hours whilst fecal excretion accounts for only 5.4% of the total 1 mg IV and 50 mg PO dose.²²²



Scheme 4. Metabolic pathway of NTX in rodents

Both parent NTX and 6 β -naltrexol are conjugated by UDP-glucuronosyltransferase (UGT2B1) to form NTX- and 6 β -naltrexol-glucuronides, which are subsequently excreted into bile/feces and urine (**Scheme 4**).²²³ The biliary excretion may result in enterohepatic recycling, prolonging the persistence of NTX and 6beta in the body.

Table 11. Opioid QSPKR obtained from Dr. Jurgen Venitz laboratory²²⁴

Y	X	slope	intercept	comments
f_u	$\log(D_{7.4})$	-0.1421	0.6633	n=29
Vd_{ss}^u	$\log(D_{7.4})$	0.3665	0.3932	n=29
CL_{tot}^u	$\log(D_{7.4})$	0.2587	1.2647	n=28
CL_{nonren}^u	$\log(D_{7.4})$	0.3627	1.0683	n=18
CL_{ren}^u	$\log(D_{7.4})$	0.0258	0.2455	n=18, ns

A previously validated QSPKR model for opioids in humans used $\log D_{7.4}$ to predict in vivo PK properties, such as f_u (fraction unbound in plasma [%]), Vd_{ss}^u (unbound volume of distribution at steady-state [L/kg]) and CL_{tot}^u (unbound total body clearance [mL/min/kg]) (**Table 11.**)²²⁴ Except for f_u , linear relationships between $\log(Y)$ and $\log(X)$ using the slope and intercept values listed below were employed: Vd_{ss} , CL_{tot} were calculated by multiplying their (QSPKR-predicted) counterparts by the (QSPKR-predicted) f_u . Thus, an assumption was made that $\log(D_{7.4})$ is directly related to the in vivo pharmacokinetic properties of opioids.²²²

The physicochemical properties of 71 opioid compounds designed and synthesized in our laboratory group together with naltrexone (NTX) were predicted using Scifinder. All the compounds had an ionizable tertiary nitrogen at position 17. Only 2 compounds had an ionizable amine at position 6, making these compounds very soluble. Also, most the compounds had an isoquinoline or pyridine ring at position 6 or 14. About half of the compounds are cations whilst the rest are neutral. Eight molecules had hydrolysable

esters at position 14. The major metabolic pathway of these compounds is expected glucuronidation at position 3 (as is the case for NTX). However, 20 of these compounds have a carbonyl group at position 6 and, therefore, can be subject to DD metabolism and form analogs to 6 β -naltrexol (which would be subject to further glucuronidation, as is the case for NTX). Across the entire series of compounds, their molecular weights, pKa, clogP and log D_{7.0} of the ranged from 342 to 562 g/mol, 6.26-8.57, 0.31-6.42 and -1.11-6.19, respectively - indicating considerable physicochemical diversity.

The physicochemical properties obtained were used to predict whether the compounds will pass Lipinsky's rule of 5, GI permeability and CNS penetration: The Lipinski rule of five (RO5) states that poor oral absorption is more likely when the molecular weight (MW) exceeds 500 Da, there are more than five hydrogen bond donors (HBD, expressed as the sum of hydroxyl and amino groups present in a molecule), the calculated octanol–water partition coefficient (clogP) exceeds 5 or there are more than 10 hydrogen bond acceptors (HBA, expressed as the sum of nitrogen and oxygen atoms in the molecule). RO5 is based on the assumption that these 5 physicochemical properties determine primarily GI solubility and GI permeability (i.e., F_{oral}) of therapeutic drug doses. Compounds that are substrates for drug transporters (in the GIT) are exceptions to the rule.²²⁵

From the studies conducted, it was observed that the 24 of the 71 compounds failed RO5. Most of the compounds that failed RO5 had molecular weights greater than 500; four of the compounds that failed had clogP values greater than 5. If a compound fails the RO5, there is a high probability that F_{oral} is insufficient to support oral dosing.

However, passing the RO5 is no guarantee that a compound is drug-like. Analysis of small drug-like molecules suggests that compounds with $0 > \log D < 3$ may have a higher probability of good intestinal permeability.²²⁶ We therefore used this criterion to assess whether the compounds will be GI permeable, and 43 of the 71 compounds passed this computational screen.

Norinder and Haerberlein used a very simple rule to predict CNS permeability: If N + O (the number of nitrogen and oxygen atoms) in a molecule is less than or equal to 5, it has a high chance of entering the brain.²²⁷ All the compounds failed this test, including NTX, which is known to penetrate the CNS - suggesting that this *in-silico* screen may not be useful.

Table 12. Comparison of predicted fu and CL_{tot} to actual of NTX, NAP and NAQ

Compound ID	Lipinsky RO5	GI Perm	f _u [%]	CL _{tot} [mL/min/kg]	(actual) fu [%]	(actual) CL _{tot} [mL/min/kg]
NTX	Pass	Pass	42%	21.3	79%	46.7
NAP	Pass	Pass	52%	17.3	85%	5
NAQ	Pass	Pass	37%	23.4	2.6%	13

Twenty of the opioid compounds in this study had a ketone at position 6 as does NTX and can therefore be metabolized by the DD enzymes to form 6β-hydroxyl derivatives, which might be their major metabolite. Only two compounds in the table (appendix) did not have a hydroxy group at position 3, but had an ester group. However, the ester at position 3 may be easily hydrolyzed by esterases, present throughout the body,

including blood. On the other hand, all compounds can undergo glucuronidation by UDP-glucuronosyltransferases to form either 3 or/and 6 glucuronides.

As discussed above, in vitro tests with human plasma show NTX to be 21% bound to plasma proteins ($f_u = 79\%$) over the therapeutic dose range. In vivo human studies after I.V. administration estimated that NTX has a $V_{d_{ss}}$ of 18 L/g, CL_{tot} of 46.7 mL/min/kg and half-life of 267 minutes. The QSPKR-model predicts that NTX is 58 % plasma protein bound, has a $V_{d_{ss}}$ of 4.4 L/kg, CL_{tot} of 21.3 mL/min/kg and half-life of 142 minutes.

Thus, the predicted $V_{d_{ss}}$ was approximately 4-fold lower than the experimental value whilst CL_{tot} and half-life were approximately 2-fold lower than the experimental values.

The predicted f_u [%] and CL_{tot} of NAP and NAQ was compared to their actual values that were obtained from experiments conducted in Dr. Phil Gerk's laboratory (**Table 12**).²⁰⁹

The predicted f_u [%] of NAP was 1.6 fold lower than the actual value whilst the predicted CL_{tot} was 3.5 fold greater than the predicted value. On the other hand, the predicted f_u [%] of NAQ was 14 fold greater than the actual value whilst the predicted CL_{tot} was 1.8 fold greater than the predicted value. The QSPKR model used only $\log D_{7.4}$ to predict the in vivo PK properties, and among the members of the opioid database used to develop and validate the model, only NTX was subject to the (unique) DD-mediated metabolic route, which may explain some of these the discrepancies.

Using this model, we predicted f_u , $V_{d_{ss}}^u$, CL_{ren}^u , and CL_{tot}^u (and counterparts based on total drug in plasma), as well as half-life for the 71 compounds designed and synthesized in our laboratory - see appendix.

The model predicted that 5 compounds, namely VZMN016, 019, 021, 023, and 024 (appendix) are more than 99% plasma bound, had very low CL_{tot} and long half-lives -

which may make them unsuitable for further studies since drugs have to be cleared from the body to avoid their toxic effect. The predicted values for $V_{d_{ss}}$ of the compounds ranged from 1.4 to 7.9 L/kg. The predictions for CL_{tot} and half-life of the compounds range from 8-26 mL/min/kg and 89-281 min.

4.4 Summary of QSPKR study

Studies have shown that physicochemical properties of a molecule can be used to predict the “drug likeness” of a compound.²¹⁷ ADME properties play an important role in determining the bioavailability and duration of action of drugs. In silico methods have been developed to quickly predict the PK properties of compounds early in the drug discovery process to reduce the likelihood of drugs failing in vivo tests later. QSPKR studies use theoretical descriptors that are calculated from the physicochemical properties of the molecule. Once a QSPKR model is generated, it can be used to predict the PK properties of similar drug molecules. A QSPKR table was therefore generated using opioid compounds synthesized in our laboratory. Most of the compounds used in this study were derived from Naltrexone (NTX).

66% of the compounds analyzed passed the Lipinsky’s RO5 and GI permeability rule, which indicates that majority of the compounds have good oral bioavailability unless they are subject to extensive first-pass metabolism (as is the case for TNX). The QSPKR-model generated property values show that 86% of the compounds have a f_u [%] greater than 10% and that 88% of the compounds have a $V_{d_{ss}}$ greater than 2 L/kg. Also, 89% of the compounds have a CL_{tot} greater than 15 mL/min/kg. The majority of the compounds will be metabolized by UGT2B1 to form glucuronides at position 3. On the other hand, about 28% of the compounds have a carbonyl group at position 6, and

hence can be metabolized by DD enzymes to form 6 β -hydroxyl derivatives. 11% of the compounds had ester groups at position 14 and/or 3 which can easily be hydrolyzed by esterases. However, in vitro binding and functional data for the compounds along with target product profiles will be needed to determine which compounds to progress to further in vitro PK screening to obtain experimental values for CL_{tot}, Vd_{ss} and F_{oral} in rodents and or in vitro drug metabolism screening, e.g., in human liver cytosol (HLC) and/or human liver microsomes (HLM). The predicted f_u [%] and CL_{tot} of NAP and NAQ was compared to their experimental.²⁰⁹ The predicted f_u [%] of NAP was 1.6 fold lower than the actual value whilst the predicted CL_{tot} was 3.5 fold greater than the predicted value. On the other hand, the predicted f_u [%] of NAQ was 14 fold greater than the actual value whilst the predicted CL_{tot} was 1.8 fold greater than the predicted value. The QSPKR model only used logD_{7.4} to predict the in vivo PK properties. From the opioid database used only NTX was subject to the (unique) DD-mediated metabolic route, which may explain some of these the discrepancies. To make further recommendations, information about (effective) target plasma concentrations (e.g., based on in vitro K_i values) as well as a target pharmaceutical profile (TPP) for the target indication(s) need to be developed and incorporated in the projection of feasible human dosing regimens.

CHAPTER 5

5.0 CONCLUSIONS

The Sumerians of Mesopotamia were the first people to cultivate the opium poppy plant and they called it Hul Gil, meaning the “joy plant”. Morphine was isolated from the poppy plant by Friedrich Serturmer in 1806 and its pharmacology was defined at the receptor level 167 years later. The addictive properties of morphine were characterized by Dr. Eduard Livenstein who also showed that morphine had withdrawal effects. The cloning of the opioid receptors in the 1990s helped in understanding the roles of the individual opioid receptors. The first crystal structure was obtained for opioid receptors (MOR) in 2012 by Dr. Brian Kobilka and his contribution in this field led to him being awarded the Nobel prize in Chemistry in 2012.

Studies using opioid receptor knock-out mice revealed that, analgesia, addiction, respiratory depression, and constipation produced by opioid agonists is because of activation of MOR. Therefore, compounds that selectively block MOR may have therapeutic potential in treating opioid addiction or serve as valuable pharmacologic tools to help in opioid receptor research.

Opioid receptor antagonists such as naltrexone and naloxone have been found to block opioid addiction relapse. However, the use of opioid antagonist as long term treatments for opioid addiction results in severe side effects such as depression, dysphoria, pulmonary edema, cardiac arrhythmias and also leads to high rates of overdose and suicide.^{189,190,191} Studies have shown that the side effects associated with opioid antagonists are due to their lack of selectivity for MOR.^{73,104,123} Thus, a highly selective MOR antagonist might lack the side effects associated with naltrexone and naloxone and may therefore be ideal to treat opioid addiction. Some selective MOR antagonist such as β -FNA and clocinnamox have been developed; however, these agents bind irreversibly to MOR and might have numerous side effects due to their covalent binding with the receptor.^{196,197} Compounds that bind reversibly to a receptor are preferred since the compounds can be washed off easily from the receptor. Again, opioid antagonists such as CTOP and CTAP have also been identified as highly selective MOR antagonists. However, these compounds are conformationally constrained and have limited bioavailability and blood-brain barrier penetration capacity.^{200,201} This makes them unsuitable as drug candidates. Therefore, the development of a potent, selective, reversible, non-peptide antagonist for MOR remains highly desirable.

GNTI and NTI are derivatives of naltrexone that are selective for KOR and DOR respectively. The selectivity of these compounds has been rationalized using the “message address concept”. The “address” domain aids in selectivity by either increasing the affinity for a particular type of receptor or by decreasing the affinity at other sub-types of receptors whilst the “message domain” is responsible for the pharmacological effects of the compound.^{199,202,203} Utilizing the “message-address

concept”, our research group has designed and synthesized novel non-peptide, reversible MOR selective ligands NAQ and NAP that were experimentally characterized through in vitro and in vivo studies.^{205–207} Further pharmacokinetic characterization revealed that NAP acts mainly peripherally whilst NAQ can also act in the central nervous system. Therefore, NAQ was used as the lead compound in this study.^{208,209}

Studies showed that NAQ significantly reversed morphine withdrawal-associated depression of intracranial self-stimulation (ICSS) in rat and did not precipitate withdrawal in morphine pelleted mice. These results agreed with the in vitro pharmacology data of NAQ and indicate that NAQ may serve as a relatively safe option for treatment of opioid addiction.^{209,210} To understand the pharmacological effects of NAQ in primates, a project was proposed to study the effects of NAQ in Rhesus monkeys. Therefore, large scale synthesis of NAQ was conducted, 8 g of NAQ was synthesized in 48% yield and characterized by ¹HNMR, ¹³CNMR, and HRMS.

NAQ, however, has low selectivity for MOR over DOR (146 fold) compared to naltrexone (435 fold).²¹¹ NAQ also showed relatively high efficacy and moderate potency in the DOR [³⁵S]GTPγS binding assay.²⁰⁵ Studies have demonstrated that DOR activation is also involved in the development of morphine dependence.²¹² Hence, second generation NAQ analogs were designed and synthesized.²¹¹ Two compounds NCQ and NNQ, were identified as MOR ligands. NCQ was identified as an opioid agonist whilst NNQ was identified as an antagonist. Therefore, the design of another generation of NAQ analogs was proposed to understand the SAR of NNQ. To investigate the role of the nitro group on NNQ at position 6, it was proposed that alkyl groups be introduced at position 6 on the isoquinoline ring. The synthesis of the 6-

methyl and t-butyl analogs of NAQ was carried out by first synthesizing their respective isoquinoline acid analogs. However, the ¹HNMR data obtained for 6-methyl isoquinoline carboxylate synthesized showed that the product was a mixture of the 6 and 7- methyl isoquinoline carboxylate isomers. The two isomers had the same R.F. value and could not be separated by column chromatography. They could not also be separated by recrystallization. Another route was then by refluxing 2-bromo-4-methylbenzaldehyde, with methyl 2-acetamidoacrylate in the presence of tris-o-tolyl phosphine and palladium acetate. However, this reaction failed and the reaction was repeated under microwave conditions but the reaction was not successful. Thus, the 6-alkyl analogs of NNQ could not be obtained.

Molecular modeling and mutagenesis studies conducted in our laboratory revealed that the selectivity of NAQ for MOR is as a result of its π - π stacking with W318.²¹³

Therefore, other heterocyclic ring systems were explored to find out if compounds with improved pharmacologic profiles would be obtained. Thus, new compounds were designed where the isoquinoline ring of NAQ was replaced with an indole ring. The newly designed compounds were indole analogs of 6 α / β -naltrexamine. The indole analogs of 6 α / β -naltrexamine were synthesized using EDCI/HOBt coupling. The ester formed at position 3 was then hydrolyzed using K₂CO₃/MeOH. The final compounds synthesized were converted to the HCl salt to improve their stability and solubility and then characterized using ¹HNMR, ¹³CNMR, IR, and HRMS. The percentage yield obtained for the synthesized compounds ranged from 22-81%.

The first assay conducted was to determine whether the designed compounds bind to their biological target, MOR. This was determined using the radioligand binding assay.

In this assay, the synthesized compounds compete with labeled naloxone for binding to MOR. Competition at KOR and DOR with labeled diprenorphine was used to determine the selectivity of these compounds for MOR over KOR and DOR. The MOR binding data for the 6 α -naltrexamine analogs revealed that the position of the substitution on the indole ring did not significantly affect the binding affinities at MOR. Compound **4** (the 5 substituted indole analog of 6 α -naltrexamine) had the least binding affinity which was 3.3 fold worse than compound **6**, (the 7 substituted indole analog of 6 α -naltrexamine) which had the best binding affinity at MOR. Also, increasing alkyl chain at position 3 did not significantly affect binding affinity at MOR. Compound **7** with the one carbon linker had the least binding affinity. It was also observed that the 6 β -naltrexamine analogs had better binding affinities at MOR than their respective 6 α -naltrexamine analogs. The K_i of all the indole analogs of 6 β -naltrexamine at MOR was approximately 0.2 nM. Thus, neither the substitution position nor the length of the alkyl group at position 3 had any significant effect on binding affinity at MOR for the 6 β -naltrexamine analogs. Again, it was observed that compound **6** and **12** had the greatest selectivity for MOR over KOR while compound **17** was more selective for MOR over DOR. Compound **6** also had a high selectivity for MOR over DOR when only the 6 α -substituted naltrexamine analogs were considered. Thus, compound **6** and **12** had the best MOR selectivity profile.

The next assay conducted was the [³⁵S]GTP γ S functional assay. This assay was conducted to determine the relative efficacy of the compound at MOR. Regarding the 6 α -naltrexamine analogs, it was observed that compound **6** had the least efficacy at MOR although very potent, while compound **1** (the 2 substituted analog) had the highest efficacy. Compound **6** was more potent than NAQ but had similar efficacy as NAQ. It

was also observed that increasing the alkyl chain at position 3 did not have a significant effect on potency and efficacy. However, compound **9** with the three carbon linker was the most potent compound. The 6 β -naltrexamine analogs, compound **10**, **11** and **14** were the most potent and most efficacious having E_{max} values greater than 70%. In fact, compound **10** with substitution at position 2 had the highest efficacy with an E_{max} value of 92% with compound **12** having the lowest efficacy with an E_{max} value of 15%. It was also observed that increasing the alkyl chain length at position 3 did not significantly affect potency but there was a corresponding decrease in efficacy.

Warm-water immersion, an in vivo assay using mice, was conducted to determine whether the synthesized compounds had antinociceptive effects and/or blocked the antinociceptive effects of morphine. The tail-flick was conducted 20 minutes after s.c. administration of the compounds since morphine's antinociceptive effects peaks at 20 min after injection. Not surprisingly, compound **10** which had the greatest efficacy in the [³⁵S]GTP γ S functional assay had the greatest antinociceptive effects in the warm-water immersion assay. Compounds **15** and **16** had partial antinociceptive effect. To find out if the compounds block morphine's antinociceptive effect, morphine was administered 5 min after administering the compounds and the tail-flick then conducted 20 mins later. Interestingly, compound **6**, which had a high potency and low efficacy at MOR in the [³⁵S]GTP γ S functional assay, almost completely blocked morphine's antinociceptive effects. However, compound **12** that had the lowest efficacy in the [³⁵S]GTP γ S functional assay did not significantly block morphine's antinociceptive effects. Compound **15**, **17**, and **18** also partly blocked morphine-mediated antinociception. The antagonist effects of compound **6**, **17**, and **18** were dose dependent and their AD₅₀

values obtained were 2.39 (0.46-12.47), 7.30 (3.38-15.74), and 9.64 (3.17-29.29) mg/kg (95% CL) respectively. Compound **6** was also identified as the most potent opioid antagonist in the warm-water immersion assay. Therefore further in vivo studies were conducted on compound **6** using morphine-pelleted mice to determine if compound **6** had opioid withdrawal effects. It was observed that compound **6** produced less significant withdrawal symptoms even at a dose of 50 mg/kg compared to naltrexone at 1 mg/kg. Thus, compound **6** produces significantly less withdrawal symptoms than naltrexone and therefore has the potential to be used in opioid addiction treatments.

Molecular modeling studies were conducted to understand the molecular interactions of compound **6** at the receptor level. This information will help guide the design of the next generation of compound **6** analogs. Molecular docking studies conducted revealed that compound **6** clustered in two binding poses in MOR. The morphinan part of the compound was docked in the same position in both sites whereas the indole ring docked differently in the two sites. In binding site 1, the nitrogen of the indole ring formed a hydrogen bond with K303 and had pi-pi interactions with W318. In binding site 2, the nitrogen of the indole ring was hydrogen bonded to K233 and did not have pi-pi interactions with W318. An MD simulation was conducted with these two poses and the results revealed that the interactions observed in binding pose 2 are the most likely interactions between compound **6** and MOR.

Future directions for this may project would be to study the SAR of compound **6**. The first will be to determine the optimum alkyl chain length between the indole ring and the carbonyl group. Therefore, compounds with 2 to 5 carbon chain length between the indole ring and the carbonyl group can be synthesized. Again, electron withdrawing and

donating groups can be introduced at different positions on the indole ring to get the next generation of compounds with improved pharmacologic activity.

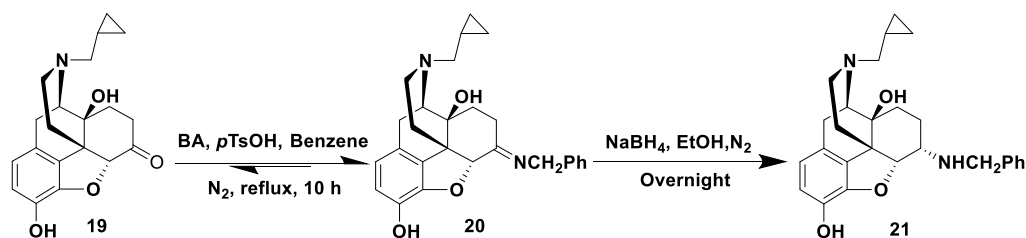
Again, further in vitro and in vivo studies will be conducted with compound 6 to have a complete pharmacologic profile for this compound. For instance, a [³⁵S]GTP_γS binding functional assay at DOR and KOR will reveal whether compound 6 activates DOR and/or KOR. Another functional assay such as the Ca²⁺ mobilization assay will corroborate the functional results obtained by the [³⁵S]GTP_γS assay. Another In vivo study such as the intracranial self-stimulation study in rats will be conducted to determine if compound **6** significantly reverses morphine withdrawal-associated depression of intracranial self-stimulation in rats.

CHAPTER 6

6.0 EXPERIMENTAL SECTION

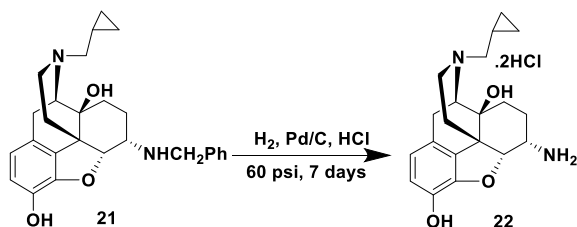
6.1 Chemical synthesis

6.1.1 Synthesis of 6 α -benzyl naltrexamine



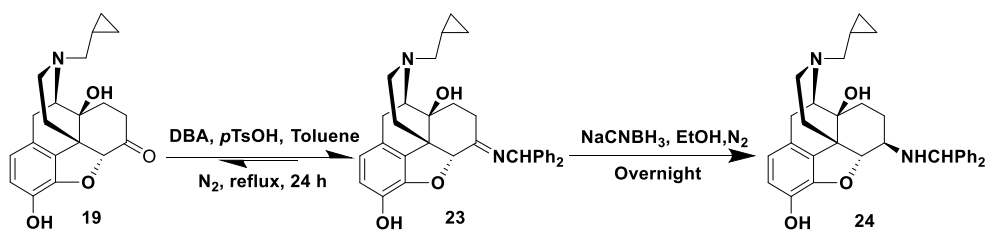
A benzene solution (150 mL) in a three-necked flask containing naltrexone base (**19**), benzyl amine (1.2 eq.) and a trace of p-toluene sulfonic acid was refluxed for 10 hours using a Dean-Stark trap for azeotropic removal of water. The mixture was then concentrated (30 mL) and NaBH₄, absolute ethanol and 4 Å molecular sieves were added to the reaction mixture and stirred under N₂ overnight. When the reaction was completed, the solvent was removed using a rotary evaporator and the product purified using column chromatography with a dichloromethane: methanol: ammonium hydroxide

(40: 1: 1 %) mobile phase system to obtain 6 α -benzyl naltrexamine (**21**) in 88 % yield.²¹⁴ **6.1.2 Synthesis of 6 α -naltrexamine HCl**



6 α -benzyl naltrexamine (**21**) was dissolved in 35-60 mL of methanol and then concentrated HCl was added to obtain a pH of 2. 10 % Pd/C (approximately 10% of the starting material) was added and hydrogenation was carried out at 60 psi for 6 days using a Parr hydrogenator. The Pd/C was changed every three days. When the reaction was completed, the Pd/C was filtered using celite to obtain pure 6 α -naltrexamine HCl (**22**) with a yield of 76 %.²¹⁴

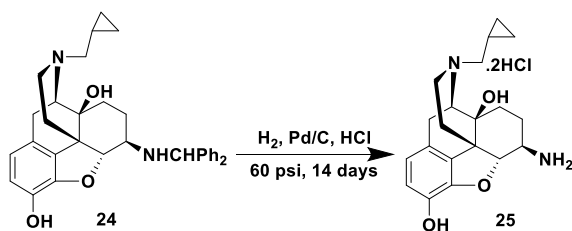
6.1.3 Synthesis of 6 β -dibenzyl naltrexamine



A toluene solution (150 mL) in a three-necked flask containing naltrexone base (**19**), benzoic acid (1.3 eq.), a trace of p-toluene sulfonic acid was stirred for 30 minutes at room temperature. Dibenzyl amine (1.3 eq.) was then added and the mixture refluxed with a Dean-Stark apparatus for 24 hours under N₂. The mixture was then concentrated to 30 mL, cooled and then 50 mL anhydrous ethanol and NaCNBH₃ (0.8 eq) were added and the reaction mixture was stirred under N₂ overnight. The mixture was then

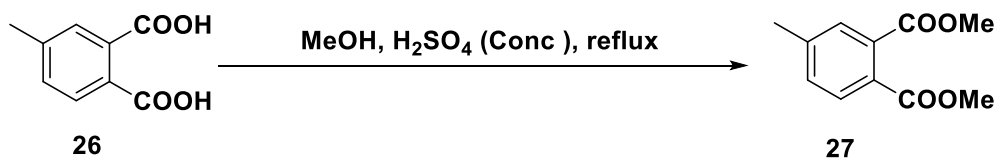
filtered with celite and the solvent was removed using a rotary evaporator apparatus. The solid obtained was refluxed with methanol for 1 hour and then cooled and filtered. The residue obtained was washed with cold methanol to obtain 6 β -dibenzyl naltrexamine (**24**) in 71 % yield.²¹⁴

6.1.4 Synthesis of 6 β -naltrexamine HCl



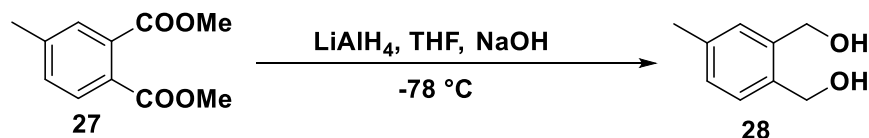
Dibenzyl naltrexamine (**24**) was dissolved in 35-60 mL of methanol and then concentrated HCl was added to obtain a pH of 2. 10% Pd/C (approximately 10 % of the starting material) was added and hydrogenation was carried out at 60 psi for 6 days using a Parr hydrogenator. The Pd/C was changed every three days. When the reaction was completed, the Pd/C was filtered using celite to obtain pure 6 β -naltrexamine HCl (**25**) with a yield of 82 %.²¹⁴

6.1.5 Synthesis of dimethyl 4-methylphthalate



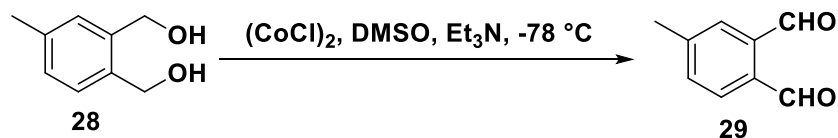
5 drops of concentrated sulfuric acid was added to 4-methylphthalic acid (**26**) dissolved in methanol. The mixture was refluxed for 24 hours and the solvent evaporated to obtain 4-methylphthalate (**27**) in 81 % yield.²¹⁶

6.1.6 Synthesis of (4-methyl-1,2-phenylene)dimethanol



To a slurry of LiAlH₄ (2 eq.) in anhydrous THF (40 mL) cooled to -78 °C, a solution of dimethyl 4-methylphthalate (**27**) in anhydrous THF (20 mL) was added dropwise over a period of 1 hour. After slow warming of the reaction mixture to room temperature, the mixture was stirred overnight. The heterogeneous mixture was then cooled to 0 °C and sodium hydroxide solution (15 %, 20 mL) cooled to 0 °C was added very slowly. This was followed by addition of ice-cold water (20 mL) and THF (40 mL). The organic layer was separated and dried with brine and Na₂SO₄. The solvent was evaporated and the compound was purified using column chromatography to obtain (4-methyl-1,2-phenylene)dimethanol (**28**) in 96 % yield.²¹⁶

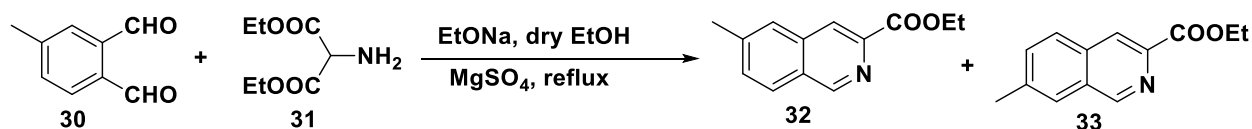
6.1.7 Synthesis of 4-methylphthalaldehyde



To an oven-dried 100 mL three-necked flask, was added 4 Å molecular sieves, a solution of anhydrous dichloromethane (6 mL) and oxalyl chloride (4 eq.) under nitrogen. The stirred solution was cooled to -78 °C and a solution of anhydrous dimethyl sulfoxide (6 eq.) in dichloromethane (1.2 mL) was added dropwise to the reaction mixture. The mixture was stirred for 5 minutes and (4-methyl-1,2-phenylene)dimethanol

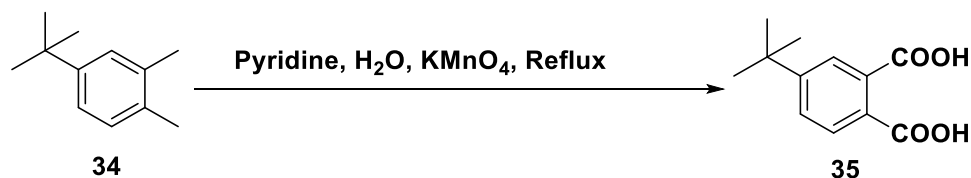
(**28**) dissolved in dichloromethane: dimethyl sulfoxide mixture (2 mL) was added dropwise. The reaction was allowed to continue stirring for 30 minutes and then anhydrous triethylamine (0.03 eq.) was added slowly at -78 °C. The reaction mixture was stirred for 10 minutes and then slowly warmed to room temperature. Ice cold water (20 mL) was added to the reaction mixture and the aqueous layer was extracted with dichloromethane and then dried the organic phase over Na₂SO₄. The mixture was then purified with hexane: ethyl acetate (70:30) to obtain 4-methylphthalaldehyde (**29**) in 39% yield.²¹⁶

6.1.8 Synthesis of ethyl 6-methylisoquinoline-3-carboxylate



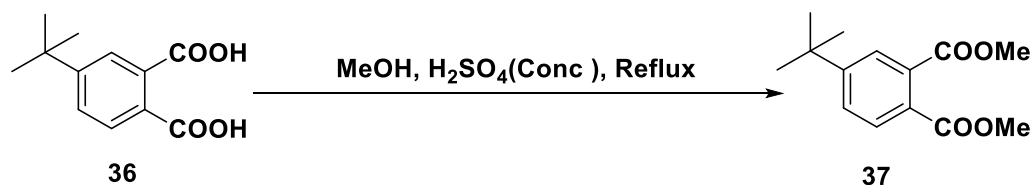
Diethyl amino malonate HCl salt was treated with saturated NaHCO₃ in dichloromethane for 12 minutes. Diethyl amino malonate (**31**) was obtained in 80 % yield after drying the organic layer over Na₂SO₄ and elimination of solvent. The compound was then stored under nitrogen at 4 °C. 4-methylphthalaldehyde (**30**), freshly prepared diethyl amino malonate (**31**) (1 eq.) and sodium ethoxide were refluxed in ethanol under nitrogen for 4 hours. After elimination of the ethanol, the mixture was extracted repeatedly with ethyl acetate and then purified by column chromatography to obtain a mixture of 6-methylisoquinoline-3-carboxylate (**32**) and 7-methylisoquinoline-3-carboxylate (**33**) in 48 % yield.²¹⁶

6.1.9 Synthesis of 4-(tert-butyl)phthalic acid



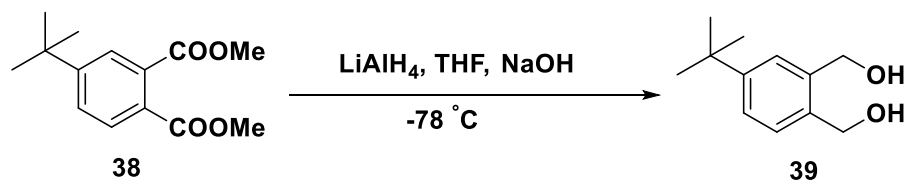
4-tertbutyl-o-xylene (**34**) was suspended in pyridine and water in a three-necked flask with a sealed stirrer. To this well-stirred, gently boiling mixture, potassium permanganate (4.8 eq.) was added slowly within a period of 2 hours. The mixture was then refluxed for 30 minutes. When the reaction was completed, ethanol was added and the mixture was filtered. The residue was washed with warm water. The filtrate was concentrated and then acidified to pH 1 with HCl to give a precipitate. The precipitate was then filtered and dried to obtain 4-(tert-butyl)phthalic acid (**35**) in 46 % yield.²²⁸

6.1.10 Synthesis of dimethyl 4-(tert-butyl)phthalate



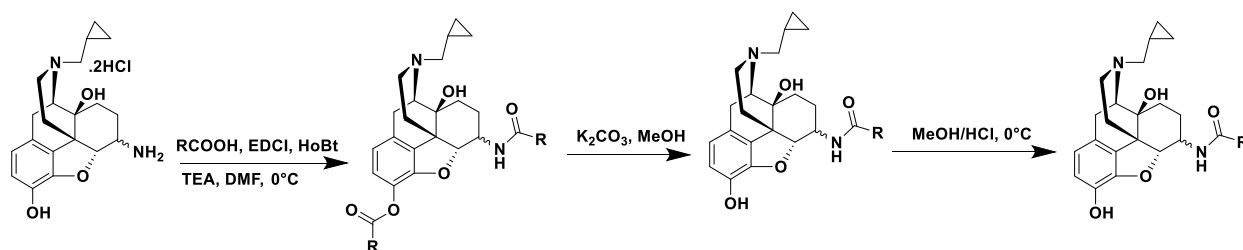
10 drops of concentrated H₂SO₄ was added to a solution of 4-(tert-butyl)phthalic acid (**36**) in methanol and then refluxed for 48 hours. The reaction mixture was concentrated to obtain an oil which was then dissolved in dichloromethane. NaHCO₃ was added making sure the pH of the aqueous layer was between 7- 8. The organic phase was dried over Na₂SO₄ concentrated and purified using column chromatography to obtain 4-(tert-butyl)phthalate (**37**) in 66 % yield.²¹⁶

6.1.11 Synthesis of (4-(tert-butyl)-1,2-phenylene)dimethanol



To a slurry of LiAlH_4 (2 eq.) in anhydrous THF (40 mL) cooled to $-78\text{ }^\circ\text{C}$, a solution of 4-(tert-butyl)phthalate (**38**) in anhydrous THF (20 mL) was added dropwise over a period of 1 hour. After slow warming of the reaction mixture to room temperature, the mixture was stirred overnight. The heterogeneous mixture was then cooled to $0\text{ }^\circ\text{C}$ and sodium hydroxide solution (15 %, 20 mL) cooled to $0\text{ }^\circ\text{C}$ was added very slowly. This was followed by the addition of ice-cold water (20 mL) and THF (40 mL). The organic layer was separated and dried with brine and Na_2SO_4 . The solvent was evaporated and the compound was purified using column chromatography to obtain (4-(tert-butyl)-1,2-phenylene)dimethanol (**39**) in 96 % yield.²¹⁶

6.1.12 General method of coupling of naltrexamine to carboxylic acid derivatives

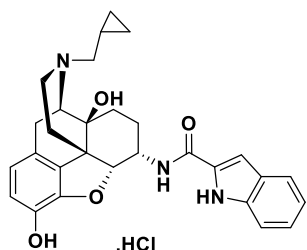


The carboxylic acid derivatives (3 eq.), hydrobenzotriazole (HoBt) (3 eq.), 4 Å molecular sieves triethylamine (9 eq.), *N*-(3-Dimethylaminopropyl)-*N*'-ethylcarbodiimide hydrochloride (EDCI) (3 eq.), and DMF (2 mL) were added into a three-necked flask on an ice-water bath and stirred for 15 minutes. Naltrexamine (1 eq.) suspended in 2 mL

DMF was added dropwise and then stirred on the water bath for 24 hours. When the reaction was completed, the reaction mixture was filtered with celite and the filtrate concentrated to remove DMF. MeOH (7 mL) and K₂CO₃ (3 eq.) were added to the concentrate and stirred at ambient temperature. When hydrolysis of the ester at position 3 was complete, the mixture was filtered through celite again and concentrated to remove MeOH. The mixture was then purified using column chromatography with dichloromethane: MeOH (20:1) and NH₄OH to give the free base.²¹¹

6.2 Characterization of compounds

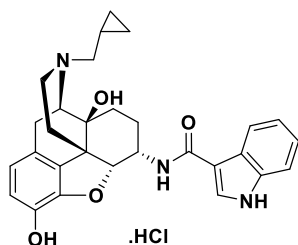
17-Cyclopropylmethyl-3,14β-dihydroxy-4,5α-epoxy-6α-(indole-2-carboxamido)morphinan (1)



The title compound was prepared by following the general procedure in 81% yield. ¹H NMR (400 MHz, DMSO-*d*₆) δ 11.65 (s, 1H, Exchangeable), 9.25 (s, 1H, Exchangeable), 8.87 (s, 1H, Exchangeable), 8.09 (d, J = 7.76 Hz, 1H, Exchangeable), 7.62 (d, J = 7.96 Hz, 1H), 7.45 (d, J = 8.2 Hz, 1H), 7.23 (dd, J = 7.96 Hz, 1.44 Hz, 1H), 7.18 (d, J = 8.2 Hz, 1H) 7.05 (t, J = 7.88 Hz, 1H), 6.72 (d, J = 8.08 Hz, 1H), 6.59 (d, J = 8.16 Hz, 1H), 6.34 (s, 1H, Exchangeable), 4.79 (d, J = 3.8 Hz, 1H) 4.62 (m, 1H), 3.93 (d, J = 7 Hz, 1H), 3.40-3.26 (m, 2H), 3.12-3.05 (m, 2H), 2.96 (m, 1H), 2.73(m, 1H), 1.92 (m, 1H) 1.66 (d, J = 10.56, 1 H) 1.56-1.45 (m, 2H), 1.2 (m, 1H) 1.09 (m, 1H), 0.71-0.61 (m, 2H), 0.51-0.40 (m, 2H). ¹³C NMR (100 MHz, DMSO-*d*₆) δ 160.45, 146.16, 138.79,

136.50, 131.46, 128.74, 126.95, 123.40, 122.16, 121.44, 119.73, 119.15, 118.55, 112.26, 103.77, 87.41, 69.41, 61.07, 59.70, 57.08, 45.57, 45.28, 30.23, 29.27, 23.57, 19.56, 5.70, 5.16, 2.60. HRMS m/z found 486.2414 $[M + H]^+$, Calculated 485.2315. IR (ATR, cm^{-1}) ν_{max} 3146, 1633, 1544.97, 1505, 1457, 1341, 1312, 1235, 1173, 1116, 989, 810, 746. % Purity 97.69%.

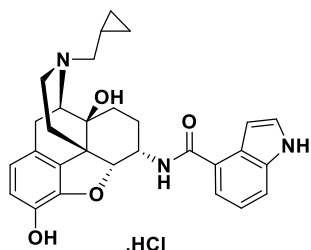
17-Cyclopropylmethyl-3,14 β -dihydroxy-4,5 α -epoxy-6 α -(indole-3-carboxamido)morphinan (2)



The title compound was prepared by following the general procedure in 29% yield.

^1H NMR (400 MHz, $\text{DMSO-}d_6$) δ 11.65 (s, 1H, exchangeable), 9.21 (s, 1H, exchangeable), 8.85 (s, 1H, exchangeable), 8.14(d, $J=2.88$, 1H, exchangeable), 8.11 (d, $J=7.56$, 1H), 7.45 (t, $J=6.68$, 2H), 7.18-7.09 (m, 2H), 6.71 (d, $J=8.08$, 1 H), 6.58 (d, $J=8.12$, 1H), 6.27(s, 1H, exchangeable), 4.80(d, $J=3.8$, 1H), 4.66-4.60(m,1H), 3.91 (d, $J=6.68$, 1H), 3.12-3.05 (m, 2H), 2.95 (m, 1H), 2.74 (m, 1H), 1.90 (m, 1H), 1.66 (d, $J=10.64$, 1H), 1.56-1.44 (m, 2H), 1.11-1.06 (m, 2H), 0.71-0.61 (m, 2H), 0.51-0.40 (m, 2H). ^{13}C NMR (100 MHz, $\text{DMSO-}d_6$) δ 164.32, 145.79, 138.41, 135.91, 128.82, 128.09, 125.73, 122.18, 122.07, 120.62, 119.31, 118.06, 111.90, 110.04, 87.85, 69.23, 60.97, 56.99, 45.13, 44.82, 30.12, 29.16, 23.36, 19.59, 5.55, 5.19, 2.41, 0.012. HRMS m/z found 486.2357 $[M + H]^+$, Calculated 585.2315. IR (ATR, cm^{-1}) ν_{max} 3269, 1667, 1540, 1504, 1459, 1318, 1174, 1118.

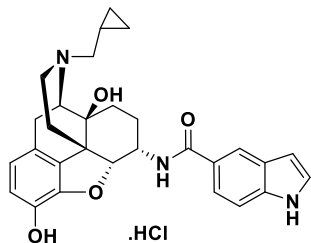
17-Cyclopropylmethyl-3,14β-dihydroxy-4,5α-epoxy-6α-(indole-4-carboxamido)morphinan (3)



The title compound was prepared by following the general procedure in 81% yield.

^1H NMR (400 MHz, $\text{DMSO-}d_6$) δ 11.37 (s, 1H, exchangeable), 9.18 (s, 1H, exchangeable) 8.92 (s, 1H, exchangeable), 7.65 (d, $J=8$, 1H, exchangeable), 7.57 (d, $J=8$, 1H), 7.46-7.44 (m, 2H), 7.16 (t, $J=7.72$, 1H), 6.85 (s, 1H), 6.71 (d, $J=8.04$, 1H), 6.58 (d, $J=8$, 1H), 6.33 (s, 1H, exchangeable), 4.83 (d, $J=3.24$, 1H), 4.66 (m, 1H), 3.94 (d, $J=6.08$, 1H), 3.32 (s, 1H), 3.10 (m, 2H), 3.05 (m, 2H), 2.74 (m, 2H), 1.94 (m, 1H), 1.67 (d, $J=12.92$, 1H), 1.58 (m, 1H), 1.47 (m, 1H), 1.09 (m, 2H), 0.69 (m, 1H), 0.62 (m, 1H), 0.49 (m, 1H), 0.41 (m, 1H). ^{13}C NMR (100 MHz, $\text{DMSO-}d_6$) δ 167, 145.62, 137.71, 136.30, 130.81, 126.53, 126.19, 125.36, 125.20, 120.34, 118.93, 118.77, 117.22, 114.36, 101.16, 88.85, 69.20, 61.27, 58.73, 54.59, 46.52, 45.99, 42.74, 29.27, 22.31, 20.32, 9.03, 3.80, 3.34. HRMS m/z found 486.2391 $[\text{M} + \text{H}]^+$, Calculated 485.2315. IR (ATR, cm^{-1}) ν_{max} 3212, 2152, 1980, 1606, 1505, 1462, 1318, 1118, 771. %Purity 98.96%.

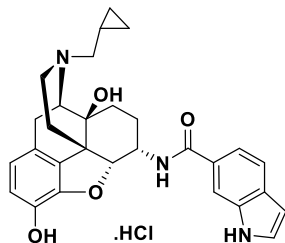
17-Cyclopropylmethyl-3,14β-dihydroxy-4,5α-epoxy-6α-(indole-5-carboxamido)morphinan (4)



The title compound was prepared by following the general procedure in 85% yield.

^1H NMR (400 MHz, $\text{DMSO-}d_6$) δ 11.39 (s, 1H, exchangeable), 9.21 (s, 1H, exchangeable), 8.89 (s, 1H, exchangeable), 8.16 (s, 1H), 7.80 (d, $J=7.76$, 1H), 7.65 (d, $J=8.44$, 1H), 7.44 (d, $J=8.84$, 1H, exchangeable), 7.43 (s, 1H), 6.72 (d, $J=8.04$, 1H), 6.58 (d, $J=8.08$, 1H), 6.55 (s, 1H), 6.37 (s, 1H, exchangeable), 4.79 (d, $J=3.52$, 1H), 4.66-4.61 (m, 1H), 3.95 (d, $J=6.24$, 1H), 3.35 (s, 2H), 3.09-2.98 (m, 4H), 2.73 (m, 2H), 1.97-1.93 (m, 1H), 1.65 (d, $J=12.04$, 1H), 1.56-1.43 (m, 2H), 1.18-1.09 (m, 2H), 0.69-0.62 (m, 2H), 0.50 (m, 1H), 0.41 (m, 1H). ^{13}C NMR (100 MHz, $\text{DMSO-}d_6$) δ 167.01, 146.10, 138.81, 137.43, 128.80, 126.92, 126.64, 125.33, 122.09, 120.66, 120.08, 119.06, 118.34, 110.85, 102.03, 87.55, 69.41, 61.02, 57.02, 45.79, 45.21, 39.54, 30.23, 29.29, 23.54, 19.61, 5.71, 5.17, 2.58. HRMS m/z found 486.2421 $[\text{M} + \text{H}]^+$, Calculated 485.2315. IR (ATR, cm^{-1}) ν_{max} 3147, 1627, 1603, 1522, 1502, 1464, 1351, 1323, 1118, 1036, 771, 755, 726. % Purity 99.99%.

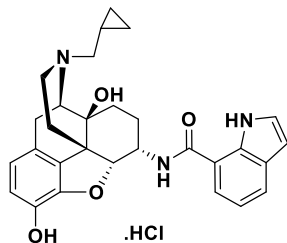
17-Cyclopropylmethyl-3,14 β -dihydroxy-4,5 α -epoxy-6 α -(indole-6-carboxamido)morphinan (5)



The title compound was prepared by following the general procedure in 75% yield.

^1H NMR (400 MHz, $\text{DMSO-}d_6$) δ 11.43 (s, 1H, exchangeable), 9.21 (s, 1H, exchangeable) 8.88 (s, 1H, exchangeable), 7.98 (s, 1H), 7.85 (d, $J=7.72$, 1H, exchangeable), 7.61 (d, $J=8.28$, 1H), 7.54 (dd, $J=1.32,8.28$, 1H), 7.50 (t, $J=2.72$, 1H), 6.73 (d, $J=8.04$, 1H), 6.58 (d, $J=8.12$, 1H) 6.49 (d, $J=1.88$, 1H), 6.35 (s, 1H, exchangeable), 4.81 (d, $J=3.76$, 1H), 4.63 (m, 1H), 3.94 (d, $J=6.76$, 1H), 3.3 (m, 2H), 3.11-3.05 (m, 2H), 2.98 (m, 1H), 2.72 (m, 1H), 1.94 (m, 1H), 1.65 (d, $J=10.96$, 1H), 1.57-1.43 (m, 2H), 1.23-1.09 (m, 3H), 0.71-0.59 (m, 2H), 0.50 (m, 1H), 0.40 (m, 1H). ^{13}C NMR (100 MHz, $\text{DMSO-}d_6$) δ 167.16, 145.92, 138.53, 134.98, 129.89, 128.76, 127.88, 127.01, 122.15, 119.46, 119.24, 118.21, 118.10, 111.31, 101.26, 87.53, 69.29, 61.04, 57.03, 45.73, 45.17, 39.28, 30.17, 29.16, 23.44, 19.44, 5.60, 5.18, 2.49. HRMS m/z found 486.2371 [$\text{M} + \text{H}$] $^+$., Calculated 485.2315. IR (ATR, cm^{-1}) ν_{max} 3225, 2162, 1975, 1605, 1540, 1503, 1318, 1119, 1066, 780, 735. % purity 99.93.

17-Cyclopropylmethyl-3,14β-dihydroxy-4,5α-epoxy-6α-(indole-7-carboxamido)morphinan (6)

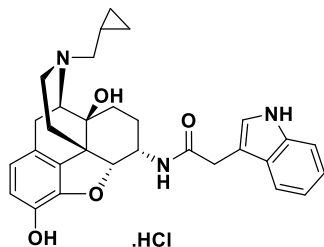


The title compound was prepared by following the general procedure in 22% yield.

^1H NMR (400 MHz, $\text{DMSO-}d_6$) δ 11.13 (s, 1H, exchangeable), 9.25 (s, 1H, exchangeable), 8.91 (s, 1H, exchangeable), 8.14 (d, $J=7.52$, 1H, exchangeable), 7.74 (m, 2H), 7.36 (t, $J=2.72$, 1H), 7.09 (t, $J=7.6$, 1H), 6.71 (d, $J=8.04$, 1H), 6.58 (d, $J=8.12$, 1H), 6.50 (m, 1H), 6.39 (s, 1H, exchangeable), 4.88 (d, $J=3.68$, 1H), 14.70 (m, 1H), 3.95 (d, $J=6.64$, 1H), 3.12-3.04 (m, 3H), 2.94 (m, 1H), 2.73 (m, 2H), 2.00-1.92 (m, 1H), 1.68 (d, $J=11.2$, 1H), 1.56-1.45 (m, 3H), 1.24-1.18 (m, 1H), 1.08 (bs, 1H), 0.70 (m, 1H), 0.62 (m, 1H), 0.50 (m, 1H), 0.41 (m, 1H). ^{13}C NMR (100 MHz, $\text{DMSO-}d_6$) δ 166.63, 145.93, 138.61, 133.95, 129.03, 128.69, 126.40, 123.86, 122.10, 120.24, 119.20, 118.17, 118.06, 116.80, 101.06, 87.30, 69.31, 69.01, 57.00, 45.61, 45.18, 30.22, 29.15, 23.45, 19.27, 5.62, 5.16, 2.53. HRMS m/z found 486.2408 $[\text{M} + \text{H}]^+$, Calculated 485.2315. IR (ATR, cm^{-1}) ν_{max} 3060, 2166, 1634, 1585, 1504, 1456, 1312, 1280, 1123, 1030, 984.

17-Cyclopropylmethyl-3,14 β -dihydroxy-4,5 α -epoxy-6 α -

[2-(indol-3-yl)acetamido)morphinan (7)

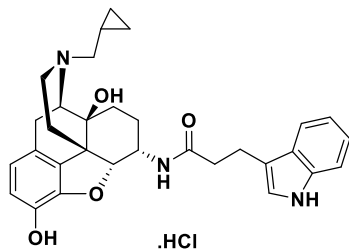


The title compound was prepared by following the general procedure in 80% yield.

^1H NMR (400 MHz, DMSO- d_6) δ 10.85 (s, 1H, exchangeable), 9.20 (s, 1H, exchangeable), 8.78 (s, 1H, exchangeable), 7.80 (d, $J=7.96$, 1H, exchangeable), 7.58 (d, $J=7.92$, 1H), 7.33 (d, $J=8.08$, 1H), 7.20 (d, $J=2.28$, 1H), 7.06 (t, $J=7.50$, 7.58, 1H), 6.96 (t, $J=7.88$, 7.04, 1H), 6.71 (d, $J=8.08$, 1H), 6.56 (d, $J=8.16$, 1H), 6.15 (s, 1H, exchangeable), 4.60 (d, $J=3.88$, 1H), 4.40 (m, 1H), 3.84 (d, $J=6.84$, 1H), 3.58 (s, 2H), 3.37 (s, 2H), 3.07-3.00 (m, 2H), 2.91 (m, 1H), 2.69 (m, 1H), 1.18 (m, 1H), 1.61 (d, $J=10.76$, 1H), 1.40 (q, $J=10.52$, 4.4, 9.92, 2H), 1.10 (m, 2H), 0.68 (m, 1H), 0.59 (m, 1H), 0.46 (m, 1H), 0.39 (m, 1H). ^{13}C NMR (100 MHz, MeOD- d_6) δ 174.63, 185.37, 146.81, 139.41, 138.03, 131.58, 128.34, 126.14, 125.26, 122.75, 120.82, 120.16, 119.49, 118.91, 112.80, 109.25, 90.01, 71.39, 63.20, 60.22, 45.06, 37.47, 34.11, 33.81, 32.11, 29.98, 23.93, 21.85, 9.43, 5.13, 4.01. HRMS m/z found 500.2539 $[\text{M} + \text{H}]^+$. Calculated 499.25. IR (ATR, cm^{-1}) ν_{max} 3218, 1640, 1506, 1317, 1234, 117, 1032, 746. % Purity 95.99%.

17-Cyclopropylmethyl-3,14β-dihydroxy-4,5α-epoxy-6α-

[3-(indol-3-yl) propanamido)morphinan (8)



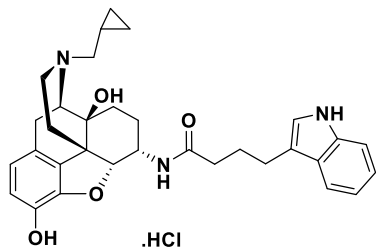
The title compound was prepared by following the general procedure in 55% yield.

¹HNMR (400 MHz, DMSO-*d*₆) δ 10.78 (s, 1H, exchangeable), 9.20 (s, 1H, exchangeable), 8.85 (s, 1H, exchangeable), 7.71 (d, *J*=8.08, 1H exchangeable), 7.53 (d, *J*=7.88, 1H), 7.32 (d, *J*=8.04, 1H), 7.12 (d, *J*=2.16, 1H), 7.05 (t, *J*=7.08, 1H), 6.97 (t, *J*=7.88, 1H), 6.71 (d, *J*=8.08, 1H), 6.55 (d, *J*=8.16, 1H), 6.28 (s, 1H, exchangeable), 4.57 (d, *J*=3.84, 1H), 4.42 (m, 1H), 3.90 (d, *J*=6.8, 1H), 3.25 (m, 1H), 3.17 (s, 2H), 3.07-3.01 (m, 2H), 2.93 (t, *J*=7.72, 3H), 2.74-2.66 (m, 1H), 2.53 (m, 1H), 2.44 (dd, *J*=4.76, 13.36, 1H), 1.90-1.82 (m, 1H), 1.60 (d, *J*=10.92, 1H), 1.42-1.36 (m, 2H), 1.11-1.06 (m, 1H), 0.96-0.90 (m, 1H), 0.70-0.59 (m, 2H), 0.50-0.46 (m, 1H), 0.42-0.37 (m, 1H).

¹³CNMR (100 MHz, DMSO-*d*₆) δ 169.37, 169.29, 143.31, 136.02, 133.54, 126.26, 124.50, 119.45, 118.46, 116.73, 115.85, 115.57, 111.26, 108.78, 85.09, 66.74, 58.46, 54.49, 45.97, 42.61, 42.29, 33.51, 27.59, 26.55, 20.90, 18.48, 17.08, 3.12, 2.70. HRMS *m/z* found 514.2691, [M + H]⁺, Calculated 513.2628. IR (ATR, cm⁻¹) ν_{\max} 3267, 3146, 2157, 1670, 1616, 1543, 1504, 1463, 1427, 1343, 1316, 1172, 1118, 1031

17-Cyclopropylmethyl-3,14β-dihydroxy-4,5α-epoxy-6α-

[4-(indol-3-yl) butanamido)morphinan (9)

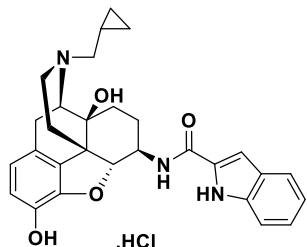


The title compound was prepared by following the general procedure in 34% yield.

$^1\text{H NMR}$ (400 MHz, $\text{DMSO-}d_6$) δ 10.79 (s, 1H, exchangeable), 9.17 (s, 1H, exchangeable), 8.86 (s, 1H, exchangeable), 7.64 (d, $J=8.04$, 1H, exchangeable), 7.51 (d, $J=7.84$, 1H), 7.32 (d, $J=8.04$, 1H), 7.11 (d, $J=2.16$, 1H), 7.05 (t, $J=7.04$, 1H), 7.96 (t, $J=7.88$, 1H), 6.71 (d, $J=8.08$, 1H), 6.54 (d, $J=8.12$, 1H), 6.29 (s, 1H, exchangeable), 4.59 (d, $J=3.88$, 1H), 4.45-4.38 (m, 1H), 3.91 (d, $J=6.8$, 1H), 3.32 (d, $J=19.72$, 1H), 3.25 (m, 1H), 3.02 (m, 2H), 2.96 (m, 1H), 2.69 (t, $J=7.4$, 3H), 2.43 (dd, $J=4.92$, 13.32, 1H), 2.22 (t, $J=7.32$, 2H), 1.92-1.83 (m, 1H), 1.60 (d, $J=13.16$, 1H), 1.38 (m, 2H), 1.07 (m, 1H), 0.99-0.87 (m, 1H), 0.69-0.59 (m, 2H), 0.50-0.45 (m, 1H), 0.41-0.36 (m, 1H).

$^{13}\text{C NMR}$ (100 MHz, $\text{DMSO-}d_6$) δ 173.08, 146.69, 139.36, 137.00, 129.64, 127.98, 123.04, 122.95, 121.78, 120.15, 119.20, 119.07, 118.97, 115.05, 112.19, 88.45, 70.11, 61.85, 57.90, 45.98, 45.66, 35.98, 30.97, 29.95, 27.11, 25.11, 24.28, 20.41, 15.92, 6.46, 6.08, 3.34. HRMS m/z found 528.2876, 556.2742, 1055.5772 $[\text{M} + \text{H}]^+$, Calculated 527.2784. IR (ATR, cm^{-1}) ν_{max} 3267, 3124, 2162, 1671, 1623, 1506, 1456, 1373, 1119

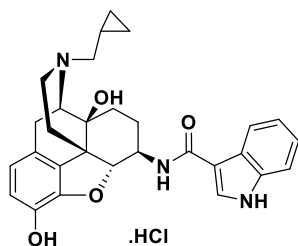
17-Cyclopropylmethyl-3,14β-dihydroxy-4,5α-epoxy-6β-(indole-2-carboxamido)morphinan (10)



The title compound was prepared by following the general procedure in 32% yield.

^1H NMR (400 MHz, DMSO- d_6) δ 11.60 (s, 1H, exchangeable), 9.33 (s, 1H, exchangeable) 8.88 (s, 1H, exchangeable), 8.73 (d, $J=7.92$, 1H, exchangeable), 7.62 (d, $J=7.96$, 1H), 7.42 (d, $J=8.24$, 1H), 7.18 (m, 2H), 7.04 (t, $J=7.52$, 1H), 6.73 (d, $J=8.08$, 1H), 6.66 (d, $J=7.96$, 1H), 6.24 (s, 1H, exchangeable), 4.84 (d, $J=7.72$, 1H), 3.89 (s, 1H), 3.71 (m, 1H), 3.33 (m, 2H), 3.11-3.06 (m, 2H), 2.88 (m, 1H), 2.50 (m, 2H), 1.96-1.78 (m, 2H), 1.63 (m, 1H), 1.49-1.40 (m, 2H), 1.09 (s, 1H), 0.68 (s, 1H), 0.60 (s, 1H), 0.52 (s, 1H), 0.42 (s, 1H). ^{13}C NMR (100 MHz, DMSO- d_6) δ 160.73, 142.02, 141.09, 136.23, 131.30, 129.62, 126.97, 125.26, 123.46, 121.52, 120.64, 119.83, 119.39, 117.87, 112.23, 102.63, 89.85, 69.62, 61.67, 56.69, 50.66, 46.37, 45.61, 29.37, 23.78, 22.91, 5.62, 5.07, 2.55. HRMS m/z found 486.2411 $[\text{M} + \text{H}]^+$, Calculated 485.2315. IR (ATR, cm^{-1}) ν_{max} 3212, 2167, 1975, 1617, 1551, 1506, 1315, 1239, 1125, 1034, 815, 747, 668. % Purity 96.75%.

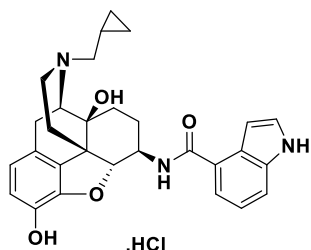
17-Cyclopropylmethyl-3,14β-dihydroxy-4,5α-epoxy-6β-(indole-3-carboxamido)morphinan (11)



The title compound was prepared by following the general procedure in 27% yield.

^1H NMR (400 MHz, $\text{DMSO-}d_6$) δ 11.64 (s, 1H, exchangeable), 9.34 (bs, 1H, exchangeable), 8.89 (s, 1H, exchangeable), 8.13-8.10 (m, 3H, 1 proton exchangeable), 7.42 (d, $J=7.88$, 1H), 7.16-7.06 (m, 2H), 6.73 (d, $J=8.08$, 1H), 6.65 (d, $J=8.12$, 1H), 6.24 (s, 1H, exchangeable), 4.82 (d, $J=7.76$, 1H), 3.90 (s, $J=4.28$, 1H), 3.70 (m, 1H), 3.36 (s, 1H), 3.12-3.05 (m, 3H), 2.88 (m, 2H), 1.89 (q, $J=12.32$, 1H), 1.78 (d, $J=13.2$, 1H), 1.63 (m, 1H), 1.48-1.41 (m, 2H), 1.22 (bs, 1H), 0.68 (m, 1H), 0.50 (m, 1H), 0.52 (m, 1H), 0.42 (m, 1H). ^{13}C NMR (100 MHz, $\text{DMSO-}d_6$) δ 164.46, 142.18, 141.03, 135.90, 129.70, 127.60, 125.86, 121.98, 120.89, 120.63, 120.43, 119.29, 117.89, 111.79, 110.30, 90.17, 69.69, 61.70, 56.70, 50.21, 46.38, 45.60, 29.40, 27.30, 23.99, 22.93, 5.61, 5.12, 2.53. HRMS m/z found 486.2411 $[\text{M} + \text{H}]^+$, Calculated 485.2315. IR (ATR, cm^{-1}) ν_{max} 3267, 1671, 1621, 1539, 1505, 1455, 1313, 1176, 1119

17-Cyclopropylmethyl-3,14β-dihydroxy-4,5α-epoxy-6β-(indole-4-carboxamido)morphinan (12)

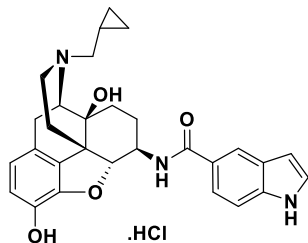


The title compound was prepared by following the general procedure in 31% yield.

^1H NMR (400 MHz, $\text{DMSO-}d_6$) δ 11.31 (s, 1H, exchangeable), 9.34 (s, 1H, exchangeable), 8.87 (bs, 1H, exchangeable), 8.39 (d, $J=8.12$, 1H, exchangeable), 7.55 (d, $J=8.04$, 1H), 7.48 (d, $J=7.16$, 1H), 7.43 (m, 1H), 7.15 (t, $J=7.72$, 1H), 6.88 (s, 1H), 6.73 (d, $J=8.12$, 1H), 6.66 (d, $J=8.16$, 1H), 6.19 (s, 1H, exchangeable), 4.89 (d, $J=7.76$, 1H), 3.88 (d, $J=4.92$, 1H), 3.77-3.72 (m, 1H), 3.32 (m, 1H), 3.13-3.04 (m, 2H), 2.87 (m, 1H), 1.93 (q, $J=12.08$, 1H), 1.78 (d, $J=13.68$, 1H), 1.65 (m, 1H), 1.46 (m, 2H), 1.09 (t, $J=6.96$, 2H), 0.70-0.68 (m, 1H), 0.60 (m, 1H), 0.53-0.50 (m, 1H), 0.43-0.41 (m, 1H).

^{13}C NMR (100 MHz, $\text{DMSO-}d_6$) δ 167.77, 142.15, 141.02, 136.35, 129.67, 126.30, 126.09, 125.75, 120.64, 120.19, 119.34, 118.50, 117.90, 114.31, 101.78, 89.92, 69.68, 61.68, 56.68, 50.89, 46.37, 45.61, 29.43, 27.29, 23.66, 22.90, 5.58, 5.11, 2.50. HRMS m/z found 486.2434 $[\text{M} + \text{H}]^+$, Calculated 485.2315. IR (ATR, cm^{-1}) ν_{max} 3207, 2166, 1639, 1503, 1455, 1319, 1237, 1195, 1123, 1037, 917.

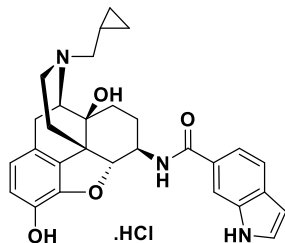
17-Cyclopropylmethyl-3,14β-dihydroxy-4,5α-epoxy-6β-(indole-5-carboxamido)morphinan (13)



The title compound was prepared by following the general procedure in 61% yield.

^1H NMR (400 MHz, $\text{DMSO-}d_6$) δ 11.36 (s, 1H, exchangeable), 9.32 (s, 1H, exchangeable) 8.88 (s, 1H, exchangeable), 8.48 (d, $J=8.08$, 1H, exchangeable), 8.18 (s, 1H), 7.66 (dd, $J=1.56, 8.56$, 1H), 7.42 (m, 2H), 6.73 (d, $J=8.12$, 1H), 6.65 (d, $J=8.16$, 1H), 6.53 (s, 1H), 6.20 (s, 1H, exchangeable), 4.89 (d, $J=7.8$, 1H), 3.88 (s, 1H), 3.71 (m, 1H), 3.35 (s, 2H), 3.11-3.04 (m, 2H), 2.87 (m, 1H), 1.90 (q, $J=12.6$, 1H), 1.78 (d, $J=13.76$, 1H), 1.62 (m, 1H), 1.49-1.39 (m, 2H), 1.09 (m, 1H), 0.68 (m, 1H), 0.59 (m, 1H), 0.52 (m, 1H), 0.42 (m, 1H). ^{13}C NMR (100 MHz, $\text{DMSO-}d_6$) δ 166.77, 142.30, 141.30, 137.41, 129.77, 126.99, 126.60, 125.29, 120.56, 120.49, 119.91, 119.16, 117.92, 110.80, 102.05, 90.06, 69.80, 61.81, 56.74, 51.11, 46.52, 45.62, 29.44, 27.41, 23.93, 23.06, 5.72, 5.09, 2.65. HRMS m/z found 486.2434 $[\text{M} + \text{H}]^+$, Calculated 485.2315. IR (ATR, cm^{-1}) ν_{max} 3125, 2162, 1980, 1622, 1595, 1547, 1360, 1311, 1249, 1124, 1037, 919, 760, 672. % Purity 98.51%.

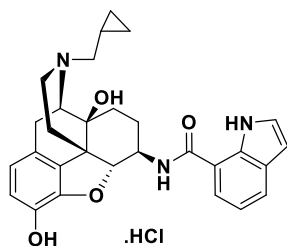
17-Cyclopropylmethyl-3,14β-dihydroxy-4,5α-epoxy-6β-(indole-6-carboxamido)morphinan (14)



The title compound was prepared by following the general procedure in 29% yield.

^1H NMR (400 MHz, $\text{DMSO-}d_6$) δ 11.43 (s, 1H, exchangeable), 9.33 (s, 1H, exchangeable) 8.87 (s, 1H, exchangeable), 8.54(d, $J=7.4$, 1H, exchangeable), 7.99 (s, 1H), 7.58 (s, 2H), 7.50 (s, 1H), 6.73 (d, $J=6.36$, 1H), 6.66 (d, $J=7.68$, 1H), 6.49 (s, 1H), 6.20 (s, 1H, exchangeable), 4.90 (d, $J=5.92$, 1H), 3.88 (s, 1H), 3.71 (s, 1H), 3.17-3.06 (m, 2H), 2.89 (m, 2H), 2.5 (s, 1H), 1.90 (m, 1H), 1.78 (d, $J=12.32$, 1H), 1.62 (d, $J=10.56$, 1H), 1.49-1.39 (m, 2H), 1.09 (t, $J=6.52$, 2H), 0.68 (s, 1H), 0.60 (s, 1H), 0.52 (s, 1H), 0.42 (s, 1H). ^{13}C NMR (100 MHz, $\text{DMSO-}d_6$) δ 166.85, 142.16, 140.23, 135.05, 129.76, 127.74, 127.20, 119.34, 118.39, 117.95, 116.98, 111.16, 101.20, 90.74, 69.62, 61.76, 58.35, 51.50, 49.99, 39.96, 39.76, 30.60, 29.99, 24.65, 22.25, 3.72, 3.46. HRMS m/z found 486.2396 $[\text{M} + \text{H}]^+$., Calculated 485.2315. IR (ATR, cm^{-1}) ν_{max} 3223, 2152, 1970, 1608, 1551, 1312, 1035, 920, 820, 740. % Purity 99.86%.

17-Cyclopropylmethyl-3,14β-dihydroxy-4,5α-epoxy-6β-(indole-7-carboxamido)morphinan (15)

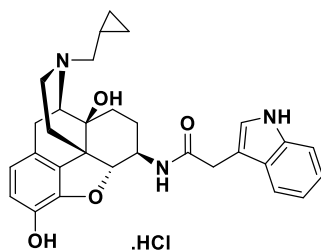


The title compound was prepared by following the general procedure in 56% yield.

^1H NMR (400 MHz, $\text{DMSO-}d_6$) δ 11.07 (s, 1H, exchangeable), 9.37 (s, 1H, exchangeable), 8.90 (s, 1H, exchangeable), 8.75 (d, $J=8.04$, 1H, exchangeable), 7.78-7.75 (dd, $J=4.24$, 3.12, 2H), 7.35 (t, $J=2.6$, 1H), 7.10 (t, $J=7.6$, 1H), 6.74 (d, $J=8.12$, 1H), 6.67 (d, $J=8.16$, 1H), 6.49 (m, 1H), 6.26 (bs, 1H, exchangeable), 4.93 (d, $J=7.8$, 1H), 3.91 (d, $J=4.84$, 1H), 3.82-3.78 (m, 2H), 3.18-3.06 (m, 3H), 2.91-2.86 (m, 1H), 2.02-1.93 (q, $J=11.56$, 1H), 1.65 (m, 1H), 1.56-1.41 (m, 2H), 1.10 (t, $J=7$, 2H), 0.71-0.68 (m, 1H), 0.62-0.60 (m, 1H), 0.55-0.52 (m, 1H), 0.44-0.42 (m, 1H). ^{13}C NMR (100 MHz, $\text{DMSO-}d_6$) δ 164.50, 139.51, 138.46, 131.48, 127.15, 126.67, 123.95, 121.72, 118.20, 117.28, 117.02, 115.79, 115.40, 113.77, 98.68, 87.35, 67.21, 62.45, 59.20, 54.25, 48.23, 43.86, 43.16, 26.96, 24.75, 21.14, 20.39, 12.43, 3.07, 2.65. HRMS m/z found 486.2411 [$\text{M} + \text{H}$] $^+$, Calculated 485.2315. IR (ATR, cm^{-1}) ν_{max} 3090, 2162, 1979, 1633, 1540, 1327, 1248, 1040

17-Cyclopropylmethyl-3,14 β -dihydroxy-4,5 α -epoxy-6 β -

[2-(indol-3-yl)acetamido)morphinan (16)

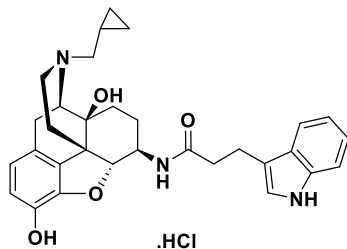


The title compound was prepared by following the general procedure in 49% yield.

^1H NMR (400 MHz, $\text{DMSO-}d_6$) δ 10.89 (s, 1H, exchangeable), 9.32 (s, 1H, exchangeable), 8.82 (s, 1H, exchangeable), 8.20 (d, $J=7.92$, 1H, exchangeable), 7.54 (d, $J=7.76$, 1H), 7.34 (d, $J=8.04$, 1H), 7.18 (d, $J=2.08$, 1H), 7.06 (t, $J=7.08$, 1H), 6.98 (t, $J=7.24$, 1H), 6.70 (d, $J=8.12$, 1H), 6.62 (d, $J=8.16$, 1H), 6.14 (s, 1H, exchangeable), 4.60 (d, $J=7.84$, 1H), 3.82 (d, $J=5.2$, 1H), 3.50 (q, $J=14.96$, 2H), 3.40 (m, 1H), 3.32 (m, 1H), 3.28 (s, 1H), 3.07-3.01 (dd, $J=5.96, 19.24$, 2H), 2.84 (m, 1H), 2.43-2.39 (m, 2H), 1.68 (m, 2H), 1.49-1.28 (m, 3H), 1.07 (m, 1H), 0.67-0.66 (m, 1H), 0.60-0.56 (m, 1H), 0.51-0.48 (m, 1H), 0.41-0.39 (m, 1H). ^{13}C NMR (100 MHz, $\text{DMSO-}d_6$) δ 170.94, 170.86, 141.99, 140.99, 135.88, 129.55, 127.03, 123.57, 121.02, 120.58, 119.36, 118.53, 118.42, 117.83, 111.28, 108.49, 99.49, 69.56, 61.54, 56.62, 46.32, 45.49, 32.78, 29.17, 27.21, 23.45, 22.82, 5.55, 5.08, 2.46. HRMS m/z found 500.2539 $[\text{M} + \text{H}]^+$, Calculated 499.2471. IR (ATR, cm^{-1}) ν_{max} 3270, 1666, 1549, 1463, 1303, 1274, 1232, 1174, 1124, 1030, 898

17-Cyclopropylmethyl-3,14β-dihydroxy-4,5α-epoxy-6β-

[3-(indol-3-yl) propanamido)morphinan (17)

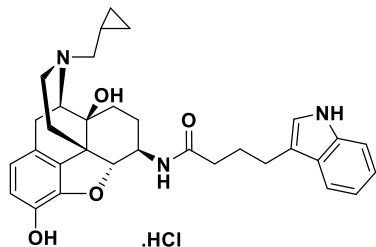


The title compound was prepared by following the general procedure in 70% yield.

^1H NMR (400 MHz, $\text{DMSO-}d_6$) δ 10.77 (s, 1H, exchangeable), 9.34 (s, 1H, exchangeable), 8.83 (s, 1H, exchangeable), 8.14 (d, $J=7.8$, 1H, exchangeable), 7.52 (d, $J=7.8$, 1H), 7.32 (d, $J=8.04$, 1H), 7.10 (s, 1H), 7.06 (t, $J=7.96$, 1H), 6.97 (t, $J=7.88$, 1H), 6.72 (d, $J=8.12$), 6.63 (d, $J=8.16$, 1H), 6.18 (s, 1H, exchangeable), 4.55 (d, $J=7.8$, 1H), 3.85 (s, 1H), 3.45 (m, 1H), 3.34-3.29 (m, 2H), 3.09-3.00 (m, 2H), 2.92-2.83 (m, 3H), 2.45-2.42 (m, 4H), 1.71-1.68 (m, 2H), 1.53-1.50 (m, 1H), 1.42 (d, $J=9.76$, 1H), 1.33 (t, $J=12.32$, 1H), 1.08 (m, 1H), 0.68-0.63 (m, 1H), 0.60-0.57 (m, 1H), 0.52-0.48 (m, 1H), 0.42-0.38 (m, 1H). ^{13}C NMR (100 MHz, $\text{DMSO-}d_6$) δ 141.98, 140.93, 135.97, 129.53, 126.86, 121.96, 120.98, 120.64, 119.41, 118.26, 117.89, 113.57, 111.27, 89.91, 69.58, 61.58, 56.67, 50.47, 46.31, 45.49, 39.62, 29.21, 27.21, 23.43, 22.83, 20.85, 5.55, 5.11, 2.47, 0.012. HRMS m/z found 514.2714, $[\text{M} + \text{H}]^+$, Calculated 513.2628. IR (ATR, cm^{-1}) ν_{max} 3187, 2160, 1640, 1541, 1505, 1450, 1325, 1271, 1234, 1124, 1032, 854

17-Cyclopropylmethyl-3,14β-dihydroxy-4,5α-epoxy-6β-

[4-(indol-3-yl) butanamido)morphinan 18

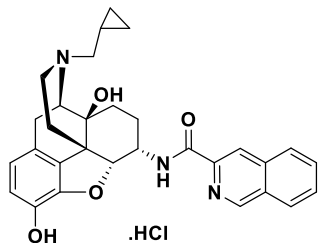


The title compound was prepared by following the general procedure in 39% yield.

¹HNMR (400 MHz, DMSO-*d*₆) δ , 10.79 (s, 1H, exchangeable), 9.35 (bs, 1H, exchangeable), 8.84 (s, 1H, exchangeable), 8.09 (d, *J*=7.88 1H, exchangeable), 7.51 (d, *J*=7.84, 1H), 7.33 (d, *J*=8.04, 1H), 7.12 (d, *J*=2.08, 1H), 7.08 (t, *J*=7.46, 1H), 6.97 (t, *J*=7.42, 1H), 6.72 (d, *J*=8.12, 1H), 6.64 (d, *J*=8.16, 1H), 6.18 (bs, *J*=1H, exchangeable), 4.56 (d, *J*=7.84, 1H), 3.85 (d, *J*=4.84, 1H), 3.09-3.03 (dd, *J*=5.88, 19.48, 2H), 2.88-2.84 (m, 1H), 2.68 (t, *J*=7.48, 2H), 2.44-2.41 (m, 2H), 2.16 (t, *J*=7.32, 2H), 1.89-1.85 (m, 2H), 1.75-1.70 (m, 2H), 1.56-1.53 (m, 1H), 1.43 (d, *J*=9.68, 1H), 1.38-1.31 (m, 1H), 1.12-1.05 (m, 2H), 0.69-0.67 (m, 1H), 0.61-0.58 (m, 1H), 0.53-0.50 (m, 1H), 0.43-0.40 (m, 1H).

¹³CNMR (100 MHz, DMSO-*d*₆) δ 142.02, 140.99, 136.07, 129.56, 127.05, 122.03, 120.88, 120.60, 119.35, 118.28, 118.18, 117.87, 114.11, 111.27, 89.88, 69.59, 67.88, 61.59, 56.65, 50.44, 46.33, 45.49, 29.24, 27.22, 26.15, 24.05, 23.53, 22.85, 15.00, 5.56, 5.10, 2.48. HRMS *m/z* found 528.2874 [M + H]⁺., Calculated 527.2784. IR (ATR, cm⁻¹) ν_{\max} 3268, 1671, 1633, 1505, 1455, 1423, 1316, 1178, 1127, 1033

17-Cyclopropylmethyl-3,14β-Dihydroxy-4,5α-Epoxy-6α-(Isoquinoline-3-Carboxamido)morphinan (NAQ)



^1H NMR (400 MHz, $\text{DMSO-}d_6$) δ 9.44 (s, 1H), 8.98 (bs, 1H, exchangeable), 8.65 (s, 1H), 8.57 (d, $J=8.76$, exchangeable), 8.28 (d, $J=8.08$, 1H), 8.24 (d, $J=8.08$, 1H), 7.94 (t, $J=8.04$, 1H), 7.85 (d, $J=8$, 1H), 6.80 (d, $J=8.04$, 1H), 6.60 (d, $J=8.16$, 1H), 4.80 (d, $J=3.76$, 1H), 4.77-4.70 (m, 1H), 4.03 (d, $J=6.68$, 1H), 3.38 (d, $J=19.68$, 1H), 3.31-3.25 (m, 1H), 3.13-3.02 (m, 3H), 2.78-2.72 (m, 1H), 2.57 (dd, $J=4.76, 13.6$, 1H), 2.04-1.98 (m, 1H), 1.68-1.65 (m, 2H), 1.50-1.44 (m, 1H), 1.14-1.02 (m, 2H), 0.72-0.66 (m, 1H), 0.65-0.62 (m, 1H), 0.53-0.50 (m, 1H), 0.43-0.41 (m, 1H). ^{13}C NMR (100 MHz, $\text{DMSO-}d_6$) δ 163.46, 151.54, 145.32, 141.94, 138.54, 135.30, 132.08, 129.72, 129.12, 128.66, 128.07, 127.91, 122.03, 120.21, 119.73, 118.12, 87.44, 69.21, 57.05, 48.43, 45.27, 45.17, 45.07, 29.92, 28.87, 23.31, 19.82, 5.50, 5.19, 2.38. HRMS m/z found 498.2461 $[\text{M} + \text{H}]^+$, Calculated 497.2315. IR (ATR, cm^{-1}) ν_{max}

6.3 Instruments used for characterization

The Bruker 400 MHz NMR was used to determine the ^1H and ^{13}C NMR spectra of the compounds. The masspec and IR spectra were determined using the Perkin Elmer ToF mass spectrometer and Thermo Scientific smart iTR instruments, respectively. The purity of the compounds was determined using Varian Prostar HPLC instrument. The HPLC parameters used were: column= C18, injection volume=5 μL , sample

concentration= 3mM, mobile phase=60 H₂O : 40 MeCN, flowrate=1 mL/min, detector= UV detection at 210 and 254 nm.

6.4 Pharmacological assays

Pharmacological assays were conducted to determine the binding affinity, selectivity and functional activity of the synthesized compounds. Chinese hamster ovary (CHO) cells expressing MOR, KOR and DOR were used in this assay. These cells were cultured in Dr. Selley's laboratory in the department of Pharmacology and Toxicology at VCU. For the in vivo study, male Swiss Webster mice were used for both the warm-water immersion and opioid withdrawal assays. The mice weighed 23-35 g and were housed five to a cage in animal care quarters maintained at 22 °C on a 12 hour light-dark cycle with food and water available ad libitum. The mice were transferred to the test room and the tests were then conducted 18 hours later. Protocols and procedures were approved by the Institutional Animal Care and Use Committee at Virginia Commonwealth University Medical Center and complied with the recommendations of the International Association for the Study of Pain.

6.4.1 Cell culture

Cells obtained from the -80 °C freezer were thawed by warming by hand. The cells were then transferred into a culture dish containing 10 mL of culture media. The culture media used for MOR CHO cells contained 500 mL DMEM/F12 media, 10% FBS, 1% penicillin/streptomycin, and 2.75 mL G418. The DOR and KOR CHO cells were cultured in the same media except that 5% FBS was used instead of 10%. The cells are placed in an incubator set at 30 °C with 5% CO₂ and 95% humidity for 24 hours. The old media containing DMSO is then replaced with fresh culture media that does not contain

DMSO. The cells are allowed to grow until they are 80-95% confluent after which they are split. The splitting is done by first aspirating the old media and then rinse the cells with 5 mL PBS. 3 mL trypsin is then added and the cells are placed in the incubator for 5 mins or until all cells are detached. The trypsin is then aspirated and the cells are suspended in 1 mL cell culture media. Aliquots of the cells suspended in media is then transferred to new culture dish containing 10 mL cell media. The cells are then placed in the incubator and the media changed regularly. During the next splitting, the size of the culture dishes are changed from (100 mm x 20 mm) to (150 mm x 25mm). The cells are continuously split while increasing the culture dishes until there are enough culture dishes (16) for harvesting.

6.4.2 Cell membrane harvesting

This step does not need sterile conditions. Once the cells in the large culture dishes are very confluent, the old media is aspirated and the cells are rinsed with 5 mL PBS. 5 mL PBS is added to each dish and the cells are then scraped off the dishes using a scraper and then transferred into a 50 mL centrifuge tube. The cells are then centrifuged at 1000 x g for 10 minutes. After centrifugation, the supernatant is poured out and membrane buffer (50 mM Tris, 3 mM MgCl₂, and 1 mM EGTA, pH 7.4) is added to the tube. The cells are then homogenized and then centrifuged again at 50000 x g for 10 minutes. The supernatant is poured away and the cells homogenized again in membrane buffer. A Bradford assay is conducted to determine the concentration of the membrane protein which are then aliquoted making sure each Eppendorf tube contains 3 mg of membrane protein. The membrane protein preparations are the stored at -80 °C.

6.4.3 Competition binding assay

The competition binding assay was conducted to determine the affinity and selectivity of the synthesized compounds to MOR over KOR and DOR. [³H]NLX was used to label MOR whilst [³H]DPN was used to label both DOR and KOR. The K_d and B_{max} values for [³H]NLX at MOR and [³H]DPN at KOR had been determined previously in Dr. Selley's laboratory. The K_d and B_{max} values for [³H]DPN at DOR were determined using varying concentrations of [³H]DPN and fixed a concentration of 30 μ g DOR membrane protein and 5 μ M SNC80. The potency of the drugs in displacing the specific binding of the radioligand was determined by linear regression analysis of Hill plots. Specific (i.e., opioid receptor-related) binding at MOR, KOR and DOR was determined as the difference in binding obtained in the absence and presence of 5 μ M naltrexone, U50,488 and SNC80, respectively. The IC_{50} values were determined and converted to K_i values using the Cheng–Prusoff equation.²¹⁵ This assay was performed as described below.

50 mL tubes containing distilled water, membrane buffer, TME (50 mM Tris, 3 mM $MgCl_2$, and 0.2 mM EGTA adjusted to 7.7 pH) buffer (without NaCl) respectively were put in an ice bucket filled with ice. The membrane protein preparations were obtained from the -80 °C freezer, thawed, and then transferred to a spin tubes containing 4 mL membrane buffer. The membrane preparations have to be kept on ice all the time. The membrane protein preparations were then homogenized, 2 mL membrane buffer is used to rinse the homogenizer, the membrane preparations were then centrifuged at 50000 x g for 10 mins. After centrifugation, the supernatant is poured away and then 4 mL of TME buffer (without NaCl) was added to the membrane protein pellet. The

membrane protein was homogenized and the homogenizer was rinsed with 2 mL TME buffer (without NaCl). The Bradford assay was then conducted to determine the concentration of the membrane protein. In Bradford assay, varying concentrations of BSA were used to construct a standard curve which was used to determine the concentration of the membrane protein preparations. Distilled water was used to dilute BSA. A stock solution 10 times the desired concentration of the radioligand was prepared and placed on ice. A stock solution 10 times the desired concentration of the compound used for non-specific binding was prepared and placed on ice. Test-tubes were added to the test-tube rack and labeled accordingly. Three sets of test-tube racks were used, one for the drug curve, one for the experiment, and another for incubation. Drug dilutions of the compounds (naltrexamine analogs) and the membrane protein were made accordingly. The desired amount of the protein per tube was 30 µg. All concentrations prepared were 10 times the desired amount since there was a 10-fold dilution when compounds were added to the experimental rack. TME buffer (without NaCl) was used for all the dilutions required. Once all the protein, radioligand, compound dilutions, and nonspecific concentrations were made, 300 mL TME buffer (without NaCl) was added to each of the test-tubes for the experimental rack. 50 µl of non-specific compound and naltrexamine analog compounds were added to their respective test-tubes in the experimental racks. 50 µl radioligand was then added to all the test-tubes and to 3 scintillation vials (these vials will be used as standards). 4 mL Scintillation fluid was then added to these vials. Finally, 100 µl of membrane protein was added to all the test-tubes to afford a total volume of 500 µl. All the test-tubes were then vortexed, rearranged in the test-tube racks for incubation and placed in the shaking

water bath at 30 °C for 90 minutes. The blue racks were filled with scintillation vials making sure the first and last slots are left open. 10 minutes before incubation was complete, the tubes of Brandel harvester were rinsed with 70% ethanol then distilled water. GF/B glass filter paper was then fixed onto the harvester and rinsed with cold Tris buffer. After 90 minutes of incubation, the bound radioligand was filtered and rinsed three times with cold Tris buffer. The filtered bound radioligand was then transferred into the scintillation tubes and the tubes were then filled with 4 mL of scintillation fluid and capped. The scintillation tubes were labelled and the bound radioligand was quantified using the liquid scintillation counter. Counting was delayed for 9 hrs to allow the radioactivity to get into solution. The percentage of bound radioligand was calculated using excel which was then subjected to nonlinear regression analysis to determine the IC₅₀ values with Prism 6.0 software (GraphPad Software, San Diego, CA).. The K_i values were determined from the IC₅₀ values using the Cheng-Prusoff equation [$K_i = IC_{50}/(1+(L^*/K_d^*))$]. The assay was performed in triplicates and repeated at least three times.

6.4.4 [³⁵S]GTP_γS functional assay

The [³⁵S]GTP_γS functional assay was used to determine the relative efficacy of the synthesized compounds. Agonists result in activation of GPCRs upon binding to the receptor. The agonist's activity of the compounds was measured relative to 3 μM DAMGO at MOR since DAMGO is a full agonist at MOR. In this assay, upon receptor activation due to agonist binding, [³⁵S]GTP_γS binds to the Gα subunit. Thus, [³⁵S]GTP_γS replaces endogenous GTP and since the γ-thiophosphate bond is resistant to hydrolysis by GTPase, [³⁵S]GTP_γS labelled Gα subunits accumulate and can be quantified by

measuring the amount of incorporated [³⁵S].²²⁹ The assay was performed as described below.

50 mL tubes containing distilled water, membrane buffer, TME (50 mM Tris, 3mM MgCl₂, 0.2 mM EGTA, and 100 mM NaCl adjusted to pH 7.7) buffer (with NaCl) respectively were put in an ice bucket filled with ice. The membrane protein preparations were obtained from the -80 °C freezer, thawed, and then transferred to a spin tubes containing 4 mL membrane buffer. The membrane preparations have to be kept on ice all the time. The membrane protein preparations were then homogenized, 2 mL membrane buffer was used to rinse the homogenizer, the membrane preparations were then centrifuged at 50000 x g for 10 mins. After centrifugation, the supernatant was poured away and then 4 mL of TME buffer (with NaCl) was added to the membrane protein pellet. The membrane protein was homogenized and the homogenizer rinsed with 2 mL TME buffer (with NaCl). The Bradford assay was then conducted to determine the concentration of the membrane protein. In Bradford assay, varying concentrations of BSA were used to construct a standard curve which was used to determine the concentration of the membrane protein preparations. Distilled water was used to dilute BSA. A stock solution 10 times the desired concentration of [³⁵S]GTP γ S was prepared by adding a specific volume of TME buffer (with NaCl) (the volume of buffer used depends on the calibration date of [³⁵S]GTP γ S) to the 15 ml vials containing pre-aliquoted [³⁵S]GTP γ S. 50 μ L of [³⁵S]GTP γ S was then transferred into three scintillation vials and then filled with 4 mL of scintillation fluid. The radioactivity was determined using the liquid scintillation counter. The DPM per tube was initially measured to make sure the value was between 115000 and 135000 before the assay

was continued. A stock solution 10 times the desired concentration of cold GTP γ S used for non-specific binding was prepared and placed on ice. A stock solution 10 times the desired concentration of DAMGO and GDP were made and also placed on ice. Test-tubes were added to the test-tube rack and labeled accordingly. Three sets of test-tube racks were used, one for the drug curve, one for the experiment, and another for incubation. Drug dilutions of the compounds (naltrexamine analogs) and the membrane protein were made accordingly. The desired amount of the protein per tube was 10 μ g. All concentrations prepared were 10 times the desired amount since there was a 10-fold dilution when compounds were added to the experimental rack. TME buffer (with NaCl) was used for all the dilutions required. Once all the protein, [35 S]GTP γ S, GDP, cold GTP γ S, and compound dilutions were made, 250 mL TME buffer (with NaCl) was added to each of the test-tubes in the experimental racks. 50 μ L of GDP was also added to all the test-tubes in the experimental racks. 50 μ L of cold GTP γ S and naltrexamine analog compounds were also added to their respective test-tubes in the experimental racks. 50 μ L [35 S]GTP γ S was then added to all the test-tubes and to 3 scintillation vials (these vials will be used as standards). 4 mL Scintillation fluid was then added to these vials. Finally, 100 μ L of membrane protein was added to all the test-tubes to afford a total volume of 500 μ L. All the test-tubes were then vortexed, rearranged into the test-tube rack for incubation and placed in the shaking water bath at 30 °C for 90 minutes. The blue racks were filled with scintillation vials making sure the first and last slots are left open. 10 minutes before incubation was complete, the tubes of Brandel harvester were rinsed with 70% ethanol then distilled water. GF/B glass filter paper was then fixed onto the harvester and rinsed with cold Tris buffer. After 90 minutes of incubation, the bound

radioligand was filtered and rinsed three times with cold Tris buffer. The filtered bound radioligand was then transferred into the scintillation tubes using the puncher/filler and the tubes were then filled with 4 mL of scintillation fluid and capped. The scintillation tubes were labelled and the bound radioligand was quantified using the liquid scintillation counter. Counting was delayed for 9 hrs to allow the radioactivity to get into solution. Percent DAMGO stimulation was defined as (net stimulated binding of test compound/ net stimulated binding of DAMGO) x 100%. The normalized data were then subjected to nonlinear regression analysis to determine EC₅₀ and E_{max} values using Prism 6.0 software (GraphPad Software, San Diego, CA). The assay was performed in triplicates and repeated at least three times.

6.4.5 warm-water immersion assay

Antinociception for the 6 α / β -naltrexamine derivatives was determined using the warm-water tail immersion assay described by Coderre and Rollman.²³⁰ The assay was conducted using male Swiss Webster mice. The a water bath temperature was maintained at 56 \pm 0.1 °C. The baseline latency (control) was determined before injecting the compounds into the mice. The average baseline latency obtained for this experiment was 3.0 \pm 0.1 s and only mice with a baseline latency of 2 to 4 s were used. To test for agonism, the tail immersion was done 20 min (time that morphine effect starts to peak) after injecting the indole analogs of 6 α / β -naltrexamine. To prevent tissue damage, a 10 s maximum cut off time was imposed. Antinociceptive response was calculated as the percentage maximum possible effect (%MPE), where %MPE = [(test – control)/ (10 – control)] x 100. In the antagonism study, the 6 α / β -naltrexamine derivatives were given 5 min before morphine. The tail immersion test was then

conducted 20 min after giving morphine. %MPE was calculated for each mouse using at least five mice per drug. AD₅₀ values were calculated using the least-squares linear regression analysis followed by calculation of 95% confidence interval by Bliss method.

6.4.6 Opioid withdrawal assay

Male Swiss Webster mice were used in this study. A 75 mg morphine pellet was implanted in to the base of the neck of the mice and the mice were then given time to recover in their home cages before the test was conducted. The mice were then allowed for 30 min habituation to an open-topped, square, clear Plexiglas observation chamber (26 x 26 x 26 cm³) with lines partitioning the bottom into quadrants before they were given antagonist. All drugs and test compounds were administered subcutaneously (s.c.). Withdrawal was precipitated at 72 h from pellet implantation with naltrexone (1.0 mg/kg, s.c.), and the test compounds at indicated doses. Withdrawal commenced within 3 min after antagonist administration. Escape jumps, paw tremors and wet dog shakes were quantified by counting their occurrences over 20 min for each mouse using five mice per drug. The data is given as the mean \pm SEM. One-way ANOVA followed by the post hoc Dunnett test were performed to assess significance using the Prism 6.0 software.

6.5 Molecular modeling study

Molecular modeling studies were conducted to observe the binding interactions of compound **6** with MOR which might help in understanding its molecular mechanism of action. Chemical structures of the compounds were sketched in SybylX-2.1, and Gasteiger–Hückel charges were assigned before energy minimization (100 000 iterations) with the Tripos Force Fields. The X-ray crystal structure for MOR (4DKL) was

retrieved from the Protein Data Bank (PDB) and prepared for docking by adding hydrogens and deleting water molecules and bound ligands inside the binding pocket.

6.5.1 Molecular docking study

Automated docking on MOR was done utilizing genetic algorithm docking program GOLD 5.4. The binding site was defined to include all atoms within 10 Å of the γ -carbon atom of Asp147 along with a hydrogen bond constraint between the 17-N of the ligand's morphinan skeleton and the carboxylate group of Asp147. Compound **6** was docked 50 times into MOR. The best CHEM-PLP scored solutions were chosen for further analyses. Pictures were generated using PyMOL Molecular Graphics System, version 1.7.4.5²¹¹

6.5.2 Molecular dynamics simulation

The best CHEM-PLP-scored solutions for binding pose 1 and 2 were chosen for molecular dynamics (MD) studies. Force field parameter and topology files for compound **6** were generated utilizing CGenFF. Coordinates for the spatial arrangement of the receptors within the lipid bilayer were retrieved from the Orientations of Proteins in Membranes (OPM) database. The simulation system, consisting of the receptor–ligand complex embedded in a lipid (POPC) bilayer surrounded with saline solution (0.15 MNaCl) was created in VMD 1.9.3 using the CHARMM force field topology file. All simulations were performed under hybrid CHARMM force field parameters that included protein, lipids and ligand with a time-step of 2 femtoseconds (fs). Periodic boundary conditions were employed, and Particle Mesh Ewald (PME) summation was used to calculate long-range electrostatic interactions. Non-bonded interactions were calculated with a smooth cutoff at 14 Å with a frequency of 2 fs. The temperature was maintained

at 310 K via Langevin dynamics. All molecular modeling simulations were performed using NAMD 2.8. MD simulations were carried out in four stages. In the first stage, equilibration of the fluid-like lipid bilayer was performed via minimization (1000 iterations) followed by NPT equilibration (pressure equilibration, 0.5 ns) of the lipid tails only. In the second stage, an NPT equilibration of the system was run for a period of 1 ns with harmonic constraints placed on protein and NNQ atoms (5 kcal/(mol-Å)). The harmonic restraint was released in stage 3 and the entire system was equilibrated using the NVT canonical ensemble for a further 1 ns. The final production run was conducted for 10 ns using an NVT ensemble. Energy landscape analysis was performed using the NAMD Energy 1.4 plug-in; non-bonded interaction analyses were performed at various distances with a dielectric constant of 6.5. The best-scored poses based on the NAMD non-bonded interactions were selected for further analysis. Figures were generated using the PyMOL Molecular Graphics System, Version 1.3.

6.6 QSPKR study

Values for molecular weight (MW), clogP, pK_a, LogD_{7.0} solubility at pH of 7 [g/L], hydrogen bond donors (HBD), and hydrogen bond acceptors (HBA) were obtained by first drawing the structures of the opioid compounds in the existing databases in Chemdraw 13.0, and their physicochemical properties were determined in Scifinder using the Scifinder search tool in Chemdraw. The physicochemical properties obtained were used to predict whether the compounds will pass Lipinsky's rule of 5, GI permeability and CNS penetration: Compounds with molecular weight (MW) exceeding 500 Da, more than five hydrogen bond donors (HBD, expressed as the sum of hydroxyl and amino groups present in a molecule), octanol–water partition coefficient (clogP)

greater 5 and more than 10 hydrogen bond acceptors (HBD, expressed as the sum of nitrogen and oxygen atoms in the molecule) failed the Lipinsky's rule of 5. To access GI permeability, $0 > \log D < 3$ was used as the criteria. Compounds with $\log D$ out of this range failed the test.²²⁶ Norinder and Haerberlein rule was used to predict CNS permeability: If $N + O$ (the number of nitrogen and oxygen atoms) in a molecule is less than or equal to 5, it has a high chance of entering the brain.²²⁷ All the compounds failed this test, including NTX, which is known to penetrate the CNS - suggesting that this *in-silico* screen may not be useful.

The values for $\log D_{7.4}$ were calculated using the equation: $\log D_{7.4} = \text{clogP} - \log(1 + 10^{(\text{pK}_a - 7.4)})$.

Values for $D_{\text{max}}^{\text{sol}}$ [mg], i.e., the maximally soluble dose in the GI tract, were calculated using the lowest solubility within a pH range of 1-8 [g/L] multiplied by 250 mL (estimated volume of GI fluid).

List of References

List of References

- (1) UNODC. *World Drug Report 2015*; United Nations: Vienna, 2015.
- (2) Center for Behavioral Health Statistics and Quality. Behavioral Health Trends in the United States: Results from the 2014 National Survey on Drug Use and Health. (*HHS Publication No. SMA 15-4927, NSDUH Ser. H-50. 2015*, 64.
- (3) Muhuri, P.; Gfroerer, J.; Davies, C. Associations of Nonmedical Pain Reliever Use and Initiation of Heroin Use in the US. *Cent. Behav. Heal. Stat. Qual. Data Rev. 2013*, No. SAMHSA.
- (4) NIDA. *Principles of Drug Addiction Treatment: A Research-Based Guide*, Third Edit.; U.S. Government Printing Office: Washington, DC, 2012.
- (5) Booth, M. *Opium: A History*; St. Martin's Press: New York, 1986.
- (6) Dikotter, F.; Laaman, L.; Xun, Z. *Narcotic Culture: A History of Drugs in China*; University of Chicago Press: Chicago, 2004.
- (7) Askitopoulou, H.; Ramoutsaki, I.; Konsolaki, E. Archaeological Evidence on the Use of Opium in the Minoan World. *Int. Congr. Ser. 2002*, 1292, 23–97.

- (8) Schiff, P. L. Opium and Its Alkaloids. *Am. J. Pharm. Educ.* **2002**, 66, 186–194.
- (9) Katz, N. P.; Adams, E. H.; Chilcoat, H.; Colucci, R. D.; Comer, S. D.; Goliber, P.; Grudzinskas, C.; Jasinski, D.; Lande, S. D.; Passik, S. D.; Schnoll, S. H.; Sellers, E.; Travers, D.; Weiss, R. Challenges in the Development of Prescription Opioid Abuse-Deterrent Formulations. *Clin. J. Pain* **2007**, 23 (8), 648–660.
- (10) Pert, B. C.; Snyder, H. S. Opiate Receptor : Demonstration in Nervous. *Science* (80-.). **1973**, 179, 1011–1014.
- (11) Meldrum, M. L. A Capsule History of Pain Management. *JAMA* **2003**, 290 (18), 2470–2475.
- (12) Musto, D. F. *The American Disease: Origins of Narcotic Control*, 3rd ed.; Oxford University Press: New York, 1999.
- (13) Ballantyne, J. C. Opioids for Chronic Nonterminal Pain. *South Med J* **2006**, 99 (11), 1245–1255.
- (14) Corbett, A. D.; Henderson, G.; McKnight, A. T.; Paterson, S. J. 75 Years of Opioid Research: The Exciting but Vain Quest for the Holy Grail. *Br. J. Pharmacol.* **2006**, 147 Suppl, S153-62.
- (15) Strain, E. C.; Stitzer, M. L. *Methadone and Other Treatments for Opioid Dependence*; John Hopkins University Press: Baltimore, 2006.
- (16) Courtwright, D. T.; Joseph, H.; DesJarlais, D. *Addicts Who Survived*; University of Tennessee Press: Knoxville, TN, 1989.
- (17) Rosenblum, A.; Marsch, L. A.; Herman, J.; Portenoy, R. K. Opioids and the

Treatment of Chronic Pain: Controversies, Current Status, and Future Directions. *Exp Clin Psychopharmacol.* **2008**, 16 (5), 405–416.

- (18) Zacny, J.; Bigelow, G.; Compton, P.; Foley, K.; Iguchi, M.; Sannerud, C. College on Problems of Drug Dependence Taskforce on Prescription Opioid Non-Medical Use and Abuse: Position Statement. *Drug Alcohol Depend.* **2003**, 69 (3), 215–232.
- (19) Cai, R.; Crane, E.; Poneleit, K.; Paulozzi, L. Emergency Department Visits Involving Nonmedical Use of Selected Prescription Drugs in the United States, 2004–2008. *J. Pain Palliat. Care Pharmacother.* **2010**, 24 (3), 293–297.
- (20) Ling, W.; Mooney, L.; Hillhouse, M. Prescription Opioid Abuse, Pain and Addiction: Clinical Issues and Implications. *Drug Alcohol Rev.* **2011**, 30 (3), 300–305.
- (21) Rudd, R.; Seth, P.; David, F.; Scholl, L. Increases in Drug and Opioid-Involved Overdose Deaths — United States, 2010–2015. **2016**, 65 (50–51), 1445–1452.
- (22) Compton, W. M.; Jones, C. M.; Baldwin, G. T. Relationship between Nonmedical Prescription-Opioid Use and Heroin Use. *N. Engl. J. Med.* **2016**, 374 (2), 154–163.
- (23) Owens, P. L.; Barrett, M. L.; Weiss, A. J.; Washington, R. E.; Kronick, R. Hospital Inpatient Utilization Related to Opioid Overuse Among Adults, 1993-2012, HCUP Statistical Brief #177. *Agency Healthc. Res. Qual.* **2014**, 1–14.
- (24) Wickramatilake, S.; Zur, J.; Mulvaney-Day, N.; von Klimo, M. C.; Selmi, E.;

- Harwood, H. How States Are Tackling the Opioid Crisis. *Public Health Rep.* **2017**, XX, 3335491668820.
- (25) Jones, C. M. Heroin Use and Heroin Use Risk Behaviors among Nonmedical Users of Prescription Opioid Pain Relievers - United States, 2002-2004 and 2008-2010. *Drug Alcohol Depend.* **2013**, 132 (1–2), 95–100.
- (26) Jones, C. M.; Logan, J.; Gladden, R. M.; Bohm, M. K.; Author, M. P. H. Vital Signs : Demographic and Substance Use Trends Among Heroin Users — United States , 2002 – 2013. *MMWR July 2015* **2015**, 64 (26), 1–7.
- (27) Xu, J.; Murphy, S. L.; Kochanek, K. D.; Bastian, B. A. Deaths: Final Data for 2013. *Natl. Vital Stat. Reports* **2016**, 64 (2), 1–119.
- (28) Medicine, A. S. of A. Opioid Addiction 2016 Facts and Figures. *Am. Soc. Addict. Med.* **2016**, No. 2014, 10–12.
- (29) US Department of Justice Drug Enforcement Administration. *2015 National Drug Threat Assessment Summary*; 2015.
- (30) Center for Behavioral Health Statistics and Quality. *2015 National Survey on Drug Use and Health : Detailed Tables*; Substance Abuse and Mental Health Services Administration: Rockville, MD, 2016.
- (31) Mansour, A.; Watson, S. J. Anatomical Distribution of Opioid Receptors in Mammals: An Overview. In *Handbook of Experimental Pharmacology*; Herz, A., Akil, H., Simon, E. J., Eds.; Springer: Berlin, 1993; pp 79–105.
- (32) Wittert, G.; Hope, P.; Pyle, D. Tissue Distribution of Opioid Receptor Gene

- Expression in the Rat. *Biochem. Biophys. Res. Commun.* **1996**, 218 (3), 877–881.
- (33) Law, P. Y.; Wong, Y. H.; Loh, H. H. Molecular Mechanisms and Regulation of Opioid Receptor Signaling. *Annu. Rev. Pharmacol. Toxicol.* **2000**, 40 (1), 389–430.
- (34) Jin, W.; Lee, N. M.; Loh, H. H.; Thayer, S. A. Opioids Mobilize Calcium from Inositol 1,4,5-Trisphosphate-Sensitive Stores in NG108-15 Cells. *J. Neurosci.* **1994**, 14 (4), 1920–1929.
- (35) Waldhoer, M.; Bartlett, S. E.; Whistler, J. L. Opioid Receptors. *Annu. Rev. Biochem.* **2004**, 73, 953–990.
- (36) Hughes, J.; Kosterlitz, H. W. Opioid Peptides: Introduction. *Br. Med. Bull.* **1983**, 39 (1), 1–3.
- (37) De Vries, L.; Zheng, B.; Fischer, T.; Elenko, E.; Farquhar, M. G. The Regulator of G Protein Signaling Family. *Annu. Rev. Pharmacol. Toxicol.* **2000**, 40 (1), 235–271.
- (38) Hamm, H. E. The Many Faces of G Protein Signaling. *J. Biol. Chem.* **1998**, 273 (2), 669–672.
- (39) Beckett, A. H.; Casy, A. F. SYNTHETIC ANALGESICS: STEREOCHEMICAL CONSIDERATIONS. *J. Pharm. Pharmacol.* **1954**, 6, 986–1001.
- (40) Portoghese, P. S. A New Concept on the Mode of Interaction of Narcotic Analgesics with Receptors. *J. Med. Chem.* **1965**, 8, 609–616.
- (41) Terenius, L. Stereospecific Interaction between Narcotic Analgesics and a

- Synaptic Plasma Membrane Fraction of Rat Cerebral Cortex. *Acta Pharmacol. Toxicol.* **1973**, *32*, 317–320.
- (42) Simon, E. J.; Hiller, J. M.; Edelman, I. Stereospecific Binding of the Potent Narcotic Analgesic (3H) Etorphine to Rat-Brain Homogenate. *Proc. Natl. Acad. Sci. USA* **1973**, *70*, 1947–1949.
- (43) Lord, J. A.; Waterfield, A. A.; Hughes, J.; Kosterlitz, H. W. Endogenous Opioid Peptides: Multiple Agonists and Receptors. *Nature* **1977**, *267*, 495–499.
- (44) Bunzow, J. R.; Saez, C.; Mortrud, M.; Bouvier, C.; Williams, J. T.; Low, M.; Grandy, D. K. Molecular Cloning and Tissue Distribution of a Putative Member of the Rat Opioid Receptor Gene Family That Is Not a Mu, Delta or Kappa Opioid Receptor Type. *FEBS Lett.* **1994**, *347* (2–3), 284–288.
- (45) Mollereau, C.; Parmentier, M.; Mailleux, P.; Butour, J. L.; Moisand, C.; Chalon, P.; Caput, D.; Vassart, G.; Meunier, J. C. ORL1, a Novel Member of the Opioid Receptor Family. Cloning, Functional Expression and Localization. *FEBS Lett.* **1994**, *341*, 33–38.
- (46) Meunier, J.; Mollereau, C.; Toll, L.; Suaudeau, C.; Moisand, D.; Alvinerie, P.; Butour, J. L.; Guillemot, J. C.; Ferrara, P.; Monsarrat, B. Isolation and Structure of the Endogenous Agonist of Opioid Receptor-like ORL1 Receptor. *Nature* **1995**, *377*, 532–535.
- (47) Hoellt, V. Multiple Endogenous Opioid Peptides. *Trends Neurosci.* **1983**, *6*, 24–26.

- (48) Dian-San, S.; Zhen-Hong, W.; Yong-Jun, Z.; Yan-Hua, Z.; Xiang-Rui, W. Dose-Dependent Neuroprotection of Delta Opioid Peptide [D-Ala², D-Leu⁵] Enkephalin in Neuronal Death and Retarded Behavior Induced by Forebrain Ischemia in Rats. *Neurosci. Lett.* **2007**, *423*, 113–117.
- (49) Onogi, T.; Minami, M.; Katao, Y.; Nakagawa, T.; Aoki, Y.; Toya, T.; Katsumata, S.; Satoh, M. DAMGO, a Mu-Opioid Receptor Selective Agonist, Distinguishes between Mu- and Delta-Opioid Receptors around Their First Extracellular Loops. *FEBS Lett.* **1995**, *357* (1), 93–97.
- (50) Gulland, J. M.; Robinson, R. The Morphine Group. Part I. A Discussion of the Constitutional Problem. *J. Chem. Soc.* **1923**, *123*, 980–998.
- (51) Takemori, A. E.; Portoghese, P. S. Evidence for the Interaction of Morphine with Kappa and Delta Opioid Receptors to Induce Analgesia in Beta-Funaltrexamine-Treated Mice. *J. pharmacol. Exp. Ther.* **1987**, *243*, 91–94.
- (52) Zhu, B. T. Mechanistic Explanation for the Unique Pharmacologic Properties of Receptor Partial Agonists. *Biomed. Pharmacother.* **2005**, *59* (3), 76–89.
- (53) Blumberg, H.; Dayton, H. B. Naloxone, Naltrexone, and Related Noroxymorphones. *Adv. Biochem. Psychopharmacol.* **1973**, *8*, 33–43.
- (54) Foldes, F. F.; Lunn, J. N.; Moore, J.; Brown, I. M. N-Allylnoroxy-Morphine: A New Potent Narcotic Antagonist. *Am. J. Med. Sci.* **1963**, *245*, 23–30.
- (55) Hart, E. R.; McCawley, E. L. The Pharmacology of N-Allynormorphine as Compared with Morphine. *J. pharmacol. Exp. Ther.* **1944**, *82*, 339–348.

- (56) Leslie, F. M. Methods Used for the Study of Opioid Receptors. *Pharmacol. Rev.* **1987**, *39*, 197–249.
- (57) Magnan, J.; Paterson, S. J.; Tavani, A.; Kosterlitz, H. W. The Binding Spectrum of Narcotic Analgesic Drugs with Different Agonist and Antagonist Properties. *Naunyn. Schmiedebergs. Arch. Pharmacol.* **1982**, *319*, 197–205.
- (58) Soyka, M. Nalmefene for the Treatment of Alcohol Use Disorders: Recent Data and Clinical Potential. *Expert Opin Pharmacother* **2016**, *17* (4), 619–626.
- (59) Yuan, Y.; Zaidi, S. A.; Elbegdorj, O.; Aschenbach, L. C. K.; Li, G.; Stevens, D. L.; Scoggins, K. L.; Dewey, W. L.; Selley, D. E.; Zhang, Y. Design, Synthesis, and Biological Evaluation of 14-Heteroaromatic- Substituted Naltrexone Derivatives: Pharmacological Profile Switch from Mu Opioid Receptor Selectivity to Mu/Kappa Opioid Receptor Dual Selectivity. *J. Med. Chem.* **2013**, *56* (22), 9156–9169.
- (60) Feng, Y.; He, X.; Yang, Y.; Chao, D.; Lazarus, L. H.; Xia, Y. Current Research on Opioid Receptor Function. *Curr. Drug Targets* **2012**, *13* (2), 230–246.
- (61) Chao, D.; Balboni, G.; Lazarus, L. H.; Salvadori, S.; Xia, Y. Na⁺ Mechanism of Delta-Opioid Receptor Induced Protection from Anoxic K⁺ Leakage in the Cortex. *Cell. Mol. Life Sci.* **2009**, *66* (6), 1105–1115.
- (62) Chao, D.; Bazy-Asaad, A.; Balboni, G.; Salvadori, S.; Xia, Y. Activation of DOR Attenuates Anoxic K⁺ Derangement via Inhibition of Na⁺ Entry in Mouse Cortex. *Cereb. Cortex* **2008**, *18* (9), 2217–2227.
- (63) Chao, D.; Donnelly, D. F.; Feng, Y.; Bazy-Asaad, A.; Xia, Y. Cortical Delta-

- Opioid Receptors Potentiate K⁺ Homeostasis during Anoxia and Oxygen-Glucose Deprivation. *J. Cereb. Blood Flow Metab.* **2007**, 27 (2), 356–368.
- (64) Chao, D.; Bazy-Asaad, A.; Balboni, G.; Xia, Y. Delta-, but Not Mu-, Opioid Receptor Stabilizes K⁽⁺⁾ Homeostasis by Reducing Ca⁽²⁺⁾ Influx in the Cortex during Acute Hypoxia. *J. Cell. Physiol.* **2007**, 212 (1), 60–67.
- (65) Jin, W.; Lee, N. M.; Loh, H. H.; Thayer, S. A. Dual Excitatory and Inhibitory Effects of Opioids on Intracellular Calcium in Neuroblastoma X Glioma Hybrid NG108-15 Cells. *Mol. Pharmacol.* **1992**, 42 (6), 1083–1089.
- (66) Wang, J. F.; Shun, X. J.; Yang, H. F.; Ren, M. F.; Han, J. S. Suppression by [D-Pen², D-Pen⁵]enkephalin on Cyclic AMP Dependent Protein Kinase-Induced, but Not Protein Kinase C-Induced Increment of Intracellular Free Calcium in NG108-15 Cells. *Life Sci.* **1993**, 52 (6), 1519–1525.
- (67) Vlaskovska, M.; Schramm, M.; Nylander, I.; Kasakov, L.; You, Z. B.; Herrera-Marschitz, M.; Terenius, L. Opioid Effects on ⁴⁵Ca²⁺ Uptake and Glutamate Release in Rat Cerebral Cortex in Primary Culture. *J. Neurochem.* **1997**, 68 (2), 517–524.
- (68) Thorlin, T.; Eriksson, P. S.; Persson, P. A. I.; Åberg, N. D.; Hansson, E.; Rönnbäck, L. Delta-Opioid Receptors on Astroglial Cells in Primary Culture: Mobilization of Intracellular Free Calcium via a Pertussis Sensitive G Protein. *Neuropharmacology* **1998**, 37 (3), 299–311.
- (69) Spadoni, F.; Martella, G.; Martorana, A.; Lavaroni, F.; D'Angelo, V.; Bernardi, G.; Stefani, A. Opioid-Mediated Modulation of Calcium Currents in Striatal and

Pallidal Neurons Following Reserpine Treatment: Focus on Kappa Response.
Synapse **2004**, 51 (3), 194–205.

- (70) Komai, H.; McDowell, T. S. Effects of Local Anesthetics on Opioid Inhibition of Calcium Current in Rat Dorsal Root Ganglion Neurons. *Neurosci. Lett.* **2007**, 418 (3), 298–303.
- (71) Rola, R.; Jarkiewicz, M.; Szulczyk, P. Modulation of Ca²⁺ Channel Current by Mu Opioid Receptors in Prefrontal Cortex Pyramidal Neurons in Rats. *Acta Neurobiol. Exp. (Wars)*. **2008**, 68 (1), 10–25.
- (72) Malendowicz, L. K.; Rebuffat, P.; Tortorella, C.; Nussdorfer, G. G.; Ziolkowska, A.; Hochol, A. Effects of Met-Enkephalin on Cell Proliferation in Different Models of Adrenocortical-Cell Growth. *Int. J. Mol. Med.* **2005**, 15 (5), 841–845.
- (73) Narita, M.; Kuzumaki, N.; Miyatake, M.; Sato, F.; Wachi, H.; Seyama, Y.; Suzuki, T. Role of Delta-Opioid Receptor Function in Neurogenesis and Neuroprotection. *J. Neurochem.* **2006**, 97 (5), 1494–1505.
- (74) Mayfield, K. P.; Alecy, L. G. Delta-1 Opioid Agonist Acutely Increases Hypoxic Tolerance. *J. Pharmacol. Exp. Ther.* **1994**, 268 (2), 683 LP-688.
- (75) Endoh, H.; Taga, K.; Yamakura, T.; Sato, K.; Watanabe, I.; Fukuda, S.; Shimoji, K. Effects of Naloxone and Morphine on Acute Hypoxic Survival in Mice. *Crit Care Med.* **1999**, 27 (9), 1929–1933.
- (76) Hayward, N. J.; McKnight, A. T.; Woodruff, G. N. Neuroprotective Effect of the χ -Agonist Enadoline (CI-977) in Rat Models of Focal Cerebral Ischaemia. *Eur. J.*

Neurosci. **1993**, 5 (7), 961–967.

- (77) Summers, R. L.; Li, Z.; Hildebrandt, D. Effect of a δ Receptor Agonist on Duration of Survival during Hemorrhagic Shock. *Acad. Emerg. Med.* **2003**, 10 (6), 587–593.
- (78) Yang, L.; Wang, H.; Shah, K.; Karamyan, V. T.; Abbruscato, T. J. Opioid Receptor Agonists Reduce Brain Edema in Stroke. *Brain Res.* **2011**, 1383, 307–316.
- (79) Hosobuchi, Y.; Baskin, D. S.; Woo, S. K. Reversal of Induced Ischemic Neurologic Deficit in Gerbils by the Opiate Antagonist Naloxone. *Science* (80-). **1982**, 215 (4528), 69 LP-71.
- (80) Adams, H. P.; Olinger, C. P.; Barsan, W. G.; Butler, M. J.; Graff-Radford, N. R.; Brott, T. G.; Biller, J.; Damasio, H.; Tomsick, T.; Goldberg, M. A Dose-Escalation Study of Large Doses of Naloxone for Treatment of Patients with Acute Cerebral Ischemia. *Stroke* **1986**, 17 (3), 404 LP-409.
- (81) SKARPHEDINSSON, J. O.; THOREN, P. Endorphin Mechanisms Are Responsible for the Beneficial Effects of Opioid Antagonists on Cerebral Function during Relative Cerebral Ischaemia in Rats. *Acta Physiol. Scand.* **1988**, 132 (3), 281–288.
- (82) Olinger, C. P.; Adams, H. P.; Brott, T. G.; Biller, J.; Barsan, W. G.; Toffol, G. J.; Eberle, R. W.; Marler, J. R. High-Dose Intravenous Naloxone for the Treatment of Acute Ischemic Stroke. *Stroke* **1990**, 21 (5), 721 LP-725.
- (83) Chen, C. J.; Liao, S. L.; Chen, W. Y.; Hong, J. S.; Kuo, J. S. Cerebral Ischemia/reperfusion Injury in Rat Brain: Effects of Naloxone. *Neuroreport* **2001**,

12 (6), 1245–1249.

- (84) Chen, C.-J.; Cheng, F.-C.; Liao, S.-L.; Chen, W.-Y.; Lin, N.-N.; Kuo, J.-S. Effects of Naloxone on Lactate, Pyruvate Metabolism and Antioxidant Enzyme Activity in Rat Cerebral Ischemia/reperfusion. *Neurosci. Lett.* **2000**, *287* (2), 113–116.
- (85) Zhang, J.; Qian, H.; Zhao, P.; Hong, S. S.; Xia, Y. Rapid Hypoxia Preconditioning Protects Cortical Neurons from Glutamate Toxicity through δ -Opioid Receptor. *Stroke* **2006**, *37*.
- (86) Ma, M. C.; Qian, H.; Ghassemi, F.; Zhao, P.; Xia, Y. Oxygen Sensitive δ -Opioid Receptor-Regulated Survival and Death Signals: Novel Insights into Neuronal Preconditioning and Protection. *J Biol Chem* **2005**, *280*.
- (87) Yang, Y.; Xia, X.; Zhang, Y.; Wang, Q.; Li, L.; Luo, G.; Xia, Y. δ -Opioid Receptor Activation Attenuates Oxidative Injury in the Ischemic Rat Brain. *BMC Biol.* **2009**, *7* (1), 55.
- (88) Chao, D.; Bazy-Asaad, A.; Balboni, G.; Xia, Y. δ -, but Not M-, Opioid Receptor Stabilizes K⁺ Homeostasis by Reducing Ca²⁺ Influx in the Cortex during Acute Hypoxia. *J. Cell. Physiol.* **2007**, *212* (1), 60–67.
- (89) Chao, D.; Donnelly, D. F.; Feng, Y.; Bazy-Asaad, A.; Xia, Y. Cortical δ -Opioid Receptors Potentiate K⁺ Homeostasis During Anoxia and Oxygen–Glucose Deprivation. *J. Cereb. Blood Flow Metab.* **2006**, *27* (2), 356–368.
- (90) Chao, D.; Bazy-Asaad, A.; Balboni, G.; Salvadori, S.; Xia, Y. Activation of DOR Attenuates Anoxic K⁺ Derangement via Inhibition of Na⁺ Entry in Mouse Cortex.

- Cereb. Cortex* **2008**, 18 (9), 2217–2227.
- (91) Chao, D.; Balboni, G.; Lazarus, L. H.; Salvadori, S.; Xia, Y. Na⁺ Mechanism of δ -Opioid Receptor Induced Protection from Anoxic K⁺ Leakage in the Cortex. *Cell. Mol. Life Sci.* **2009**, 66 (6), 1105–1115.
- (92) Kang, X. Z.; Chao, D. M.; Gu, Q. B.; Ding, G. H.; Wang, Y. W.; Balboni, G.; Lazarus, L. H.; Xia, Y. δ -Opioid Receptors Protect from Anoxic Disruption of Na⁺ Homeostasis via Na⁺channel Regulation BT - *Cell Mol Life Sci*; 2009.
- (93) Zhang, J. H.; Gibney, G. T.; Xia, Y. Effect of Prolonged Hypoxia on Na⁺ Channel mRNA Subtypes in the Developing Rat Cortex. *Mol. Brain Res.* **2001**, 91 (1–2), 154–158.
- (94) Zhang, J. H.; Gibney, G. T.; Zhao, P.; Xia, Y. Neuroprotective Role of δ -Opioid Receptors in the Cortical Neurons. *Am J Physiol* **2002**, 282.
- (95) Zhang, J. H.; Xia, Y.; Haddad, G. G. Activation of δ -Opioid Receptors Protects Cortical Neurons from Glutamate Excitotoxic Injury. *Soc Neurosci* **1999**, 28.
- (96) Borlongan, C. V.; Hayashi, T.; Oeltgen, P. R.; Su, T. P.; Wang, Y. Hibernation-like State Induced by an Opioid Peptide Protects against Experimental Stroke. *BMC Biol* **2009**, 7.
- (97) Borlongan, C. V.; Wang, Y.; Su, T. P. δ Opioid Peptide (D-Ala 2, D-Leu 5) Enkephalin: Linking Hibernation and Neuroprotection. *Front Biosci* **2004**, 9.
- (98) Horiuchi, T.; Kawaguchi, M.; Kurita, N.; Inoue, S.; Sakamoto, T.; Nakamura, M.; Konishi, N.; Furuya, H. Effects of Delta-Opioid Agonist SNC80 on White Matter

- Injury Following Spinal Cord Ischemia in Normothermic and Mildly Hypothermic Rats. *J. Anesth.* **2008**, 22 (1), 32–37.
- (99) Horiuchi, T.; Kawaguchi, M.; Sakamoto, T.; Kurita, N.; Inoue, S.; Nakamura, M.; Konishi, N.; Furuya, H. The Effects of the δ -Opioid Agonist SNC80 on Hind-Limb Motor Function and Neuronal Injury After Spinal Cord Ischemia in Rats. *Anesth. Analg.* **2004**, 99 (1), 235–240.
- (100) Charron, C.; Messier, C.; Plamondon, H. Neuroprotection and Functional Recovery Conferred by Administration of Kappa- and delta1-Opioid Agonists in a Rat Model of Global Ischemia. *Physiol. Behav.* **2008**, 93 (3), 502–511.
- (101) Iwata, M.; Inoue, S.; Kawaguchi, M.; Nakamura, M.; Konishi, N.; Furuya, H. Effects of Delta-Opioid Receptor Stimulation and Inhibition on Hippocampal Survival in a Rat Model of Forebrain Ischaemia. *Br. J. Anaesth.* **2007**, 99 (4), 538–546.
- (102) Govindaswami, M.; Brown, S. A.; Yu, J.; Zhu, H.; Bishop, P. D.; Kindy, M. S.; Oeltgen, P. R. Delta 2 -Specific Opioid Receptor Agonist and Hibernating Woodchuck Plasma Fraction Provide Ischemic Neuroprotection. *Acad. Emerg. Med.* **2008**, 15 (3), 250–257.
- (103) Pamenter, M. E.; Buck, L. T. δ -Opioid Receptor Antagonism Induces NMDA Receptor-Dependent Excitotoxicity in Anoxic Turtle Cortex. *J Exp Biol* **2008**, 211.
- (104) Zhang, J.; Haddad, G. G.; Xia, Y. δ -, but Not μ - and κ -, Opioid Receptor Activation Protects Neocortical Neurons from Glutamate-Induced Excitotoxic Injury. *Brain Res.* **2000**, 885 (2), 143–153.

- (105) Borlongan, C. V.; Wang, Y.; Su, T.-P. Delta Opioid Peptide (D-Ala 2, D-Leu 5) Enkephalin: Linking Hibernation and Neuroprotection. *Front. Biosci.* **2004**, *9*, 3392–3398.
- (106) Bruce, D. S.; Bailey, E. C.; Setran, D. P.; Tramell, M. S.; Jacobson, D.; Oeltgen, P. R.; Horton, N. D.; Hellgren, E. C. Circannual Variations in Bear Plasma Albumin and Its Opioid-like Effects on Guinea Pig Ileum. *Pharmacol. Biochem. Behav.* **1996**, *53* (4), 885–889.
- (107) Bourhim, N.; Kabine, M.; Elkebbaj, M. S. Characterization of Opioid Peptides and Opioid Receptors in the Brain of Jerboa (*Jaculus Orientalis*), a Hibernating Rodent. *Brain Res. Bull.* **1997**, *44* (5), 615–620.
- (108) Peart, J. N.; Gross, E. R.; Gross, G. J. Opioid-Induced Preconditioning: Recent Advances and Future Perspectives. *Vascul. Pharmacol.* **2005**, *42* (5–6), 211–218.
- (109) Wu, T.; Dong, P.; Chen, C.; Yang, J.; Hou, X. The Myocardial Protection of Polarizing Cardioplegia Combined With Delta-Opioid Receptor Agonist in Swine. *Ann. Thorac. Surg.* **2011**, *91* (6), 1914–1920.
- (110) Yu, L. C.; Cai, Y. P. Arousal Following Intra-Preoptic Area Administration of Naltrexone, ICI 174864 or nor-BNI in Hibernating Ground Squirrels. *Behav. Brain Res.* **1993**, *57* (1), 31–35.
- (111) Kieffer, B. L.; Gavériaux-Ruff, C. Exploring the Opioid System by Gene Knockout. *Prog. Neurobiol.* **2002**, *66* (5), 285–306.
- (112) Eisinger, D. A.; Schulz, R. Mechanism and Consequences of Delta-Opioid

- Receptor Internalization. *Crit. Rev. Neurobiol.* **2005**, *17* (1), 1–26.
- (113) Hanlon, K. E.; Herman, D. S.; Agnes, R. S.; Largent-Milnes, T. M.; Kumarasinghe, I. R.; Ma, S. W.; Guo, W.; Lee, Y.-S.; Ossipov, M. H.; Hruby, V. J.; Lai, J.; Porreca, F.; Vanderah, T. W. Novel Peptide Ligands with Dual Acting Pharmacophores Designed for the Pathophysiology of Neuropathic Pain. *Brain Res.* **2011**, *1395*, 1–11.
- (114) Molina, P. E. Stress-Specific Opioid Modulation of Haemodynamic Counter-Regulation. *Clin. Exp. Pharmacol. Physiol.* **2002**, *29* (3), 248–253.
- (115) Kho, H. G.; Kloppenborg, P. W.; van Egmond, J. Effects of Acupuncture and Transcutaneous Stimulation Analgesia on Plasma Hormone Levels during and after Major Abdominal Surgery. *Eur. J. Anaesthesiol.* **1993**, *10* (3), 197–208.
- (116) LaBuda, C. J.; Sora, I.; Uhl, G. R.; Fuchs, P. N. Stress-Induced Analgesia in Mu-Opioid Receptor Knockout Mice Reveals Normal Function of the Delta-Opioid Receptor System. *Brain Res.* **2000**, *869* (1–2), 1–5.
- (117) Gavériaux-Ruff, C.; Kieffer, B. L. Opioid Receptor Genes Inactivated in Mice: The Highlights. *Neuropeptides* **2002**, *36* (2–3), 62–71.
- (118) Matthes, H. W. D.; Maldonado, R.; Simonin, F.; Valverde, O.; Slowe, S.; Kitchen, I.; Befort, K.; Dierich, A.; Le Meur, M.; Dollé, P.; Tzavara, E.; Hanoune, J.; Roques, B. P.; Kieffer, B. L. Loss of Morphine-Induced Analgesia, Reward Effect and Withdrawal Symptoms in Mice Lacking the M-Opioid-Receptor Gene. *Nature* **1996**, *383* (6603), 819–823.

- (119) Yamada, H.; Shimoyama, N.; Sora, I.; Uhl, G. R.; Fukuda, Y.; Moriya, H.; Shimoyama, M. Morphine Can Produce Analgesia via Spinal Kappa Opioid Receptors in the Absence of Mu Opioid Receptors. *Brain Res.* **2006**, *1083* (1), 61–69.
- (120) Ananthan, S. Opioid Ligands with Mixed M/ δ Opioid Receptor Interactions: An Emerging Approach to Novel Analgesics. *AAPS J.* **2006**, *8* (1), E118–E125.
- (121) Gebhart, G. J.J. Bonica lecture—2000: Physiology, Pathophysiology, and Pharmacology of Visceral Pain. *Reg. Anesth. Pain Med.* **2000**, *25* (6), 632–638.
- (122) Filliol, D.; Kieffer, B. L.; Ghozland, S.; Chluba, J.; Martin, M.; Matthes, H. W. D.; Simonin, F.; Befort, K.; Gavériaux-Ruff, C.; Dierich, A.; LeMeur, M.; Valverde, O.; Maldonado, R. Mice Deficient for Delta- and Mu-Opioid Receptors Exhibit Opposing Alterations of Emotional Responses. *Nat. Genet.* **2000**, *25* (2), 195–200.
- (123) Saitoh, A.; Yoshikawa, Y.; Onodera, K.; Kamei, J. Role of δ -Opioid Receptor Subtypes in Anxiety-Related Behaviors in the Elevated plus-Maze in Rats. *Psychopharmacology (Berl)*. **2005**, *182* (3), 327–334.
- (124) Roth, B. L.; Baner, K.; Westkaemper, R.; Siebert, D.; Rice, K. C.; Steinberg, S.; Ernsberger, P.; Rothman, R. B. Salvinorin A: A Potent Naturally Occurring Nonnitrogenous Kappa Opioid Selective Agonist. *Proc. Natl. Acad. Sci. U. S. A.* **2002**, *99* (18), 11934–11939.
- (125) Sheng, W. S.; Hu, S.; Gekker, G.; Zhu, S.; Peterson, P. K.; Chao, C. C. Immunomodulatory Role of Opioids in the Central Nervous System. *Arch.*

- Immunol. Ther. Exp. (Warsz)*. **1997**, 45 (5–6), 359–366.
- (126) Welters, I. D. Is Immunomodulation by Opioid Drugs of Clinical Relevance? *Curr. Opin. Anaesthesiol.* **2003**, 16 (5), 509–513.
- (127) Vallejo, R.; de Leon-Casasola, O.; Benyamin, R. Opioid Therapy and Immunosuppression: A Review. *Am. J. Ther.* 11 (5), 354–365.
- (128) Čeřido, M. A.; Idova, G. V. [Role of Serotonin Receptors in the Delta-Opioid Immunosuppression]. *Ross. Fiziol. zhurnal Im. I.M. Sechenova* **2010**, 96 (12), 1234–1240.
- (129) Eisenstein, T. K.; Rahim, R. T.; Feng, P.; Thingalaya, N. K.; Meissler, J. J. Effects of Opioid Tolerance and Withdrawal on the Immune System. *J. Neuroimmune Pharmacol.* **2006**, 1 (3), 237–249.
- (130) Jamali, A.; Bamdad, T.; Soleimanjahi, H.; Pakdel, F. G.; Arefian, E. Acute Morphine Administration Reduces White Blood Cells' Capability to Induce Innate Resistance against HSV-1 Infection in BALB/c Mice. *Neuroimmunomodulation* **2007**, 14 (1), 16–23.
- (131) Zou, W.; Guo, Q.; Wang, E.; Cai, J.; Cheng, Z. Intrathecal Morphine Suppresses Immune Function in Rats with Inflammatory-Induced Pain. *J. Int. Med. Res.* **2007**, 35 (5), 626–636.
- (132) Menzebach, A.; Hirsch, J.; Nöst, R.; Mogk, M.; Hempelmann, G.; Welters, I. D. Morphin Hemmt Die Expression von Komplementrezeptoren Sowie Phagozytose Und Oxidativen Burst in Monozyten Über Einen NO-Abhängigen Mechanismus.

ains · Anästhesiologie · Intensivmed. · Notfallmedizin · Schmerztherapie **2004**, 39
(4), 204–211.

(133) Welters, I. D.; Menzebach, A.; Goumon, Y.; Langefeld, T. W.; Teschemacher, H.; Hempelmann, G.; Stefano, G. B. Morphine Suppresses Complement Receptor Expression, Phagocytosis, and Respiratory Burst in Neutrophils by a Nitric Oxide and mu(3) Opiate Receptor-Dependent Mechanism. *J. Neuroimmunol.* **2000**, 111 (1–2), 139–145.

(134) Carr, D. J.; Gebhardt, B. M.; Paul, D. Alpha Adrenergic and Mu-2 Opioid Receptors Are Involved in Morphine-Induced Suppression of Splenocyte Natural Killer Activity. *J. Pharmacol. Exp. Ther.* **1993**, 264 (3), 1179–1186.

(135) Grimm, M. C.; Ben-Baruch, A.; Taub, D. D.; Howard, O. M.; Resau, J. H.; Wang, J. M.; Ali, H.; Richardson, R.; Snyderman, R.; Oppenheim, J. J. Opiates Transdeactivate Chemokine Receptors: Delta and Mu Opiate Receptor-Mediated Heterologous Desensitization. *J. Exp. Med.* **1998**, 188 (2), 317–325.

(136) Roy, S.; Cain, K. J.; Chapin, R. B.; Charboneau, R. G.; Barke, R. A. Morphine Modulates NFκB Activation in Macrophages. *Biochem. Biophys. Res. Commun.* **1998**, 245 (2), 392–396.

(137) Barnes, M. J.; Holmes, G.; Primeaux, S. D.; York, D. A.; Bray, G. A. Increased Expression of Mu Opioid Receptors in Animals Susceptible to Diet-Induced Obesity. *Peptides* **2006**, 27 (12), 3292–3298.

(138) Zuberi, A. R.; Townsend, L.; Patterson, L.; Zheng, H.; Berthoud, H.-R. Increased Adiposity on Normal Diet, but Decreased Susceptibility to Diet-Induced Obesity in

- μ -Opioid Receptor-Deficient Mice. *Eur. J. Pharmacol.* **2008**, *585* (1), 14–23.
- (139) Czyzyk, T. A.; Nogueiras, R.; Lockwood, J. F.; McKinzie, J. H.; Coskun, T.; Pintar, J. E.; Hammond, C.; Tschop, M. H.; Statnick, M. A. Kappa-Opioid Receptors Control the Metabolic Response to a High-Energy Diet in Mice. *FASEB J.* **2010**, *24* (4), 1151–1159.
- (140) Ivanov, I. S.; Schulz, K. P.; Palmero, R. C.; Newcorn, J. H. Neurobiology and Evidence-Based Biological Treatments for Substance Abuse Disorders. *CNS Spectr.* **2006**, *11* (11), 864–877.
- (141) Birnbaum, H. G.; White, A. G.; Reynolds, J. L.; Greenberg, P. E.; Zhang, M.; Vallow, S.; Schein, J. R.; Katz, N. P. Estimated Costs of Prescription Opioid Analgesic Abuse in the United States in 2001. *Clin. J. Pain* **2006**, *22* (8), 667–676.
- (142) Karow, A.; Verthein, U.; Krausz, M.; Schäfer, I. Association of Personality Disorders, Family Conflicts and Treatment with Quality of Life in Opiate Addiction. *Eur. Addict. Res.* **2008**, *14* (1), 38–46.
- (143) Li, A. H.; Wang, H.-L. G Protein-Coupled Receptor Kinase 2 Mediates M-Opioid Receptor Desensitization in GABAergic Neurons of the Nucleus Raphe Magnus. *J. Neurochem.* **2001**, *77* (2), 435–444.
- (144) Zastrow, M. von; Svingos, A.; Haberstock-Debic, H.; Evans, C. Regulated Endocytosis of Opioid Receptors: Cellular Mechanisms and Proposed Roles in Physiological Adaptation to Opiate Drugs. *Curr. Opin. Neurobiol.* **2003**, *13* (3), 348–353.

- (145) Matthes, H. W. D.; Maldonado, R.; Simonin, F.; Valverde, O.; Slowe, S.; Kitchen, I.; Befort, K.; Dierich, A.; Le Meur, M.; Dollé, P.; Tzavara, E.; Hanoune, J.; Roques, B. P.; Kieffer, B. L. Loss of Morphine-Induced Analgesia, Reward Effect and Withdrawal Symptoms in Mice Lacking the M-Opioid-Receptor Gene. *Nature* **1996**, 383 (6603), 819–823.
- (146) Koch, T.; Höllt, V. Role of Receptor Internalization in Opioid Tolerance and Dependence. *Pharmacol. Ther.* **2008**, 117 (2), 199–206.
- (147) Christie, M. J. Cellular Neuroadaptations to Chronic Opioids: Tolerance, Withdrawal and Addiction. *Br. J. Pharmacol.* **2009**, 154 (2), 384–396.
- (148) Przewlocki, R. Opioid Abuse and Brain Gene Expression. *Eur. J. Pharmacol.* **2004**, 500 (1–3), 331–349.
- (149) Bohn, L. M.; Dykstra, L. A.; Lefkowitz, R. J.; Caron, M. G.; Barak, L. S. Relative Opioid Efficacy Is Determined by the Complements of the G Protein-Coupled Receptor Desensitization Machinery. *Mol. Pharmacol.* **2004**, 66 (1), 106–112.
- (150) Bohn, L. M.; Gainetdinov, R. R.; Lin, F. T.; Lefkowitz, R. J.; Caron, M. G. Mu-Opioid Receptor Desensitization by Beta-Arrestin-2 Determines Morphine Tolerance but Not Dependence. *Nature* **2000**, 408 (6813), 720–723.
- (151) Bohn, L. M.; Lefkowitz, R. J.; Caron, M. G. Differential Mechanisms of Morphine Antinociceptive Tolerance Revealed in (Beta)arrestin-2 Knock-out Mice. *J. Neurosci.* **2002**, 22 (23), 10494–10500.
- (152) Gomes, I.; Gupta, A.; Filipovska, J.; Szeto, H. H.; Pintar, J. E.; Devi, L. A. A Role

- for Heterodimerization of Mu and Delta Opiate Receptors in Enhancing Morphine Analgesia. *Proc. Natl. Acad. Sci. U. S. A.* **2004**, *101* (14), 5135–5139.
- (153) Nitsche, J. F.; Schuller, A. G. P.; King, M. A.; Zengh, M.; Pasternak, G. W.; Pintar, J. E. Genetic Dissociation of Opiate Tolerance and Physical Dependence in Delta-Opioid Receptor-1 and Preproenkephalin Knock-out Mice. *J. Neurosci.* **2002**, *22* (24), 10906–10913.
- (154) Zhu, Y.; King, M. A.; Schuller, A. G.; Nitsche, J. F.; Reidl, M.; Elde, R. P.; Unterwald, E.; Pasternak, G. W.; Pintar, J. E. Retention of Supraspinal Delta-like Analgesia and Loss of Morphine Tolerance in Delta Opioid Receptor Knockout Mice. *Neuron* **1999**, *24* (1), 243–252.
- (155) Land, B. B.; Bruchas, M. R.; Schattauer, S.; Giardino, W. J.; Aita, M.; Messinger, D.; Hnasko, T. S.; Palmiter, R. D.; Chavkin, C. Activation of the Kappa Opioid Receptor in the Dorsal Raphe Nucleus Mediates the Aversive Effects of Stress and Reinstates Drug Seeking. *Proc. Natl. Acad. Sci. U. S. A.* **2009**, *106* (45), 19168–19173.
- (156) Cunha-Oliveira, T.; Rego, A. C.; Oliveira, C. R. Cellular and Molecular Mechanisms Involved in the Neurotoxicity of Opioid and Psychostimulant Drugs. *Brain Res. Rev.* **2008**, *58* (1), 192–208.
- (157) LaLumiere, R. T.; Kalivas, P. W. Glutamate Release in the Nucleus Accumbens Core Is Necessary for Heroin Seeking. *J. Neurosci.* **2008**, *28* (12), 3170–3177.
- (158) Harrison, L. M.; Kastin, A. J.; Zadina, J. E. Opiate Tolerance and Dependence: Receptors, G-Proteins, and Antiopiates. *Peptides* **1998**, *19* (9), 1603–1630.

- (159) Kreek, M. J.; Nielsen, D. A.; LaForge, K. S. Genes Associated With Addiction: Alcoholism, Opiate, and Cocaine Addiction. *NeuroMolecular Med.* **2004**, *5* (1), 085–108.
- (160) Mayer, P.; Höllt, V. Pharmacogenetics of Opioid Receptors and Addiction. *Pharmacogenet. Genomics* **2006**, *16* (1), 1–7.
- (161) Saboory, E.; Derchansky, M.; Ismaili, M.; Jahromi, S. S.; Brull, R.; Carlen, P. L.; El Beheiry, H. Mechanisms of Morphine Enhancement of Spontaneous Seizure Activity. *Anesth. Analg.* **2007**, *105* (6), 1729–1735.
- (162) DANIELSSON, I.; GASIOR, M.; STEVENSON, G.; FOLK, J.; RICE, K.; NEGUS, S. Electroencephalographic and Convulsant Effects of the Delta Opioid Agonist SNC80 in Rhesus Monkeys. *Pharmacol. Biochem. Behav.* **2006**, *85* (2), 428–434.
- (163) Grecksch, G.; Becker, A.; Schroeder, H.; Höllt, V. Involvement of Delta-Opioid Receptors in Pentylentetrazol Kindling Development and Kindling-Related Processes in Rats. *Naunyn. Schmiedeberg's. Arch. Pharmacol.* **1999**, *360* (2), 151–156.
- (164) Tortella, F. C.; Long, J. B. Endogenous Anticonvulsant Substance in Rat Cerebrospinal Fluid after a Generalized Seizure. *Science* **1985**, *228* (4703), 1106–1108.
- (165) Tortella, F. C.; Echevarria, E.; Robles, L.; Mosberg, H. I.; Holaday, J. W. Anticonvulsant Effects of Mu (DAGO) and Delta (DPDPE) Enkephalins in Rats. *Peptides* *9* (5), 1177–1181.

- (166) Tortella, F. C.; Robles, L.; Holaday, J. W. The Anticonvulsant Effects of DADLE Are Primarily Mediated by Activation of Delta Opioid Receptors: Interactions between Delta and Mu Receptor Antagonists. *Life Sci.* **1985**, *37* (6), 497–503.
- (167) Pinsky, C.; Bose, R.; Frederickson, R. C. Mu- and Delta-Opioid Modulation of Electrically-Induced Epileptic Seizures in Mice. *NIDA Res. Monogr.* **1986**, *75*, 543–546.
- (168) Marczak, E. D.; Jinsmaa, Y.; Myers, P. H.; Blankenship, T.; Wilson, R.; Balboni, G.; Salvadori, S.; Lazarus, L. H. Orally Administered H-Dmt-Tic-Lys-NH-CH₂-Ph (MZ-2), a Potent M- δ -Opioid Receptor Antagonist, Regulates Obese-Related Factors in Mice. *Eur. J. Pharmacol.* **2009**, *616* (1–3), 115–121.
- (169) Gosnell, B. A.; Levine, A. S. Reward Systems and Food Intake: Role of Opioids. *Int. J. Obes.* **2009**, *33*, S54–S58.
- (170) Yeadon, M.; Kitchen, I. Opioids and Respiration. *Prog. Neurobiol.* **1989**, *33* (1), 1–16.
- (171) Pattinson, K. T. S. Opioids and the Control of Respiration. *Br. J. Anaesth.* **2008**, *100* (6), 747–758.
- (172) Wu, S.; Li, H. Y.; Wong, T. M. Cardioprotection of Preconditioning by Metabolic Inhibition in the Rat Ventricular Myocyte. Involvement of Kappa-Opioid Receptor. *Circ. Res.* **1999**, *84* (12), 1388–1395.
- (173) Schultz, J. J.; Hsu, A. K.; Gross, G. J. Ischemic Preconditioning and Morphine-Induced Cardioprotection Involve the Delta (δ)-Opioid Receptor in the Intact Rat

- Heart. *J. Mol. Cell. Cardiol.* **1997**, 29 (8), 2187–2195.
- (174) Wang, G. Y.; Wu, S.; Pei, J. M.; Yu, X. C.; Wong, T. M. Kappa- but Not Delta-Opioid Receptors Mediate Effects of Ischemic Preconditioning on Both Infarct and Arrhythmia in Rats. *Am. J. Physiol. Heart Circ. Physiol.* **2001**, 280 (1), H384-91.
- (175) Spampinato, S.; Goldstein, A. Immunoreactive Dynorphin in Rat Tissues and Plasma. *Neuropeptides* **1983**, 3 (3), 193–212.
- (176) Barron, B. A.; Gu, H.; Gaugl, J. F.; Caffrey, J. L. Screening for Opioids in Dog Heart. *J. Mol. Cell. Cardiol.* **1992**, 24 (1), 67–77.
- (177) Weihe, E.; McKnight, A. T.; Corbett, A. D.; Kosterlitz, H. W. Proenkephalin- and Prodynorphin- Derived Opioid Peptides in Guinea-Pig Heart. *Neuropeptides* **1985**, 5 (4–6), 453–456.
- (178) Weihe, E.; McKnight, A. T.; Corbett, A. D.; Hartschuh, W.; Reinecke, M.; Kosterlitz, H. W. Characterization of Opioid Peptides in Guinea-Pig Heart and Skin. *Life Sci.* **1983**, 33 Suppl 1, 711–714.
- (179) Lang, R. E.; Hermann, K.; Dietz, R.; Gaida, W.; Ganten, D.; Kraft, K.; Unger, T. Evidence for the Presence of Enkephalins in the Heart. *Life Sci.* **1983**, 32 (4), 399–406.
- (180) Forman, L. J.; Estilow, S.; Hock, C. E. Localization of Beta-Endorphin in the Rat Heart and Modulation by Testosterone. *Proc. Soc. Exp. Biol. Med.* **1989**, 190 (3), 240–245.
- (181) Mabrouk, O. S.; Volta, M.; Marti, M.; Morari, M. Stimulation of Delta Opioid

- Receptors Located in Substantia Nigra Reticulata but Not Globus Pallidus or Striatum Restores Motor Activity in 6-Hydroxydopamine Lesioned Rats: New Insights into the Role of Delta Receptors in Parkinsonism. *J. Neurochem.* **2008**, *107* (6), 1647–1659.
- (182) Hill, M. P.; Hille, C. J.; Brotchie, J. M. Delta-Opioid Receptor Agonists as a Therapeutic Approach in Parkinson's Disease. *Drug News Perspect.* **2000**, *13* (5), 261–268.
- (183) Zagon, I. S.; Rahn, K. A.; Bonneau, R. H.; Turel, A. P.; McLaughlin, P. J. Opioid Growth Factor Suppresses Expression of Experimental Autoimmune Encephalomyelitis. *Brain Res.* **2010**, *1310*, 154–161.
- (184) Kampman, K.; Jarvis, M. American Society of Addiction Medicine (ASAM) National Practice Guideline for the Use of Medications in the Treatment of Addiction Involving Opioid Use. *J. Addict. Med.* **2015**, *9* (5), 358–367.
- (185) Dugosh, K.; Abraham, A.; Seymour, B.; McLoyd, K.; Chalk, M.; Festinger, D. A Systematic Review on the Use of Psychosocial Interventions in Conjunction With Medications for the Treatment of Opioid Addiction. *J. Addict. Med.* **2016**, *10* (2), 93–103.
- (186) Chen, H.; Wu, J.; Zhang, J.; Hashimoto, K. Recent Topics on Pharmacotherapy for Amphetamine-Type Stimulants Abuse and Dependence. *Curr. Drug Abuse Rev.* **2010**, *3* (4), 222–238.
- (187) George, S.; Ekhtiari, H. Naltrexone in the Treatment of Opioid Dependence. *Br. J. Hosp. Med. (Lond).* **2010**, *71* (10), 568–570.

- (188) Minozzi, S.; Amato, L.; Vecchi, S.; Davoli, M.; Kirchmayer, U.; Verster, A. Oral Naltrexone Maintenance Treatment for Opioid Dependence. In *Cochrane Database of Systematic Reviews*; Minozzi, S., Ed.; John Wiley & Sons, Ltd: Chichester, UK, 2011; p CD001333.
- (189) Miotto, K.; McCann, M.; Basch, J.; Rawson, R.; Ling, W. Naltrexone and Dysphoria: Fact or Myth? *Am. J. Addict.* **2002**, *11* (2), 151–160.
- (190) Ritter, A. J. Naltrexone in the Treatment of Heroin Dependence: Relationship with Depression and Risk of Overdose. *Aust. N. Z. J. Psychiatry* **2002**, *36* (2), 224–228.
- (191) van Dorp, E. L. A.; Yassen, A.; Dahan, A. Naloxone Treatment in Opioid Addiction: The Risks and Benefits. *Expert Opin. Drug Saf.* **2007**, *6* (2), 125–132.
- (192) Wentland, M. P.; Lou, R.; Lu, Q.; Bu, Y.; Denhardt, C.; Jin, J.; Ganorkar, R.; VanAlstine, M. A.; Guo, C.; Cohen, D. J.; Bidlack, J. M. Syntheses of Novel High Affinity Ligands for Opioid Receptors. *Bioorg. Med. Chem. Lett.* **2009**, *19* (8), 2289–2294.
- (193) White, K. L.; Roth, B. L. Psychotomimetic Effects of Kappa Opioid Receptor Agonists. *Biol. Psychiatry* **2012**, *72* (10), 797–798.
- (194) Matthes, H. W. D.; Maldonado, R.; Simonin, F.; Valverde, O.; Slowe, S.; Kitchen, I.; Befort, K.; Dierich, A.; Le Meur, M.; Dollé, P.; Tzavara, E.; Hanoune, J.; Roques, B. P.; Kieffer, B. L. Loss of Morphine-Induced Analgesia, Reward Effect and Withdrawal Symptoms in Mice Lacking the M-Opioid-Receptor Gene. *Nature* **1996**, *383* (6603), 819–823.

- (195) Skoubis, P. D.; Matthes, H. W.; Walwyn, W. M.; Kieffer, B. L.; Maidment, N. T. Naloxone Fails to Produce Conditioned Place Aversion in Mu-Opioid Receptor Knock-out Mice. *Neuroscience* **2001**, *106* (4), 757–763.
- (196) Burke, T. F.; Woods, J. H.; Lewis, J. W.; Medzihradsky, F. Irreversible Opioid Antagonist Effects of Cloccinamox on Opioid Analgesia and Mu Receptor Binding in Mice. *J. Pharmacol. Exp. Ther.* **1994**, *271* (2), 715–721.
- (197) Hawkins, K. N.; Knapp, R. J.; Lui, G. K.; Gulya, K.; Kazmierski, W.; Wan, Y. P.; Pelton, J. T.; Hruby, V. J.; Yamamura, H. I. [3H]-[H-D-Phe-Cys-Tyr-D-Trp-Orn-Thr-Pen-Thr-NH₂] ([3H]CTOP), a Potent and Highly Selective Peptide for Mu Opioid Receptors in Rat Brain. *J. Pharmacol. Exp. Ther.* **1989**, *248* (1), 73–80.
- (198) Spetea, M.; Schüllner, F.; Moisa, R. C.; Berzetei-Gurske, I. P.; Schraml, B.; Dörfler, C.; Aceto, M. D.; Harris, L. S.; Coop, A.; Schmidhammer, H. Synthesis and Biological Evaluation of 14-Alkoymorphinans. 21. Novel 4-Alkoxy and 14-Phenylpropoxy Derivatives of the Mu Opioid Receptor Antagonist Cyprodime. *J. Med. Chem.* **2004**, *47* (12), 3242–3247.
- (199) Schmidhammer, H.; Burkard, W. P.; Eggstein-Aeppli, L.; Smith, C. F. Synthesis and Biological Evaluation of 14-Alkoymorphinans. 2. (-)-N-(Cyclopropylmethyl)-4,14-Dimethoxymorphinan-6-One, a Selective Mu Opioid Receptor Antagonist. *J. Med. Chem.* **1989**, *32* (2), 418–421.
- (200) Hruby, V. J.; Toth, G.; Gehrig, C. A.; Kao, L. F.; Knapp, R.; Lui, G. K.; Yamamura, H. I.; Kramer, T. H.; Davis, P.; Burks, T. F. Topographically Designed Analogues of [D-Pen,D-Pen⁵]enkephalin. *J. Med. Chem.* **1991**, *34* (6), 1823–1830.

- (201) Abbruscato, T. J.; Thomas, S. A.; Hruby, V. J.; Davis, T. P. Blood-Brain Barrier Permeability and Bioavailability of a Highly Potent and Mu-Selective Opioid Receptor Antagonist, CTAP: Comparison with Morphine. *J. Pharmacol. Exp. Ther.* **1997**, *280* (1), 402–409.
- (202) Portoghese, P. S.; Sultana, M.; Nagase, H.; Takemori, A. E. Application of the Message-Address Concept in the Design of Highly Potent and Selective Non-Peptide Delta Opioid Receptor Antagonists. *J. Med. Chem.* **1988**, *31* (2), 281–282.
- (203) Jones, R. M.; Hjorth, S. A.; Schwartz, T. W.; Portoghese, P. S. Mutational Evidence for a Common Kappa Antagonist Binding Pocket in the Wild-Type Kappa and Mutant mu[K303E] Opioid Receptors. *J. Med. Chem.* **1998**, *41* (25), 4911–4914.
- (204) Jones, R. M.; Portoghese, P. S. 5'-Guanidinonaltrindole, a Highly Selective and Potent Kappa-Opioid Receptor Antagonist. *Eur. J. Pharmacol.* **2000**, *396* (1), 49–52.
- (205) Yuan, Y.; Li, G.; He, H.; Stevens, D. L.; Kozak, P.; Scoggins, K. L.; Mitra, P.; Gerk, P. M.; Selley, D. E.; Dewey, W. L.; Zhang, Y. Characterization of 6 α - and 6 β -N-Heterocyclic Substituted Naltrexamine Derivatives as Novel Leads to Development of Mu Opioid Receptor Selective Antagonists. *ACS Chem. Neurosci.* **2011**, *2* (7), 346–351.
- (206) Yuan, Y.; Elbegdorj, O.; Beletskaya, I. O.; Selley, D. E.; Zhang, Y. Structure Activity Relationship Studies of 17-Cyclopropylmethyl-3,14 β -Dihydroxy-4,5 α -

- Epoxy-6 α -(Isoquinoline-3'-Carboxamido)morphinan (NAQ) Analogues as Potent Opioid Receptor Ligands: Preliminary Results on the Role of Electronic Characteristics for Affin. *Bioorg. Med. Chem. Lett.* **2013**, 23 (18), 5045–5048.
- (207) Li, G.; Aschenbach, L. C.; Chen, J.; Cassidy, M. P.; Stevens, D. L.; Gabra, B. H.; Selley, D. E.; Dewey, W. L.; Westkaemper, R. B.; Zhang, Y. Design, Synthesis, and Biological Evaluation of 6 α - and 6 β -N-Heterocyclic Substituted Naltrexamine Derivatives as Mu Opioid Receptor Selective Antagonists. *J. Med. Chem.* **2009**, 52 (5), 1416–1427.
- (208) Yuan, Y.; Stevens, D. L.; Braithwaite, A.; Scoggins, K. L.; Bilsky, E. J.; Akbarali, H. I.; Dewey, W. L.; Zhang, Y. 6 β -N-Heterocyclic Substituted Naltrexamine Derivative NAP as a Potential Lead to Develop Peripheral Mu Opioid Receptor Selective Antagonists. *Bioorganic Med. Chem. Lett.* **2012**, 22 (14), 4731–4734.
- (209) Mitra, P.; Venitz, J.; Yuan, Y.; Zhang, Y.; Gerk, P. M. Preclinical Disposition (in Vitro) of Novel μ -Opioid Receptor Selective Antagonists. *Drug Metab. Dispos.* **2011**, 39 (9), 1589–1596.
- (210) Altarifi, A. A.; Yuan, Y.; Zhang, Y.; Selley, D. E.; Negus, S. S. Effects of the Novel, Selective and Low-Efficacy Mu Opioid Receptor Ligand NAQ on Intracranial Self-Stimulation in Rats. *Psychopharmacology (Berl)*. **2015**, 232 (4), 815–824.
- (211) Yuan, Y.; Zaidi, S. A.; Stevens, D. L.; Scoggins, K. L.; Mosier, P. D.; Kellogg, G. E.; Dewey, W. L.; Selley, D. E.; Zhang, Y. Design, Syntheses, and Pharmacological Characterization of 17-Cyclopropylmethyl-3,14 β -Dihydroxy-4,5 α -Epoxy-6 α -(Isoquinoline-3'-Carboxamido)morphinan Analogues as Opioid

- Receptor Ligands. *Bioorganic Med. Chem.* **2015**, 23 (8), 1701–1715.
- (212) Abdelhamid, E. E.; Sultana, M.; Portoghese, P. S.; Takemori, A. E. Selective Blockage of Delta Opioid Receptors Prevents the Development of Morphine Tolerance and Dependence in Mice. *J. Pharmacol. Exp. Ther.* **1991**, 258 (1), 299–303.
- (213) Zaidi, S. A.; Arnatt, C. K.; He, H.; Selley, D. E.; Mosier, P. D.; Kellogg, G. E.; Zhang, Y. Binding Mode Characterization of 6 α - and 6 β -N-Heterocyclic Substituted Naltrexamine Derivatives via Docking in Opioid Receptor Crystal Structures and Site-Directed Mutagenesis Studies: Application of the “Message-Address” Concept in Development of Mu Opioid. *Bioorganic Med. Chem.* **2013**, 21 (21), 6405–6413.
- (214) Sayre, L. M.; Portoghese, P. S. Stereospecific Synthesis of the 6.alpha.- and 6.beta.-Amino Derivatives of Naltrexone and Oxymorphone. *J. Org. Chem.* **1980**, 45 (16), 3366–3368.
- (215) Yung-Chi, C.; Prusoff, W. H. Relationship between the Inhibition Constant (KI) and the Concentration of Inhibitor Which Causes 50 per Cent Inhibition (I50) of an Enzymatic Reaction. *Biochem. Pharmacol.* **1973**, 22 (23), 3099–3108.
- (216) Jacobsen, E. J.; Myers, J. K.; Walker, D. P.; Wishka, D. G.; Reitz, S. C.; Piotrowski, D. W.; Acker, B. A.; Groppi, J. V. E. Azabicyclic Compounds with alpha7 Nicotinic Acetylcholine Receptor Activity, 2003.
- (217) Navia, M. A.; Chatuverdi, P. R. Design Principles for Orally Bioavailable Drugs. *Drug Discov. Today* **1996**, 1 (5), 179–189.

- (218) Turner, J. V.; Glass, B. D.; Agatonovic-Kustrin, S. Prediction of Drug Bioavailability Based on Molecular Structure. *Anal. Chim. Acta* **2003**, *485* (1), 89–102.
- (219) Ohara, H.; Miyabe, Y.; Deyashiki, Y.; Matsuura, K.; Hara, A. REDUCTION OF DRUG KETONES BY DIHYDRODIOL DEHYDROGENASES, CARBONYL REDUCTASE AND ALDEHYDE REDUCTASE OF HUMAN LIVER. *Biochem. Pharmacol.* **1995**, *50* (2), 221–227.
- (220) Cone, E. J. HUMAN METABOLITE OF NALTREXONE (N-CTCLOPROPYLMBTHTLNOROXYMORPHINE) WITH A NOVEL C-6 ISOMORPHINE CONFIGURATION. *Tetrahedron Lett.* **1973**, *14* (28), 2607–2610.
- (221) Meyer, M. C.; Straughn, A. B.; Lo, M. W.; Schary, W. L.; Whitney, C. C. Bioequivalence, Dose-Proportionality, and Pharmacokinetics of Naltrexone after Oral Administration. *J. Clin. Psychiatry* **1984**, *45* (9 Pt 2), 15–19.
- (222) Wall, M. E.; Brine, D. R.; Perez-Reyes, M. Metabolism and Disposition of Naltrexone in Man after Oral and Intravenous Administration. *Drug Metab. Dispos.* **1981**, *9* (4), 369–375.
- (223) Porter, S. J.; Somogyi, A. A.; White, J. M. Kinetics and Inhibition of the Formation of 6beta-Naltrexol from Naltrexone in Human Liver Cytosol. *Br. J. Clin. Pharmacol.* **2000**, *50* (5), 465–471.
- (224) Badri, P.; Venitz, J. *Quantitative Structure -Pharmacokinetic Relationships of Opioids in Humans*; Richmond, VA, 2010.
- (225) Lipinski, C. A.; Lombardo, F.; Dominy, B. W.; Feeney, P. J. Experimental and

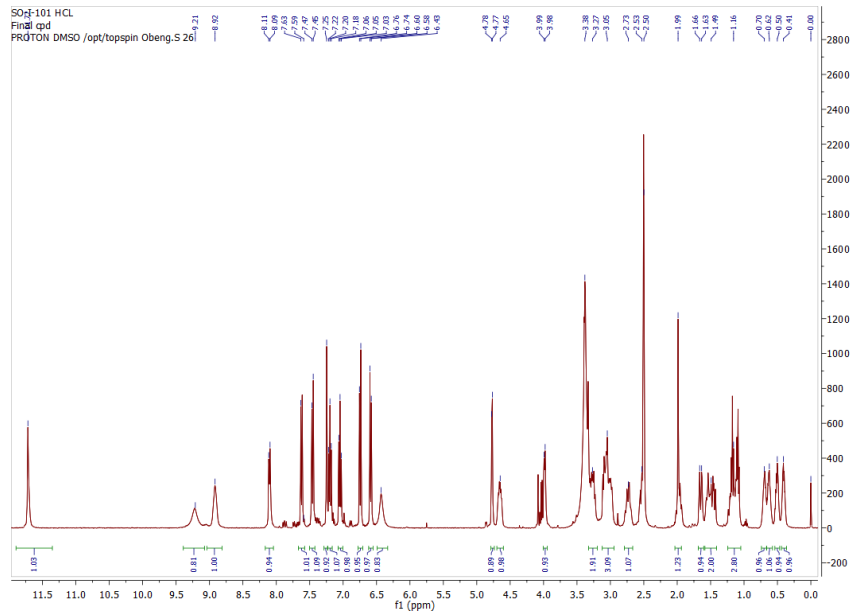
- Computational Approaches to Estimate Solubility and Permeability in Drug Discovery and Development. *Adv. Drug Deliv. Rev.* **2001**, *46* (1–3), 3–26.
- (226) Fichert, T.; Yazdanian, M.; Proudfoot, J. R. A structure–Permeability Study of Small Drug-like Molecules. *Bioorg. Med. Chem. Lett.* **2003**, *13* (4), 719–722.
- (227) Norinder, U.; Haeberlein, M. Computational Approaches to the Prediction of the Blood–brain Distribution. *Adv. Drug Deliv. Rev.* **2002**, *54* (3), 291–313.
- (228) Contractor, R. B.; Peters, A. T.; Hodgson, H. H.; Ratcliffe, J.; Mackie, A.; Ward, E. R. Notes. New Intermediates and Dyes. Part I. 4-Tert.-ButyZphthaZic Acid and Its Anhydride. *J. Chem. Soc.* **1949**, 1314–1317.
- (229) Harrison, C.; Traynor, J. R. The [35S]GTPgS Binding Assay: Approaches and Applications in Pharmacology. *Life Sci.* **2003**, *74* (4), 489–508.
- (230) Coderre, T. J.; Rollman, G. B. Naloxone Hyperalgesia and Stress-Induced Analgesia in Rats. *Life Sci.* **1983**, *32* (18), 2139–2146.

Appendix

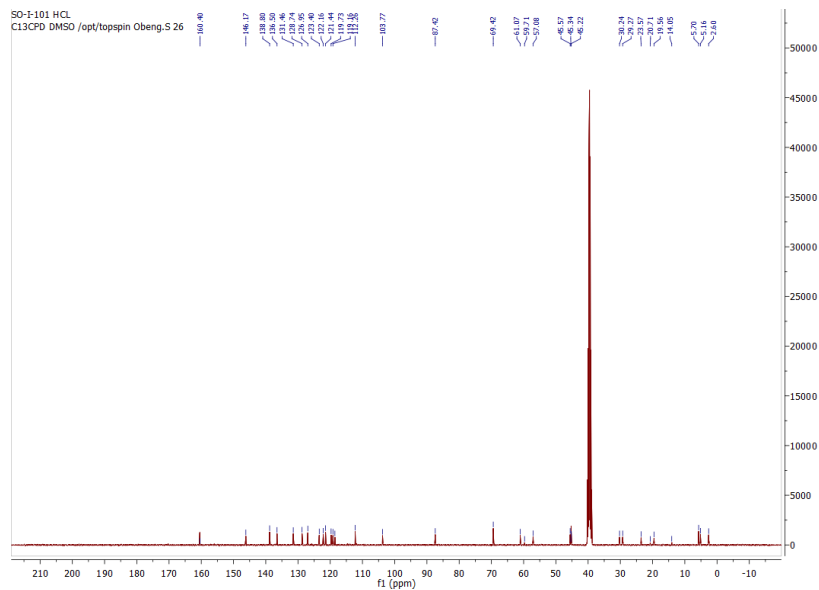
Spectra

Compound 1

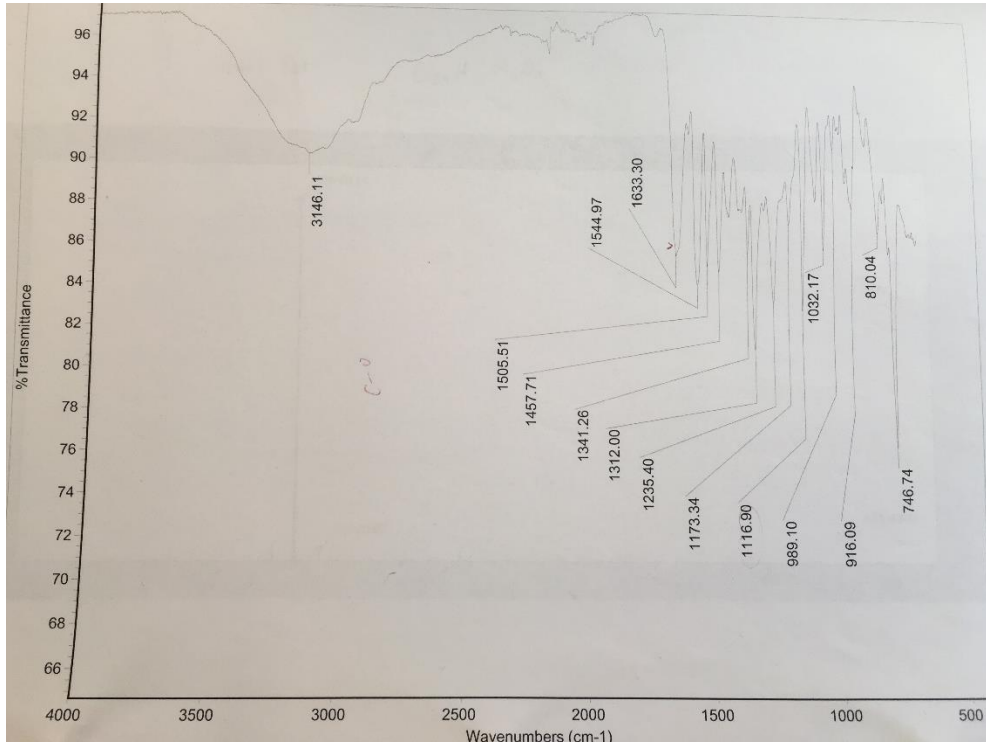
¹H NMR



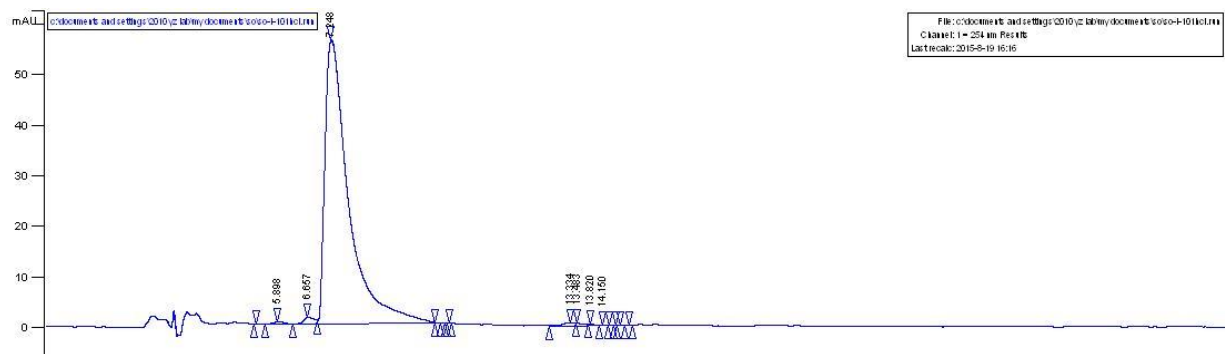
¹³CNMR



IR

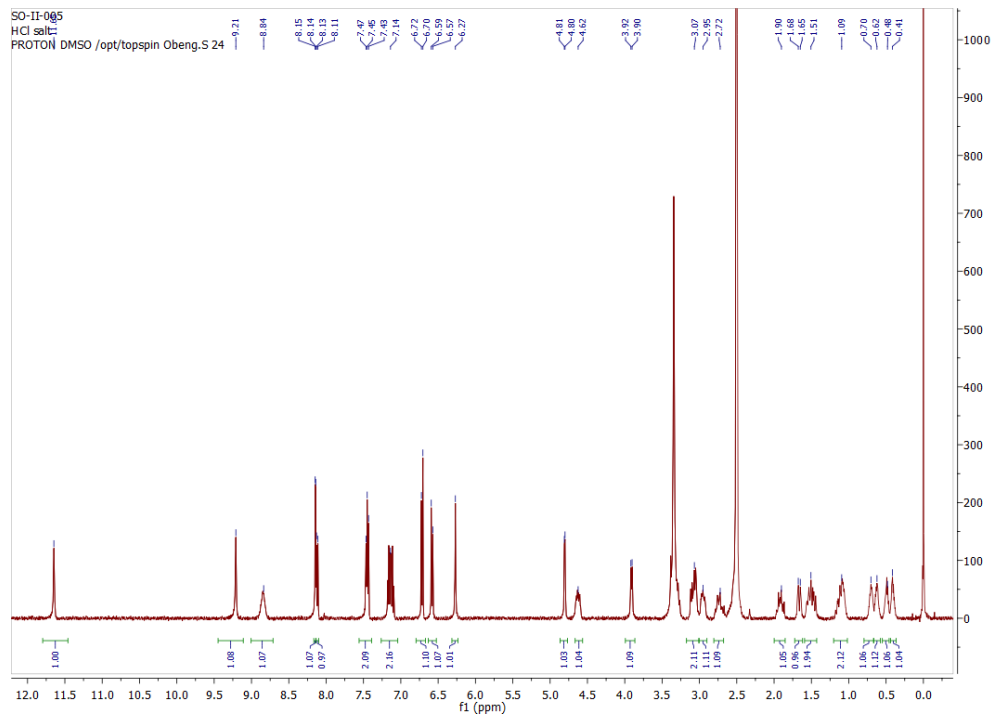


HPLC

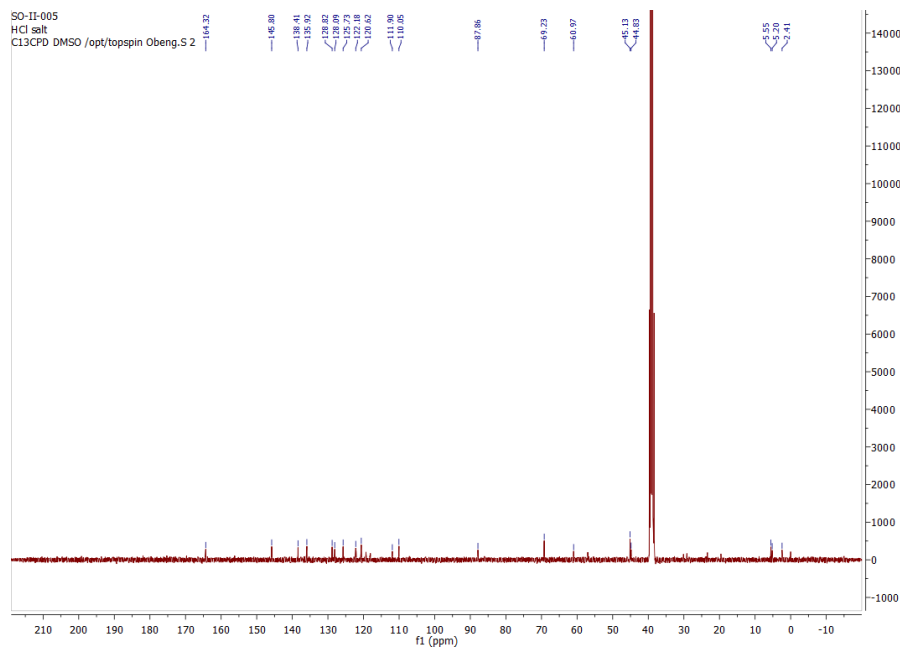


Compound 2

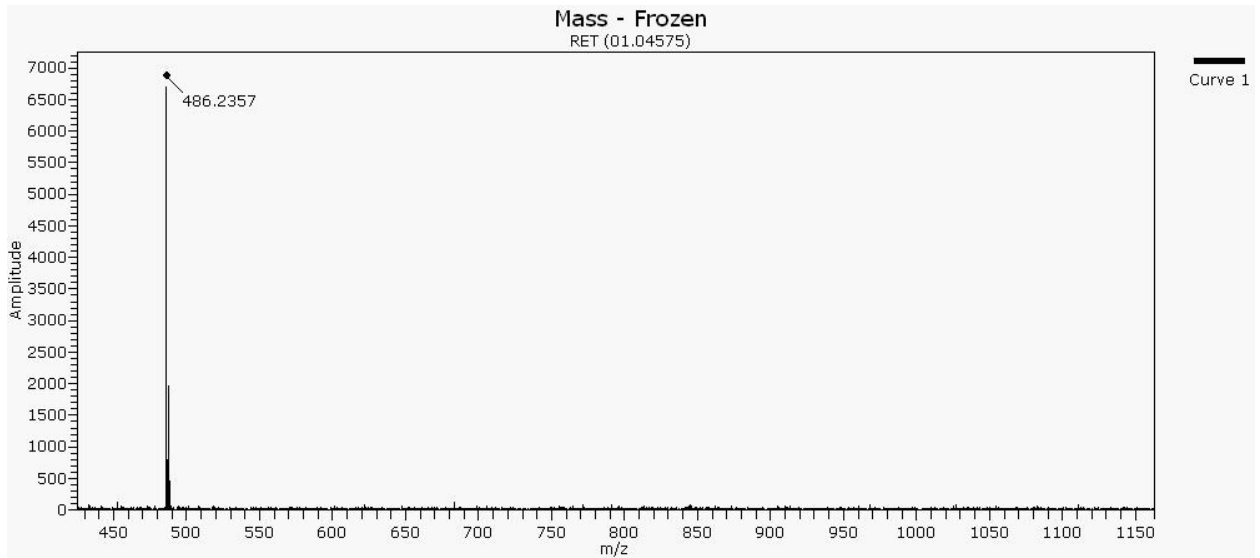
¹H NMR



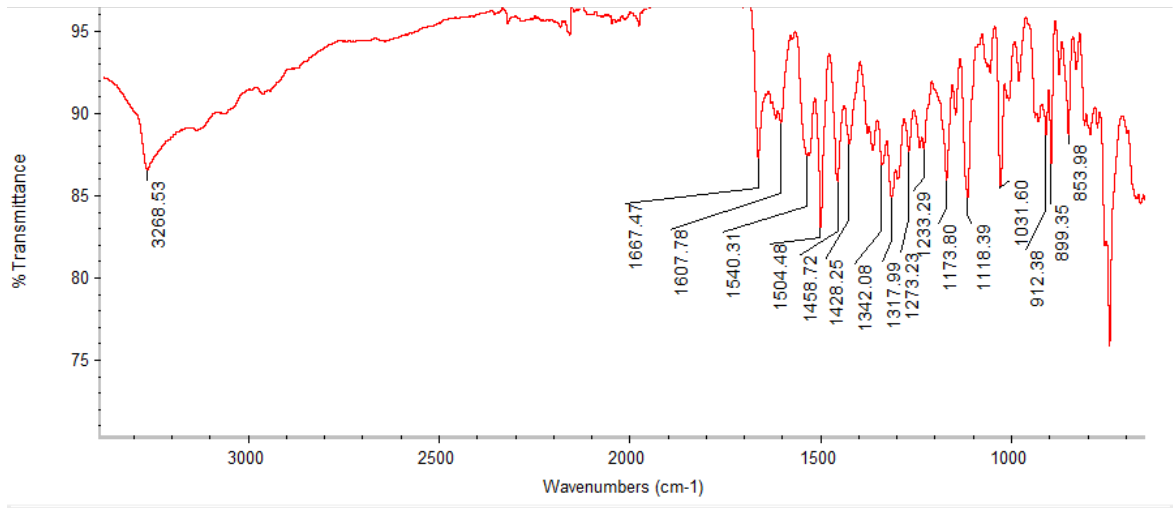
¹³C NMR



High resolution Masspec

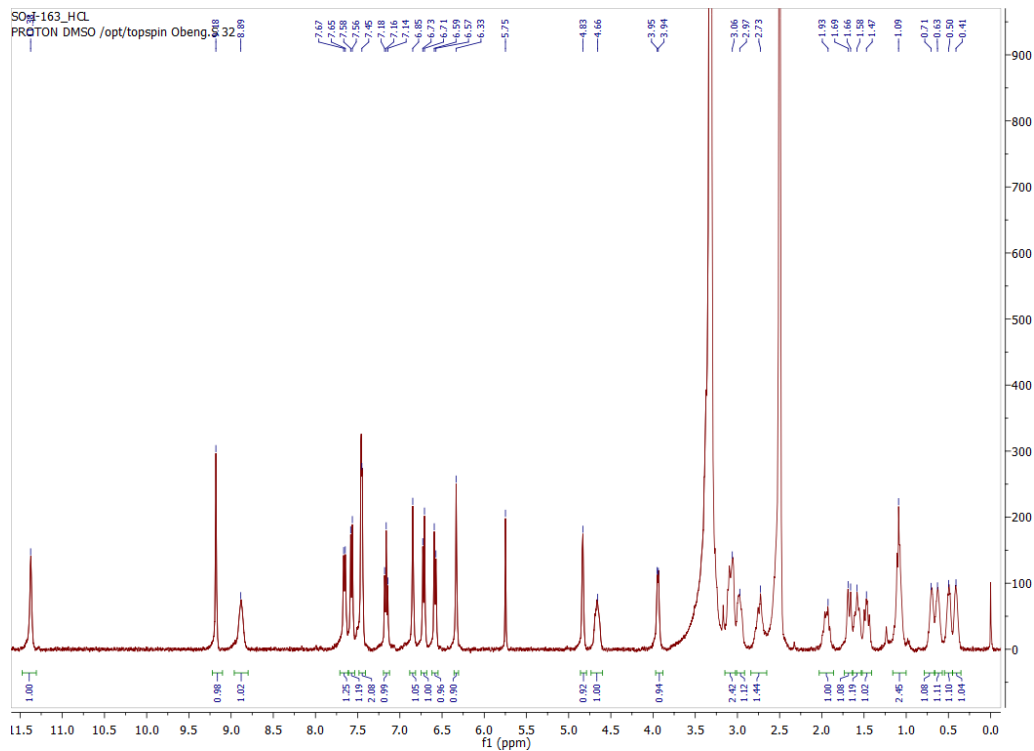


IR

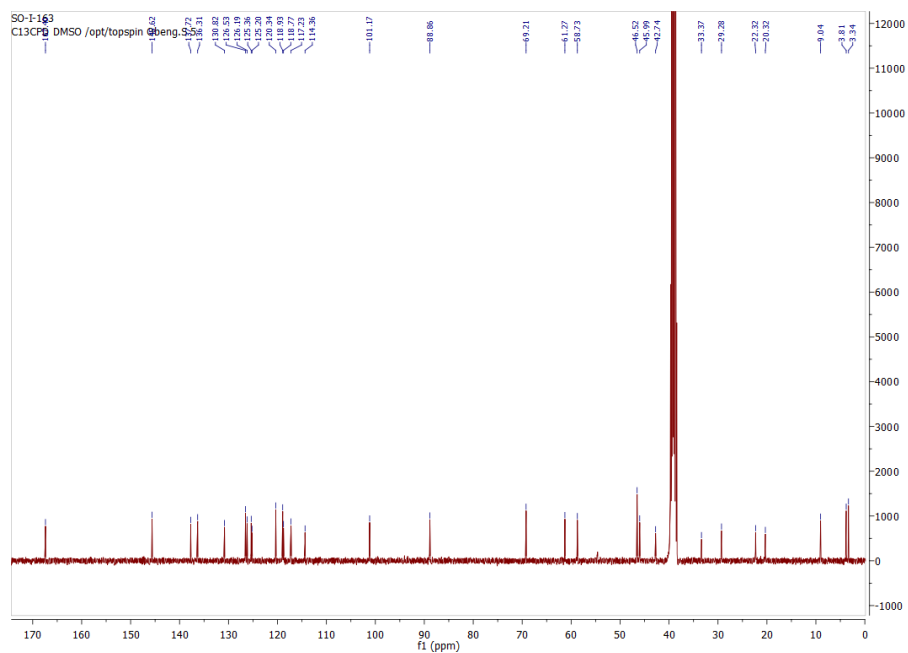


Compound 3

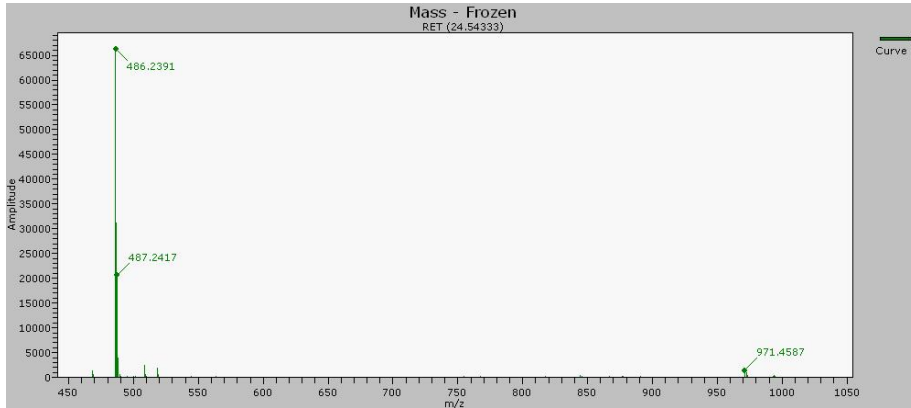
¹H NMR



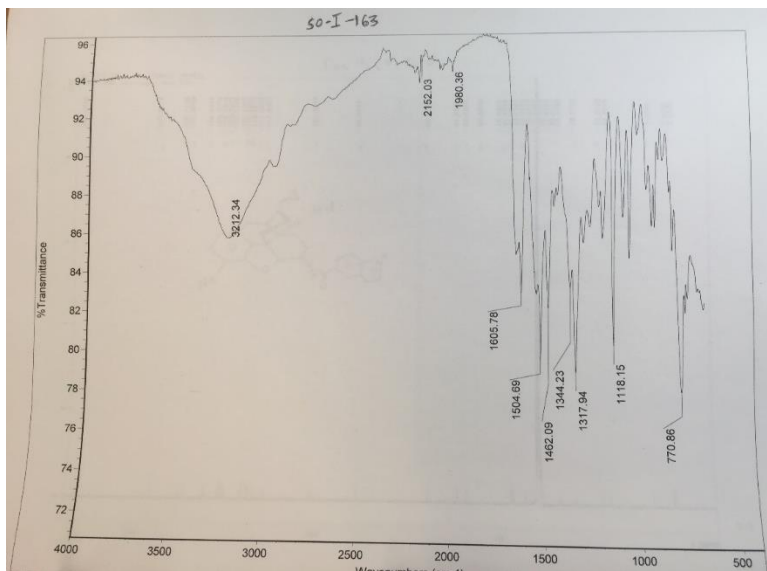
¹³C NMR



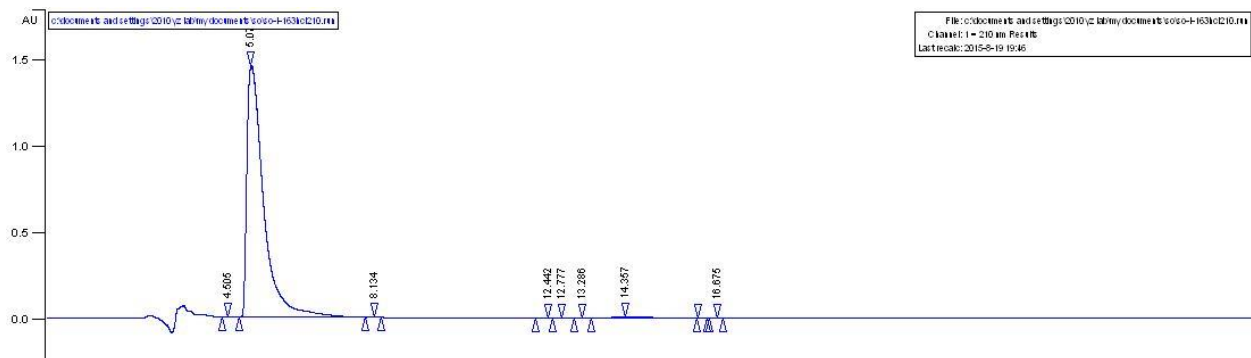
High resolution Masspec



IR

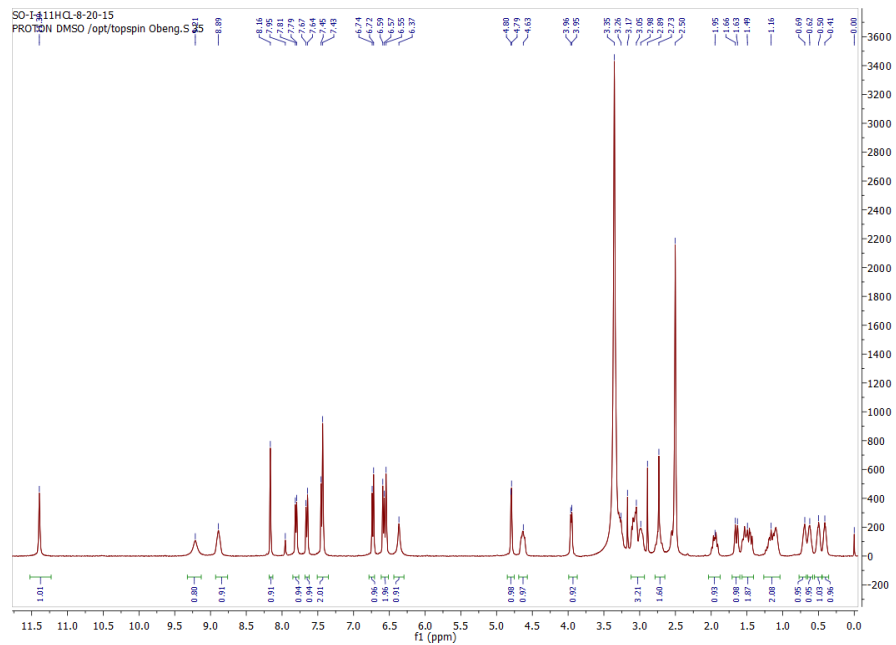


HPLC

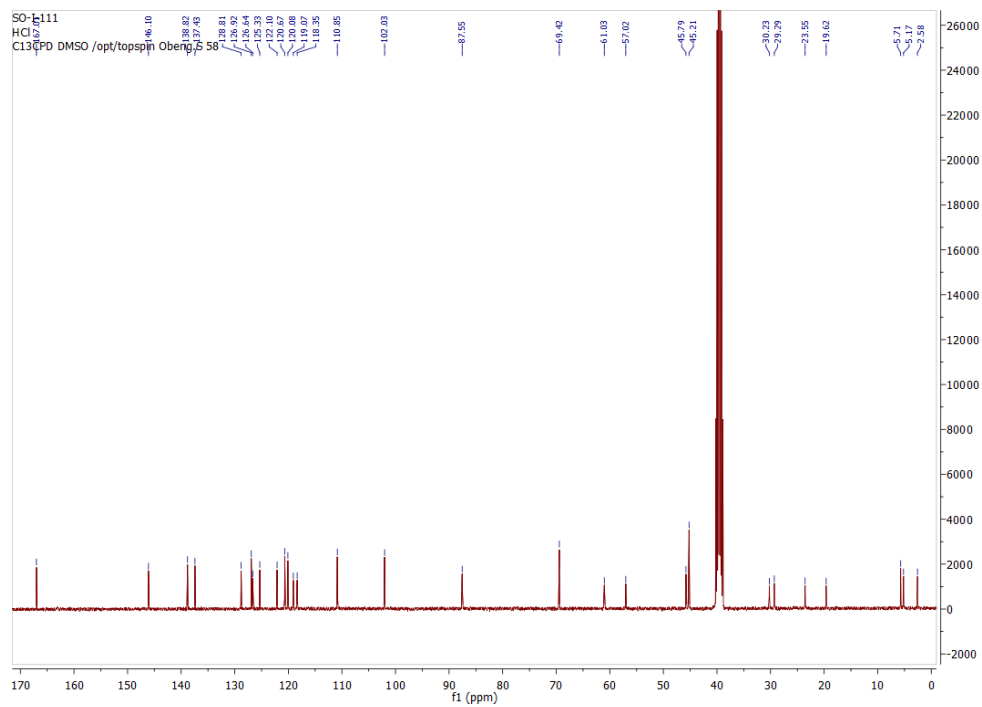


Compound 4

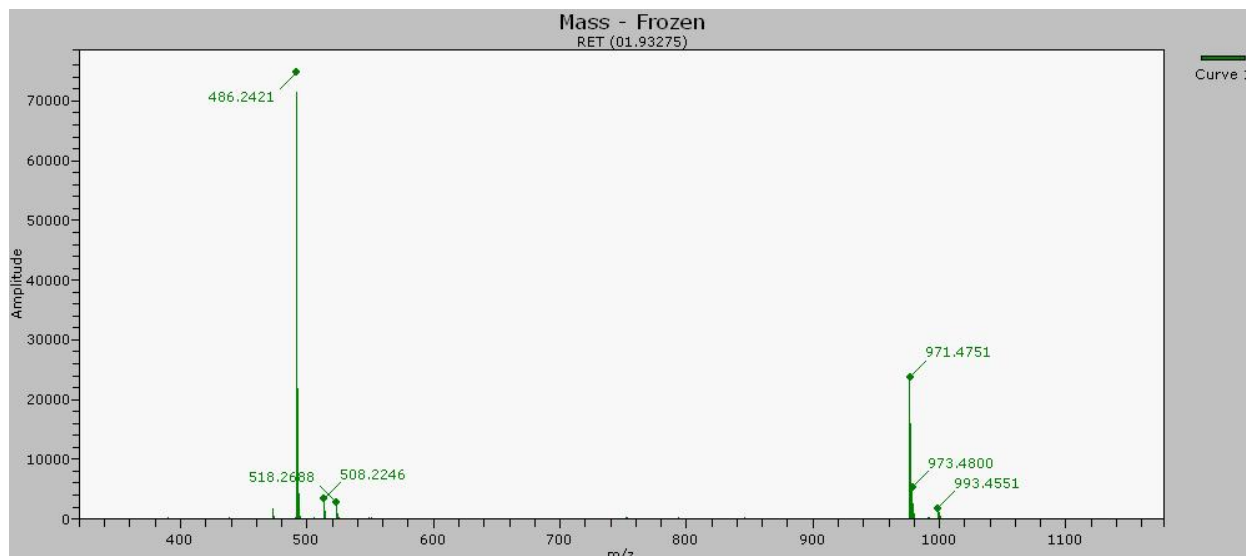
¹H NMR



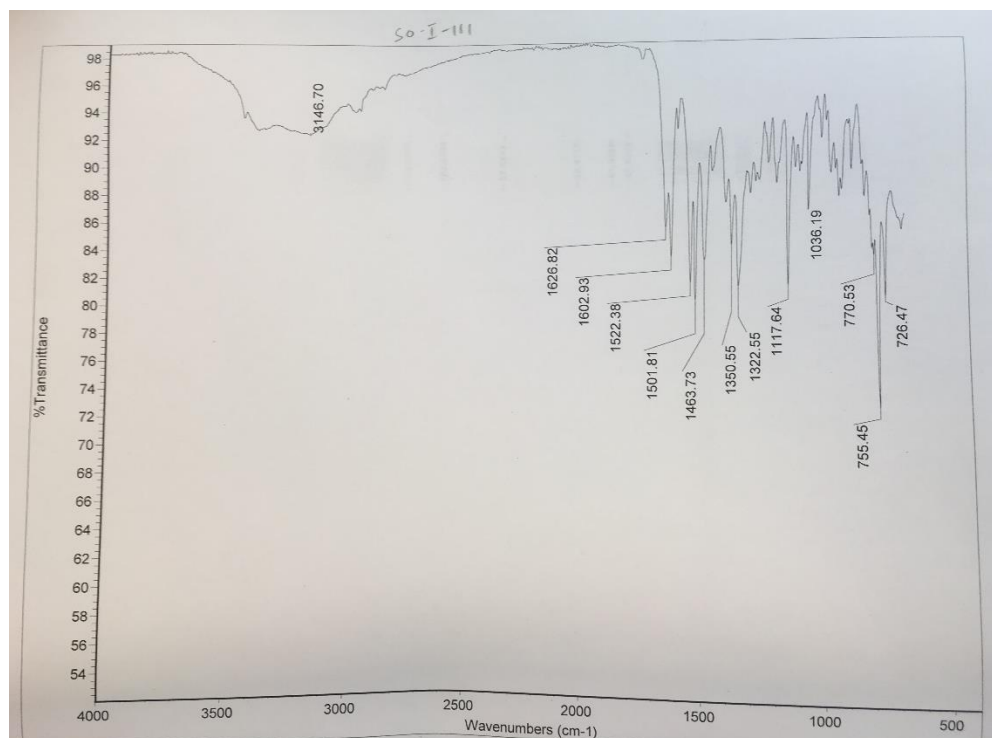
¹³C NMR



High resolution Masspec



IR

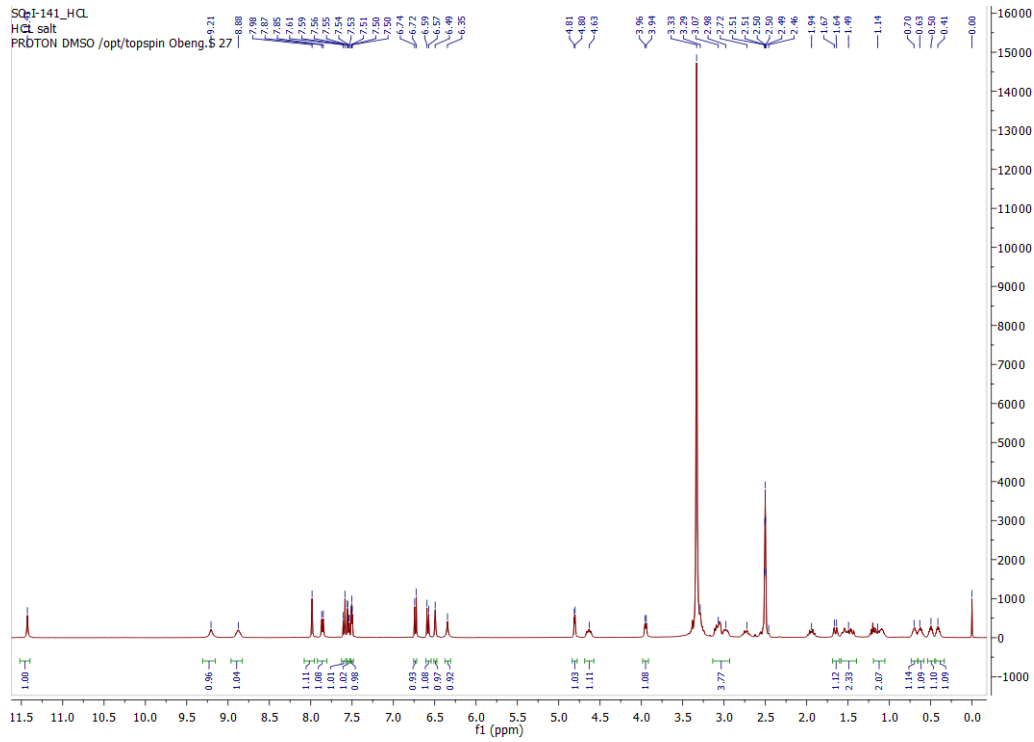


HPLC

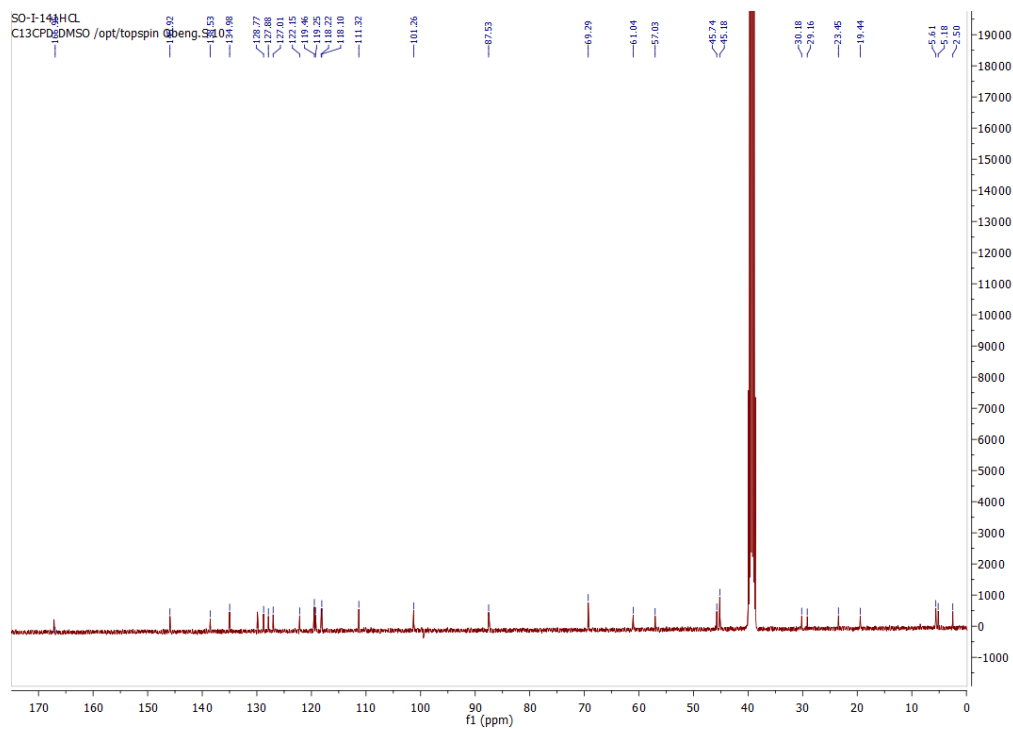


Compound 5

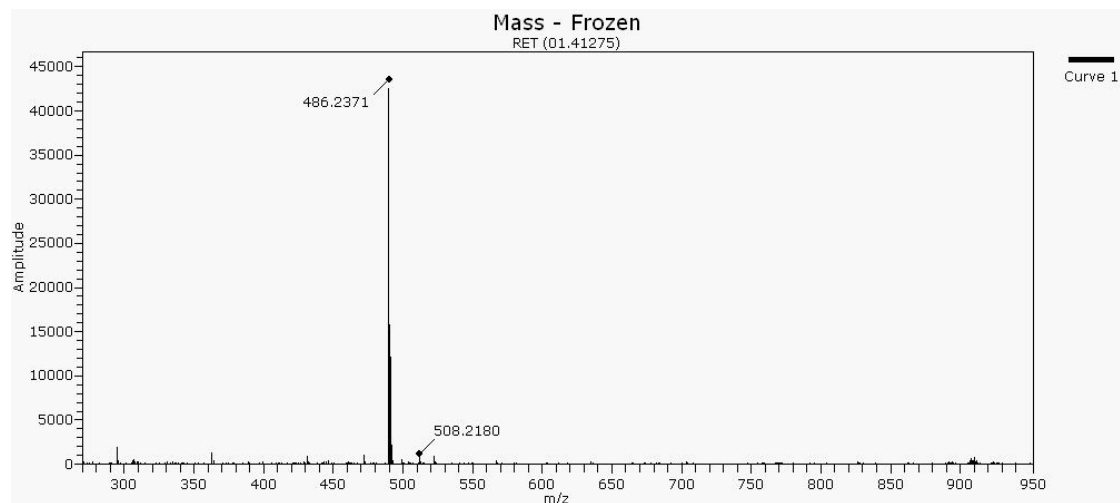
¹H NMR



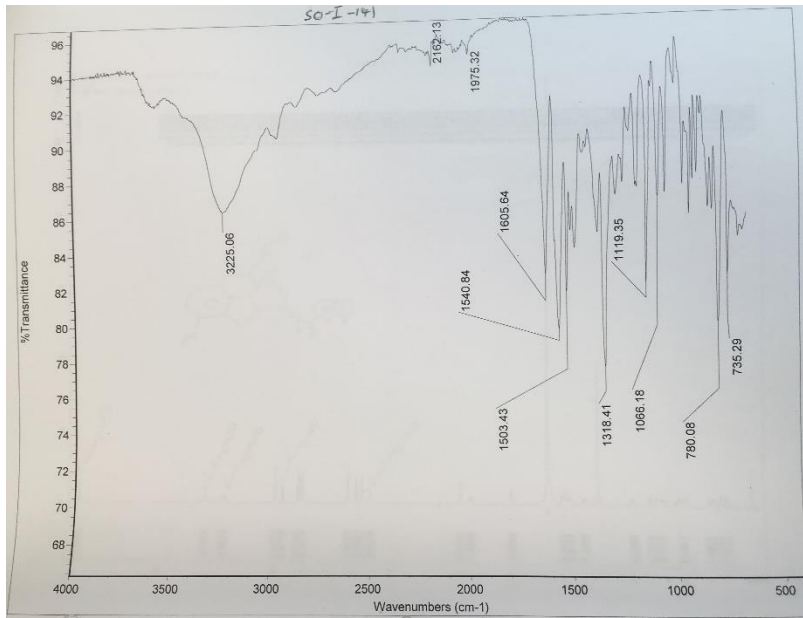
¹³CNMR



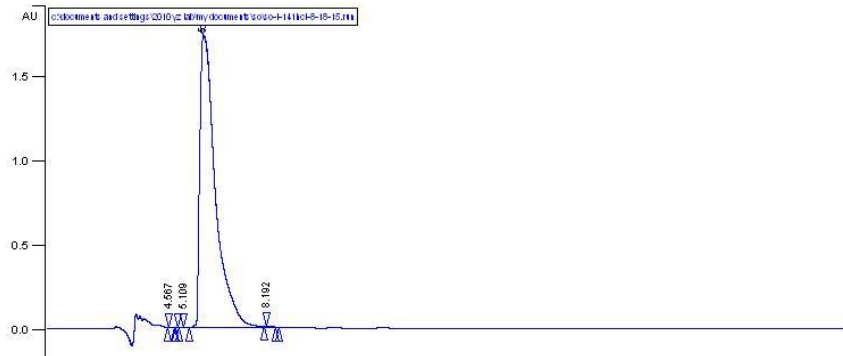
High resolution masspec



IR

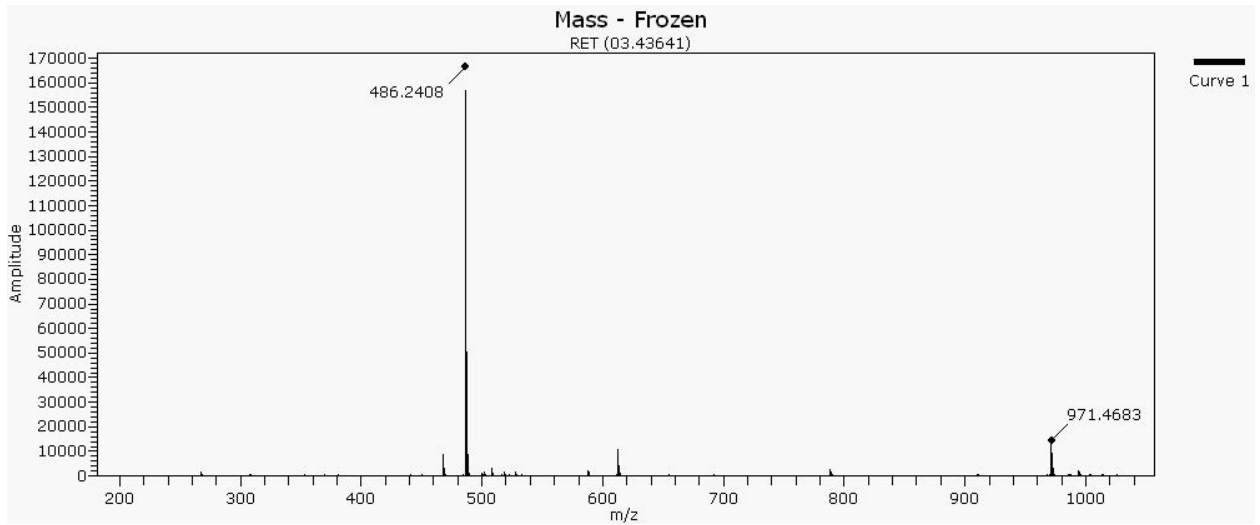


HPLC

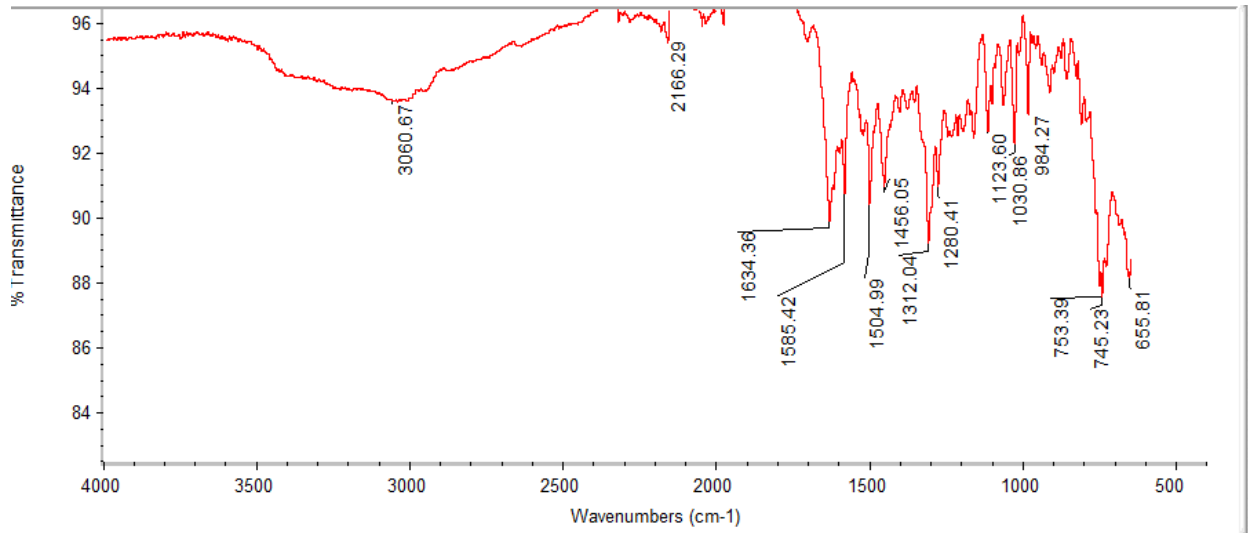


File: c:\documents and settings\2010\c\l\my documents\2010-11\10-18-15.11
Client: 1 - 210 ml Peptide
LastResak: 2015-5-19 12:25

High resolution masspec

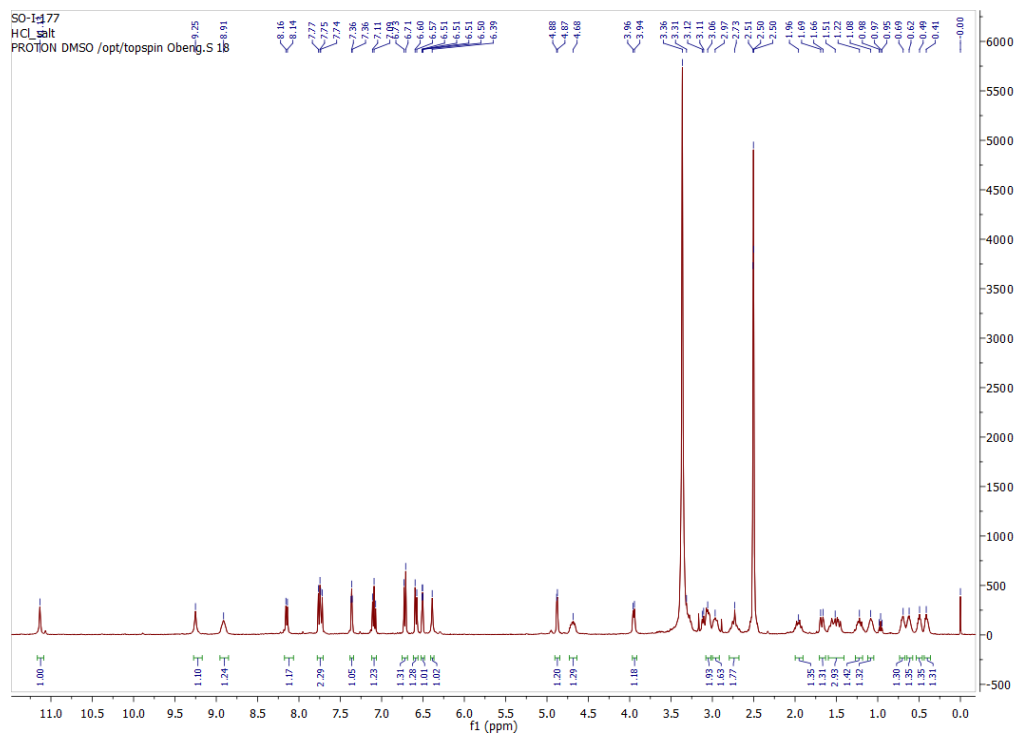


IR

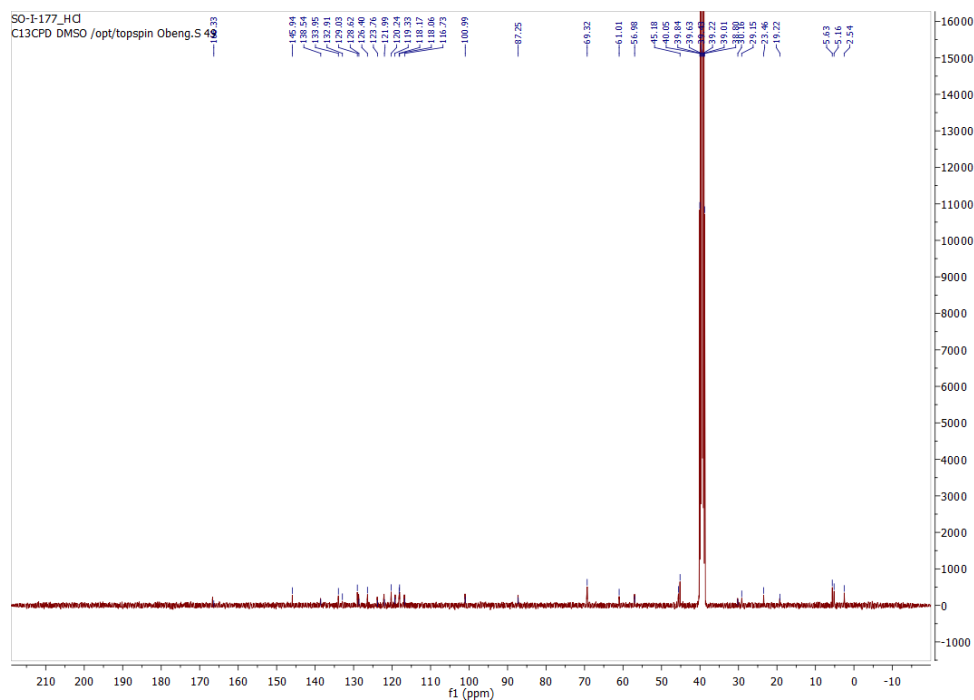


Compound 7

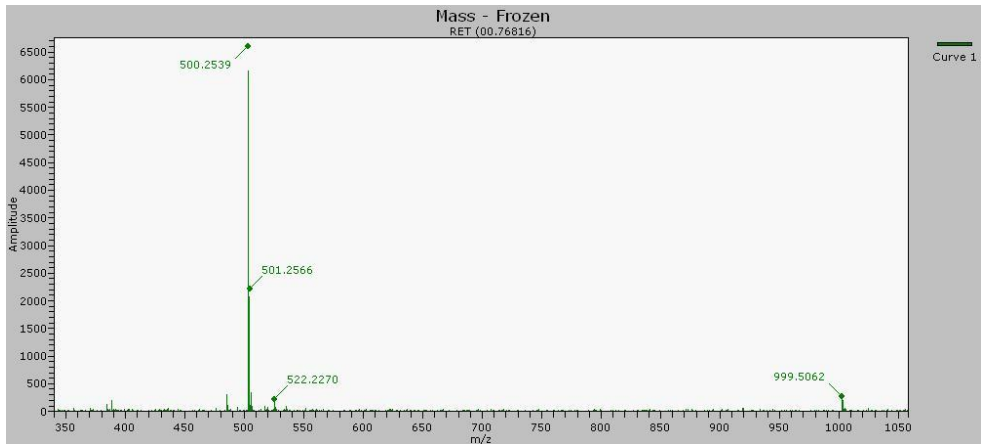
¹H NMR



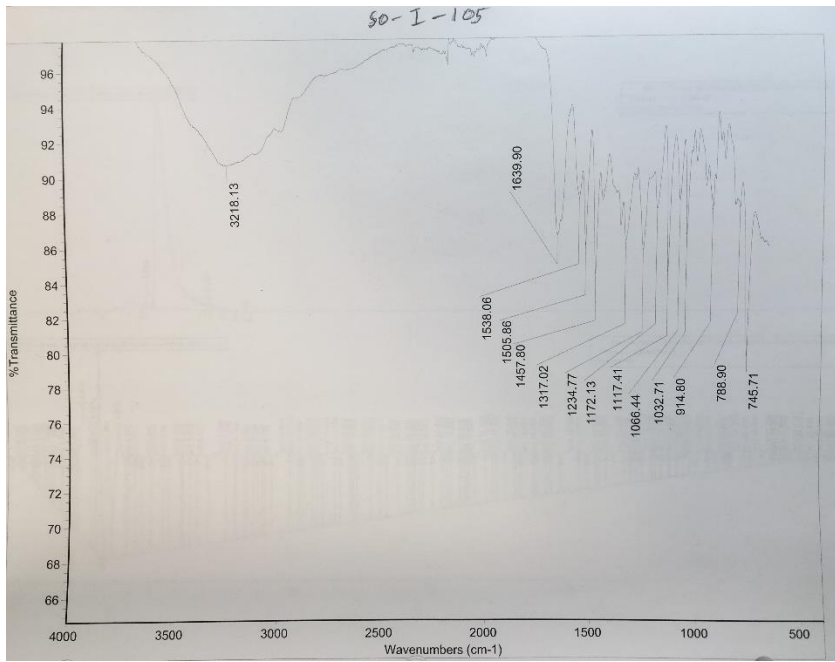
¹³C NMR



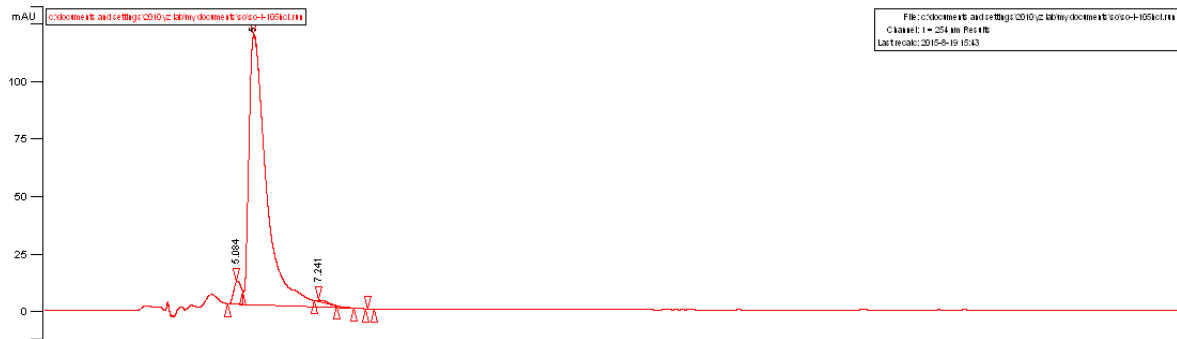
High resolution masspec



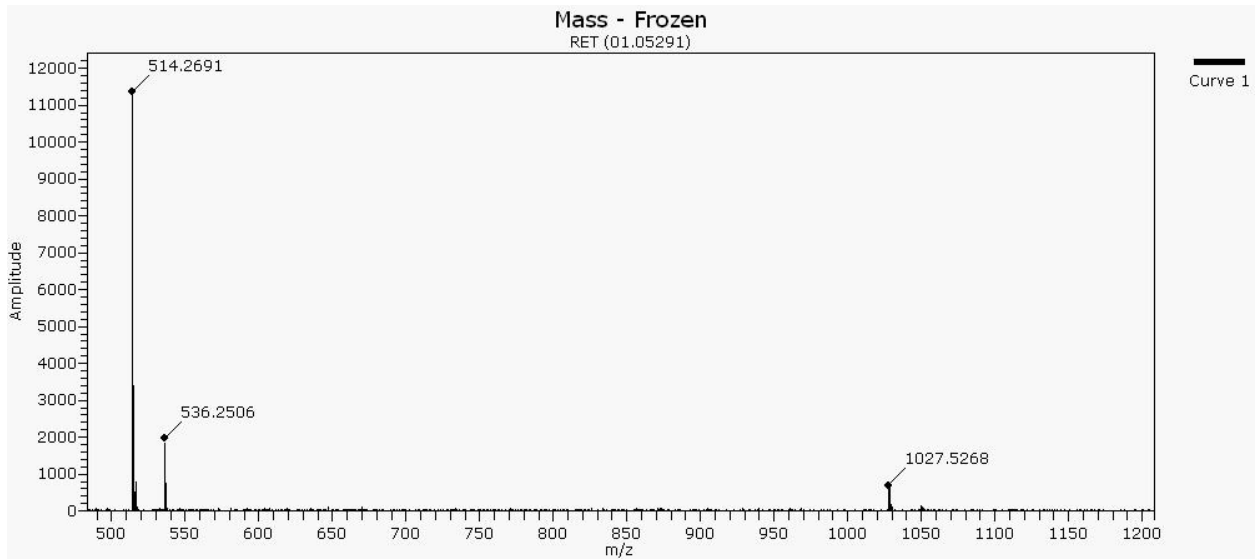
IR



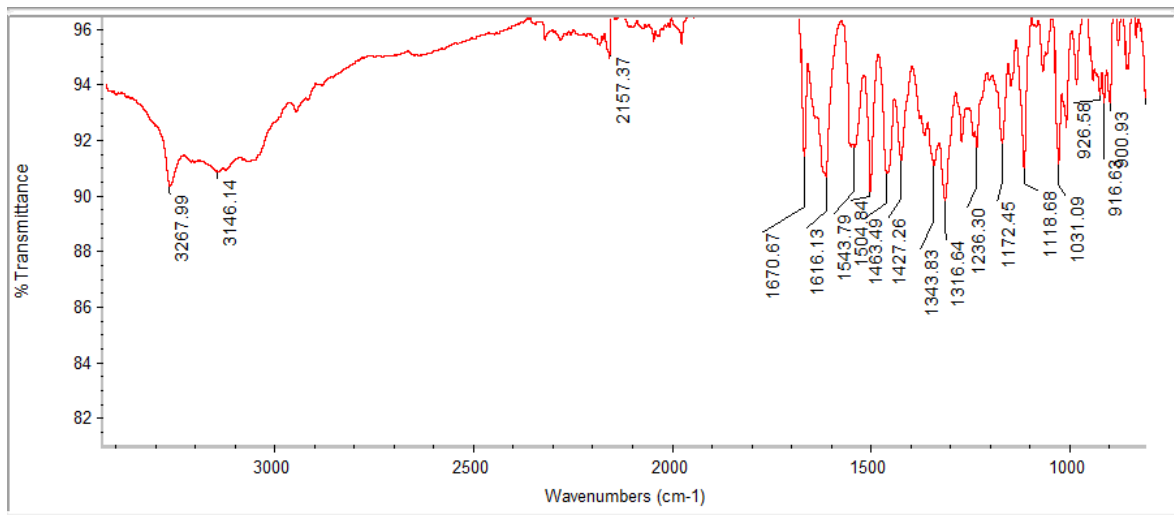
HPLC



High resolution masspec

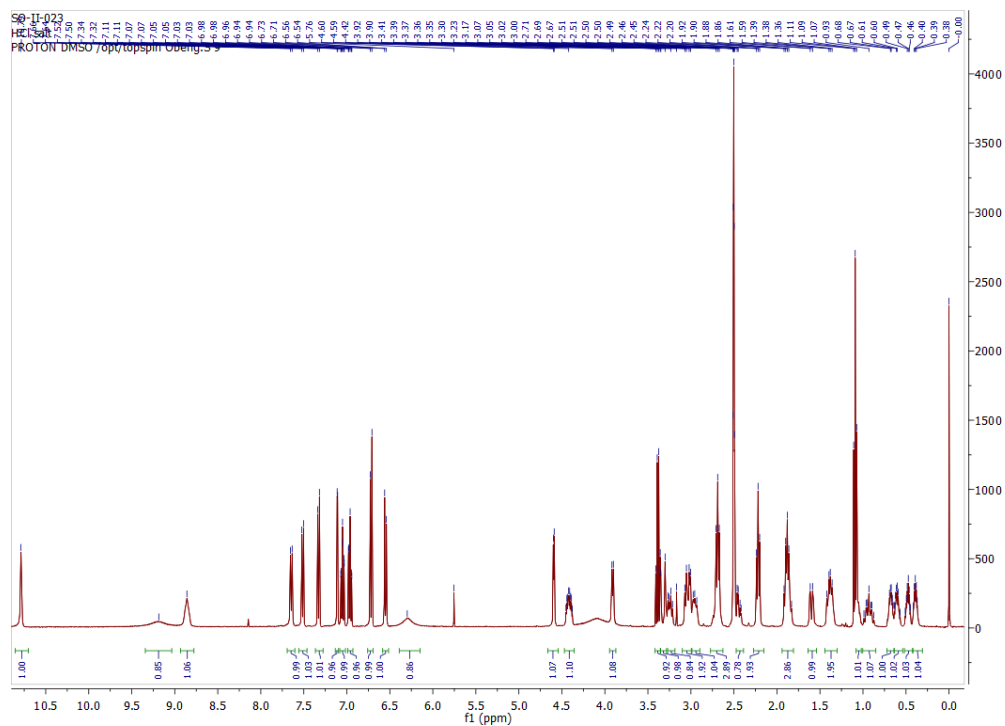


IR

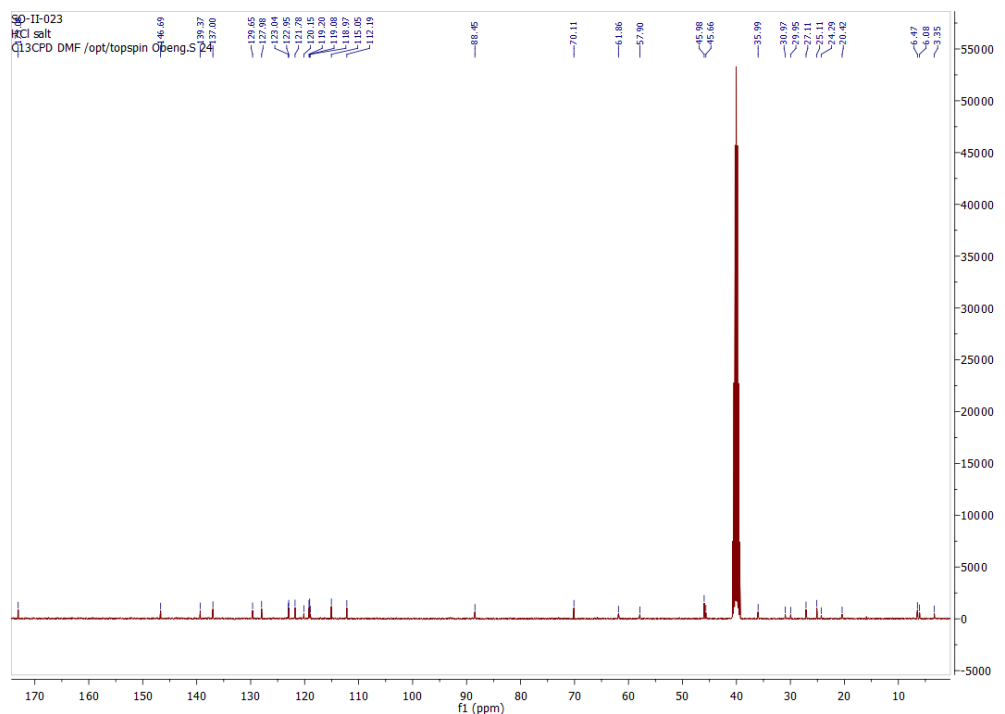


Compound 9

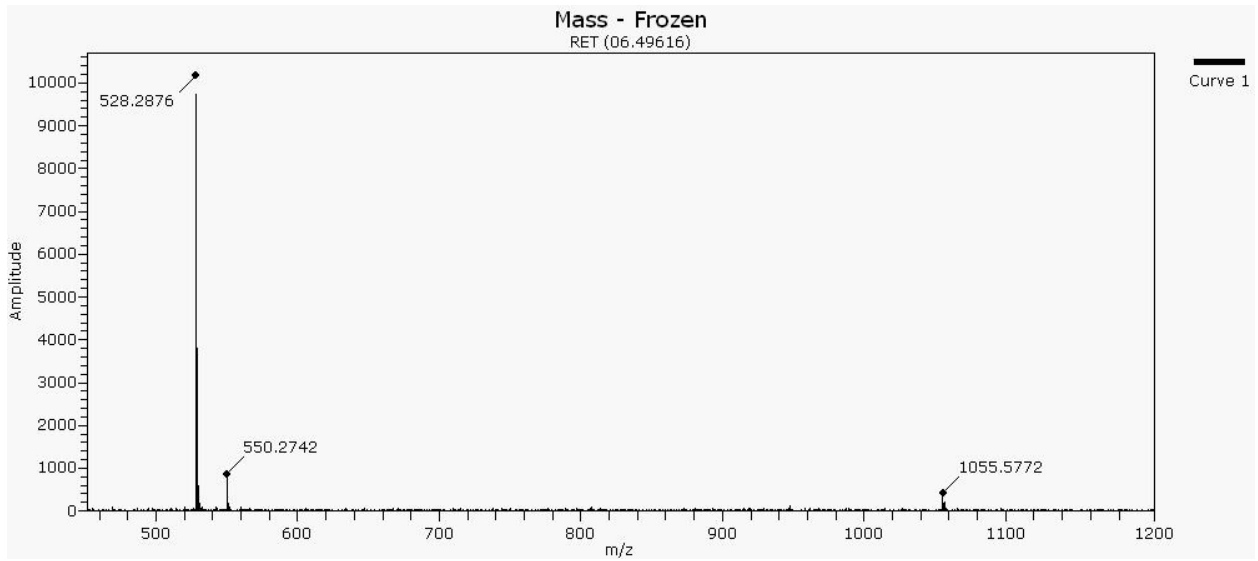
¹H NMR



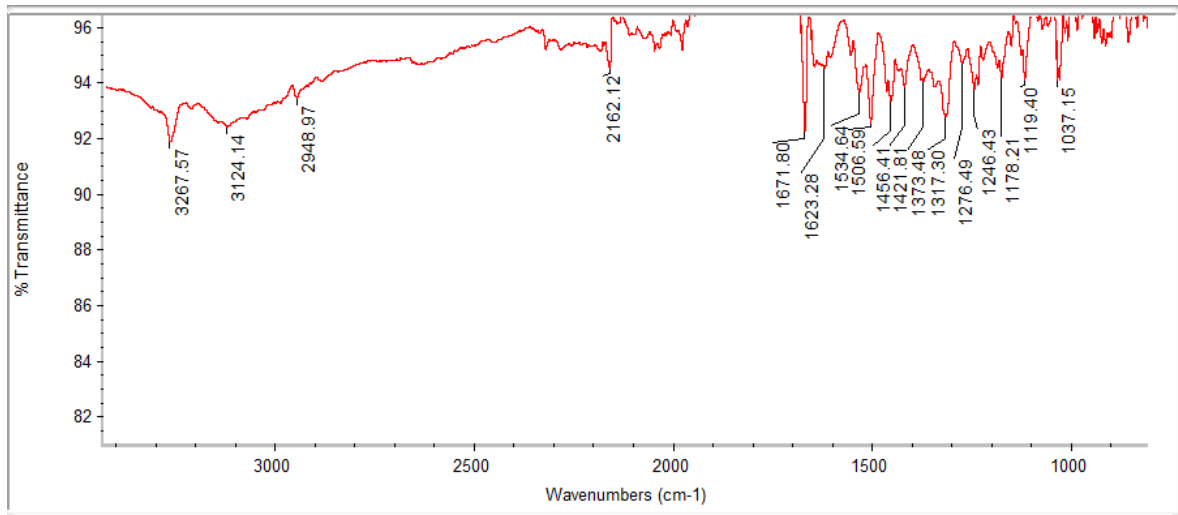
¹³C NMR



High resolution masspec

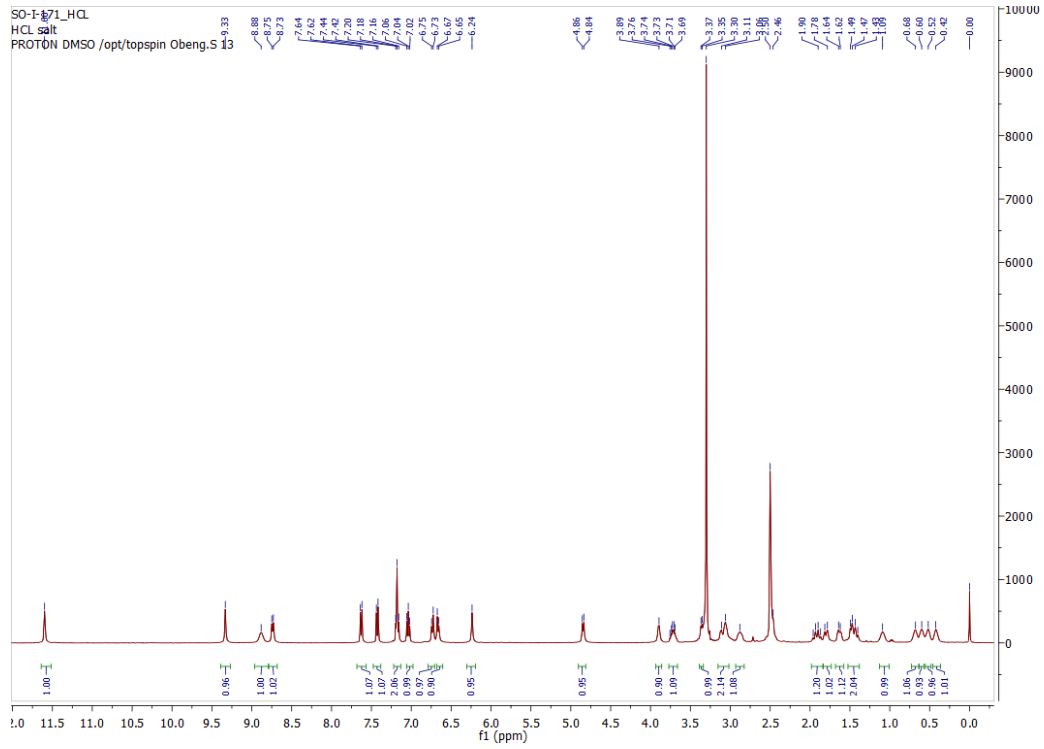


IR

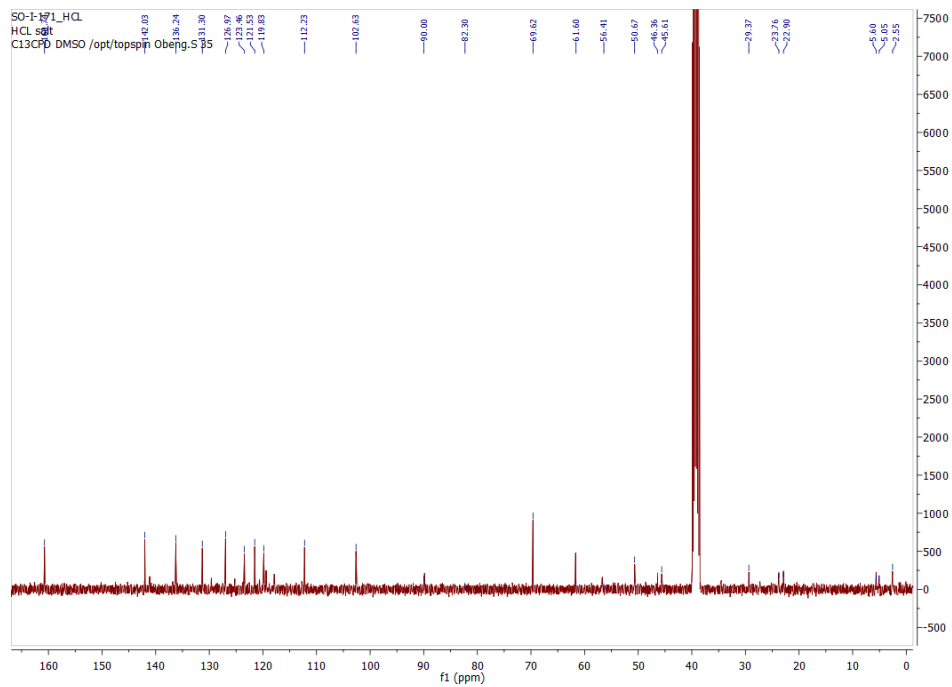


Compound 10

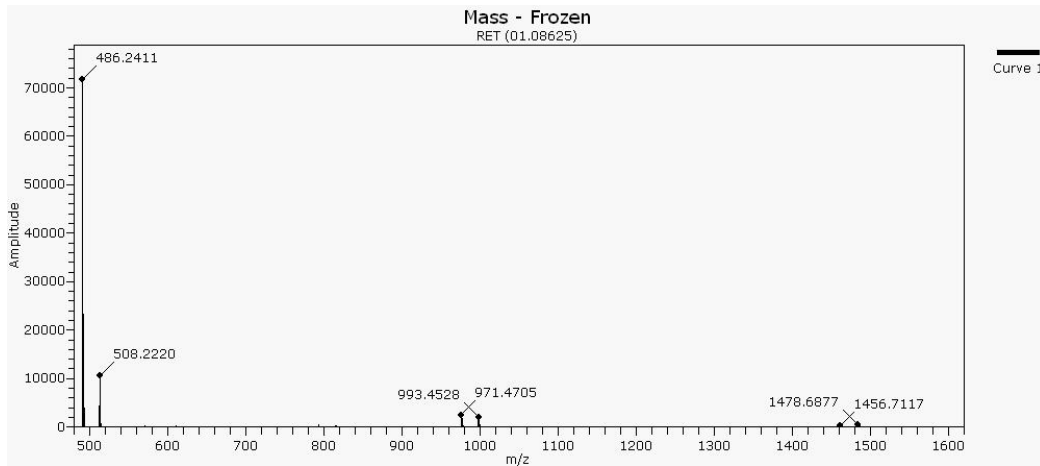
¹H NMR



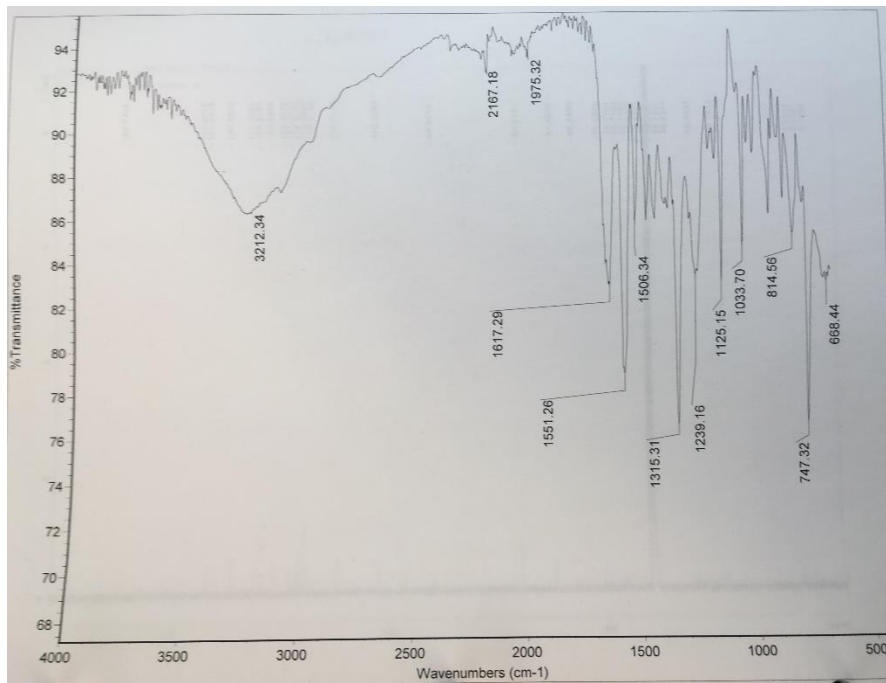
¹³C NMR



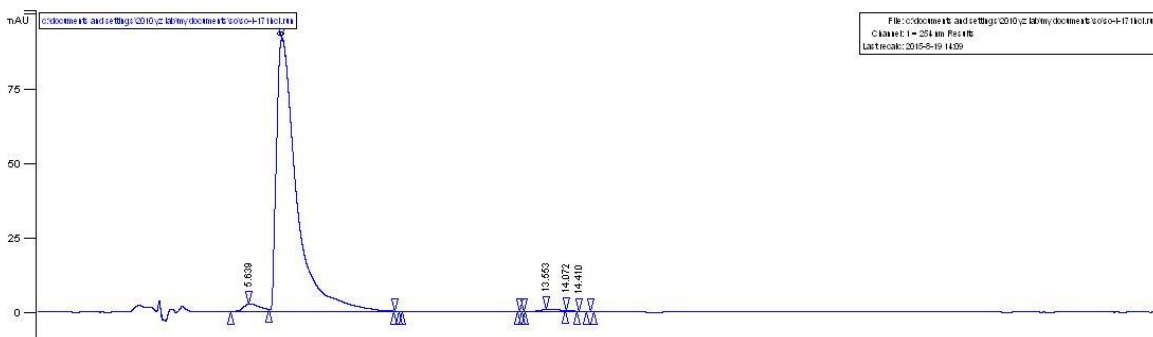
High resolution masspec



IR

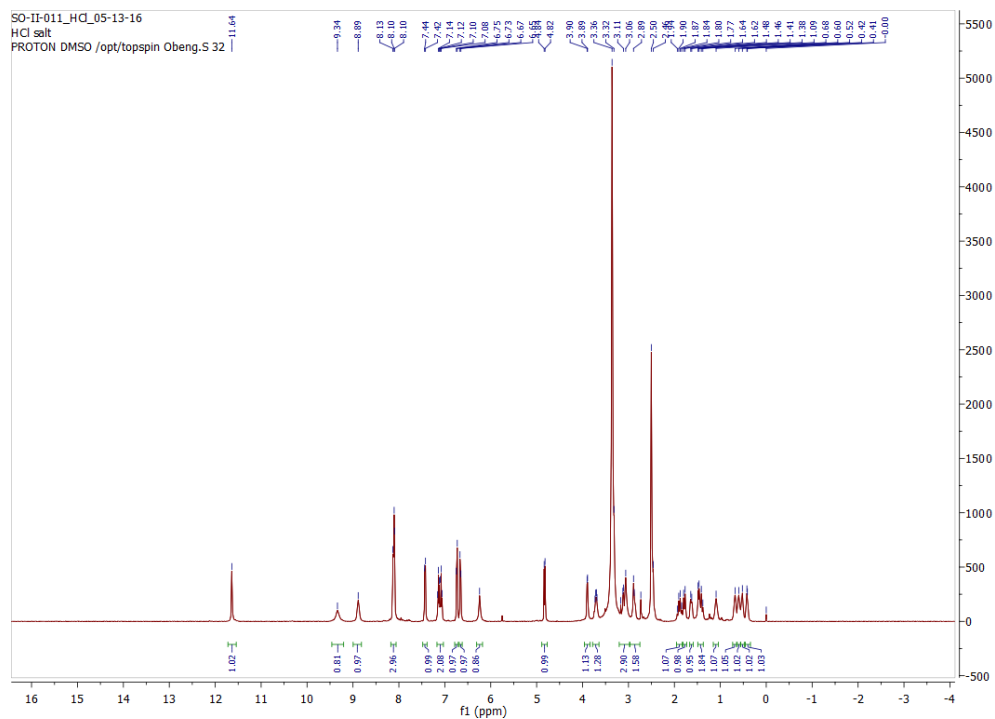


HPLC

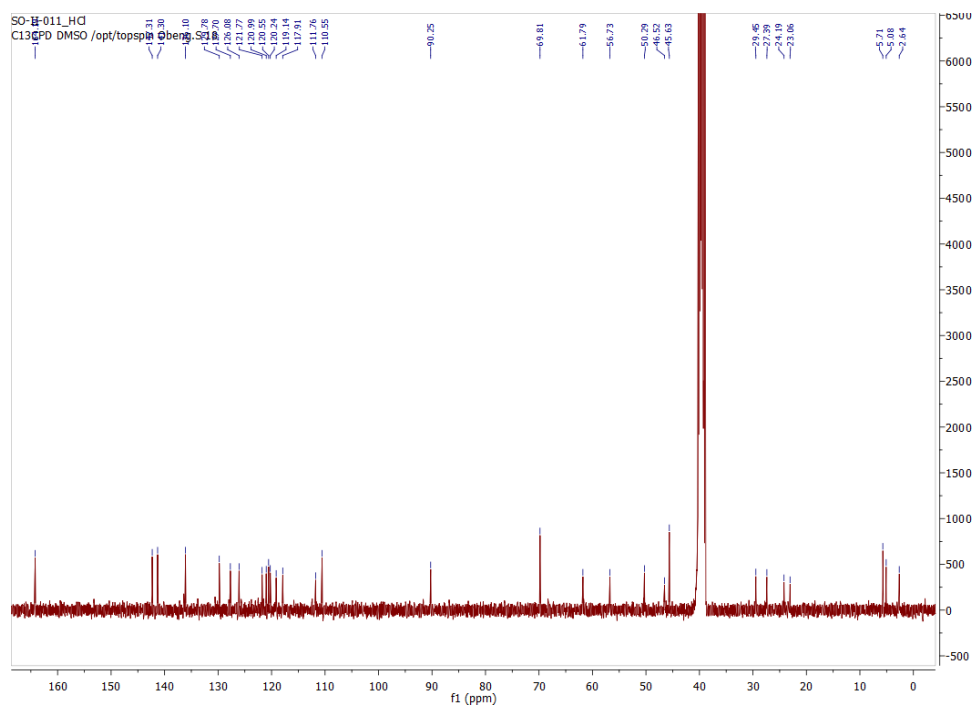


Compound 11

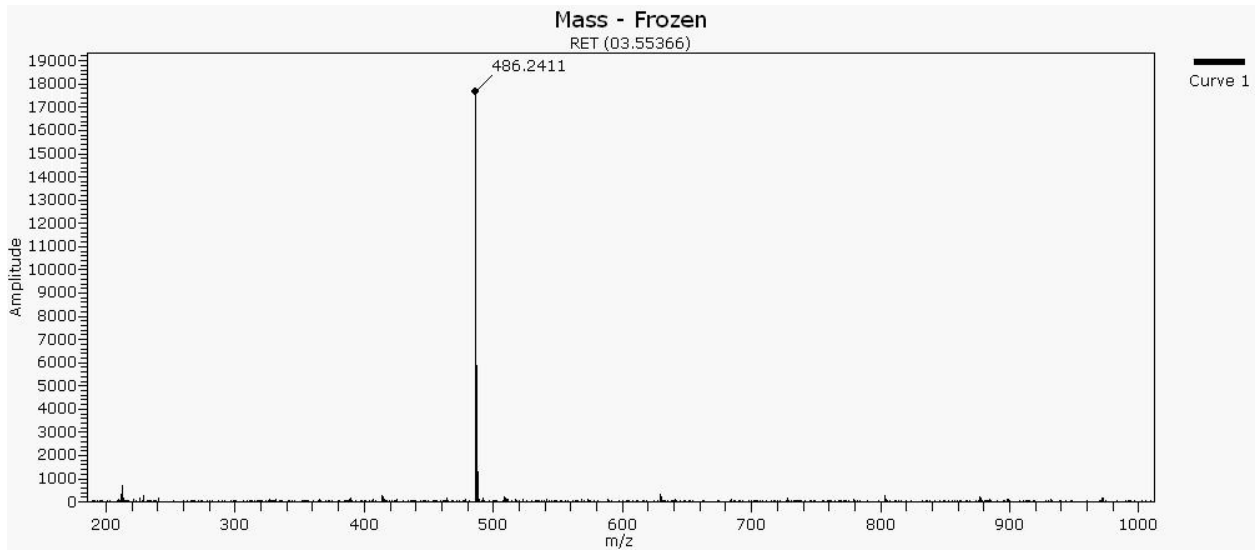
¹H NMR



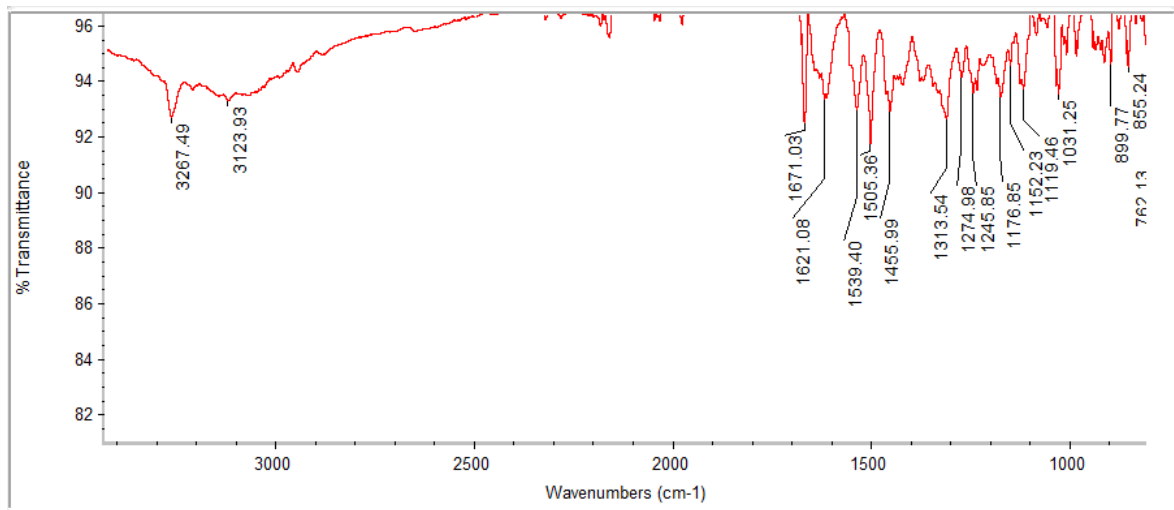
¹³C NMR



High resolution masspec

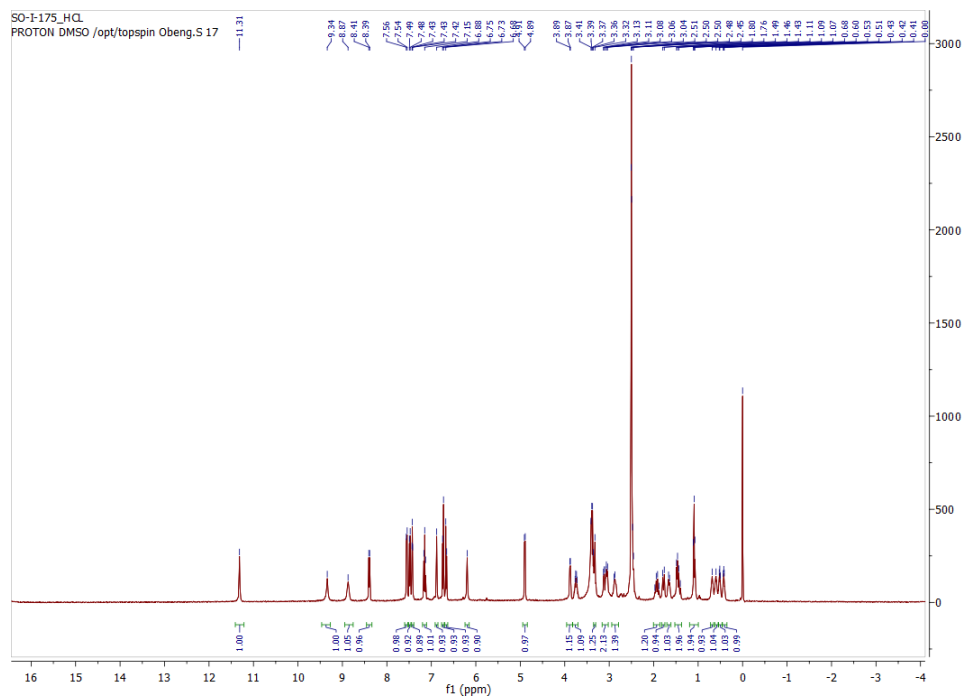


IR

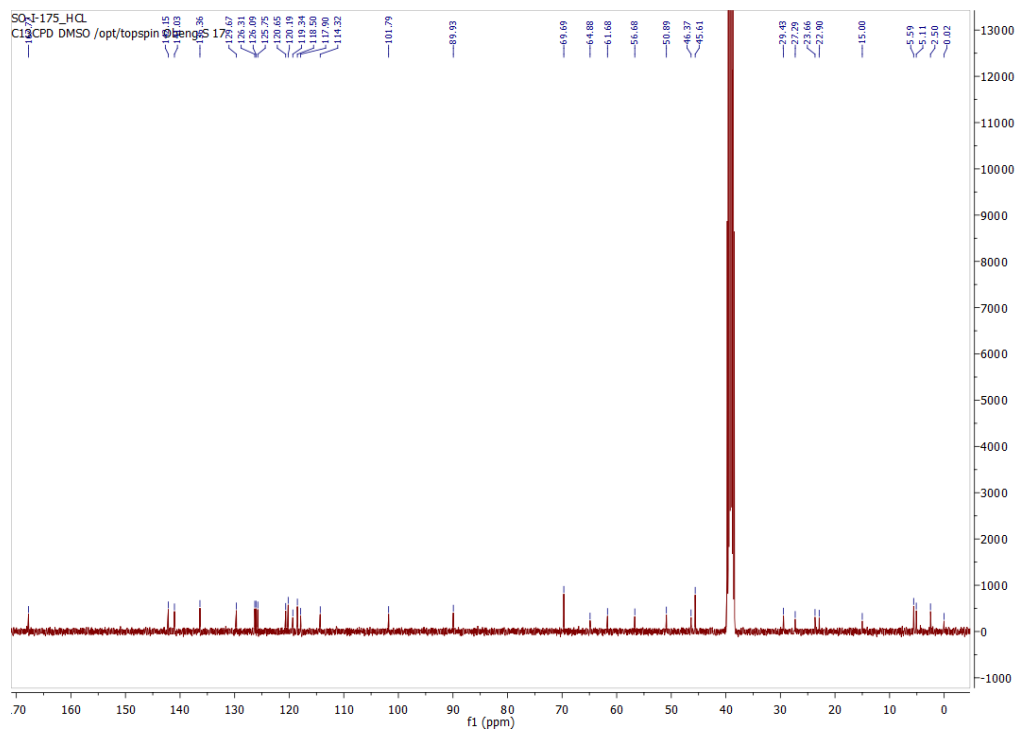


Compound 12

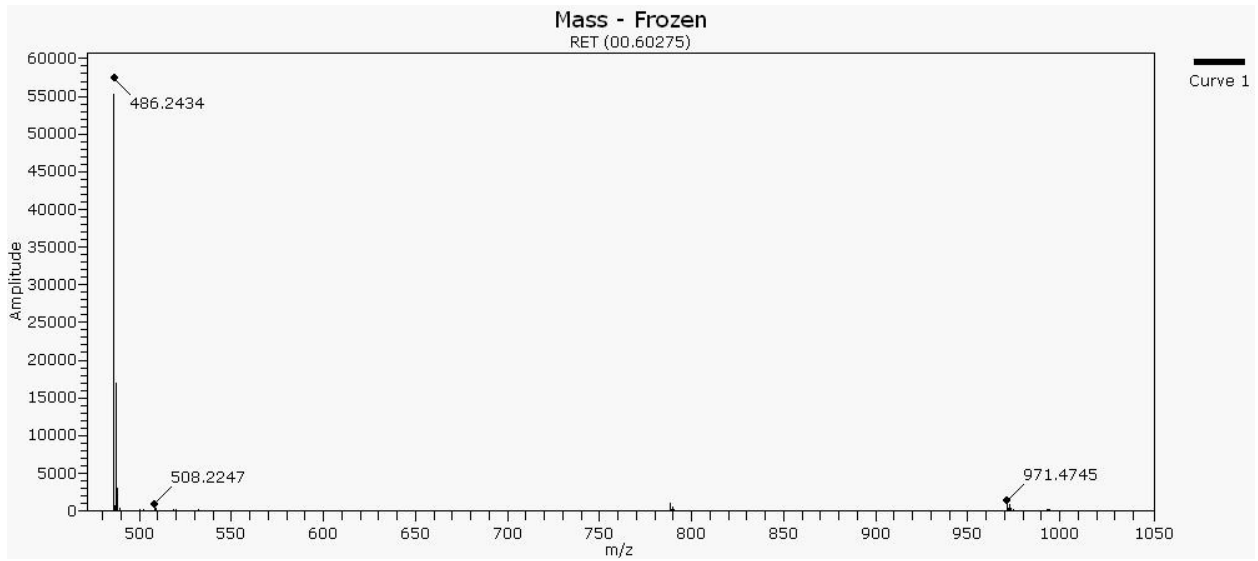
¹H NMR



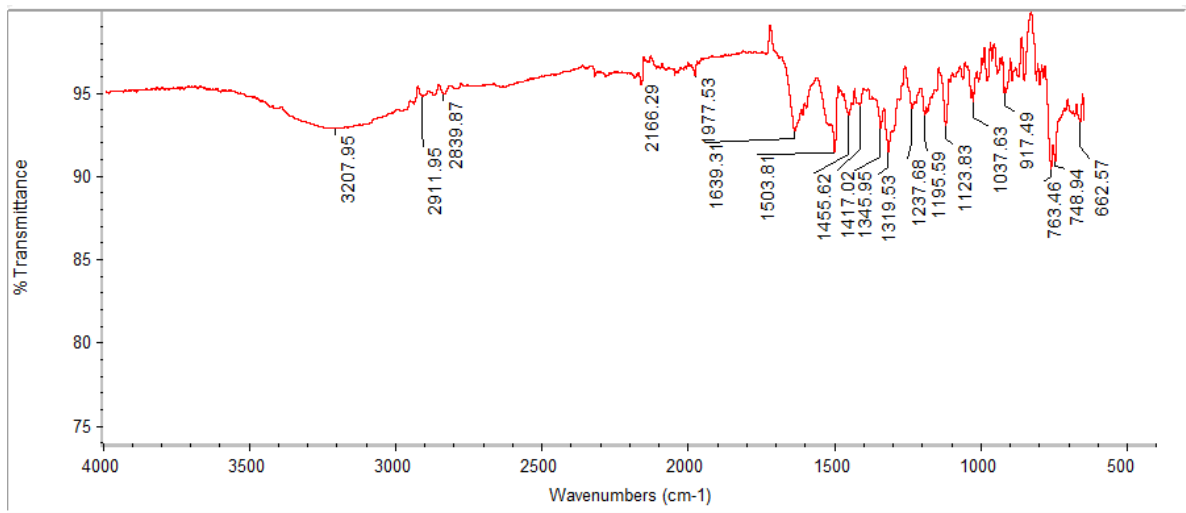
¹³C NMR



High resolution masspec

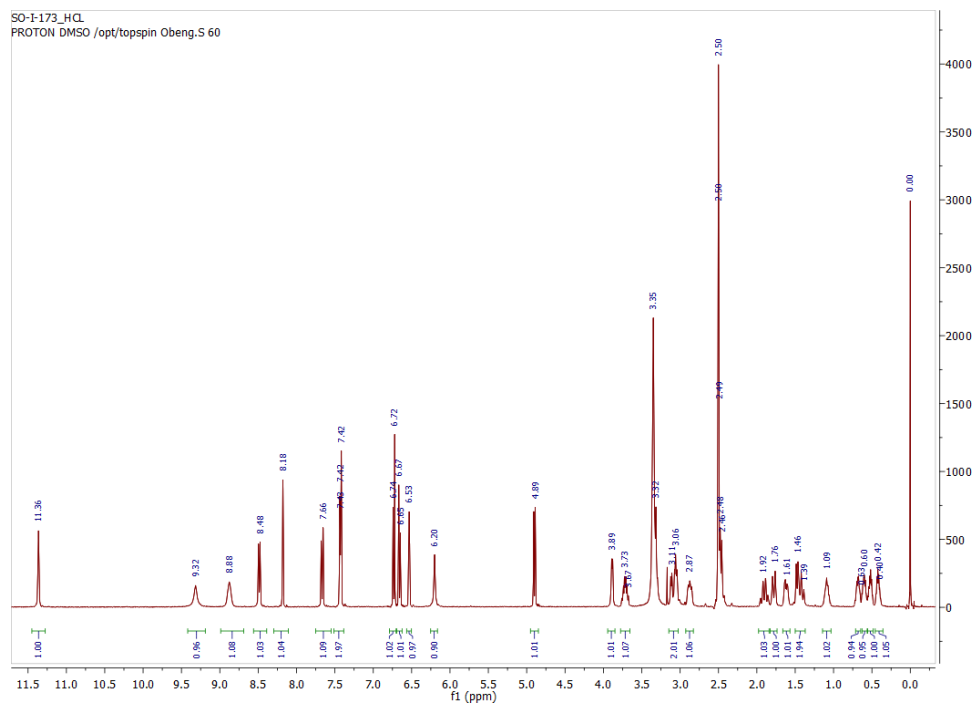


IR

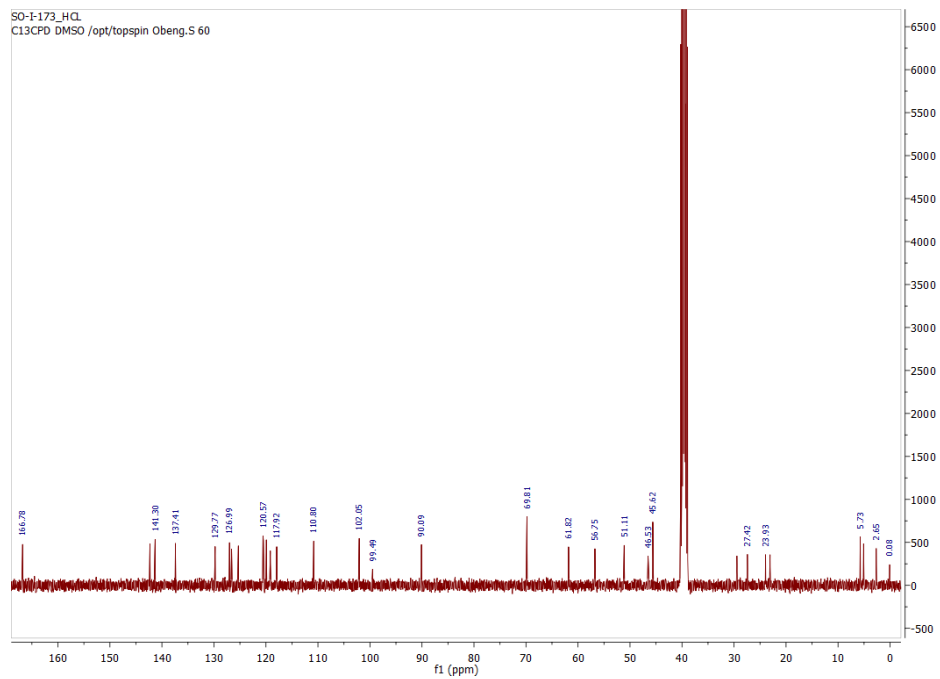


Compound 13

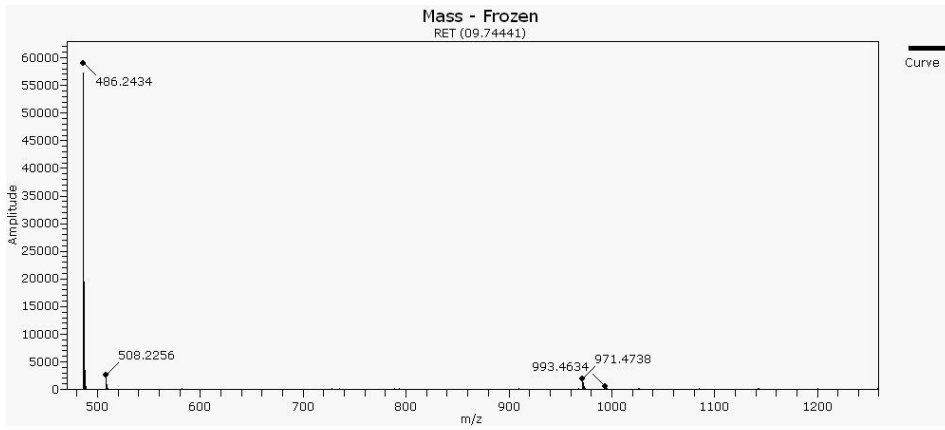
¹H NMR



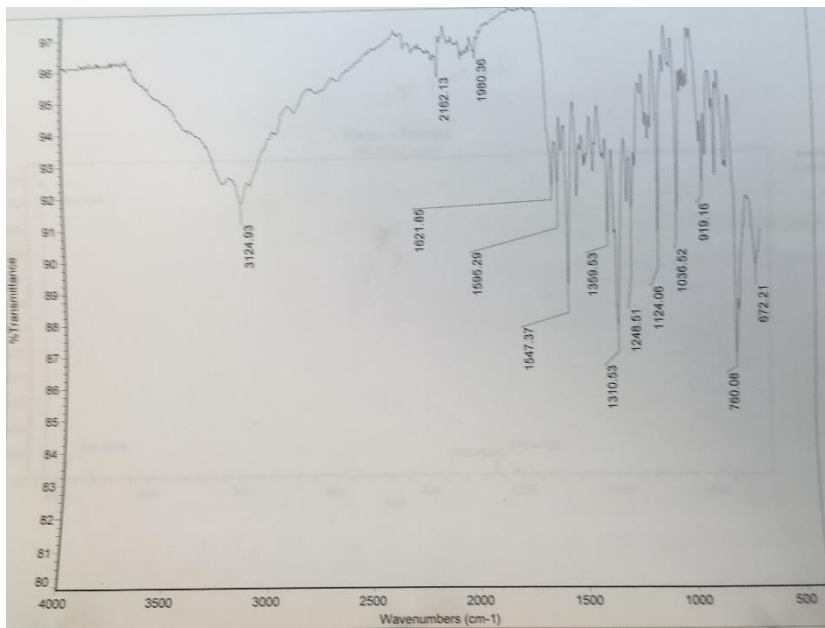
¹³C NMR



High resolution masspec



IR

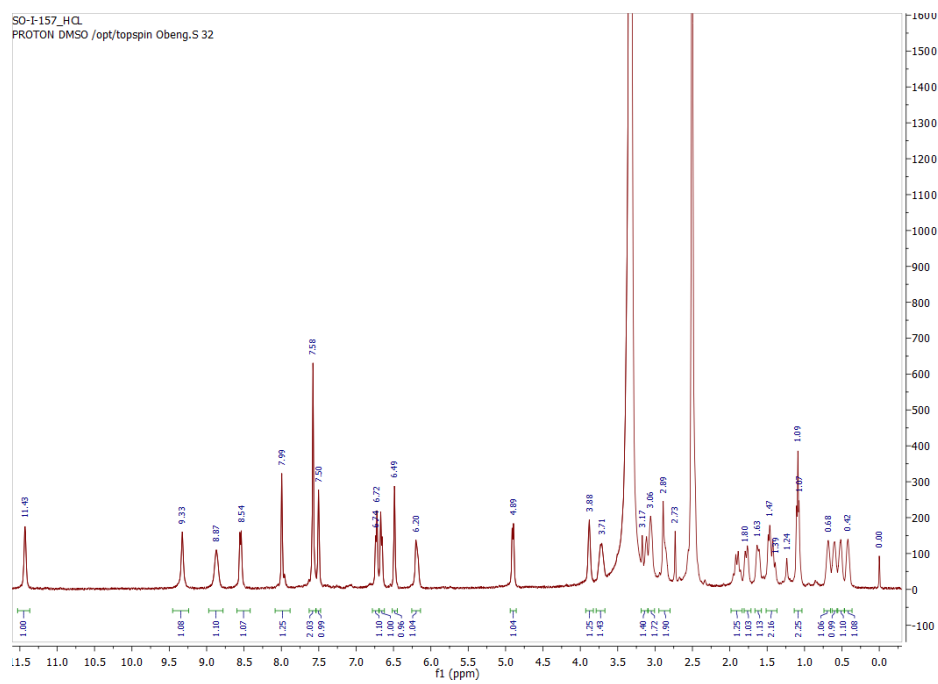


HPLC

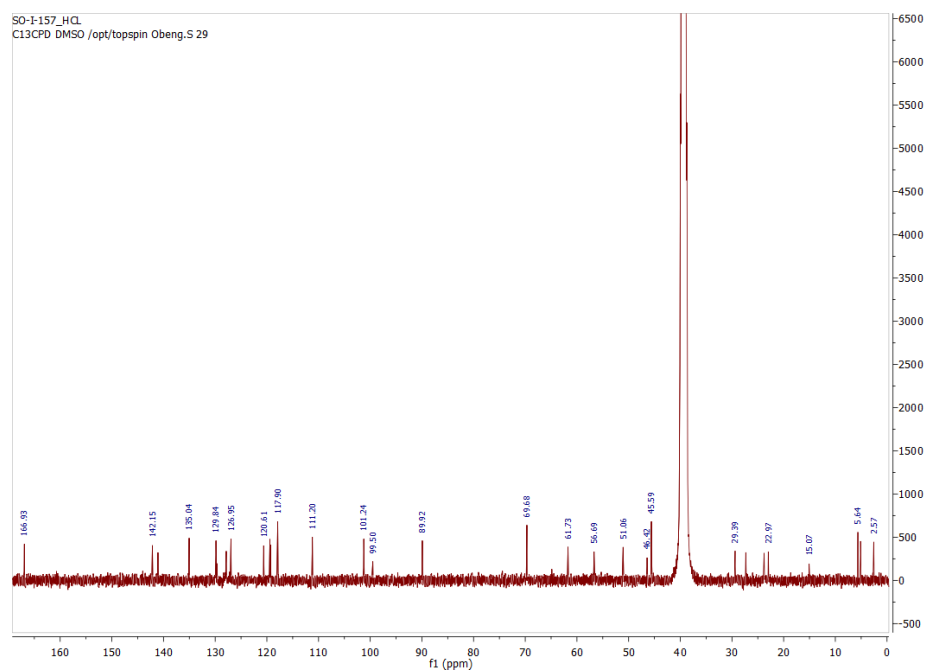


Compound 14

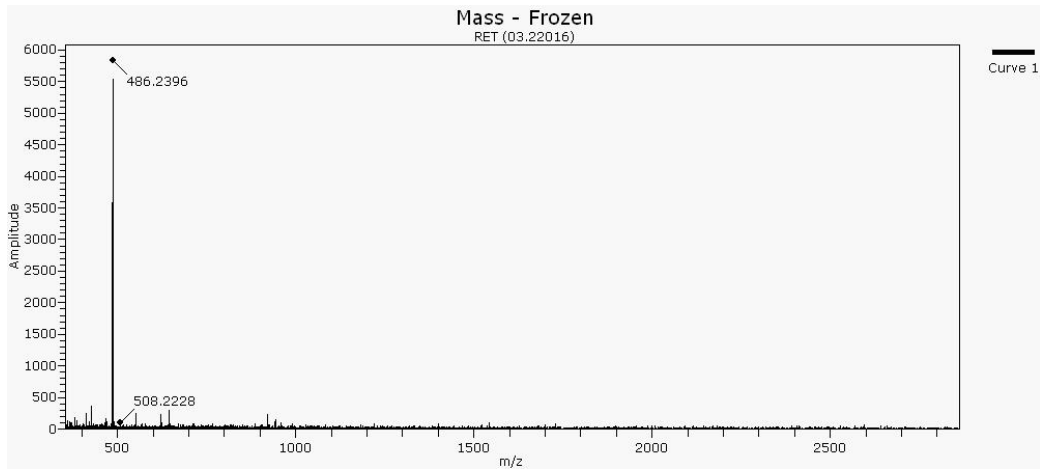
¹H NMR



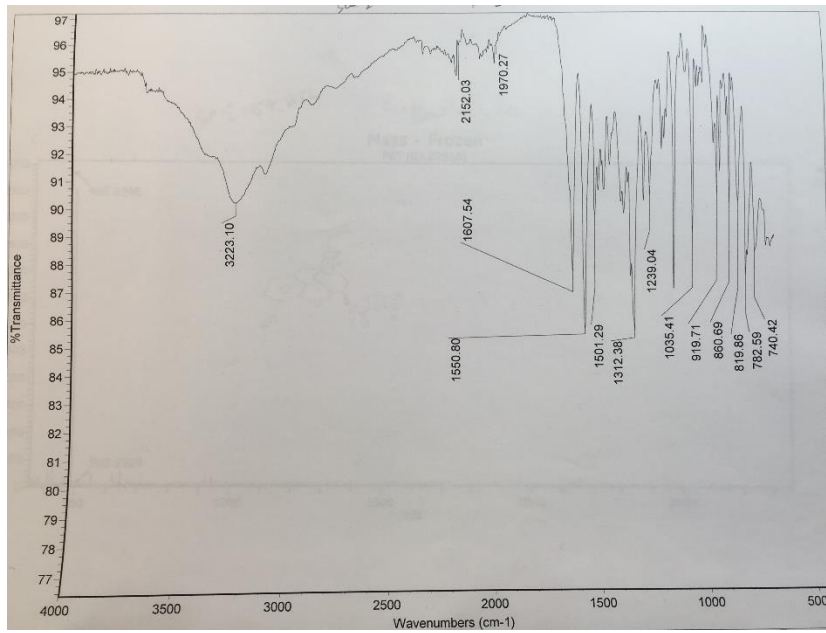
¹³C NMR



High resolution masspec



IR

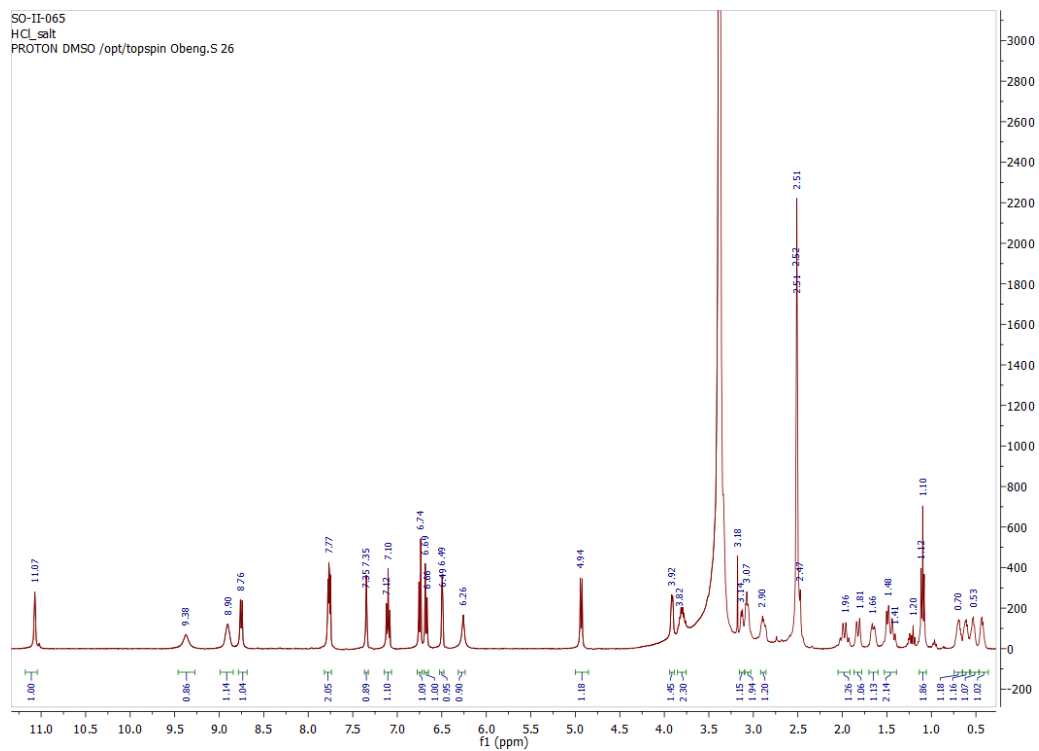


HPLC

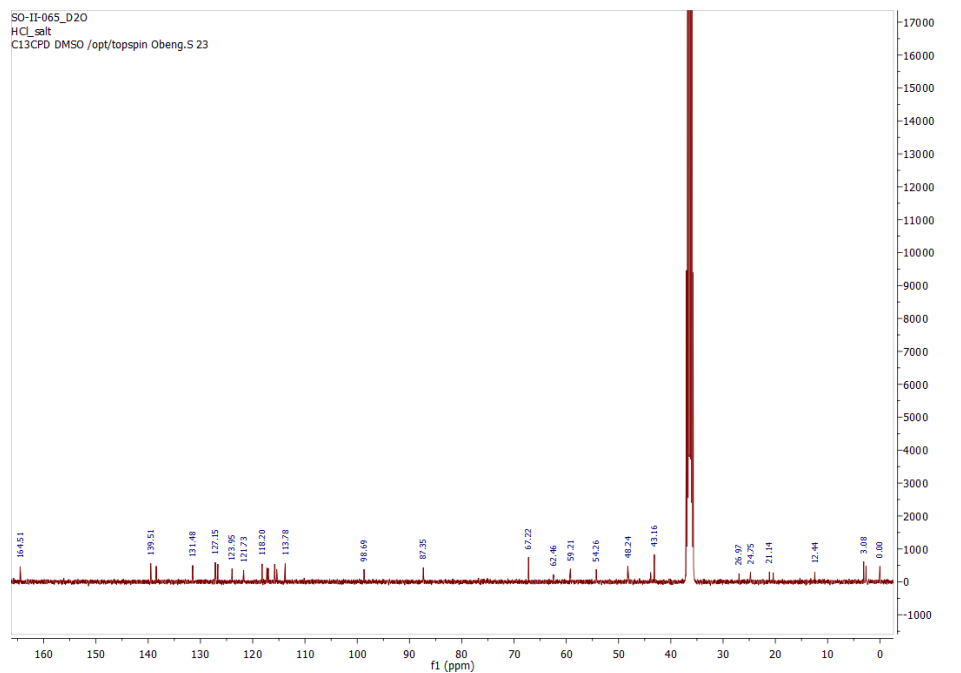


Compound 15

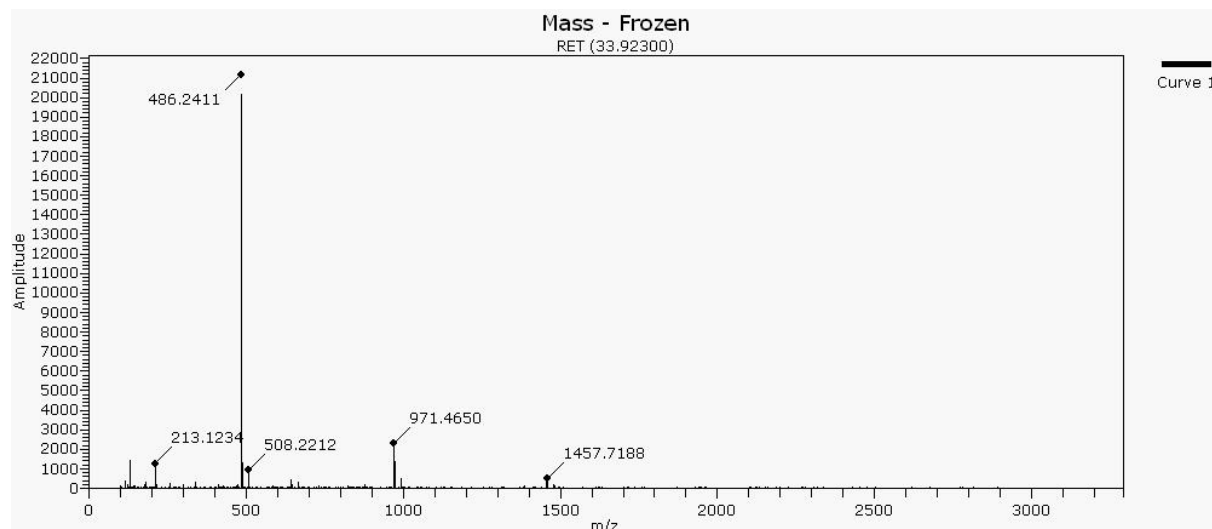
¹H NMR



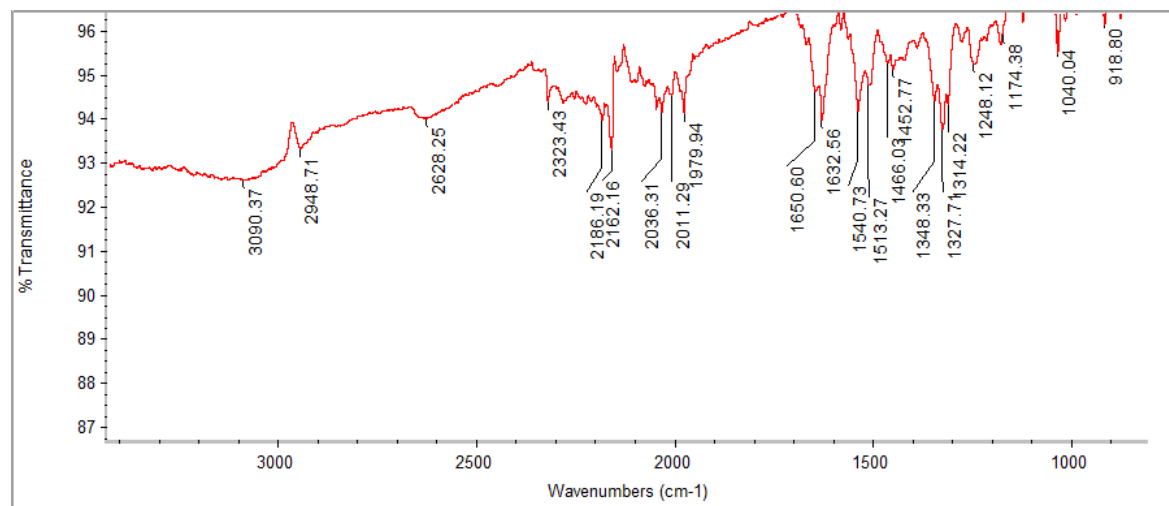
¹³C NMR



High resolution masspec

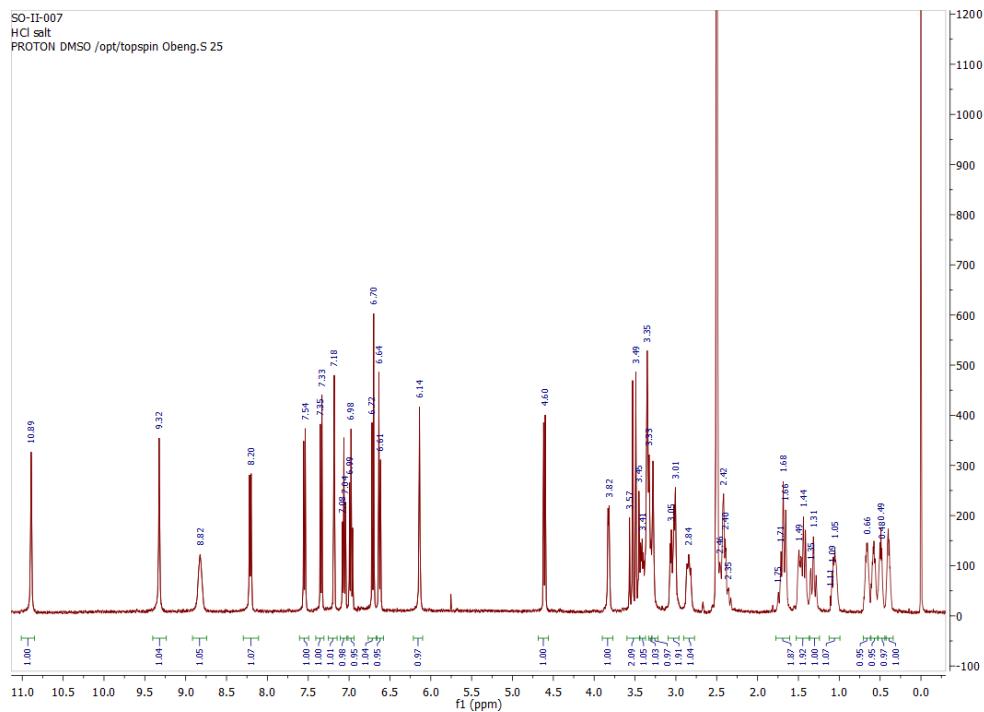


IR

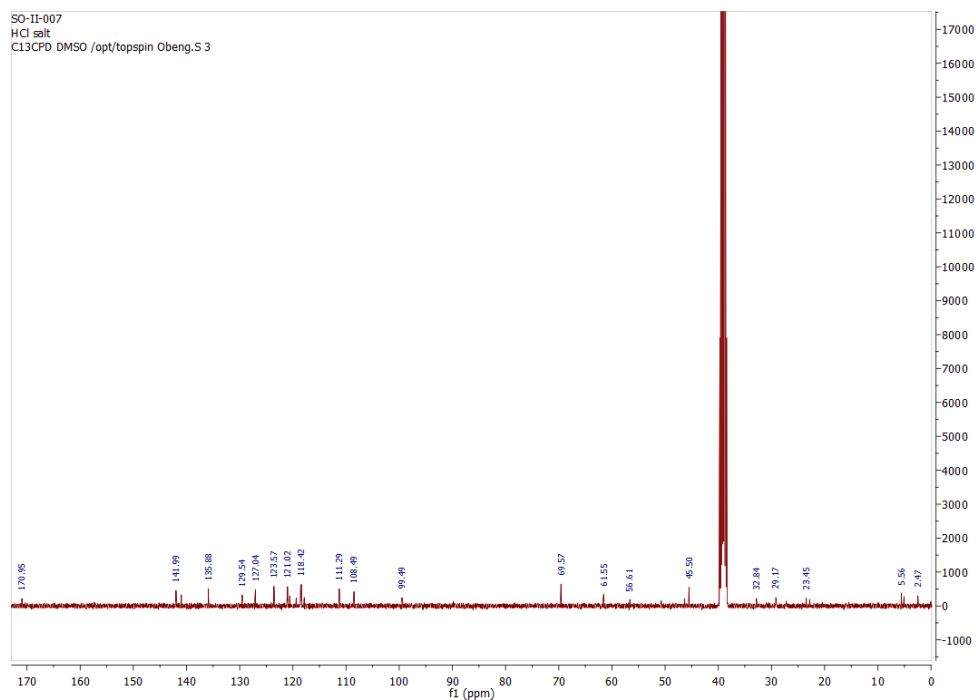


Compound 16

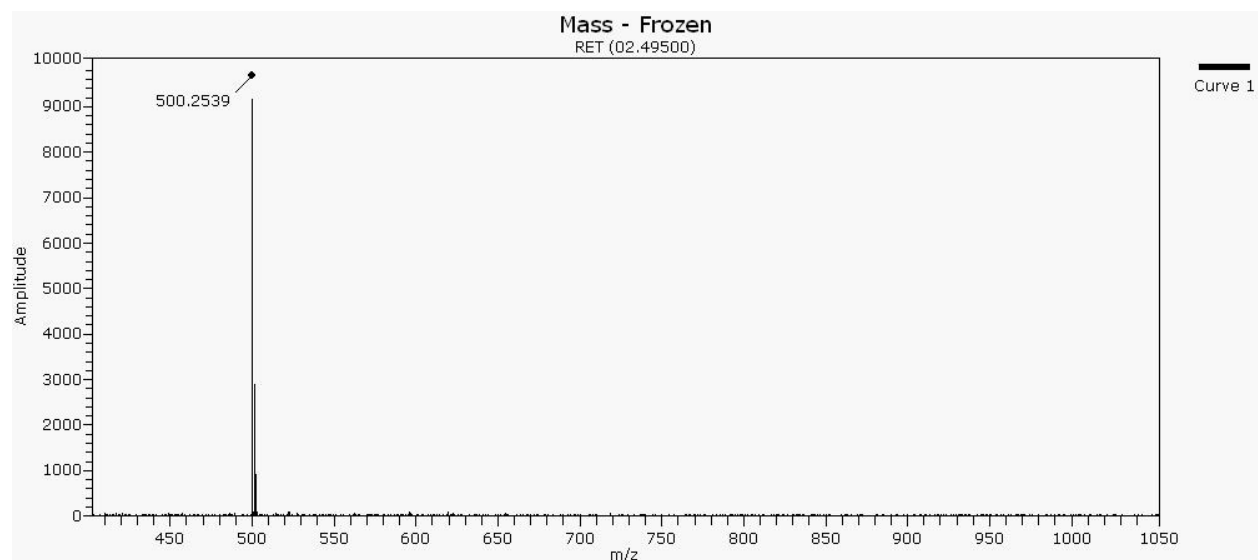
¹H NMR



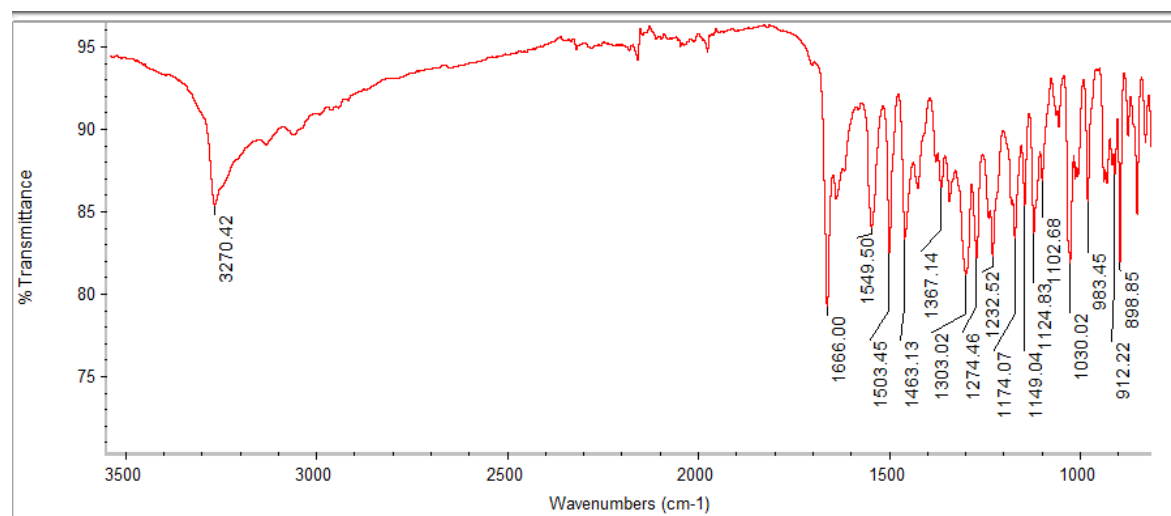
¹³C NMR



High resolution Masspec

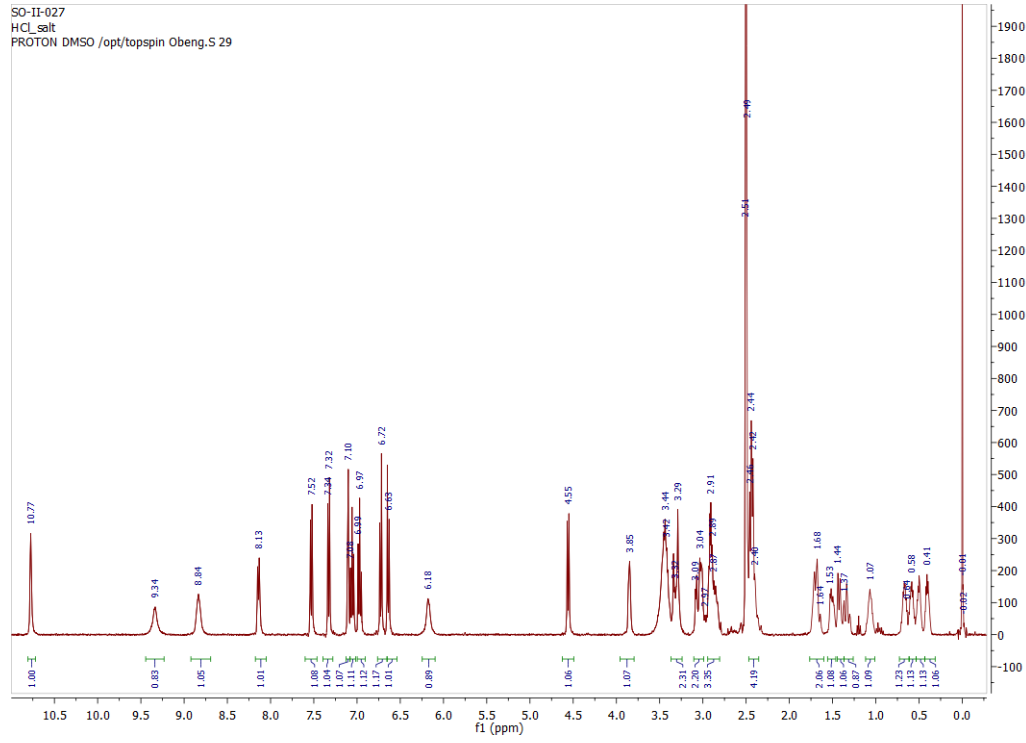


IR

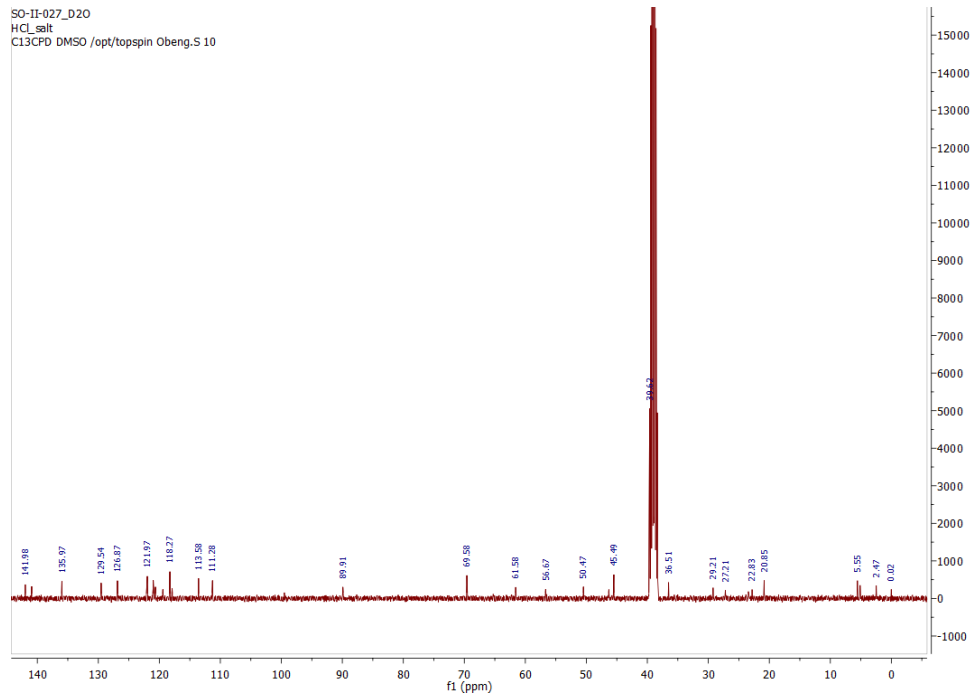


Compound 17

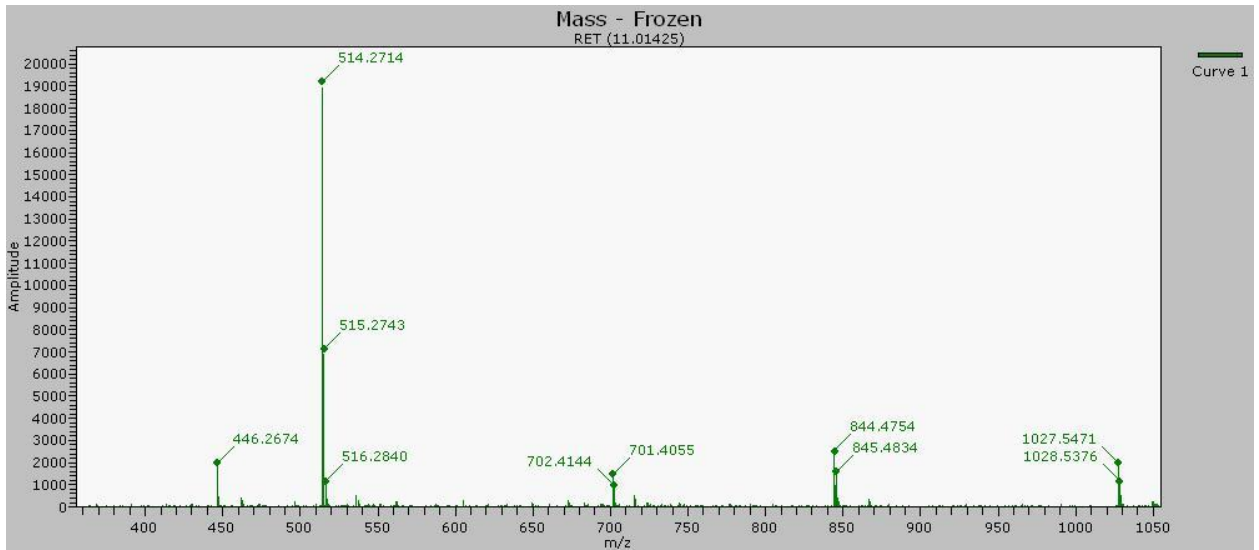
¹H NMR



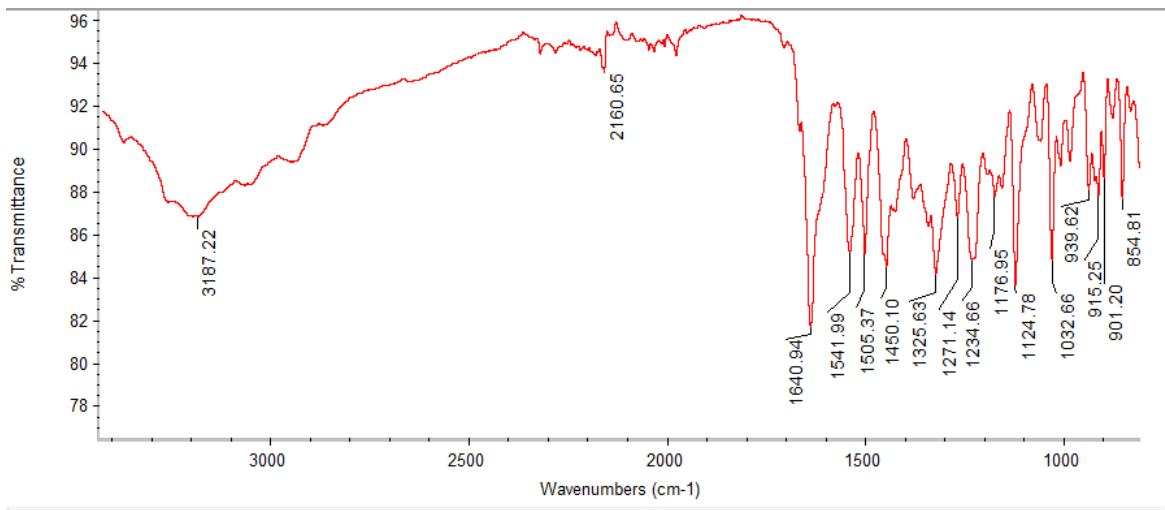
¹³C NMR



High resolution masspec

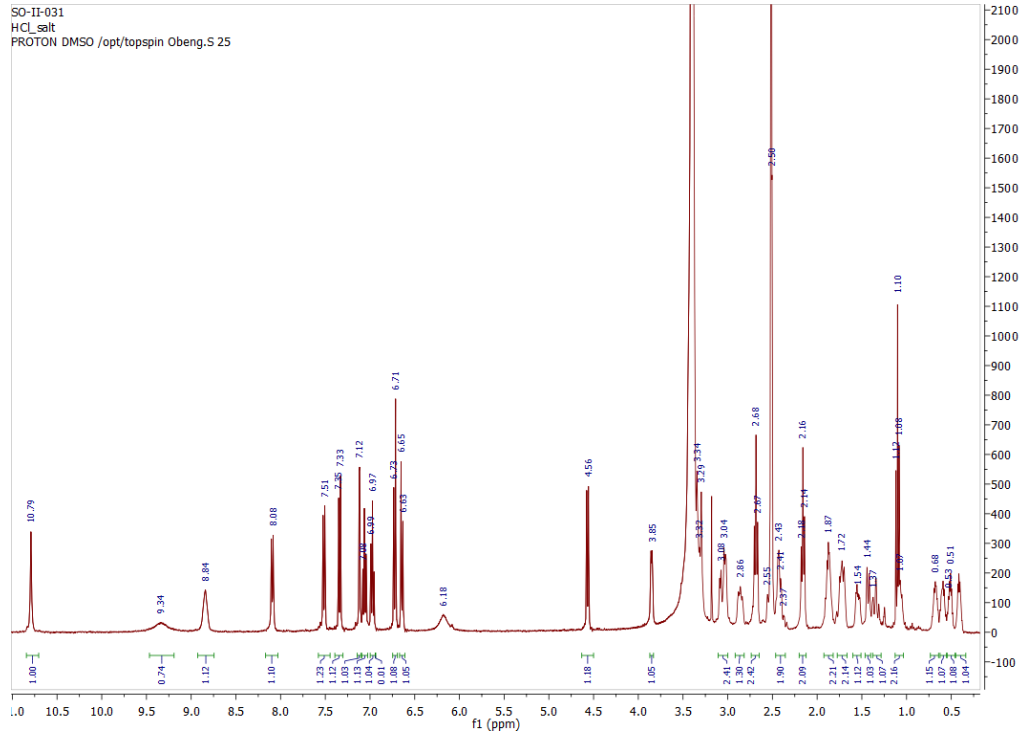


IR

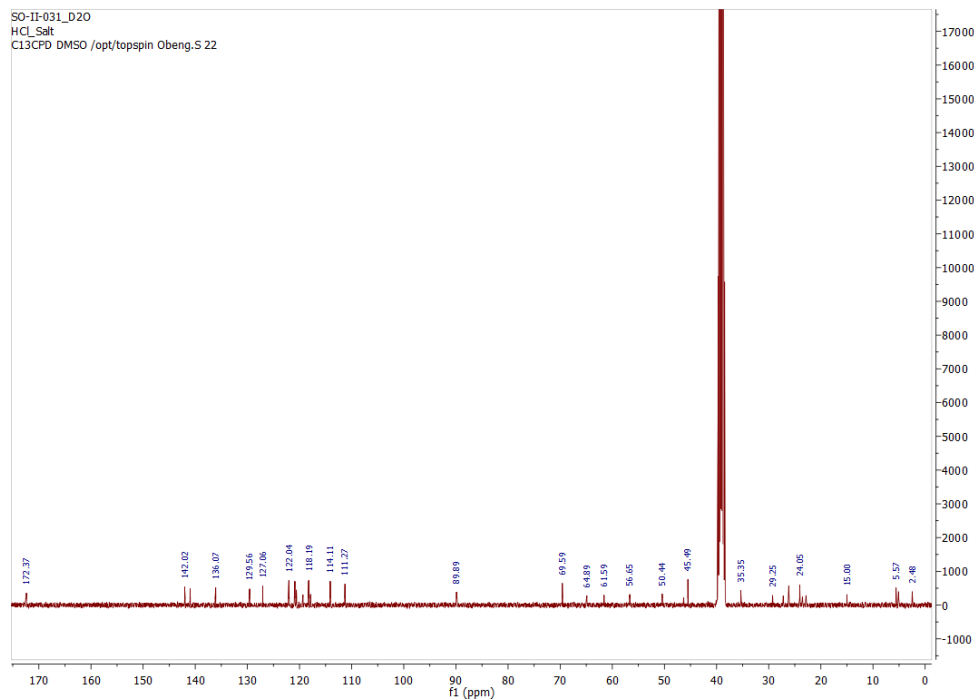


Compound 18

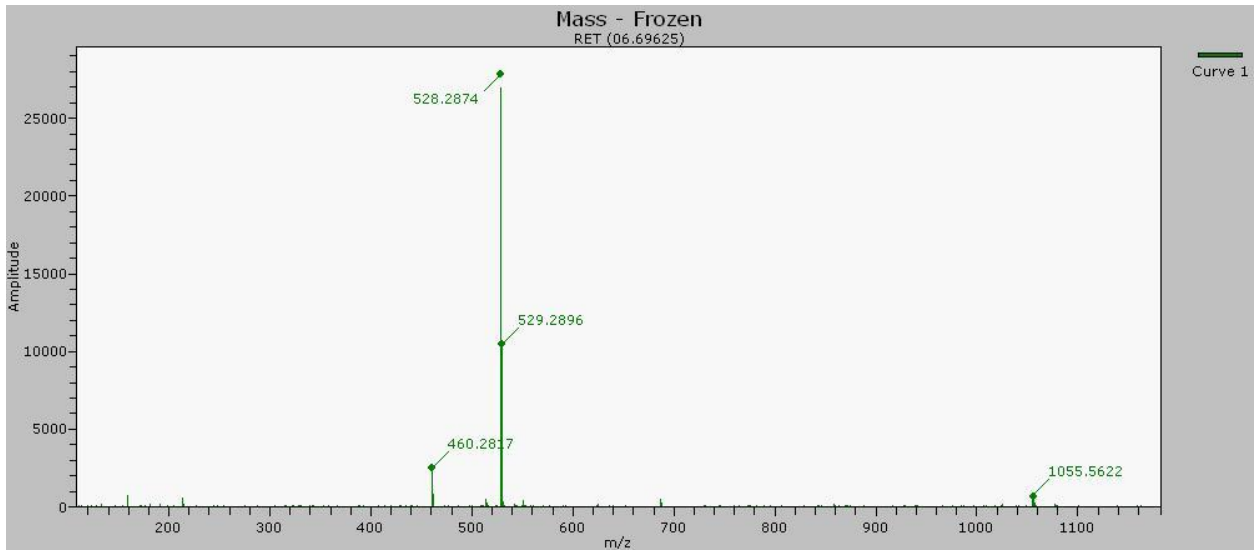
¹H NMR



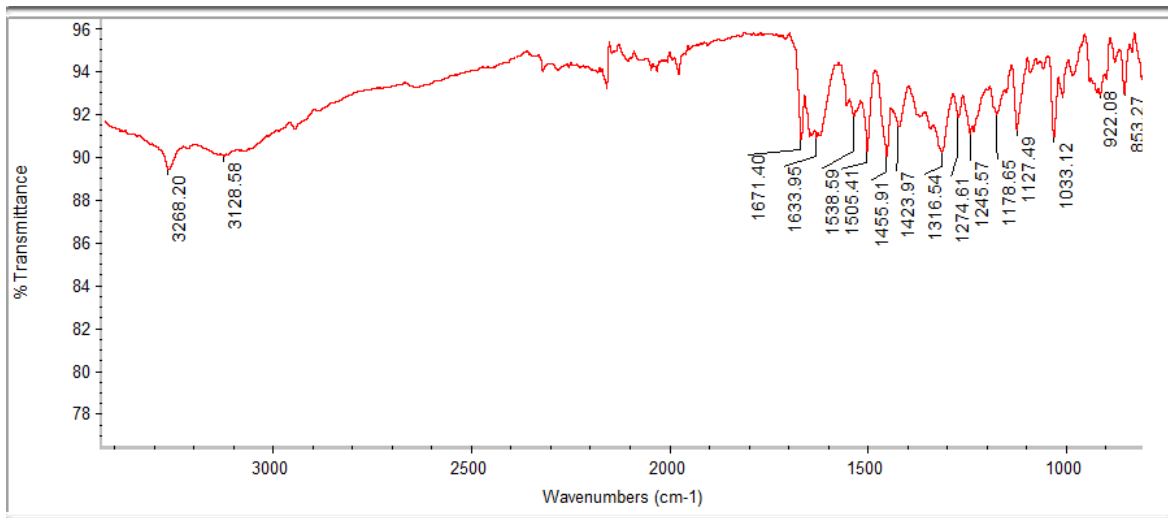
¹³C NMR



High resolution masspec

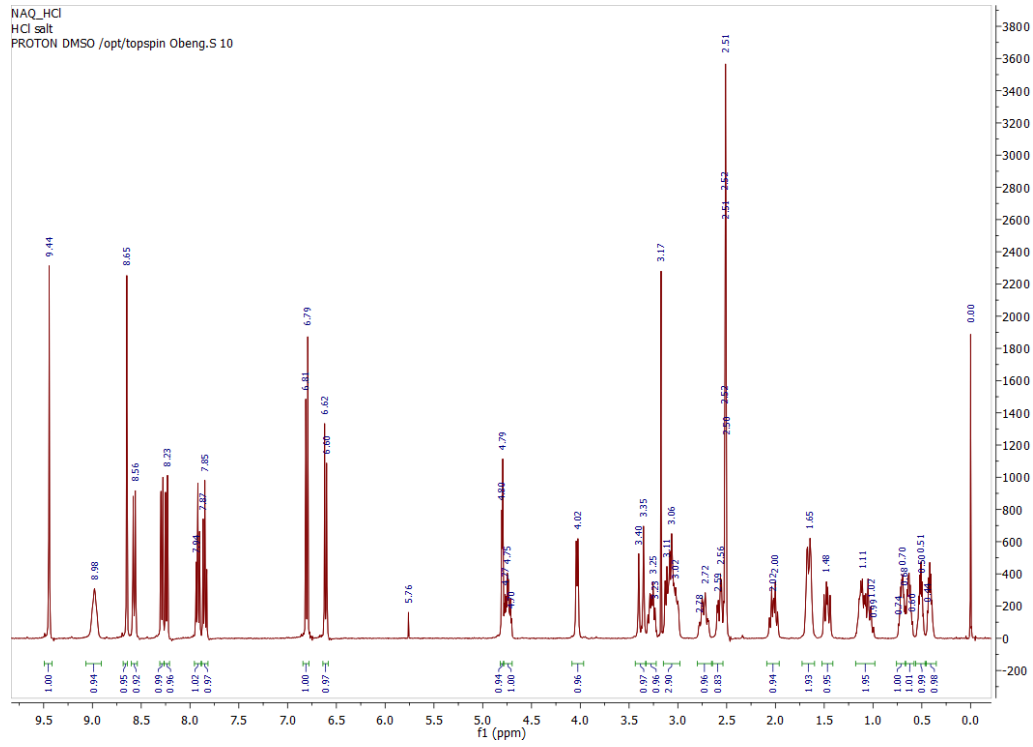


IR

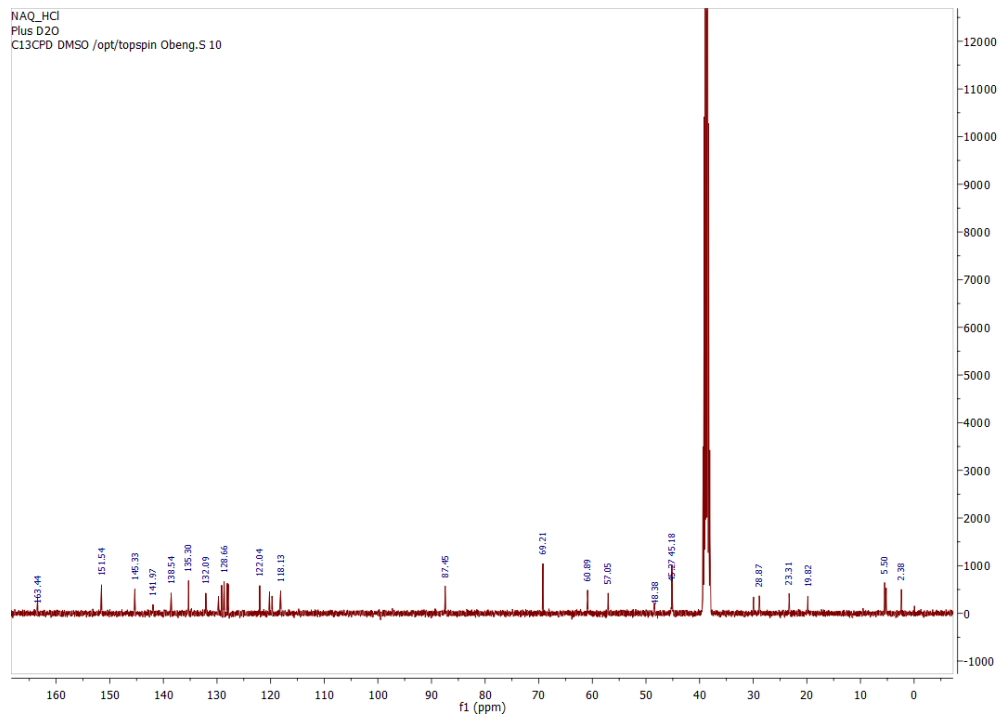


NAQ

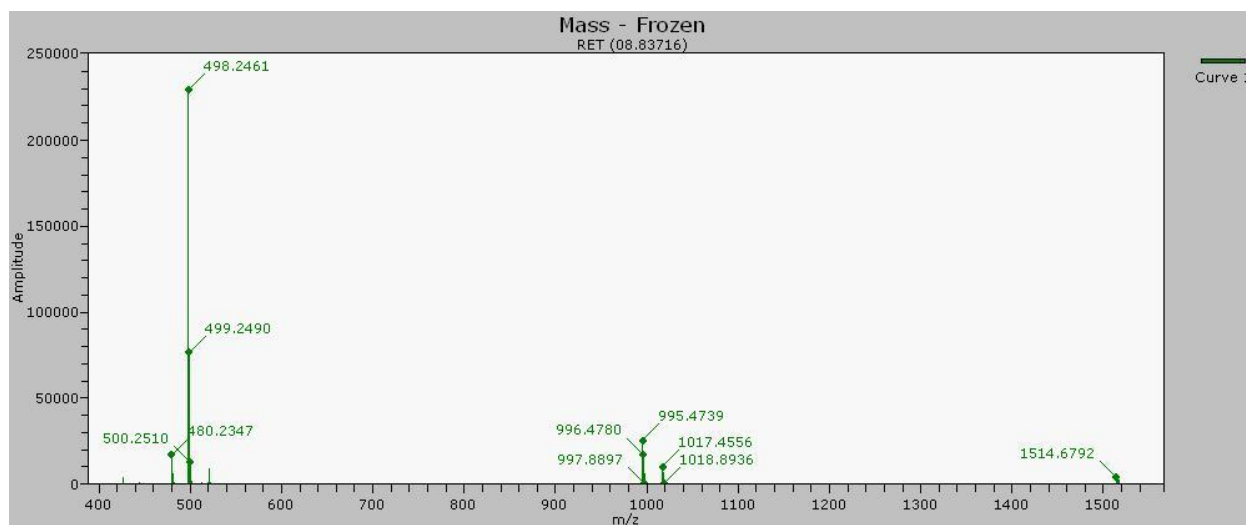
¹H NMR



¹³C NMR



High resolution masspec



QSPKR Table

Quantitative Structure Pharmacokinetic Relationship (QSPKR) TABLE																								
Compound ID	MW	cLogP	pK _a	logD _{7.4}	HB ₁	HB ₂	O ₁	nRo	C/A	LogD _{7.4} - Δ at pH7	Note1	Note2	Lipinski ROS	GI Perm	D _{max} ⁵⁰ [mg]	CNSPen	t _{1/2} [%]	Vd _{ss} [L/kg]	CL _{ven} ¹ [mL/min/kg]	CL _{corrected} ² [mL/min/kg]	CL _{tot} ³ [mL/min/kg]	Vd _{ss} [L/kg]	CL _{ss} [mL/min/kg]	syst t _{1/2} [min]
1. VZM001	342	0.49	7.99	-0.20	4	5	5	5	CI	-1.11	120	ketone at position 6	Pass	Pass	30000	Fail	69%	2.1	1.7	9.9	16.3	1.4	11.3	89
2. VZM002	342	0.49	7.99	-0.20	4	5	5	5	CI	-1.11	120	ketone at position 6	Pass	Pass	30000	Fail	69%	2.1	1.7	9.9	16.3	1.4	11.3	89
30. VZM045	449	0.31	7.19	0.10	3	8	8	6	N	-0.29	5.4		Pass	Pass	1350	Fail	65%	2.7	1.8	12.8	19.6	1.8	12.7	96
35. VZM038	468	1.65	8.57	0.45	3	7	7	6	CI	-0.35	4.7		Pass	Pass	11750	Fail	60%	3.6	1.8	17.1	24.1	2.2	14.4	104
34. VZM037	505	0.85	7.31	0.59	4	9	9	8	N	0.36	1.7		FAIL	Pass	425	Fail	58%	4.1	1.8	19.1	26.1	2.4	15.1	108
6. VZM006	499	1.23	7.72	0.74	3	8	8	6	CI	0.12	0.75		Pass	Pass	187.5	Fail	56%	4.6	1.8	21.6	28.5	2.6	15.9	112
7. VZM007	448	1.04	7.24	0.81	3	7	7	6	N	0.39	2.2		Pass	Pass	550	Fail	55%	4.9	1.8	23.0	29.8	2.7	16.3	114
12. VZM013	448	1.04	7.24	0.81	3	7	7	6	N	0.39	2.2		Pass	Pass	550	Fail	55%	4.9	1.8	23.0	29.8	2.7	16.3	114
59. VZM066	478	1.02	7.11	0.84	3	8	8	7	N	0.44	1.6		Pass	Pass	400	Fail	54%	5.0	1.8	23.5	30.3	2.7	16.5	115
43. VZM049	449	1.08	7.09	0.91	3	8	8	6	N	0.51	1.3		Pass	Pass	325	Fail	53%	5.3	1.9	25.0	31.6	2.8	16.9	117
13. VZM014	448	1.18	7.24	0.95	3	7	7	6	N	0.57	1.8		Pass	Pass	450	Fail	53%	5.5	1.9	26.0	32.5	2.9	17.1	118
8. VZM008	448	1.18	7.17	0.98	3	7	7	6	N	0.57	1.8		Pass	Pass	450	Fail	52%	5.7	1.9	26.6	33.0	3.0	17.3	119
33. VZM036	462	1.29	7.17	1.09	3	7	7	6	N	0.67	1.3		Pass	Pass	325	Fail	51%	6.2	1.9	29.0	35.1	3.1	17.9	122
60. VZM067	559	1.84	7.94	1.19	3	8	8	7	CI	0.36	1.3		FAIL	Pass	325	Fail	49%	6.8	1.9	31.7	37.4	3.3	18.5	125
5. VZM005	498	1.77	7.84	1.20	3	7	7	6	CI	0.61	0.26		Pass	Pass	65	Fail	49%	6.8	1.9	31.8	37.5	3.3	18.5	125
11. VZM011	498	1.77	7.84	1.20	3	7	7	6	CI	0.61	0.26		Pass	Pass	65	Fail	49%	6.8	1.9	31.8	37.5	3.3	18.5	125
37. VZM043	462	1.42	7.17	1.22	3	7	7	6	N	0.80	1.2		Pass	Pass	300	Fail	49%	6.9	1.9	32.3	37.9	3.4	18.6	126
26. VZM029	448	1.52	7.29	1.27	3	7	7	6	N	0.88	1.4		Pass	Pass	350	Fail	48%	7.2	1.9	33.9	39.2	3.5	18.9	128
27. VZM030	448	1.52	7.29	1.27	3	7	7	6	N	0.88	1.4		Pass	Pass	350	Fail	48%	7.2	1.9	33.9	39.2	3.5	18.9	128
50. VZM056	473	1.51	7.12	1.33	3	8	8	6	N	0.92	0.28		Pass	Pass	70	Fail	47%	7.6	1.9	35.6	40.6	3.6	19.3	130
49. VZM055	516	2.00	7.94	1.35	3	7	7	6	CI	0.55	2.9		FAIL	Pass	725	Fail	47%	7.7	1.9	36.0	41.0	3.6	19.4	130
30. VZM033	482	1.59	7.09	1.42	3	7	7	6	N	1.03	0.41		Pass	Pass	102.5	Fail	46%	8.2	1.9	38.2	42.8	3.8	19.8	132
32. VZM035	462	1.69	7.34	1.42	3	7	7	7	N	0.97	0.96		Pass	Pass	240	Fail	46%	8.2	1.9	38.4	42.9	3.8	19.8	133
31. VZM034	526	1.70	7.08	1.53	3	7	7	6	N	1.14	0.46		FAIL	Pass	115	Fail	45%	9.0	1.9	42.0	45.7	4.0	20.4	136
55. VZM061	558	2.16	7.85	1.57	3	9	9	8	CI	1.02	0.2		FAIL	Pass	50	Fail	44%	9.3	1.9	43.6	47.0	4.1	20.7	138
3. VZM003	498	2.16	7.79	1.62	3	7	7	6	CI	1.06	0.16		Pass	Pass	40	Fail	43%	9.7	1.9	45.4	48.4	4.2	20.9	139
9. VZM009	498	2.16	7.79	1.62	3	7	7	6	CI	1.06	0.16		Pass	Pass	40	Fail	43%	9.7	1.9	45.4	48.4	4.2	20.9	139
0. NTX	341	2.05	7.50	1.60	2	5	5	4	N	1.32	1.8	ketone at position 6 DO	Pass	Pass	450	Fail	42%	10.3	1.9	48.2	50.5	4.4	21.3	142
38. VZM044	476	2.01	7.36	1.72	3	7	7	8	CI	1.24	0.62		Pass	Pass	155	Fail	42%	10.6	1.9	49.4	51.3	4.4	21.5	143
23. VZM026	447	2.04	7.35	1.76	3	6	6	6	N	1.30	0.34		Pass	Pass	85	Fail	41%	10.9	2.0	51.0	52.5	4.5	21.7	144
25. VZM028	447	2.04	7.35	1.76	3	6	6	6	N	1.30	0.34		Pass	Pass	85	Fail	41%	10.9	2.0	51.0	52.5	4.5	21.7	144
36. VZM042	482	1.97	7.13	1.79	3	7	7	6	N	1.39	0.31		Pass	Pass	77.5	Fail	41%	11.2	2.0	52.0	53.3	4.6	21.8	145
29. VZM032	526	1.99	7.12	1.81	3	7	7	6	N	1.41	0.38		FAIL	Pass	95	Fail	41%	11.4	2.0	53.0	54.0	4.6	22.0	146
53. VZM059	543	2.45	7.85	1.87	3	10	10	7	CI	1.32	0.06		FAIL	Pass	15	Fail	40%	12.0	2.0	55.7	59.0	4.8	22.3	148
54. VZM060	543	2.45	7.85	1.87	3	10	10	7	CI	1.32	0.06		FAIL	Pass	15	Fail	40%	12.0	2.0	55.7	59.0	4.8	22.3	148
64. VZM072	499	2.37	7.73	1.88	3	8	8	6	CI	1.33	0.048		Pass	Pass	12	Fail	40%	12.1	2.0	56.1	56.3	4.8	22.3	148
63. VZM071	514	2.61	7.95	1.95	4	8	8	7	CI	0.49	0.021		FAIL	Pass	5.25	Fail	39%	12.8	2.0	59.7	59.8	5.0	22.7	151
42. VZM048	478	2.17	7.14	1.98	3	8	8	7	N	1.57	0.57		Pass	Pass	142.5	Fail	38%	13.1	2.0	61.1	59.8	5.0	22.8	152
48. VZM054	555	2.63	7.92	2.00	4	9	9	8	CI	1.66	0.13		FAIL	Pass	32.5	Fail	38%	13.3	2.0	61.9	60.4	5.1	22.9	153
58. VZM064	541	2.67	7.88	2.06	3	8	8	7	CI	1.51	0.065		FAIL	Pass	16.25	Fail	37%	14.1	2.0	65.4	62.8	5.2	23.3	155
4. VZM004	498	2.71	7.89	2.10	3	7	7	6	CI	1.55	0.19		Pass	Pass	47.5	Fail	37%	14.5	2.0	67.3	64.1	5.3	23.4	157
10. VZM010	498	2.71	7.89	2.10	3	7	7	6	CI	1.55	0.19		Pass	Pass	47.5	Fail	37%	14.5	2.0	67.3	64.1	5.3	23.4	157
71. VZM096	486	3.09	7.99	2.40	4	7	7	4	CI	1.76	0.26		Pass	FAIL	65	Fail	32%	18.7	2.0	86.7	76.7	6.0	24.7	169
70. VZM078	523	3.04	7.75	2.53	3	8	8	6	CI	1.92	0.029		FAIL	FAIL	7.25	Fail	30%	20.8	2.0	96.5	82.8	6.3	25.2	174
69. VZM077	512	3.09	7.80	2.54	3	7	7	6	CI	1.98	0.097		FAIL	FAIL	24.25	Fail	30%	21.2	2.0	98.0	83.7	6.4	25.3	175
22. VZM025	497	3.22	7.93	2.58	3	6	6	6	CI	1.97	0.045		Pass	FAIL	11.25	Fail	30%	21.8	2.1	101.1	85.6	6.5	25.4	177
24. VZM027	497	3.22	7.93	2.58	3	6	6	6	CI	1.97	0.045		Pass	FAIL	11.25	Fail	30%	21.8	2.1	101.1	85.6	6.5	25.4	177
41. VZM047	446	2.87	7.06	2.70	2	7	7	5	N	2.36	0.12	ketone at position 6	Pass	Pass	30	Fail	28%	24.2	2.1	111.7	91.9	6.8	25.7	182
61. VZM069	512	3.42	7.93	2.77	3	7	7	7	CI	2.17	0.062		FAIL	FAIL	20.5	Fail	27%	25.7	2.1	118.5	95.9	6.9	25.8	185
61. VZM068	526	3.53	7.96	2.86	3	7	7	8	CI	2.25	0.063	ketone at position 6	FAIL	FAIL	15.75	Fail	26%	27.6	2.1	127.4	101.0	7.1	26.0	189
40. VZM046	446	3.01	6.88	2.90	2	7	7	5	N	2.57	0.094		Pass	FAIL	23.5	Fail	25%	28.5	2.1	131.5	103.3	7.2	26.0	191
57. VZM063	562	3.43	7.78	2.90	3	8	8	7	CI	2.34	0.025		FAIL	FAIL	6.25	Fail	25%	28.5	2.1	131.7	103.4	7.2	26.0	191
65. VZM073	532	3.50	7.84	2.92	3	7	7	6	CI	2.37	0.033		FAIL	FAIL	8.25	Fail	25%	29.1	2.1	134.2	104.8	7.2	26.0	192
56. VZM062	548	3.61	7.90	2.99	4	8	8	7	CI	1.37	4.70E-03		FAIL	FAIL	1.175	Fail	24%	30.9	2.1	142.3	109.3	7.4	26.0	196
46. VZM052	446	3.35	7.18	3.15	2	7	7	5	N	2.84	0.08	ketone at position 6	Pass	FAIL	20	Fail	22%	35.2	2.1	162.1	119.9	7.6	25.9	204
44. VZM050	496	3.60	7.66	3.15	2	7	7	5	CI	2.61	0.013	ketone at position 6	Pass	FAIL	3.25	Fail	22%	35.3	2.1	162.4	120.1	7.6	25.9	204
28. VZM031	446	3.69	7.35	3.42	1	7	7	6	N	3.61	0.03	ketone at position 6	Pass	FAIL	7.5	Fail	18%	44.2	2.2	203.0	140.8	7.9	25.0	218
68. VZM076	503	3.70	7.26	3.46	3	9	9	7	N	3.18	0.046	ketone at position 6	FAIL	FAIL	11.5	Fail	17%	45.9	2.2	210.7	144.5	7.9	24.8	220
47. VZM053	445	3.87	7.34	3.60	2	6	6	5	N	3.23	0.021	ketone at position 6	Pass	FAIL	5.25	Fail	15%	51.4	2.2	235.9	156.7	7.8	23.9	228
52. VZM058	496	3.99	7.53	3.62	2	7	7	5	CI	3.13	7.40E-03	ketone at position 6	Pass</											

Vita

Samuel Obeng was born on October 25, 1986, in Koforidua, Ghana, and is a Ghanaian citizen. He graduated from St. Peter's Senior High School, Ghana in 2005. He received his Bachelor of Pharmacy degree and Master's degree in Pharmaceutical Chemistry from Kwame Nkrumah University of Science and Technology, Ghana in 2010 and 2014, respectively. He joined the Medicinal Chemistry department in the School of Pharmacy at Virginia Commonwealth University in August 2013.